



The detection of stress-related diseases: establishment of two unique methods to discover circulatory phospho- and glycoproteins

by
Logan Jason Smith

Thesis presented in fulfilment of the requirements for the degree of Master of Physiological Sciences in the Faculty of Science at Stellenbosch University

Supervisor: Prof. Faadiel Essop
Co-supervisor: Dr. Danzil Joseph

December 2023



ACKNOWLEDGEMENTS

First and foremost, I would like to thank my supervisor, Professor Faadiel Essop. Thank you for always motivating me to keep going. Your philosophy and goal of creating a holistic individual who can take on the challenges of life is what I have always looked up to. The lessons which I have learnt from you, not only as my supervisor, but also as a mentor, are those which I will carry with me always. Thank you for your eternal optimism and composure despite the unforeseen circumstances which, at times, seemed never-ending. You were an immense source of positivity and strength.

To my co-supervisor, Dr Danzil Joseph, thank you for being available when I would randomly pitch up at your office door or needed to meet online. I am grateful for your willingness to help in whichever way you could despite being flooded with your own work. Thank you for always assuring me that things would work out just fine, and for always looking out for me. I really appreciate all your constructive inputs and insights.

To my CARMA family, thank you for all the support in the form of coffee shakes, adventures and tennis matches. Even when you girls didn't fully understand what was wrong, you were always willing to help me destress whenever you could, whether it be in the form of having a laugh in the lab or going for a walk to My Brew. I will always have time for each one of you.

A special thanks is reserved for Prof Bienyameen Baker, Prof David Tabb, Dr Liam Bell and Dr Stoyan Stoychev. All of you were always open to my questions, and making the best out of this project despite its limitations and struggles. Your reliable expertise me to grasp complex concepts. Thanks for always communicating this to me in a way which is understandable.

To the staff and students in the Division of Medical Physiology and the Department of Biomedical Sciences, thank you for always being willing to assist me, and for all the snacks when I was under immense pressure. I would never have gotten through this without your support and positivity.

To my friends and family, thank you for always believing in me and re-assuring me, and for always praying for me. A special mention goes to my mother, brother, and aunty, for

always supporting me and doing all the chores towards the end of my thesis to give me time to sit down and write. I am grateful to always have you by my side.

Lastly, I would like to thank my Heavenly Father and Saviour Jesus Christ, for giving me the strength to complete this project. Without His everlasting grace and mercy, none of this would have been possible. He is also responsible for placing these incredible individuals in my life, who have helped me get through this challenging period. Despite these challenges, I am grateful for the growth I have experienced as an individual.

DECLARATION

By submitting this thesis electronically, I declare that the entirety of the work contained therein is my own, original work, that I am the sole author thereof (save to the extent explicitly otherwise stated), that reproduction and publication thereof by Stellenbosch University will not infringe any third-party rights and that I have not previously in its entirety or in part submitted it for obtaining any qualification.

LIST OF FIGURES**CHAPTER 1:**

Figure 1.1: An integrative representation of the consequences of chronic psychosocial stress.....	14
Figure 1.2: A diagrammatic summary of the pathways and proteins involved in phosphorylation and stress.....	25
Figure 1.3: A diagram that illustrates the potential links between stress-linked glycosylation and diseases.....	30
Figure 1.4: An integrative diagram representing the relationship between glycosylation, phosphorylation, and chronic psychosocial stress pathways in no particular order.....	34
Figure 1.5: A summarized visual representation of our workflow.....	51

CHAPTER 2:

Figure 2.1: A visual summary of the workflow for evaluating the efficacy of phosphoprotein enrichment.....	62
Figure 2.2: Figure 2.2. 4% - 20% gradient gel displays the (A) total protein stain of OVA and (B) the fluorescent intensity of OVA.....	63
Figure 2.3: Stain free 10% mini-protean gels which display the efficiency of the intact protein enrichment technique.....	63

CHAPTER 3:

Figure 3.1: A basic representation of the workflow in building, testing and utilizing the novel affinity material.....	81
Figure 3.2: 4% - 20% gradient gel displays the (A) total protein stain of OVA and (B) the fluorescent intensity of OVA.....	83
Figure 3.3: A stain free 10% mini-protean gel which displays the enrichment efficiency of the unique method.....	84
Figure 3.4: The total protein image of an increase in affinity material for enrichment for both positive (A) and negative (B) controls.....	85

Figure 3.5: Optimization of chemical deglycosylation was assessed using increasing amounts of TFMS.....	86
Figure 3.6: One microliter of acid was employed to deglycosylate serum for three different time intervals.....	87
Figure 3.7: Two microliters of TFMS were employed for deglycosylation of the eluted serum fraction.....	88

Chapter 4:

Figure 4.1: An overview of the proteomics workflow from sample preparation to data processing	103
Figure 4.2: A 16% tricine gel was employed to assess phosphopeptide enrichment.....	107

LIST OF TABLES

CHAPTER 1:

Table 1.1: A summary of studies where the direct links between stress and negative health outcomes were demonstrated.....	6
Table 1.2: General overview of known PTMs that are frequently mentioned in literature	19
Table 1.3 A brief overview of glycosylation and phosphorylation usage in the clinical setting.....	32
Table 1.4 A brief description of proteomics analyses in stress pathology research and the methods involved.....	45

CHAPTER 2:

Table 2.1 A comparison between the originally specified buffers and their replacements, including the reason for their substitutions.....	58
Table 2.2 Protein (including unprocessed from serum), DNA and RNA concentrations obtained from the Nanodrop One are listed, including purity ratios.....	64

CHAPTER 3:

Table 3.1 The buffers, their respective constituents, and explanations for use..	71
--	----

CHAPTER 4:

Table 4.1: The variance observed between each sample within their respective sample populations.....	104
Table 4.2: The percentage fraction of PSMs identified and reported from raw spectral data. PSM, peptide spectral match.....	104
Table 4.3: The percentage fraction of PSMs identified and reported from raw spectral data. PSM, peptide spectral match.....	105
Table 4.4: The number of PSMs and distinct peptides present in the positive control samples.....	106

LIST OF ABBREVIATIONS

2-DE	2-Dimensional electrophoresis
ACTH	Adrenocorticotrophic hormone
Akt	Ak transforming
AP-1	Activator protein 1
Arg	Arginine
Asn	Asparagine
Asp	Aspartic acid
BP	Blood pressure
BSA	Bovine serum albumin
CBG	Corticosteroid-binding globulin
ConA	Concanavalin A
COVID-19	Coronavirus disease of 2019
CPGR	Centre for Proteomic and Genomic Research
CREB	cyclic Adenosine monophosphate response element-binding protein
CRS	Chronic restraint stress
CVD	Cardiovascular disease
Da	Dalton
DHEA-S	Dehydroepiandrosterone sulfate
DNA	Deoxyribonucleic acid
EDC	1-ethyl-3-(3-dimethylamino) propyl carbodiimide
EDTA	Ethylenediamine tetraacetic acid
ER	Endoplasmic reticulum
ERK	Extracellular signal regulated kinase
FDR	False discovery rate
GC	Glucocorticoid
Glu	Glutamic acid
GR	Glucocorticoid receptor
HILIC	Hydrophilic liquid interaction chromatography
HPA	Hypothalamic pituitary adrenal
HPLC	High performance liquid chromatography
HR	Heart rate
IκB	Inhibitor of nuclear factor kappa B

IL-6	Interleukin-6
IMAC	Immobilized metal affinity chromatography
JNK	c-Jun amino-terminal kinases
kDa	Kilodaltons
LAC	Lectin affinity chromatography
LC	Liquid chromatography
Lys	Lysine
m/z	Mass-to-charge
MAPK	Mitogen activated protein kinase
MetS	Metabolic syndrome
miRNA	microRNA
MOAC	Metal oxide affinity chromatography
MS	Mass spectrometry
MS/MS	Tandem mass spectrometry
NAFLD	Non-alcoholic fatty liver disease
NCDs	Non-communicable diseases
NFκB	Nuclear factor kappa B
NHS	N-Hydroxysuccinimide
OVA	Ovalbumin
PBS	Phosphate-buffered saline
PGC-1α	Peroxisome proliferator-activated receptor-gamma coactivator 1α
Phe	Phenylalanine
PKA	Protein kinase A
Pro	Proline
PSM	Peptide spectrum match
PTM	Post-translational modification
PTSD	Post-traumatic stress disorder
RNS	Reactive nitrogen species
ROS	Reactive oxygen species
SAM	Sympathetic-adreno-medullary
SAX	Strong anion exchange
SCX	Strong cation exchange
SDS-PAGE	Sodium dodecyl sulfate polyacrylamide gel electrophoresis
Ser	Serine

StAR	Steroidogenic acute regulatory protein
T2D	Type 2 diabetes
TFMS	Trifluoromethane sulfonic acid
Thr	Threonine
TNF-α	Tumor necrosis factor-alpha
Tyr	Tyrosine
Zr	Zirconium

TABLE OF CONTENTS

ACKNOWLEDGMENTS	i
DECLARATION	iii
LIST OF FIGURES	iv
LIST OF TABLES	v
LIST OF ABBREVIATIONS	vii
FOREWORD	xv
Abstract	xvi
Opsomming	xviii
CHAPTER 1 – LITERATURE REVIEW	1
1.1 INTRODUCTION	2
1.2 THE ROLE OF STRESS	3
1.2.1 The burden of stress	3
1.2.1.1 The direct links between stress and negative health outcomes	4
1.2.2 The caveats of stress research	8
1.2.3 The physiological stress response	9
1.2.3.1 The integrated stress response	10
1.2.3.1(a) <i>The metabolic effects of stress</i>	11
1.2.3.1(b) <i>The anti-inflammatory effects of cortisol</i>	11
1.2.4 Chronic stress pathology	12
1.2.4.1 Chronic stress-induced oxidative stress	15
1.2.4.1(a) <i>The mitochondria and oxidative stress</i>	15
1.2.4.2 Chronic stress and inflammation	16
1.3 POST-TRANSLATIONAL MODIFICATIONS	18
1.3.1 Protein phosphorylation	21
1.3.1.1 Pathways and proteins in stress and phosphorylation	22
1.3.1.2 The direct involvement of phosphorylation in stress-related disease	23
1.3.1.2(a) <i>Phosphorylation of the glucocorticoid receptor</i>	24
1.3.2 Glycosylation	25
1.3.2.1 The relationship between disease and protein glycosylation	27
1.3.2.2 Strengthening the link between stress and glycosylation	28

1.3.2.2(a) <i>Endoplasmic reticulum stress</i>	29
1.3.2.2(b) <i>The corticosteroid-binding globulin</i>	30
1.4 THE EXPLORATION OF BIOMARKERS LINKED TO CHRONIC STRESS	35
1.4.1 Current potential biomarkers of psychosocial stress	35
1.4.2 Methods employed for biomarker discovery	37
1.5 A RAT MODEL OF CHRONIC STRESS	38
1.5.1 Chronic restraint stress	38
1.5.2 Serum as the biological sample	39
1.6 PROTEOMICS METHODOLOGIES	40
1.6.1 Bottom-up versus top-down approaches	41
1.6.2 Methods in proteomics	41
1.6.2.1 Sample preparation	41
1.6.2.1(a) <i>General modes of protein enrichment</i>	42
1.6.2.2 Chromatography as a mode of separation	43
1.6.2.3 Mass spectrometry as a high-throughput technique	47
1.6.2.4 Data analysis	47
1.7 AIMS AND OBJECTIVES	48
CHAPTER 2 – PHOSPHOPROTEIN ENRICHMENT USING ZR-IMAC MAGNETIC MICROPARTICLES	52
2.1 INTRODUCTION	53
2.1.1 The enrichment of phosphoproteins	53
2.1.2 Phosphopeptide versus phosphoprotein enrichment	54
2.1.3 Metal oxide affinity chromatography	54
2.1.3.1 Immobilized metal affinity chromatography	55
2.1.3.2 The presence of nucleic acids in serum	56
2.2 AIMS AND OBJECTIVES	56
2.3 METHODS AND MATERIALS	57
2.3.1 Chemicals and Materials	57
2.3.2 TRIzol extraction	57
2.3.3 Phosphoprotein enrichment	58
2.3.4 Protein determination, SDS-PAGE analysis and staining	59
2.3.4.1 Laemmli sample preparation	60
2.3.4.2 Protein loading and staining	60

2.4 RESULTS	63
2.4.1 OVA results	63
2.4.2 Nucleic acids in rat serum	64
2.5 DISCUSSION	64
2.5.1 The efficiency of the unique phosphoprotein enrichment technique	65
2.5.2 The presence of nucleic acids in rat serum	66
2.6 CONCLUSION	66
2.7 LIMITATIONS AND RECOMMENDATIONS	66
CHAPTER 3– THE ENRICHMENT OF GLYCOPROTEINS USING LECTIN AFFINITY CHROMATOGRAPHY	68
3.1 INTRODUCTION	69
3.1.1 Enrichment strategies for glycoproteins	69
3.1.2 The use of lectins for affinity chromatography	70
3.1.3 Support structures for lectin affinity chromatography	71
3.1.4 ConA immobilized onto carboxyl magnetic microparticles	73
3.1.5 The importance of deglycosylation in proteomics workflows	74
3.2 AIMS AND OBJECTIVES	75
3.3 MATERIALS AND METHODS	75
3.3.1 Biological sample origin	76
3.3.2 Building and testing novel affinity material for glycoprotein enrichment	77
3.3.3 Ensuring sufficient deglycosylation for downstream analysis	79
3.3.4 Protein determination and SDS-PAGE analysis	82
3.3.4.1 Total protein and glyco-fluorescent staining	82
3.4 RESULTS	83
3.4.1 Protein determination results	83
3.4.2 The glycosylation of OVA	83
3.4.3 Testing the affinity material with OVA	84
3.4.4 Fifty microliters of affinity material employed with 50 µg of OVA	85
3.4.5 The efficacy of deglycosylation	86
3.4.6 Serum deglycosylation	87
3.5 DISCUSSION	89
3.5.1 Investigation of affinity material competence	89
3.5.2 Ensuring deglycosylation for downstream analysis	90

3.5.2.1 OVA deglycosylation	90
3.5.2.2 Serum deglycosylation	91
3.6 CONCLUSION	91
3.7 LIMITATIONS AND FUTURE RECOMMENDATIONS	92
<i>CHAPTER 4 – THE EVALUATION OF THE ENRICHMENT METHODS BY LC-MS</i>	93
4.1 INTRODUCTION	94
4.1.1 Chromatography as an integral tool	94
4.1.2 Electrospray ionization-MS/MS	94
4.1.3 The role of trypsin	95
4.1.4 Ensuring quality control in the proteomics workflow	96
4.2 AIMS AND OBJECTIVES	97
4.3 METHODS AND MATERIALS	97
4.3.1 Sample size	97
4.3.2 On-bead digestion procedure	98
4.3.3 Phosphopeptide enrichment	98
4.3.4 Glycopeptide sample processing	99
4.3.5 Data acquisition by LC-MS/MS	99
4.3.6 Data interpretation	100
4.3.7 Supplementary SDS-PAGE experiments	101
4.4 RESULTS	104
4.4.1 The variation of the acquired data	104
4.4.2 PSMs identified from RAW spectra	104
4.4.3 The number of phospho- and glyco-PSMs identified	105
4.4.4 The identification of phosphopeptides and glycopeptides in the positive controls	105
4.4.5 Enrichment of OVA	106
4.4.6 Tricine-SDS-PAGE results	106
4.5 DISCUSSION	107
4.5.1 The variance between samples	107
4.5.2 Fewer identifications in the enriched samples compared to controls	108
4.5.2.1 The loss of the peptide/modification	108
4.5.3 The challenges associated with serum enrichment	110
4.6 CONCLUSION	111

4.7 LIMITATIONS AND FUTURE RECOMMENDATIONS	112
5 A UNIFIED CONCLUSION	113
6 REFERENCES	114
APPENDICES	189
Appendix A – CRS study	189
Appendix B – Phosphoprotein enrichment	192
Appendix C – Glycoprotein enrichment	200
Appendix D – SDS-PAGE, fluorescent staining and protein determination protocols	209
Appendix E – HILIC digestion and LC-MS settings	223
Appendix F – Data from LC-MS/MS	227
Appendix G – Turnitin Report	229

FOREWORD

This dissertation is presented in article format and written in US English. Chapter 1 reviews the literature relevant to the topic and the following chapters provide a more detailed explanation of their respective subject matters. The second, third and fourth chapters each contain a more focused introduction, methods and materials, results, discussion, a concluding paragraph and limitations and future recommendations. An overall conclusion summarizes and unifies the findings from each chapter.

ABSTRACT

Introduction: Psychosocial stress has strong links to numerous chronic diseases related to the dysregulated activation of the physiological stress system. This heightens the burden of mortality as there is a robust relationship between chronic psychosocial stress and non-communicable diseases. Hence there is a robust impetus for the identification of novel, circulating biomarkers to earlier detect stress-related chronic diseases. Although protein post-translational modifications such as glycosylation and phosphorylation can act as putative markers of pathophysiology, their relatively low abundance complicates extraction and identification from samples with a high dynamic range. The main aim of this study was therefore to establish two unique enrichment methods for circulatory glycoprotein and phosphoprotein extraction that would then be applied in a preclinical model of chronic psychosocial stress.

Methods: Phosphoprotein enrichment was performed using functionalized magnetic particles while glycoprotein enrichment occurred using lectin-bound magnetic particles. Both these methods were tested using a known purified phosphorylated and glycosylated protein and compared to bottom-up proteomics methodology using rat serum. The latter was obtained from a rat model of chronic stress that is well-established in our laboratory (n = 16 controls versus n = 16 stressed rats). These were randomly selected for proteomics analysis to assess the efficiency of retrieval in enriched versus unenriched samples. Fractions were analyzed by sodium dodecyl sulfate polyacrylamide gel electrophoresis (SDS-PAGE) and proteins visualized using Coomassie and specific fluorescent staining. Here, the relevant Pro-Q stains were employed for the identification of glycosylation and phosphorylation, respectively. The coupling of such enrichment methods to LC – tandem mass spectrometry (MS/MS) was enabled by employing various preparation steps such as deglycosylation and digestion. An exogenous protein was also included as part of the sample preparation to ensure quality control analysis of the LC-MS/MS experiment.

Results: SDS-PAGE analyses and staining methods revealed non-specific enrichment with regards to intact protein retrieval. In addition, LC-MS/MS data demonstrated that enrichment using the current set of affinity materials was inadequate for glycopeptide and phosphopeptide retrieval in serum.

Conclusion: A lack of enrichment indicates that stringent sample preparation is needed for biological materials with a high dynamic range. This may also be due to the porous nature of both materials employed for phospho- and glycoprotein/peptide enrichment respectively. A combination of enrichment and/or depletion methods may therefore be beneficial for deeper analysis of the blood proteome. These enrichment techniques and the subsequent

sample preparation still require further optimization to derive more definitive conclusions in the chronic stress context.

OPSOMMING

Inleiding: Psigososiale stres het sterk skakels met talle chroniese siektes wat verband hou met die gedisreguleerde aktivering van die fisiologiese stresstelsel. Dit verhoog die las van sterftes aangesien daar 'n sterk verband tussen chroniese psigososiale stres en nie-oordraagbare siektes is. Daar is dus 'n sterk motivering vir die identifisering van nuwe, sirkulerende biomerkers om stresverwante chroniese siektes vroeër op te spoor. Alhoewel proteïen-post-translasionele modifikasies soos glikosilasie en fosforilering as herkende merkers van patofisiologie kan dien, bemoeilik hul relatief lae hoeveelheid ekstraksie en identifikasie vanuit monsters met 'n hoë dinamiese omvang. Die hoofdoel van hierdie studie was dus om twee unieke verrykingsmetodes vir sirkulatoriese glikoproteïen- en fosfoproteïenontginning daar te stel, wat dan in 'n prekliniese model van chroniese psigososiale stres toegepas sou word.

Metodes: Fosfoproteïenverryking is uitgevoer met behulp van gefunksioneerde magnetiese partikels, terwyl glikoproteïenverryking plaasgevind het met behulp van lektiengebode magnetiese partikels. Albei hierdie metodes is getoets met behulp van 'n bekende gesuiwerde gefosforileerde en glikosileerde proteïen en in vergelyking met onder-na-bo proteomiese-metodologie met behulp van rotserum. Laasgenoemde is verkry uit 'n rotmodel van chroniese stres wat goed gevestig is in ons laboratorium (n = 16 kontroles teenoor n = 16 gestresde rotte). Dit is lukraak gekies vir proteomiese-analise om die doeltreffendheid van herwinning in verrykte teenoor onverrykte monsters te bepaal. Fraksies is ontleed deur natriumdodesielsulfaat poliakrylamiedgelelektroforese (SDS-PAGE) en proteïene gevisualiseer met behulp van Coomassie en spesifieke fluoresserende kleuring. Hier is die relevante Pro-Q-kleurstowwe gebruik vir die identifisering van onderskeidelik glikosilasie en fosforilering. Die koppeling van sulke verrykingsmetodes aan vloeistofchromatografie (VC) - tandemmassaspektrometrie (MS/MS) is moontlik gemaak deur gebruik te maak van verskillende voorbereidingsstappe soos deglikosilasie en vertering. 'n Eksogene proteïen is ook ingesluit as deel van die monstervoorbereiding om kwaliteitsbeheeranalyse van die VC-MS/MS-eksperiment te verseker.

Resultate: SDS-PAGE-ontledings en kleuringsmetodes het nie-spesifieke verryking met betrekking tot ongeskonde proteïenherwinning aan die lig gebring. Daarbenewens het VC-MS/MS-data getoon dat verryking met behulp van die huidige stel affiniteitsmateriaal onvoldoende was vir glikopeptied- en fosfopeptied-herwinning in serum.

Gevolgtrekking: 'n Gebrek aan verryking dui daarop dat streng monstervoorbereiding nodig is vir biologiese materiale met 'n hoë dinamiese omvang. Dit kan ook te wyte wees aan die poreuse aard van beide materiale wat onderskeidelik vir fosfoproteïen- en

glikoproteïenverryking gebruik word. 'n Kombinasie van verrykings- en/of uitputtingsmetodes kan dus voordelig wees vir dieper ontleding van die bloedproteoom. Hierdie verrykingstegnieke en die daaropvolgende steekproefvoorbereiding vereis steeds verdere optimalisering om meer definitiewe gevolgtrekkings in die chroniese streskonteks af te lei.

CHAPTER 1 - LITERATURE REVIEW

1.1 INTRODUCTION

In 1936, a young medical student named Hans Selye wrote a letter to the editor of *Nature* where he coined “the general adaptation syndrome” (581). Many years later, this concept is known as stress and refers to an inadequate response to any demand, whether it be emotional, physical, or mental (474, 572). This response may also occur if the demand taking place is imagined, emphasizing the importance of the individual’s perception of stressors in stress processing (234, 572). Psychosocial stress in particular has recently emerged as a major risk factor for numerous non-communicable diseases (NCDs) (214, 447, 528, 608) as it becomes increasingly prevalent in contemporary society (162, 617). Moreover, the 21st century is plagued with NCDs as it attributes up to 74% of global mortalities (700). The prevalence of such complications continue to increase in sub-Saharan Africa, as low- to middle-income countries are most at risk due to various genetic, physiological and environmental factors (700). Such risk factors together with psychosocial stress increase susceptibility to cancer, neurodegenerative diseases, mental illnesses and cardio-metabolic diseases (271, 321, 473, 556, 633).

Cardiovascular diseases remain the largest contributor towards global mortality with up to ~18,6 million deaths recorded each year (548). Cardiomyopathy, diabetes mellitus, hypertension, coronary artery disease and stroke all fall under the umbrella term of “cardio-metabolic diseases” (548). South African citizens are not exempt from this as ~225 residents succumb daily to cardiovascular diseases (CVD), demonstrating the magnitude of this burden (89). The current coronavirus disease of 2019 (COVID-19) pandemic further heightens the risk of mortality, as many individuals are now experiencing extreme stress (464). This indicates the need for novel and unique methods to discover specific biomarkers of high prognostic value that link chronic stress to NCD pathogenesis. Proteins often make good disease markers as they participate in numerous interactive processes and are altered under various conditions (238). More specifically, protein post-translational modifications (PTMs) such as glycosylation and phosphorylation are highly sensitive to physiological changes (525), making such modifications excellent candidates for the discovery of novel biomarkers.

Despite such promise, PTMs are difficult to examine due to masking effects of other molecules (100). Enrichment methods therefore need to be employed to do extractions not only at the peptide, but also at the protein level (195). These methods must be specific and reproducible for coupling to high-throughput proteomic workflows (36, 377). To the best of

our knowledge, no known biomarkers which consist of phosphorylated or glycosylated proteins relating to chronic stress-induced diseases exist. This is mainly due to such proteins not yet being sufficiently examined in this context. More importantly, unique enrichment techniques must be designed for protein retrieval and hence our aim is to design novel material for serum glycoprotein retrieval. Phosphoprotein extraction will be perfected through the adaptation of a previously described method (160). The efficacy of such techniques will be further validated via sensitive and specific proteomic approaches. The following text will now discuss stress in relation to each of these aspects in greater detail, with the focus placed on method development.

1.2 THE ROLE OF STRESS

1.2.1 The burden of stress

A review of the literature demonstrates that psychosocial stress confers significant risk for many of the leading sources of morbidity and mortality (126, 395, 405, 499, 528). The recent COVID-19 pandemic has further exacerbated feelings of distress, which plays a major role in poor mental health outcomes (83, 219, 464, 708). Moreover, infected individuals appear to be at risk of poor mental health outcomes compared to controls, with increased prevalence of stress, depressive and anxiety disorders observed (14, 708). A report by Gallup (2021) stated that negative experiences continue to rise worldwide, with a record high of 40% of adults experiencing stress throughout the day (222). Countries with advanced health care services are not exempt, as almost two thirds of the American population report being under constant stress versus only 20% in 2019 (163). Furthermore, 1 in every 3 Americans report to be so stressed about the pandemic that they struggle to make even the most basic decisions (18). Psychosocial stress does not only influence mental and physical health, but also adds to the financial burden as up to \$7 billion are lost each year in the United States due to stress-related incidences (163).

During the pandemic, the stress levels of South Africans increased by 56%, as half of the population felt anxious and frustrated, while 31% suffered from depression (498). The state of mental wellbeing was not optimal before the pandemic either, as the Sunday Times published an article in 2014 entitled “South Africa’s sick state of mental health” (664). Even though the negative emotions directly related to the pandemic may have subsided, stress is still rife within the nation (117, 230). Reasons for this include increased cases of gender-based violence, corruption, unemployment, poverty, and an overall low standard of living (110, 230, 503). Hence South Africa is ranked as the second most stressed nation in the

world (118, 177). Moreover, the global burden of stress is borne unequally as younger persons seem to bear the brunt of it (19).

A meta-analysis involving the prevalence of depression and anxiety in children and adolescents revealed that 1 in 4, and 1 in 5 of the global youth population experienced clinically elevated levels of depression and anxiety, respectively (520). Likewise, younger female students from South Africa seem to display higher levels of stress compared to their older counterparts, indicative of possible gender differences in stress perception (605). The dilemma of increased stress levels amongst the youth compounds the burden of poor health and wellbeing. Findings from the INTERHEART study which consisted of 15 152 cases and 14 820 controls from 52 different countries indicated that 40% - 60% of chronic disease is attributable to psychosocial, behavioral and environmental factors (561). NCDs are the cause of up to 74% of mortality, of which most occur in low- to middle-income countries (700). These include CVD, Type 2 diabetes (T2D), neurodegenerative diseases, mental illnesses and cancer, which literature links to the stress system (270, 338, 473, 528, 608, 633). Such statistics are sobering and emphasize the importance of understanding the links between psychosocial stress and diseases onset and progression.

1.2.1.1 The direct links between stress and negative health outcomes

The association between stress and negative health outcomes in humans was demonstrated through research involving diverse people in a variety of settings (321, 528, 545, 564). Such studies range for example from young males and females to individuals over 65, while also assessing situations that involve their employment location(s) and places of residence (94, 338, 473, 545). Here, a variety of study designs were employed and hence the collective data displays certain strengths and also weaknesses (191). Table 1.1 summarizes associations between stress and lesser cardiometabolic- and mental wellbeing-related outcomes (the focus of our research group). However, the overall link between chronic stress stretches far wider than such complications, for example it includes complications such as neurodegeneration and cancer. For example, Sulkava *et al.* (2022) found a significant association between psychological distress and all-cause dementia, where such findings were not influenced by cardiovascular risk factors or reverse causation due to the prodromal phase of dementia (633). Likewise, others identified psychological distress as a risk factor for dementia-related mortality when pooling 10 large community-based cohort studies (555). This association remained after adjustment for multiple variables such as age and sex. Moreover, others demonstrated that self-reported stress levels

predicted a 2-fold increase in breast cancer incidence versus their female counterparts who reported no significant degree of stress (270).

Table 1.1. A summary of studies where the direct links between stress and negative health outcomes were demonstrated. CVD, cardiovascular disease; T2D, type 2 diabetes.

Brief description of research study	Outcomes	Reference
This study examined specific psychosocial stressors implicated in juvenile male and female youths suffering from depression	A link between more severe, prolonged and common psychosocial stressors to major depression was in found in young people compared to typically developing controls (10-18 years old)	(499)
The incidence of atrial fibrillation in relation to psychosocial stress in the form of long working hours was evaluated in both men and women	Both males and females with longer working hours displayed an increased risk for atrial fibrillation compared with those normal working hours	(338)
By utilizing data from the INTERSTROKE study the risk of acute stroke was evaluated in relation to psychosocial stress	Increased stress at home and recent stressful life events were positively correlated with risk of stroke Psychosocial stress was also found to be a common risk factor for acute stroke	(528)
The impact of psychosocial work traits on severe depressive incidence symptoms among men and women was evaluated	Job insecurity was found to be a predictor of increased depressive symptoms for men, while women with low influence and support were at greater risk for severe depressive symptoms	(552)
25, 000 participants from the INTERHEART study were analyzed in relation to lifestyle factors and acute myocardial infarction	There was a statistically significant increased risk for acute myocardial infarction with work stress Permanent stress increased the risk of an acute myocardial infarction by 2-fold	(545)
The state of psychosocial stress was examined in women who suffered from coronary heart disease	Marital stress was associated with a 2.9-fold increased risk of recurrent coronary events	(483)
Individual data from 13 European cohort studies was extracted to examine the association between job strain (as a risk factor) and T2D	Job strain was associated with an increased risk for diabetes mellitus, independent of other lifestyle factors	(473)
The assessment of mental stress-induced myocardial ischemia or conventional stress ischemia with recurrent adverse cardiovascular events in patients with coronary heart disease was evaluated	Patients with mental-stress-induced ischemia displayed an increased risk for adverse events such as cardiovascular death or non-fatal myocardial infarction	(673)
The investigation of associations between earlier cancer caregiving exposure and the development of physical impairments was done over a period of 6 years	The caregivers that were highly stressed were more likely to develop adverse long-term health effects such as arthritis and CVD	(332)
The association of stress in the form of job strain was investigated in relation to atrial fibrillation in a Swedish cohort	Almost 50% higher risk of atrial fibrillation was found for those experiencing job strain (after adjusting for confounders) versus matched controls	(209)
843 college students were surveyed to assess the relationship between academic stress and mental wellbeing	A significant correlation between worse academic stress and poor mental health was discovered	(51)

Six areas which can be considered as stressful (love life, family, friends, finances, work/school relationships and health issues of loved ones) were evaluated in relation to mental disorders (major depressive disorder, bipolar disorder, generalized anxiety disorder, panic disorder, alcohol use disorder, drug use disorder)	A significant dose-response association was found between the degree of stress (for each area) and the odds of one of the six mental disorders Increased stress enhanced the chances of onset and progression of such mental disorders	(321)
The relationship between obesity and psychosocial stressors (including psychological outcomes such as depression and anxiety) was evaluated	Psychosocial stress was significantly and positively related to overweight and obese classes 1-3 over life-course, without relation to anxiety and depression and while controlling for confounding variables	(186)
Heart rate variability (as an indicator of early onset prehypertension and other cardiovascular diseases) was assessed in medical students (both sexes)	Females exhibited lower heart rate variability and higher levels of stress, with increased stress intensity associated with decreased cardiovascular health in terms of heart rate variability, blood pressure and rate pressure product	(516)
The incidence of CVD was assessed in 55-year-old Estonian men and women as the country underwent major socio-economic changes	Decreased quality of life was found among those with hypertension, exhibiting links with depression and negative stressful life experiences	(563)
The effects of psychosocial risk factors and CVD/mortality were investigated in several high-, middle-, and low-income countries	Increased psychosocial stress showed a significant relationship with mortality and CVD	(564)
The relationship between job insecurity and CVD was evaluated and compared versus securely employed individuals	Job insecurity was associated with excess risk of new onset coronary heart disease - post-adjustment for physiological and cardiovascular risk factors	(197)
The relationship between financial stress and the risk of coronary heart disease was evaluated using data from the Jackson Heart Study	Moderate to high stress was associated with higher chances of incident coronary heart disease but was also linked to traditional risk factors such as depression, smoking and diabetes mellitus	(447)
Data from the INTERHEART case control study was evaluated to assess the relationship between physical activity, anger, or emotional upset in relation to acute myocardial infarction	Emotional upsets strongly increased the risk of acute myocardial infarction	(608)

1.2.2 The caveats of stress research

Although the table summarized studies linking psychosocial stress to adverse human health outcomes (cardiometabolic and mental wellbeing focused), it remains challenging to derive a framework that standardizes the mechanisms involved and also the outcomes of those exposed to psychosocial stress. This may be due to the multi-dimensional nature of the stress response and the multiple steps/factors involved, that can all influence the translation of especially preclinical stress research (259, 481). For example, such factors include the chronicity level of the stressor(s), an individual's interpretation of whether a situation is stressful or not, an individual's genetic predisposition, and the environmental setting regarding the standard of living (26, 135, 145, 410).

Individual variability may be one of the most striking factors which confound the outcome of stress research. For example, individuals may possess distinct coping strategies in response to stress exposures and this may elicit different (patho)physiologic outcomes, both within a cohort and also when doing comparisons between different studies (212). The magnitude of the stressor may also vary with its degree of perceived uncontrollability/unpredictability, as individuals may exhibit variability in behavioral and physiological responses (51, 182). The unique genetic predisposition of individuals may also influence the development of mental disorders related to stress (607). Moreover, personality traits (shaped by internal and/or external environments) may render some individuals more susceptible to stress. This is demonstrated in a meta-analysis that found that agreeableness, openness and conscientiousness were negatively related to stress (410). These traits also affect one another, for example an important characteristic such as resilience may be affected by the degree of neuroticism (427). In support, some found that increased resilience was associated with reduced stress and enhanced well-being (328).

Ethnicity and socio-demographic factors may also influence outcomes (366, 430). For example, some researchers found that South African women rape survivors who resided in KwaZulu-Natal were more likely to develop depressive symptoms versus others living in different provinces (430). Furthermore, the recent COVID-19 pandemic differently affected marginalized communities compared to others (366) and may be due to those with access to social support experiencing less adverse effects compared to those without (618). Although the pandemic's importance is noteworthy, it may not be uniformly representative of the usual stressors experienced on a daily basis. This could add further confounding variables and emphasizes the heterogeneity of stressor(s) (21, 497). Some data collection

occurs in the form of surveys (552, 562) which can also add variability as personal, social and cultural factors often determine the expression of emotions and symptoms (290, 558). Another important caveat of stress research includes the population under study. Although global studies such as the INTERHEART and INTERSTROKE were successfully completed (528, 545), it is still difficult to engage with vulnerable communities and therefore they are understudied in terms of stress-related susceptibility and complications (327, 466, 587).

Sex differences is another major factor that further pose challenges for stress-related research and there are clear differences in their response to stress (271, 408). Although preclinical research studies are now slowly incorporating females into their cohorts, conflicting results may be generated compared to the human context (271). For example, although rodent studies found that females exhibited less anxious and depressive symptoms in comparison to males (289, 343), human females exhibited the opposite pattern (63, 155). Furthermore, various pre-clinical models of stress exist and each offer their unique advantages and disadvantages (224). *In vitro* models of stress is not really appropriate to employ in this research field as such experimental models lack insight into the complex stress-related organ-level responses found in intact organisms (54, 229).

Lastly, a general overlap exists between fields of study regarding stress as a construct. For example, psychologists may focus more on the emotional aspects while the medical scientists may place a greater emphasis on (patho)physiological outcomes (191). Some researchers also assume that stress as a concept is too broad and hence use unvalidated measures to study its effects (135). Together this reveals a general lack of uniformity in stress research and emphasizes the fact that a common conceptual model to examine psychosocial stress and its effects on health does not currently exist.

1.2.3 The physiological stress response

Although stress presents a significant threat to homeostasis, the body is fine-tuned to overcome and adapt to such challenges (358, 405, 659). It can be subdivided into either acute or chronic stress. Acute stress refers to the adaptive physiological mechanisms overcoming the stressor, whereas adaptive mechanisms fail during prolonged periods of stress leading to a more chronic condition (433, 572). The brain is at the center of this process and initiates a cascade of events to combat the threatening stimulus (405, 411, 572). This creates an integrated systemic response that involves numerous organ systems to re-establish homeostasis (234, 576).

1.2.3.1 The integrated stress response

The general and non-specific initiation of the stress axis takes place to counteract any perceived change in an organism's environment which may threaten homeostasis (474, 576, 667). This response ultimately converges upon the hypothalamus-pituitary-adrenal (HPA) and sympathetic-adreno-medullary (SAM) axes, the latter immediately involved while the former produces a longer lasting response. The physiological reaction produced may be subject to inter-individual variability, leading to a subject-specific experience of stress (182, 212, 544).

When a stressful situation is encountered, the information is perceived by the auditory and ocular systems that send a signal to the limbic regions of the brain (265). These regions include the amygdala, prefrontal cortex and hippocampus which process the situation and in turn activate neurons in the paraventricular nucleus of the hypothalamus (265, 591, 667). These neurons aid in the secretion of corticotropin-releasing hormone and arginine vasopressin which synergistically act upon the adeno-hypophysis of the anterior pituitary to release adrenocorticotrophic hormone (ACTH) (101, 248). Corticotropin-releasing hormone also stimulates the locus coeruleus to secrete norepinephrine at sympathetic nerve endings (115). The central activation of the sympathetic nervous system further translates to the release of epinephrine from chromaffin cells within the adrenal medulla. These catecholamines rapidly escalate the capacity of the sympathetic division's influence over the body with increased metabolic rate, oxygen consumption, blood pressure and blood flow to important organs (115, 405). The SAM axis acts synergistically with the HPA axis to generate longer lasting effects through the release of glucocorticoids (GCs) (468).

Circulating ACTH acts upon the adrenocortical zona fasciculata to release GC hormones that are synthesized from cholesterol (152, 439). The large majority of released GCs are inactive and bound to the glycoprotein corticosteroid-binding globulin (CBG) and albumin, while the remaining ~5% are able to undergo catalysis into its active form (659). This form is known as cortisol (corticosterone in rodents) and exerts the main effects of the HPA axis (411, 439). Cortisol can bind to a mineralocorticoid receptor and a glucocorticoid receptor (GR) (152, 213). The latter mediates its signaling and is present ubiquitously (681). Experiments with rats show that under stressful conditions the GR becomes saturated with cortisol and forms homodimers before translocating to the nucleus (101, 132, 621). Here, it performs its genomic effects by interacting with glucocorticoid responsive elements on deoxyribonucleic acid (DNA) to transactivate or transrepress specific genes (337, 667). Non-

genomic effects of GCs are much faster and include the modulation of the mitogen-activated protein kinase (MAPK) pathway, direct interaction with mitochondria, and interaction with membrane-bound GR and its isoforms (168, 449, 659). Glucocorticoids can also elicit a negative feedback response by inhibiting the activity of paraventricular neurons/corticotropin-releasing hormone neuronal pathways, as well as afferent pathways involving ACTH release (33, 233). The main role of the genomic and non-genomic effects of the HPA axis include modulation of metabolism and immune function, with catecholamines also playing a part (468, 667).

1.2.3.1(a) The metabolic effects of stress

Glucocorticoids act as potent modulators of metabolism and immune function while repressing less essential outcomes such as growth and reproduction (101, 526). The metabolic effects of GCs and catecholamines include tissue-specific mechanisms to eventually result in increased glycemia (468). The main reason is to increase substrate availability for improved neurological, skeletal and cardiovascular activity during periods of stress (468). The liver is heavily involved in this process, as upregulation of glycogenolysis and gluconeogenesis coincides with decreased glycogenesis to increase circulating glucose availability (159, 353, 675). This is achieved through the upregulation of enzymes involved in glucose metabolism such as phosphoenolpyruvate carboxylase and glucose-6-phosphatase (468, 683). Other tissue-specific mechanisms include decreased glucose oxidation and glycogen storage along with increased proteolysis in skeletal muscle, subsequently providing amino acids as precursors for gluconeogenesis (353, 621). Similarly, white adipose tissue glucose oxidation decreases with a parallel increase in lipolysis to ensure glycerol availability for metabolism (353, 621). The pancreas is an important mediator of metabolism and hence a role player in metabolic diseases, for e.g. during periods of psychological stress, cortisol inhibits β -cell insulin secretions with a concomitant rise in glucagon secretion (via α -cells) (353). This may result in temporary insulin resistance, which together with an uncontrolled increase in metabolism and substrate breakdown can potentiate dysregulation and disease progression (101, 357, 620, 683).

1.2.3.1(b) The anti-inflammatory effects of cortisol

The potent anti-inflammatory effects of GCs is the basis for its usage as a therapeutic intervention (538). Although cortisol does this through the GR's interaction with glucocorticoid responsive elements, its interaction with specific components in signaling pathways and membranes can also modulate inflammation (43, 88, 136, 475). Evidence for

the anti-inflammatory effects of the GR demonstrates the (genomic) relationship between stress and the immune system, with transrepression of genes such as nuclear factor kappa B (NFκB) and activator protein 1 (AP-1) (136).

Both NFκB and AP-1 are crucial for the induction of inflammation through their genomic effects. This ultimately leads to the secretion of pro-inflammatory cytokines such as tumor necrosis factor alpha (TNFα), interleukin-1β, IL-6 and interferon-gamma (150). Moreover, direct interaction between GCs, the GR, and the subunits of NFκB and AP-1 can inhibit an inflammatory response. For example, upregulation of the cytoplasmic inhibitor nuclear factor of kappa light polypeptide gene enhancer in B-cells inhibitor, alpha (IκBα), increases the retention time of NFκB in the cell cytoplasm (149, 469). In addition, the manipulation of PTMs such as phosphorylation, ubiquitination and acetylation attenuates the immune response during stressful conditions (150, 538), for e.g. by inhibiting MAPK signaling pathways (66, 88).

Overall, GCs repress the formation of pro-inflammatory cytokines while simultaneously increasing the expression of anti-inflammatory cytokines (136, 149, 475, 616). It is important to note that pro-inflammatory cytokines can stimulate the HPA axis and downregulate inflammation (599). Despite these immune changes, acute stress is known to cause a transient increase in inflammation mainly through the inflammasome, with sterile inflammation a consequence thereof (203, 295). Chronic stress may upregulate inflammation by downregulating GRs, which in turn can increase oxidative stress (125, 439, 599). Together, oxidative stress and inflammation are major role players in physiological dysregulation, highlighting that excessive psychosocial stress has the potential to increase the risk for diseases onset and progression (223, 395).

1.2.4 Chronic stress pathology

The cumulative science linking stress to adverse health outcomes is robust and implicates chronic stress as a major role player (474, 528, 545, 561) (refer Table 1.1). Excessive HPA axis activity has long been associated with NCDs such as mental illnesses, CVD and autoimmune diseases (101, 114, 235, 357, 432). However, evidence also points to the role of acute stress in pathology (203, 234, 295, 416, 421). The innate immune system is profoundly involved as acute psychosocial stress is associated with memory and cognitive impairments in humans (480). Rodent studies involving aggressive social stress confirm this phenomenon, with deficits in spatial and learning memory coupled to increased interleukin-

1 β and IL-6 levels (40). Moreover, neuroinflammation is a common outcome due to an increase in pro-inflammatory cytokines and activated microglia. These are associated with the pathogenesis of stress-induced mental illnesses (41, 537). Figure 1.1 summarizes the effects of the major role players in chronic stressed-induced pathology, namely oxidative stress, and inflammation.

Chronic psychosocial stress

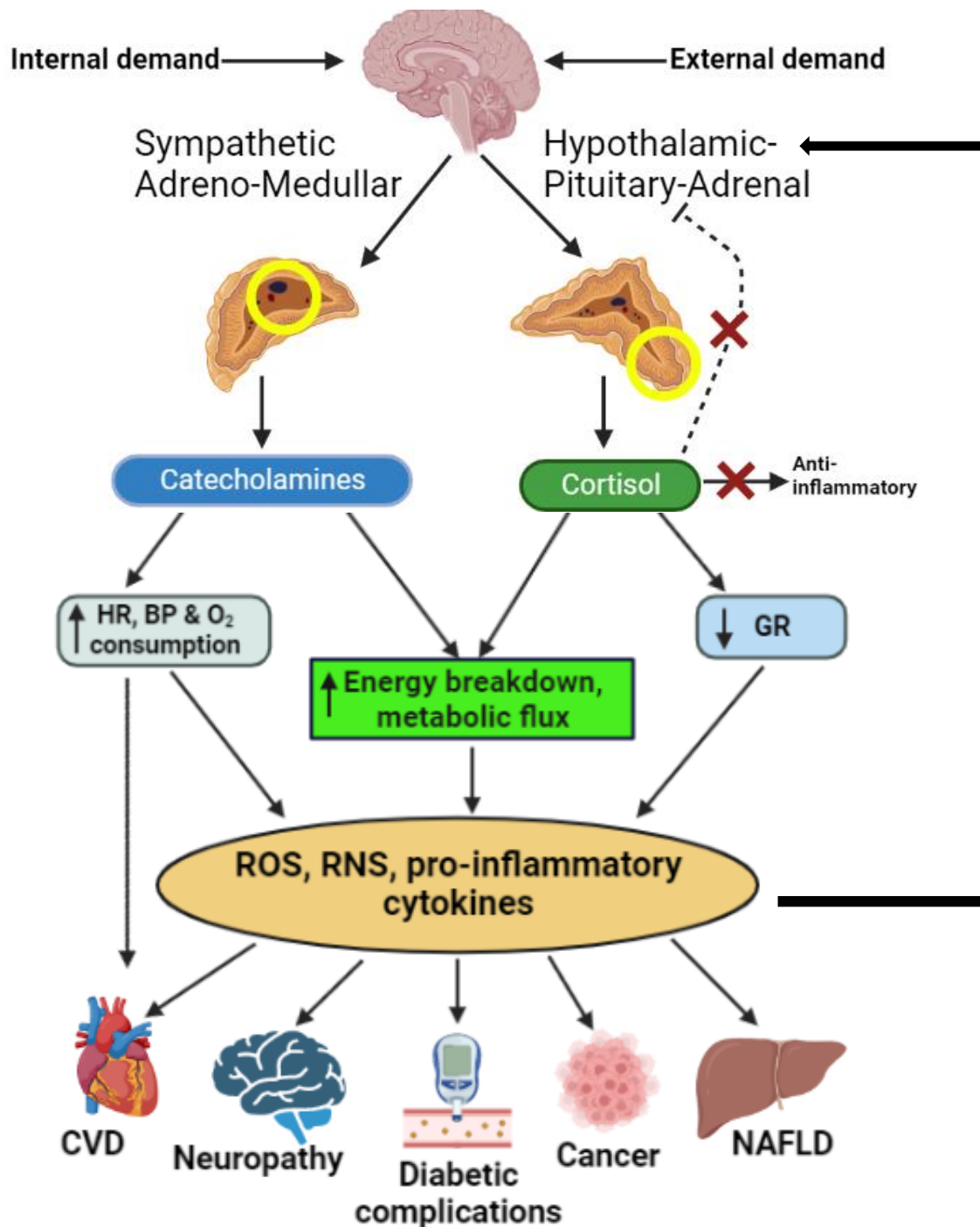


Figure 1.1. An integrative representation of the consequences of chronic psychosocial stress. HR, heart rate; BP, blood pressure; O₂, oxygen; GR, glucocorticoid receptor; ROS, reactive oxygen species; RNS, reactive nitrogen species; CVD, cardiovascular disease; NAFLD, non-alcoholic fatty liver disease. The yellow circles highlight specific regions of the adrenal glands, whereas the red 'X' illustrates an inhibitory effect. Image created using Biorender.com.

1.2.4.1 Chronic stress-induced oxidative stress

Literature confirms that oxidative stress is a central component of pathology associated with prolonged stress (35, 146, 572). Oxidative stress refers to the disequilibrium in cellular redox balance due to an excess of pro-oxidants such as reactive oxygen species (ROS) and reactive nitrogen species (RNS), and/or a decrease in antioxidant capacity (425, 508, 522). Major endogenous sources of prooxidants include the mitochondrial electron transport chain and nitric oxide synthases (199). Alternative sources include phagocytic cells such as macrophages and microglia (508, 601). Such reactive species are normal byproducts of metabolism and play a crucial role in usual intracellular signaling, proliferation and programmed cell death (568, 601). However, its dysregulation and links to various pathologies are well documented (34, 35, 422, 572).

1.2.4.1(a) The mitochondria and oxidative stress

The enhancement of mitochondrial respiratory activity is the main contributor to increased oxidative stress due to excessive cortisol secretion (620). This organelle is involved in a complex stress signaling network where it aims to re-establish homeostasis by adjusting its bioenergetic, thermogenic and oxidative properties (420). Upregulated glucose metabolism is a significant contributor to increased mitochondrial metabolism for e.g. oxidative phosphorylation, fatty acid β -oxidation, the tricarboxylic acid cycle, and the urea cycle (25, 420, 675). Moreover, an abrupt increase in rodent corticosterone facilitates its binding to the GR and complexing with anti-apoptotic factors. This later translocates to the mitochondrial membrane and ultimately enhances mitochondrial oxidation and ROS production (168, 169, 620).

Excess ROS levels can damage mitochondria and overwhelm antioxidant defense systems (420). In support, male Swiss Albino rats undergoing chronic restraint stress and corticosterone administration for 21 days displayed an overall decrease in antioxidant capacity (725). Apoptosis was also significantly increased due to damaged mitochondria (161, 476). Of note, they found decreased hippocampal GR expression, which was linked to oxidative stress and indicative of a dysregulated HPA axis (566). A vicious cycle can be established as increased ROS can attenuate negative feedback mechanisms of the stress response (33). This may result in HPA axis hyperactivity and a further increase in reactive species production. Such species can react with one another, such as in the case of superoxide and nitric oxide (560). These interactions exacerbate oxidative stress through the production of RNS (199). This increases inflammation by converging upon the I κ B

complex to facilitate its phosphorylation and ultimately blunting its inhibition of NF κ B (420). The resultant NF κ B localization within mitochondria negatively impacts on its optimal functioning (120). Conversely, an important positive modulator of mitochondrial function is peroxisome proliferator-activated receptor-gamma coactivator 1 α (PGC-1 α) which is also influenced by chronic stress exposure (420, 444).

PGC-1 α regulates mitochondrial biogenesis and oxidative phosphorylation and responds to stressful stimuli (389). These include catecholamines, cytokines and nitric oxide that stimulate pathways involved in protein phosphorylation which can activate PGC-1 α (79, 420, 702). Despite its indispensable role, prolonged psychological stress can negate its positive effects through increased mitochondrial ROS generation. This translates to decreased adenosine triphosphate levels, followed by mitochondrial DNA damage, cytochrome c release and apoptosis (99, 161). Furthermore, higher activity may also lead to intracellular signaling pathways becoming maladaptive, for e.g. adult mice displayed cardiomyopathy due to increased PGC-1 α activity (557). Diabetic animal hearts also exhibited increased mitochondrial biogenesis that is linked to excessive PGC-1 α activity (175). Evidence suggests that diabetic outcomes such as insulin resistance are mediated by phosphorylation of the insulin receptor substrates (672). Thus another potential link exists between chronic stress and diseases such as T2D and CVD (357, 510, 636). Of note, oxidative stress and inflammation share a bidirectional relationship (223), with a direct link involving the GR also connecting chronic stress and inflammation (395).

1.2.4.2 Chronic stress and inflammation

Inflammation is a natural protective mechanism and plays a crucial role in the immune response (613). However, when chronically upregulated under conditions of extensive psychosocial stress it may elicit adverse biological effects and pathophysiologic complications (544). These include NCDs such as CVD, T2D, neurodegenerative disease and cancer (12, 223, 396, 582, 710). Reviews of literature indicate the (preclinical and clinical) effects of psychologically traumatic stress in upregulating a neural and systemic inflammatory response through increased transcription of NF κ B and pro-inflammatory cytokines such as TNF α (9, 77). The relationship between chronic stress and inflammation is not yet fully understood, but oxidative stress and the GR are likely to be implicated in this process.

Glucocorticoid receptor downregulation is a significant link between chronic stress and abnormal inflammation (125, 599). Although GCs are well-known for their anti-inflammatory effects, their atypical upregulation can augment the immune response (centrally and peripherally) (90, 616). Constant HPA axis activity coupled with diminished GR expression induces a state of so-called “GC resistance” (125). This can attenuate the anti-inflammatory functions (genomic and non-genomic) of GCs that results in chronic low-grade inflammation (125). Thus a lack of inflammatory control exacerbates the occurrence of pro-inflammatory markers and increases the risk of pathogenic outcomes (124, 599). Here, stressor type and duration should also be considered as numerous stressors (specifically restraint stress) significantly elevate GC levels, for example in male mice (76). Furthermore, others found that acute GC administration elicited an increased pro-inflammatory response prior to *ex vivo* lipopolysaccharide exposure in rats, implicating microglia in specific neural regions (208). The heightened expression of microglia are also involved in upregulating inflammation within the limbic regions of the brain, as well as aggravating oxidative stress (53, 573, 585, 615, 620).

There is a robust relationship between oxidative stress and inflammation and *vice versa* (284, 317). For example, upregulated ROS/RNS secretion can activate pro-inflammatory transcription factors such as AP-1 and NF κ B (384, 613). Moreover, signaling cascades that involve increased kinase activation and decreased phosphatase activity can enhance the expression of pro-inflammatory cytokines (206). The PTMs involving kinases can alter the functionality of a variety proteins, resulting in increased inflammation and hence strengthens the importance of aberrant protein PTM in disease progression (657). This forms a vicious cycle by recruiting lymphocytes that secrete ROS and enhance DNA damage, cell death and tissue injury (62). DNA breaks can also cause transcription of pro-oncogenes which increases cancer risk (111, 613).

The plethora of literature regarding the relationship between chronic stress, oxidative stress and inflammation (234, 591, 613) provides a reasonable explanation for the pathological outcomes observed in these conditions. The above-mentioned physiological changes also affect proteins (47, 158), and more specifically PTMs that are highly dynamic and responsive to environmental changes (525).

1.3 POST-TRANSLATIONAL MODIFICATIONS OF PROTEINS

The cellular machinery of an organism is not static and is constantly changing due to external or internal stimuli (579) and means that proteins undergo numerous PTMs to be able to respond to such challenges (579, 686). External stimuli can for e.g. present as psychosocial stress, while examples of internal stimuli include DNA damage and changes in nutrient flux (579). Although PTMs provide a unique and versatile mechanism to counteract threatening stimuli, its dysregulation can lead to diseases onset/progression (525). To put things into perspective, the human genome consists of 20 000 – 25 000 protein-encoding genes while the number of proteins exceed one million (291, 303). This is partly due to the PTM of proteins where the universal protein resource database states that there are more than 400 PTMs that can interact with each other (525). Out of these, ~24 major PTMs have been identified (525). A continuous interplay exists within/between different modified proteins, with a protein able to possess numerous modified residues of the same or different types of modification on either the peptide backbone or side chains of the amino acid (121, 246). Table 1 summarizes the regularly occurring modifications noted in literature.

Table 1.2. General overview of known PTMs that are frequently mentioned in literature. NA, non-applicable; CVD, cardiovascular diseases; MetS, metabolic syndrome; T2D, Type 2 diabetes mellitus; Ser, serine; Thr, threonine; Tyr, tyrosine; Asn, asparagine; Lys, lysine; Asp, aspartic acid; Glu, glutamic acid; Arg, arginine; Pro, proline; Phe, phenylalanine.

Type	Forms	Attachment site	Enzymes	Function	Discovery	Associated diseases	References
Phosphorylation	NA	Ser, Thr, Tyr	Protein kinases & phosphatases	Cell signaling, growth, apoptosis	1906: discovery of phosphate in vitellin	Cancer, Alzheimer's disease, CVD	(184, 471, 525, 577, 643, 665, 670)
Glycosylation	O-linked	Asn	Glycosyltransferases & glycosidases	Molecular trafficking, signal transduction, cell adhesion & interaction	1961: detection of <i>N</i> -linked on ovalbumin	Congenital disorders, CVD, cancer, T2D	(49, 242, 320, 365, 698)
	<i>N</i> -linked	Ser & Thr					
Acetylation	N α , N ϵ & O-acyl	Lys, alanine, Arg, Asp, cysteine, glycine, glutamine, methionine, Pro, valine, Thr, Ser	Lysine acetyl transferase, histone acetyltransferase, histone deacetyltransferase	Protein interaction, chromatin stability, cellular metabolism	1964: experiments in isolated calf thymus nuclei	Cancer, CVD, neurological disorders, aging	(17, 112, 347, 525, 693)
Ubiquitylation	Mono- or polyubiquitylation	All 20 amino acids, but usually Lys residues	E1 – Activating E2 – Conjugating E3 – Ligating & deubiquitinases	Degradation of proteins via UPP, immune signaling	1975: polypeptide involved in immune cell differentiation	MetS, T2D, inflammatory disorders	(205, 236, 320, 438, 511, 521, 525, 684)
SUMOylation	NA	E amino group of Lys residues	Multi-enzymatic use, E1, E2 & E3	Transcription control, signal transduction, chromatin organization	1996: experiments involving Ran GTP-ase activating protein	Cancer, Alzheimer's disease, CVD, Diabetes Mellitus	(56, 167, 185, 204, 350)
Methylation	NA	Mainly Lys & Arg, but also alanine, Asn, cysteine, glycine, glutamine, histidine, Pro, phenylalanine	Methyltransferases	Histone modification	1939: experiments involving protein metabolism	Cancer, mental retardation	(108, 320, 524, 525, 539, 634, 705)
Lipidation	N-myristoylation	N-terminal of Glycine	N-myristoyl transferase	Targets proteins to organelles and membranes, increases hydrophobicity, signal transduction	1951 (myristoylation), 1978 (prenylation) & 1982 (palmitoylation)	Neurological disorders & cancer	(11, 72, 81, 534, 656, 695, 722)
	S-palmitoylation	Lys, cysteine, Thr, Ser, glycine	Palmitoyltransferases				
	S-prenylation	Cysteine	Farnesyltransferase & geranyl transferases				

The PTM of proteins refers to the covalent attachment of simple or complex chemical groups that can alter their structure and function (246). Such unique functional changes can lead to enhanced enzymatic activity and assembly, alterations in protein lifespan, receptor activation, and increased inter-protein interactions and localization (156, 170, 559). These changes can occur in organelles such as the endoplasmic reticulum (ER), Golgi apparatus, cytoplasm and nucleus, and also extracellularly through sugar-carrying units (73, 574). Since proteins are “chief actors” in living cells and required for overall cellular stability, minute PTM defects are a major cause for disease onset/progression (525) and can therefore be exploited as putative markers for disease (320).

PTMs can also be reversible (covalently modified) or irreversible (proteolytically modified), with side chains that undergo modification (73, 686, 690). Ten residues (aspartic acid [Asp], glutamic acid [Glu], serine [Ser], threonine [Thr], tyrosine [Tyr], histidine, lysine [Lys], cysteine, methionine, arginine [Arg]) possess a nitrogen, oxygen or sulfuric atom(s) that can function as nucleophiles in modification reactions (340). Asparagine (Asn) and glutamine react via their side chain amide groups where the nitrogen atom of the carboxamide group acts as a weak nucleophile (451, 686). Three major PTMs comprise more than 90% of all modifications, i.e. phosphorylation, ubiquitination and acetylation (330). However, glycosylation, lipidation, acetylation and SUMOylation are reported to be most involved in terms of disease onset/progression (525). Each amino acid can also undergo at least three different modifications (525).

It is important to note that the modulation of protein function has become a major center of attention in recent years (156, 170, 281, 559). These are often viewed in isolation and not well-related to one another as their separation and analysis from complex mixtures/samples with high dynamic range can be an arduous task (246). For this purpose, proteomic analyses involving LC-MS have developed well over the years to identify and critically investigate the manifestation of PTMs. This is often in relation to disease pathogenesis and the establishment of novel therapeutic treatments (100, 113, 412, 426). Phosphorylation and glycosylation are well-investigated and play crucial roles in terms of the disease burden and could hence serve as potential biomarkers (102, 574). Moreover, disease associations are likely to occur when these two PTM types are co-involved in central functions (170). Bearing this in mind, the rest of this review will focus on phosphorylation and glycosylation in the context of chronic diseases linked to stress. Although mechanisms linking chronic stress to PTM changes are not entirely clear, the current evidence links

adverse psychosocial events and its negative downstream effects to changes in enzyme activity involved in protein phosphorylation and glycosylation (442, 443).

1.3.1 Protein phosphorylation

The phosphorylation of proteins was first discovered in 1906 by Levene *et al.* (1906), with enzymatic phosphorylation of proteins described many years later (86). Protein phosphorylation is the most widespread and well-studied PTM and can be reversibly attached to multiple amino acid residues, principally on Ser, Thr and Tyr (29). This occurs through the action of the nucleophilic hydroxyl group on the terminal phosphate group of adenosine triphosphate to form phospho-Ser, phospho-Tyr and phospho-Thr (686). Protein kinases facilitate this attachment, whereas the detachment is catalyzed by phosphatases (671). The phosphoproteome is therefore dependent on these two enzyme classes as they regulate the dynamic nature of the cell (400). Their localization is therefore important as this is indicative of phosphorylation occurring in the nucleus or cytosol (170). Diverse substrates for this modification exist and include lipids, nucleotides, carbohydrates and proteins (671). Only on unique occasions does guanosine triphosphate replace adenosine triphosphate as co-substrate in such reactions (543).

Approximately 30% of all human proteins can be phosphorylated at any given time by the activity of the indicated enzymes (400). Kinases may alter proteins in a transient manner on single or multiple amino acid residues (121). Protein kinases contain regulatory subunits which activate or inhibit their function. In most cases, basal state kinases are dephosphorylated and require phosphorylation for activation (184, 728), for e.g. MAPK and protein kinase A (PKA) are phosphorylated and phosphorylate downstream targets in a linear or amplified manner (610). The downstream effects modulate virtually all cellular and biological processes such as cell growth, apoptosis and signal transduction (232, 546). These diverse outcomes are mediated by two main downstream consequences of protein phosphorylation, i.e. (1) conformational changes and (2) recruitment of neighboring proteins whose domains bind to phosphomotifs of the modified protein (306). The latter is crucial for signal transduction as such protein-protein interactions assist in recruiting downstream targets for functional adaptations.

1.3.1.1 Pathways and proteins in stress and phosphorylation

The induction of the MAPK pathways can be attributed to the stress response (43, 66) and include three signal transduction links, namely extracellular signal regulated kinases (ERKs), c-Jun amino-terminal kinases (JNK) and p38 MAPKs (309). The propagation of phosphorylation is the principal method of target protein activation and these are complex interactions and highly integrative with one another and other signaling events (595). A high level of specificity and constancy characterizes the activation of such pathways in response to diverse signals for e.g. growth factors, cytokines, environmental stress and exogenous toxicity (309). More specifically, the ERK and p38 MAPK pathways are upregulated under conditions of environmental stress, ROS and inflammatory signals which in turn can further upregulate inflammation and oxidative stress through immune cellular proliferation and differentiation (43, 66).

The JNK pathway converges upon the transcription of AP-1 (43). This can add to the formation of vicious cycles involving inflammation and oxidative stress, culminating in diseases such as T2D and cancer (316, 494). These mechanisms are not fully understood as stress can induce decreased ERK phosphorylation as discovered in male Wistar rats undergoing chronic restraint stress (CRS) (689). Conversely, a study involving mice exposed to acute/chronic social stress showed increased ERK activation through upregulated phosphorylation in specific neural regions (131). It is noteworthy that such pathways (involving phosphorylation) can be convolutedly linked to similar signal transduction mechanisms like the phosphatidylinositol 3 kinase (PI3K) and Akt strain transforming (Akt) signaling cascade (309, 595).

The PI3K/Akt pathway also increases ROS production to thereby enhance intracellular oxidative stress (59). However, a bidirectional relationship exists between such pathway activation and ROS production, as pro-oxidants produced (through cellular events) may result in its activation. This involves the transcription of NF κ B, a prominent role player in chronic stress and pathology, which further demonstrates the potential link between adverse psychosocial events and protein phosphorylation (59). Increased research efforts revealed the phosphorylation of NF κ B subunits as a mediator of its transcription (420). Another pathway implicated in this process is the PKA phosphorylating cascade which forms part of the cyclic adenosine monophosphate response element-binding protein (CREB) family (333, 688).

CREB-family kinases and proteins are both activated by phosphorylation of proteins and are linked to diseases which involve chronic oxidative stress and inflammation (7, 688). Of note, neurodegenerative diseases are linked to the phosphorylating activity of CREB (688). Moreover, brain-derived neurotrophic factor is a crucial modulator that regulates and phosphorylates CREB (688). This neurotrophin is a regulator of neural plasticity and development and is linked to systemic metabolism (549). CREB abnormalities are further linked to patients of schizophrenia with MAPK pathways involved in this instance (688).

Psychological stress and CREB activity have been directly linked to cancer progression (550). Moreover, neurological complications are observed in the hyperphosphorylation of tau in Alzheimer's disease (268, 645). Not only is phosphorylation involved, but aberrant glycosylation also increases tauopathies associated with neurodegeneration (268). Researchers also found that male rats undergoing acute noise exposure displayed increased phospho-tau levels in brain tissues (138). This strengthens the link between psychosocial stress exposure and NCDs, while implicating protein modification in this process. Numerous animal stress models exhibit relationships between phosphorylation and microglial activation with upregulation in ROS and inflammatory cytokine activity contributing to disease onset/progression (467). However, the evidence is not fully conclusive (467). Another important protein in the control of oxidative stress is the transcription factor nuclear factor erythroid-derived 2-like 2 which governs antioxidant activity and status (391). Nuclear factor erythroid-derived 2-like 2's activity is regulated by phosphorylation and possibly glycosylation, with dysregulation in such modifications linked to CVD, neurodegenerative disease and cancer (391). The implication of oxidative stress further associates chronic stress with diseases onset/progression and with links to PTMs.

1.3.1.2 The direct involvement of phosphorylation in stress-related disease

The phosphorylation of the steroidogenic acute regulatory protein (StAR) and GR perform important roles in the physiological outputs of the stress axes (106, 621). StAR aids in steroidogenesis by controlling the rate-limiting step of shuttling cholesterol (cortisol precursor) from the outer to the inner mitochondrial membrane (419). Phosphorylation of StAR is an outcome of PKA activity which may increase its biological activity, thus increasing cortisol production (27, 621). A more important role for phosphorylation involves the GR as it is also subject to modulation by MAPK family members (221).

1.3.1.2(a) *Phosphorylation of the glucocorticoid receptor*

Phosphorylation is a vital component in the stress response through the GR, with the absence/presence of a phosphate group on a specific amino acid residue influencing downstream signaling (221). Multiple Ser and Thr residues can be altered which can each lead to changes in terms of localization, availability and transcription activity of this stress receptor (221, 329). Furthermore, certain phosphorylated amino acids and sequences associated with them are conserved between rats and humans (221). Regarding these residues, a large body of data suggests that phospho-GR is induced by ligand binding (221). Prior phospho-events may also play a role in the pattern of modification with kinases and phosphatases catalyzing changes in composition and structure (221). However, knowledge is sparse regarding the role of phosphatases in GR PTM although kinase activity is well-documented (221, 293, 311).

Differential MAPK pathways such as ERK and JNK, as well as non-MAPK-related ones such as the cyclin kinase pathways can specifically change the GR's modification (221). For example, phospho-Ser203 of the GR is correlated with inactivity by its containment in the cytosol. Conversely, human phospho-Ser211 (rat Ser232/mouse Ser220) produces increased transcriptional activity due to changes in conformation (221). Alternative outcomes of GR signaling through serine residue phosphorylation include blunted GC downstream effects and altered outcomes of the stress hormones (221, 311).

The Ser226 residue has gained major attention due to its link to diseases such as major depressive disorder where patients exhibited relatively higher levels of this site-specific modification compared to controls (311). c-Jun amino-terminal kinases -mediated modification of this residue is also associated with GR resistance and could therefore implicate other inflammatory diseases (311). This occurs through GR export from the nucleus after Ser226 phosphorylation (106). Rodents undergoing acute and chronic stress also display higher phospho-Ser226 levels (Ser246 in rodents which is analogous to Ser226 in humans) (509, 590), while rats receiving standard antidepressant treatment exhibited decreased JNK expression in hippocampal regions together with an alleviation of depressive symptoms (388). Gender differences can also play a role in altered PTM activity through disparate kinase activity (442). For example, male and female rats undergoing chronic isolation stress exhibited distinct changes in terms of Ser phosphorylation (443). A general overview of the involvement of phosphorylation in stress is depicted in Figure 1.2.

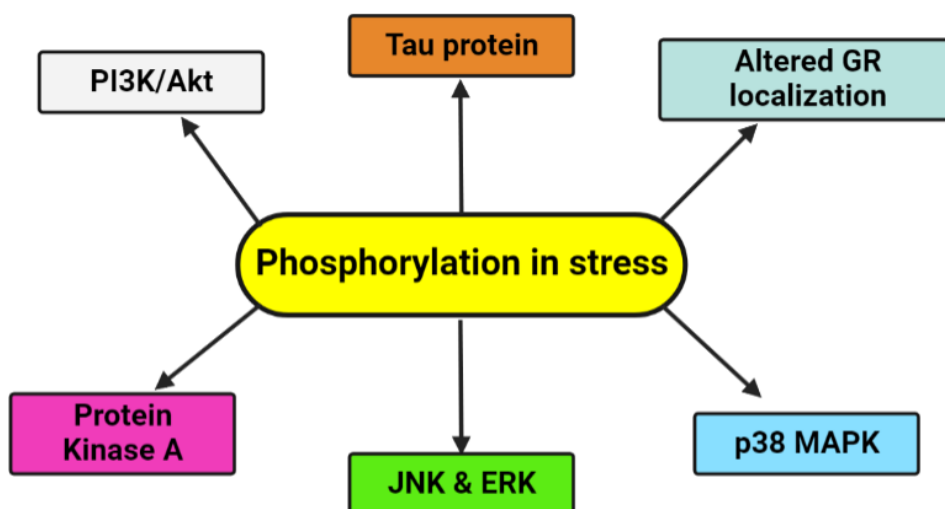


Figure 1.2. A diagrammatic summary of the pathways and proteins involved in phosphorylation and stress. PI3K, phosphatidylinositol-3-kinase; Akt, Ak strain transforming; JNK, c-Jun N-terminal kinases; ERK, extracellular signal-regulated kinase; p38 MAPK, mitogen-activated protein kinase. Image created using Biorender.com.

The modification status of the GR can clearly be linked to current therapeutic strategies for chronic stress-induced diseases and may offer utility as a diagnostic biomarker as certain amino acid residues and their diverse phosphorylation can lead to GC resistance (221) and diseases onset/progression (599). Glycosylation is another important PTM involved with GR function (384). Here, the downstream pathology of stress can be linked to aberrant glycosylation, although this relationship remains enigmatic (144). Phosphorylation is known to have direct links to the protein glycoproteome and *vice versa* as they can preclude one another's activity, or work in tandem to deliver vital functional alterations in a physiologic system (264, 504). This interaction and competition usually takes place on Ser and Thr residues (262, 263).

1.3.2 Glycosylation

Protein glycosylation refers to the covalent attachment of sugar moieties to specific residues such as Asn, Ser and Thr (262). Almost 200 glycosyltransferases catalyze the addition of sugar moieties in the multistep process of glycosylation. This process exponentially increases the diversity and complexity of the proteome, far more than any other PTM (574). In contrast, glycosidases cleave the sugar moieties from such proteins (574). This dynamic process is dependent on enzyme availability, cellular circumstances and the nature of the amino acid sequence(s) (533). The majority of nuclear and cytoplasmic proteins undergo this dynamic form of modification which many propose can rival the phosphorylation process as the most abundant PTM (261, 263). Multiple important functions of this regulation exist

and it is crucial for normal cellular function across all species (262), for e.g. intermolecular and intercellular interaction, correct protein folding, signaling, transport and delivery (679). Moreover, glycosylation affects blood type, T-cell regulation, β 1 adrenergic receptor signaling and the immune system (240, 465, 574). This can be cell/tissue specific as heterogeneity between enzyme localization and activation plays an important role in the dynamic regulation of glycosylation (574). Proteins are not restricted to one type of glycosylation as multiple sites of glycan attachment are available. This adds to the tremendous structural diversity elicited by glycosylation, with 16 distinct pathways producing *N*- and *O*-linked glycans that are the most common forms represented in humans (263, 574).

N-linked glycans refer to those which are bound to the amino group of Asn, where the anomeric carbon present in the sugar side chain forms a link with the nitrogen atom of the resident amine to result in an *N*-glycosidic bond (698). An *O*-glycosidic bond is attained when the anomeric carbon attaches to the oxygen atom within the hydroxyl group of Ser and Thr (622). A requirement of sugar attachment is often a specific consensus sequence which glycosyltransferases recognize to perform their duty (157). For *N*-linked glycans, this sequence is Asn-X-Ser/Thr, where X denotes any amino acid except proline (Pro) (403). The specific monosaccharides which are involved in this attachment includes: D-glucose, D-mannose, D-galactose, D-xylose, D-ribose, D-glucuronic acid, L-fucose, N-acetylneuraminic acid, N-acetyl-D-galactosamine, and N-acetylglucosamine which are all derived from sugar nucleotides or dolichol-linked donors (574).

Many of such attachments originate in the ER, with two initiating in the Golgi apparatus (574, 622). After it is formed, further processing occurs within the Golgi complex where different compartments are allocated for specific processing steps, often ending in the capping of the glycan with a negatively charged sialic acid (sialyltransferase action) (533). It may also occur co-translationally rather than post-translationally, with separate events such as attachment, maturation and trimming aiding in its biosynthesis (574, 679). The resulting attached glycan structures are classified as either complex oligosaccharides, high-mannose oligosaccharides or a combination (hybrid) of the two (172, 663, 679). *N*-glycosylation and a large number of its enzymes are conserved across eukaryotes (663). Although *N*-linked glycans are the most prevalent, *O*-glycosyl attachments are important in regulating cell biology and rival phosphorylation (49, 261).

The O-glycoproteome is extensive in nature and can induce complex pathways and outcomes which are yet to be fully understood. Thus far, more than 3, 000 O-glycoproteins in humans are known together with up to 15, 000 identified sites of attachment on a myriad of proteins (310). This clearly demonstrates the need for specific, reproducible and high-throughput methods to be designed for the complete detection of such PTMs (361, 721). Thus current workflows need to be considered along with the exponential increase in proteomic tools to allow for further pioneering in this rapidly growing field. However, due to the context and cellular specific nature of this PTM, continuous glycan processing occurs alongside the non-specific catalyzation of certain glycosyltransferases. This creates large volumes of heterogeneity and difficulties in terms of glycoproteome assessment (717).

Analytical challenges often present due to the low stoichiometry of glycosylated residues versus other highly abundant proteins (574). Further side chain modifications which involve acetylation, sulfation and phosphorylation play a regulatory role in glycan processing which adds to its complexity (574, 588). The latter acts as gatekeeper for the elongation and complexity of oligosaccharide moieties through the activation of synthesis of elaborate glycans (588). Moreover, glycosylation is highly sensitive to cellular and physiological changes and hence implicates it in the progression of pathologies such as congenital diseases and cancer (436, 477).

1.3.2.1 The relationship between disease and protein glycosylation

Disease progression tied to protein glycosylation is often rooted in genetic mutations which demonstrate complex mechanisms (533, 574). More than 100 disorders involving glycosylation display a genetic basis such as autosomal recessive inheritance traits (211, 298). These result in congenital glycosylation disorders which display a wide spectrum (211). Profiling of *N*-glycans of the abundant serum proteome is used to identify such genetic perturbations which often involve enzymatic malfunctions, specifically glycosyltransferase activity deficiencies (298). O-glycosyl residues can influence such congenital disorders and manifest in the form of poly-organ diseases. Single organ diseases also exist for e.g. cardiovascular, neurological, muscular, retinal and hepatic dysfunction with varying degrees of severity (297, 298). However, genetic alterations are not the sole cause of disorders linked to deviant glycosylation as Golgi fragmentation, ER stress and metabolic perturbations are processes that are all implicated (49, 496, 574).

Mental illnesses such as schizophrenia can also exhibit wide changes in the *N*-glycoproteome of patients compared to controls (624). Of note, severe acute respiratory syndrome coronavirus 2 displays specific glycans on its cell surface which is the foundation of vaccine efficacy (691). Although glycosylation is a significant contributor to diseases onset/progression, little is known regarding its role in chronic stress-related pathology. Potential links therefore need to be stringently examined to help clarify this relationship as it could potentially unlock numerous benefits for individuals suffering from such mental illnesses.

1.3.2.2 Strengthening the link between stress and glycosylation

The influence of stress on glycosylation profiles was first studied in 1989 by Tsukada and colleagues by employing rats subjected to water immersion tests (669). These data revealed that gastric mucosal cells of stressed rodents displayed up to 50% lower *N*-acetylgalactosamine levels versus matched controls. However, a paucity of information still exists that directly links deviant glycosylation events with chronic psychosocial stress. The high sensitivity of glycan attachment to physiological status offers potential to infer a unique relationship between these two concepts (477). Evidence for the role of glycosylation in the immune response and illnesses which involve chronic inflammation strengthens the possibility of stress-related glycosylation deficiencies (533). An example of this is the effect of glycosylation patterns on the function of different immunoglobulins, as well as T-cell regulation and death promotion (69, 465). Here, especially immunoglobulin G can be modulated as changes in *N*-glycan is a characteristic trait of acute and chronic inflammation (532). Evidence also suggests that glycosyltransferases are affected by psychosocial stress (364).

Enzyme activity (e.g. sialyltransferases) can be modulated under pathological conditions such as stress (144). Furthermore, post-traumatic stress disorder (PTSD) patients display increased glycome alterations that are associated with extreme traumatic experiences and aging (346). Moreover, glycoproteins are involved in a wide array of psychological disorders (e.g. Alzheimer's disease and major depressive disorder) which exhibit significant *N*-glycosylation disturbances (409, 488). In support, some found strong associations between major depressive disorder severity and aberrant *N*-glycosylation (488), while others discovered significant differences in the serum *N*-glycan profile of female major depressive disorder patients that correlated with increased IL-6 and C-reactive protein levels (74).

Although enigmatic, psychosocial stress and increased levels of circulating cytokines exhibit a correlation (658). This is important as such pro-inflammatory cytokines are involved in modulation of the HPA axis and chronic inflammation (599). Such cytokines can also induce *N*-glycan changes of endothelial cells which can contribute to inflammatory vascular disease (Figure 1.3) (97). Schizophrenic individuals also display glycan structural changes in serum and cerebrospinal fluid that are linked to chronic inflammation (624). Moreover, rats undergoing acute and chronic stress exhibited altered sialyltransferase activity in an organ-specific manner (144).

1.3.2.2(a) Endoplasmic reticulum stress

Endoplasmic reticulum stress is a major determining factor for the correct glycosylation pattern of cells (724). This could play a pivotal role in the outcomes observed with chronic stress as numerous studies show a direct correlation between stress and markers of ER damage (267, 719, 731). In support, a 21-day chronic restraint stress study using adult male rats showed increased ER stress pathway activation in the hippocampus together with cognitive impairments (731). Moreover, they found upregulated caspase cleavage that is indicative of ER stress-induced apoptosis (731). In a similar study, rats that underwent restraint stress (forced swimming) exhibited increased ER stress proteins in the hypothalamus versus controls (719). Since excessive psychological stress induces oxidative stress, this further implicates the ER and dysregulated protein synthesis and folding in this process (Figure 1.3) (267).

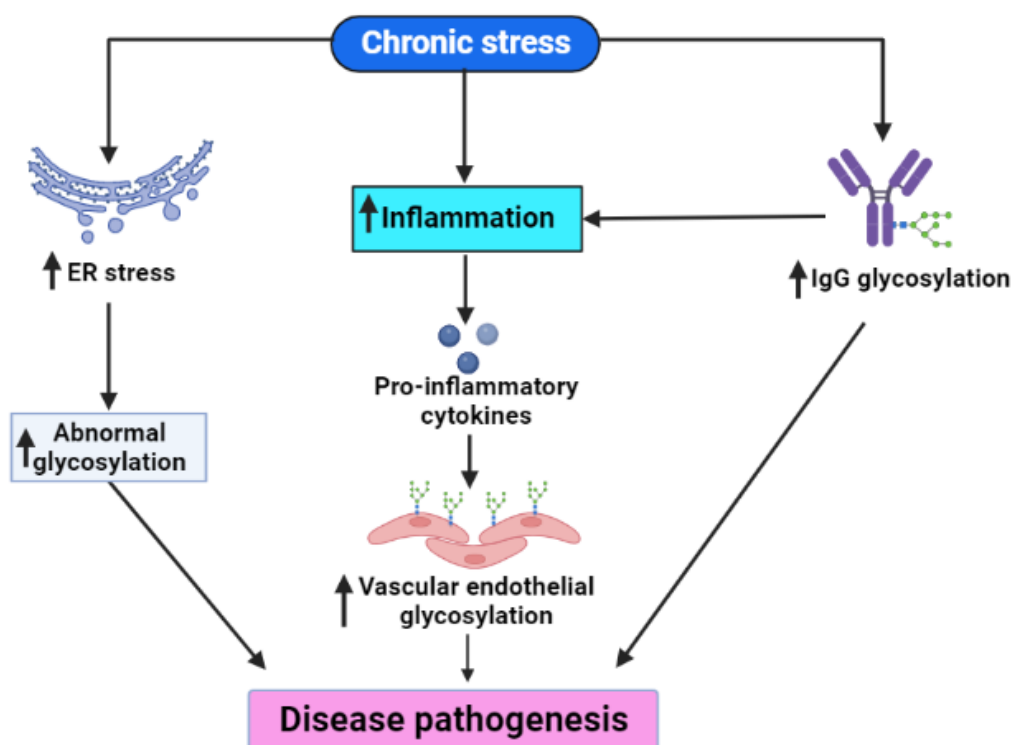


Figure 1.3. A diagram that illustrates the potential links between stress-linked glycosylation and diseases. IgG, immunoglobulin G; ER, endoplasmic reticulum. Image created using Biorender.com.

1.3.2.2(b) *The corticosteroid-binding globulin*

The plasma carrier CBG is an important regulator of the effects of the GCs as it determines the availability of steroid hormone accessible to target cells (378, 600). This hepatically produced protein exhibits six *N*-linked glycosylation sites which are conserved across humans and rats and account for ~30% of its mass (600). These sites are essential for the half-life, stability and solubility of the CBG and if lost/modified may result in disrupted steroid binding potential (42).

Corticosteroid-binding globulin glycoforms can also be altered via the stress axes as revealed by dexamethasone treatment of hepatic cells (440). Hypothalamic pituitary axis-related inflammatory effects form part of CBG functionality as the severity of chronic inflammation in female rats negatively correlated with the weight and levels of circulating CBG (275). Likewise, some indicated that CBG shuttles cortisol to inflammatory locations, with a bidirectional influence of pro-inflammatory cytokines taking place via a 50% decrease in serum CBG levels (493). This was demonstrated by exogenous IL-6 administration to patients enduring acute trauma and surgery (668). A lesser known role of glycosylation in the stress response is the modification of the corticotropin-releasing hormone receptor type 1 (37). It was found that *N*-glycosylation of the receptor subtype is needed for the proper

functioning of the hormone itself (37). However, these observations were done in an *in vitro* model and hence misses the well-known systemic effects of the stress response.

Although some glycan attachments seem inert, non-deleterious glycan events can still impart subtle advantageous characteristics (477). However, most of the literature supports the notion that aberrant PTM changes such as phosphorylation and glycosylation are linked to the development of chronic stress-induced diseases. This concept may therefore unlock utility as improved methodologies that allow for better detection of such PTMs may result in the development of novel clinical biomarkers. The use of phosphorylation and glycosylation as modes of diagnoses are not new concepts as they are frequent reporters of disease and are already used in the clinical environment for examining cancer and neurodegenerative diseases (268, 642, 645). Table 1.3 gives a brief overview of the current use of these PTMs as clinical biomarkers.

Table 1.3. A brief overview of glycosylation and phosphorylation usage in the clinical setting. CDG, Congenital Disorders of Glycosylation.

PTM	Biomarker	How it is used	Diagnosis	Reference
Glycosylation	Serum transferrin	The change in protein glycoforms is assessed by monitoring whether a loss of a specific glycan has occurred, or an alteration in glycan structure has occurred This ultimately leads to an overall molecular weight change	CDG-type 1 and 2	(207, 247, 372)
			Chronic alcohol abuse	(269, 273)
	Alpha-1 acid glycoprotein & haptoglobin	A change in the form of the <i>N</i> -glycan is related to molecular weight change	CDG-type 1 and 2	(82)
	Apolipoprotein C-3	The presence of <i>O</i> -glycan abnormalities is evaluated	N-acetyl-galactosamine-transferase 2 deficiency CDG	(718, 738)
	Anti-thrombin	Interrogation of altered glycosylation patterns, including hypoglycosylation	Thrombophilia	(153, 154, 448)
	Alpha fetoprotein	Glycoforms are used to predict the risk of developing a specific form of cancer	Hepatocellular carcinoma	(174, 567)
	Immunoglobulin G	Alteration of glycosylation patterns is associated with aging	Chronological age	(348)
	Cancer antigen 15-3	Examination of the sialylated <i>O</i> -linked glycan, including protein concentrations	Breast cancer	(173, 336)
Phosphorylation	Phospho-tau181 (Thr 181)	The examination of hyperphosphorylated protein tau in cerebrospinal fluid	Alzheimer's disease	(296, 428, 678)

Although only one phospho-biomarker has been established, treatment relating to this PTM emphasizes the importance of a continuous investigation into its effects and the machinery involved. Since abnormal phosphorylation is linked to disease progression, the function and manipulation of kinase activity have been emphasized in treatment strategies for diseases such as cancer (123, 407, 546). Numerous kinase inhibitors are therefore employed to treat this disease (547). Such a therapeutic approach is not limited to cancer as other drugs (e.g. abemaciclib and tofacitinib) have been used in conjunction with endocrine therapy for early breast cancer and rheumatoid arthritis, respectively (349, 551). Together this strengthens the importance of investigating such PTMs in the context of biomarker discovery and by extension into the realm of stress research. If successful, such experimental advances may lead to various breakthroughs in terms of diagnostic and therapeutic strategies. Figure 1.4 summarizes the potential inter-linking relationship between glycosylation, phosphorylation, and chronic psychosocial stress.

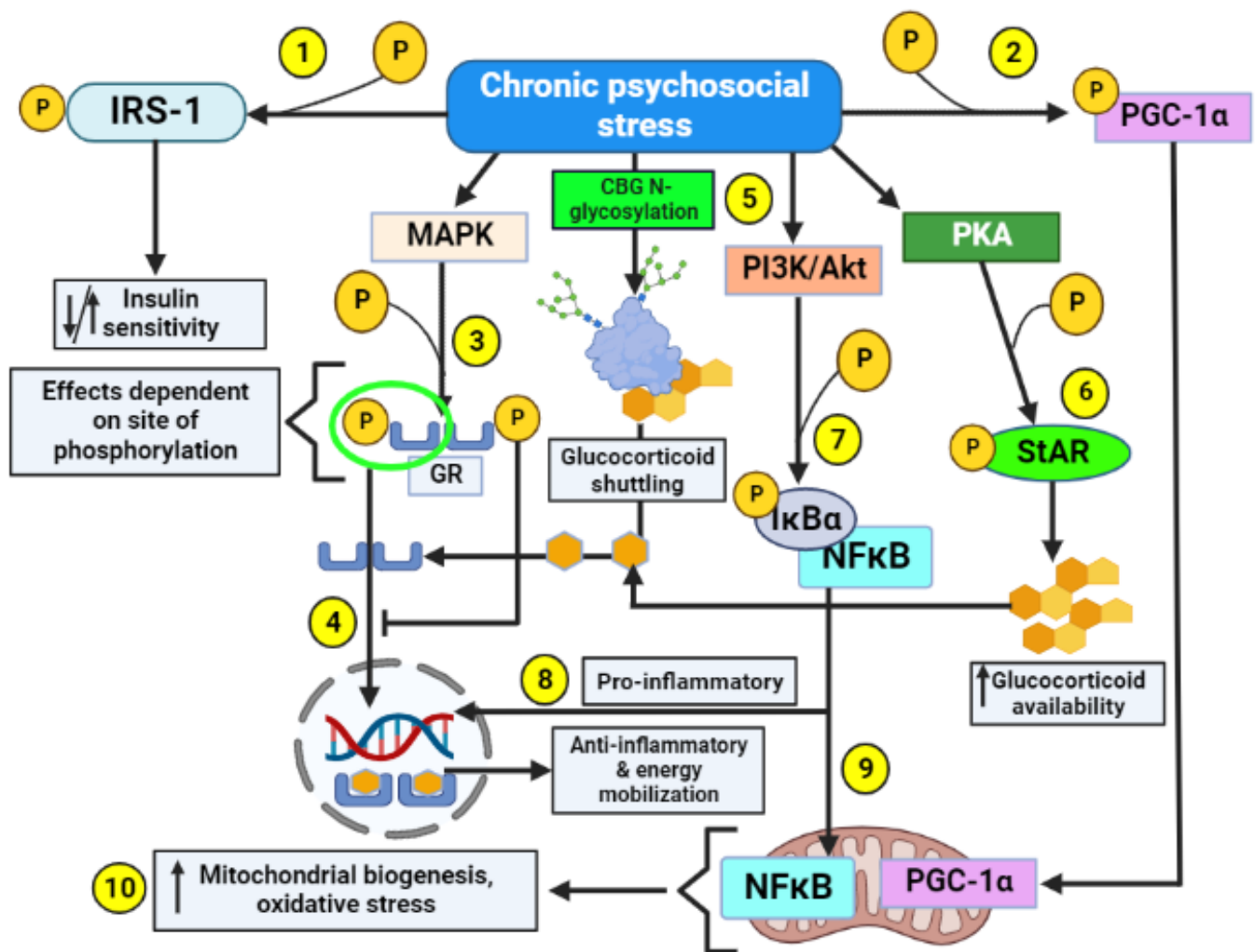


Figure 1.4. An integrative diagram representing the relationship between glycosylation, phosphorylation, and chronic psychosocial stress pathways in no particular order. Step 1: Chronic stress enables IRS-1 phosphorylation, which may either increase insulin sensitivity or insulin resistance; Step 2: Phosphorylation of PGC-1 α results in mitochondrial translocation; Step 3: Phosphorylation of specific Ser residues on the GR (indicated by green circle) can cause cytoplasmic retention or nuclear translocation; Step 4: Translocation of the GR results in cortisol's anti-inflammatory effects; Step 5: N-linked glycosylation of CBG can increase glucocorticoid shuttling, linking to; Step 6: Phosphorylation of StAR increases glucocorticoid availability which CBG can carry; Step 7: Phosphorylation of I κ B's substrates increases/decreases NF κ B translocation/retention, with translocation causing; Step 8: Pro-inflammatory cytokine gene transcription, as well as; Step 9: Increased mitochondrial ROS release and thus; Step 10: Increased oxidative stress, which can also be due to increased mitochondrial biogenesis from PGC-1 α . IRS-1, insulin receptor substrate 1, MAPK, mitogen-activated protein kinase, CBG, corticosteroid-binding globulin; GR, glucocorticoid receptor; PI3K, phosphatidylinositol 3 kinase; Akt, Ak strain transforming; PKA, protein kinase A; PGC-1 α , peroxisome proliferator-activated receptor-gamma coactivator; StAR, steroidogenic acute regulatory protein; I κ B α , inhibitor of nuclear factor kappa B; NF κ B, nuclear factor kappa B; ROS, reactive oxygen species. Image created using BioRender.com.

1.4 THE EXPLORATION OF BIOMARKERS LINKED TO CHRONIC STRESS

Biomarkers are molecules, genes or phenotypic characteristics that appear naturally during a physiological process, disease or reaction to a pharmacologic stimulation (38). They may also appear in response to environmental cues and need to be objectively measured and distinct from the direct measurement of an individual's state of emotional wellbeing and functioning (91). Numerous forms exist such as diagnostic, prognostic, pharmacodynamic, predictive and susceptibility biomarkers (91). However, a limitation exists due to the highly complex nature of biomarkers where they form part of physiologic systems that involve multi-dimensional levels of functioning. Likewise, multiple biomarkers play a role in the summative outcomes of interest and interrelationships therefore also need to be considered (48, 91).

1.4.1 Current potential biomarkers of psychosocial stress

Since cortisol has a variety of functions it is often employed as a potential serum biomarker of stress-linked mental disorders (181, 647). For example, some studies found elevated cortisol levels in a range of depressive disorders (292, 711). However, serum/plasma is not always utilized as a resource for biomarker assessment as levels can be affected by the circadian rhythm (245). Less invasive measures such as salivary and hair cortisol are therefore preferred to assess the nature and degree of stress (312, 556). It has also become difficult to assess whether cortisol measurements directly relate to acute or chronic stress, as prolonged exposure to stress can result in HPA-axis changes (181). Cortisol as a biomarker may also prove to be more elusive than informative as a dissociation between chronic stress and cortisol secretion may result due to downregulated GR expression or habituation to chronic stress and hypocortisolism (125, 411). Hypo- and hypercortisolism also relate to Cushing's syndrome and Addison's disease, respectively (245) and this further complicates cortisol's clinical utility as a biomarker. It is noteworthy that circulating cortisol levels are also influenced by individual characteristics such as weight, age, sleep cycle and other lifestyle factors (e.g. smoking) (44, 368, 655).

As a key cortisol-mediated metabolic effect include increased glycemia (114), HbA1c levels may also be associated with chronic stress (431). For example, a comparison between caregivers and controls revealed that the former displayed increased plasma glucose levels (10). However, although HbA1c may appear to serve as a promising blood biomarker, conditions such as T2D will make such analyses much harder due to associated perturbations in blood glucose levels (7).

Dehydroepiandrosterone sulfate (DHEA-S) is a steroid hormone that is released in response to ACTH and plays a protective and regenerative role (158). Thus, it can be posited that increased DHEA-S serum levels may offer prognostic value by correlating with improved health. However, in practice contradictory results have thus far been obtained in the context of psychosocial stress. For example, Lennartson *et al.* (2016) found that half of their cohort (treated for burnout) experienced increased DHEA-S, whereas the remainder displayed decreased levels (374). In addition, DHEA-S levels peak in young people and start to decline with age, together with its associations with CVD (375).

MicroRNA (miRNA) is another promising serum biomarker to consider in the stress research context as they are a) present in serum and b) play a central role in the regulation of a myriad of cell processes, including physiological and psychological pathways (697). Moreover, miRNAs also offer promise as potential biomarkers for other diseases such as T2D (674). Of note, miRNAs have been associated with psychosocial stress (academic stress) (276, 322). However, such studies often lack standardization and control subjects (128). Their analysis can also be time-consuming and expensive despite being readily available in bodily fluids (239).

Serum immunological biomarkers have also been assessed in relation to psychosocial stress (241, 369, 596). These include well-known pro-inflammatory cytokines such as IL-6 and CRP that are often increased in response to stress (241, 596). However, despite such promise their circulatory levels are affected by infection, lifestyle choices and medication (460). Such factors confound their use as serum stress biomarkers. Catecholamines have also been touted as stress-related biomarkers because of the involvement of the ANS in this context (158, 470). However, catecholamine half-lives are very short which makes it difficult to employ them as clinical biomarkers in the context of psychosocial stress (723).

Chromogranin A is a prohormone that is stored in, and released by the adrenal gland and has also been proposed as a potential biomarker of mental stress (216, 712). In support, some showed that work stress was associated with increased plasma chromogranin A levels (392). Despite such potential, it lacks specificity (252) and is therefore also considered as a potential biomarker of other complications (78, 484, 515). Alpha-klotho is another potential serum biomarker for psychosocial stress and some found that male students exhibited increased levels due to poor sleep and stress management (457). However, this study has several weaknesses as only healthy male students were investigated while it also did not

include any matched controls. As alpha-klotho levels are also associated with lifestyle factors such as smoking, this further weakens its claim to act as a stress-specific biomarker (456).

Together this summary shows the problems linked with the current crop of stress biomarkers and emphasizes the need for further research to identify novel biomarkers in this context (457). It is evident that phosphorylation and glycosylation are integral components of human health and functioning, and when adversely altered may result in pathogenic outcomes (320, 525). Literature indicates that some of these outcomes are associated with psychosocial stress (59, 69, 138, 346, 488, 550, 624, 689). This therefore points toward the potential implication of these PTMs in stress exposure and poor health. Moreover, phosphorylation of the GR impacts its systemic role (329), whereas glycosylation of the CBG is essential for its function (600). The use of such PTMs as biomarkers is well-known in the clinical setting. For example, Table 1.3 demonstrates its employment for complications such as CDG, cancer and neurodegeneration. As protein kinases form the basis of some therapeutic interventions (546, 547), this demonstrates a link between stress and such PTMs. Collectively, such information together with the current lack of a suitable biological parameter for measuring the effects and outcomes of psychosocial stress (457), points toward the potential of phosphorylation and glycosylation PTMs as putative markers of stress-related diseases. This project therefore aimed to begin to address this research gap by initially setting out to establish a method that should eventually help lead to the discovery of novel and specific biomarkers in this context.

1.4.2 Methods employed for biomarker discovery

Studies can generate fragmented outcomes due to disparities in the measurements of such biomarkers (470). Measures include immunoassays such as enzyme-linked immunosorbent assays, Western blotting, immunohistochemistry and flow cytometry (470, 501). However, their limitations include lack of sensitivity, availability of adequate sample amounts, decreased global profiling, denatured samples and lowered availability of analytes (501). This is a major factor that hinders the evaluation of phospho- and glycoproteins as they exist in sub-stoichiometric levels (151, 288). Methods such as novel enrichment techniques are thus necessary to facilitate their evaluation. To the best of our knowledge, the careful enrichment of such proteins for evaluation in the context of stress-related CVD onset/progression has not yet been rigorously pursued. Here, a rat model of chronic stress

will be utilized to allow for suitable biological material to be obtained for the testing and validation of the enrichment material.

1.5 A RAT MODEL OF CHRONIC STRESS

The complexity and multi-dimensional nature of stress means that care should be taken to select the most suitable experimental model to optimally simulate such processes and phenotypes (591, 604). As stress is almost never contained or localized to a specific region and implicates numerous organ systems, it makes rodent models particularly suitable due to a similar physiological make-up compared to humans (489, 604). These models provide important information and insight into the mechanistic basis of stress pathophysiology and related disorders such as PTSD, depression, cognitive impairments and related CVD onset and progression (39, 591). Although similarities exist between rodents and humans, fundamental differences do occur for e.g. sleep-wake cycles, metabolic rates and social hierarchies that may cause variations in results obtained (604).

Two main forms of stressors employed in rodent models include physical and psycho-emotional stress constructs (299, 489). The former includes those that inflict physical pain such as foot shock and forced swim tests, whereas the latter focuses on producing the anticipation of pain, discomfort and fear (64). Examples of psycho-emotional stressors include maternal separation, isolation, environmental disturbances such as altered light/dark cycles, and animal restraint (39). Both these forms can be employed to induce an acute or chronic stress setting, although our focus is placed on the chronicity of stress and its relation to pathological outcomes. Of note, chronic stress models often display greater effectivity and reliability when the aim is to model depressive-like behavior in rodents, as well as phenotypes of anhedonia and anxiety (39, 57, 580). Despite the wide variety of models that can be employed for stress research, the ideal does not exist as confounding factors and questions of validity remain problematic (489, 604). Thus a suitable model should rather be chosen according to the unique pathological features that form the subject of investigation.

1.5.1 Chronic restraint stress

The restraint stress model was previously validated to mimic rodent-like mental disorders (282, 699, 709). Although it is considered a milder form of stress, it remains ideal for studying acute and chronic conditions while maintaining easy standardization and replicability (604, 676). Here, HPA axis alterations and significantly increased corticosterone levels are often observed in experimental animals compared to controls, thereby confirming the successful

induction of the stress response (76, 225, 604). A major advantage of this stress protocol over unpredictable mild stressors includes the fact that rodents may adapt to the multiple mild stressors over time (225). In the case of CRS, rodents are rendered less capable of adaptation and full recovery which mimics occupation-like stressors in humans when considering the long term, inescapable and psychological nature of this model (64, 604). The literature also highlights CRS eliciting changes such as mitochondrial respiratory alterations and enzymatic adaptations (39, 190, 315, 689). Increased CRS-related ER stress markers in the brain is also an outcome in rodents (676, 731, 737). This demonstrates the potential link between this chronic stress paradigm and aberrant phosphorylation and glycosylation outcomes.

Potential limitations of the CRS model include habituation together with the introduction of adverse stimuli such as isolation and/or food and water deprivation in the animal facility. Our model of restraint aims to bypass such confounding factors as rats will be restrained for one hour per day for four weeks in Perspex cages placed next to one another. This should prevent the introduction of social isolation as an unintended stressor since rats prefer to be with one another (660). In addition, food and water deprivation should not occur as the restraint protocol will be done during the natural inactive periods of the rat cycle, with limited requirements for food and water (604). After completion of the CRS protocol, serum will be harvested to try and establish unique proteomics methods that will be designed to enrich for, and examine, glycosylation and phosphorylation changes due to chronic stress (refer Chapter 2 for a detailed description of the restraint stress protocol).

1.5.2 Serum as the biological sample

Blood samples pose significant difficulty regarding the prevalence of high abundance proteins as they decrease the concentration of proteins of interest (such as PTMs) to the range of 10^{-9} to 10^{-12} mol (52). Thus enrichment of serum samples for target proteins is vital (412) and compounded by the even lower abundance of PTMs (100).

Plasma and serum differ from one another with respect to coagulation factors as well as processing techniques to collect such fractions from whole blood (412). Biomarker identification often involves serum as it is considered more stable due to the absence of clotting factors. These overall differences are regularly viewed in their proteomic profiles as no proteome is identical, despite similar biological origins (279). This highlights the complexity which inter-variation adds between differing biological samples. Nevertheless, serum is considered the most informative and complex proteome as it provides valuable

insights into disease onset and progression through high protein content and contact with the entire physiological system (23, 60, 429). Our laboratory will therefore first test the efficacy of the enrichment material on the biological samples intended for biomarker discovery. One way to conclude whether sample preparation was effective is by utilizing a quality control that consists of an exogenous protein. This is crucial as data comparison and integration across laboratories depend upon it (70, 75, 220). Later chapters will discuss the novel and optimized sample preparation procedures in more depth, with a focus placed on the modes of enrichment. These methods form part of techniques employed in proteomics.

1.6 PROTEOMICS METHODOLOGIES

Proteomics was derived in 1994 from the genomics field, with Mark Wilkins referring to it as the study of the entire set of proteins that can be expressed by a genome at any point in time (583). Protein content is affected by the corresponding mRNA levels and host translational regulation and control, establishing proteomics as the best way to characterize a biological system (36). This methodology involves analyzing the structure, function, localization and interactions between different proteins, while ultimately identifying and quantifying the overall protein content present in an organism, cell, or tissue (36, 687). This provides an opportunity to visualize, quantify and hypothesize about the various protein interaction networks involved in disease pathophysiology. This rapidly growing field is therefore regularly employed to identify novel biomarkers in relation to diseases onset and progression (67, 377, 492). Thus proteomics remains a highly promising tool to investigate and diagnose the early onset and progression of various diseases (20, 36, 687). Despite studies employing proteomics methodologies to discover biomarkers (127, 592, 720), the implementation of such findings are often hindered due to ethical standards and sample complexity (412, 418, 714). Clinical proteomics also faces the physiochemical complexity of biological samples and hence numerous methodologies are required in this instance (685). Therefore, samples must be depleted/enriched to analyze target proteins (507), and this need is heightened when assessing low-abundance PTMs (201, 736). Thus, method refinements and developments are continuously implemented to render this process less complicated.

1.6.1 Bottom-up versus top-down approaches

Two approaches in proteomics can be applied even though diverse sub-fields are pursued. These include bottom-up (shotgun) and top-down proteomics (30, 96). The former requires proteins to be digested by specific proteases prior to being analyzed by MS (682), whereas the latter evaluates the intact protein by MS (96). Bottom-up approaches are typically employed by biologists to gain valuable insight into the nature of the proteome, as well as to discover unique biomarkers (67, 640, 730). Here, protein inference is employed to identify proteins from their peptide sequences (730). Despite its general use, a key limitation of this approach is that information describing the individual intact protein is lost (569). The digestion step also increases the complexity of the sample since each protein can now be related to multiple peptides (285). Therefore, protein inference may decrease the chances of biomarker discovery due to ambiguities encountered with a bottom-up approach (325). For this reason, top-down approaches which include intact protein enrichment may be preferred to overcome this and identify various proteoforms (6, 80). This also means that top-down methods can be beneficial for PTM analysis (96). Although this seems promising, the approach still has limitations such as the co-elution of intact proteins after LC (140). In addition, both approaches make use of core proteomic methods which include sample preparation, LC-MS and bioinformatic processing.

1.6.2 Methods in proteomics

Techniques in proteomics are employed in a specific way to best answer the research question posed. The main components of a proteomics workflow include sample preparation, data acquisition with LC-MS, and data interpretation using bioinformatic analyses (100, 189, 682, 730). Here, sample preparation is the most important step (450). New techniques are continuously being implemented to render this process less complicated.

1.6.2.1 Sample preparation

Sample preparation remains the “Achilles heel” of proteomics as this will determine the quality and accuracy of results in later stages (36, 631). Sample handling procedures must therefore be optimized based on the required outcome which ensures compatibility and maximal ranges of detection. These include appropriate storage, freeze-thawing (441), and protein separation/extraction techniques (70). A commonly used method for separation of proteins occurs through SDS-PAGE whereby 1-D or 2-D polyacrylamide gels ensure the separation of proteins based on their molecular weight (244). Stains such as Coomassie

blue or fluorescent stains that possess a unique affinity for specific groups assist in the visualization of molecules of interest (1, 627, 628). Such protein spots are then excised from the gel and digested by proteases for downstream analysis (244, 626). However, such preparation is labor intensive with certain proteins exhibiting a general inability to separate (127). Moreover, biological samples such as blood are often difficult to analyze due to the masking effects of highly abundant proteins (513). This heavily affects the identification of PTMs such as glycosylation and phosphorylation (412). Thus protein enrichment must be included in sample preparation to enable the analyses of these modifications.

1.6.2.1(a) General modes of protein enrichment

The sub-stoichiometric nature of glyco- and phosphoproteins requires specific and reproducible methods of abundant protein depletion/low-abundant protein enrichment (151, 288). A variety of abundant protein depletion methods are available and used in research, for e.g. removal by immuno-depletion and chromatography, with the general implementation of monoclonal antibodies and hydrophobic dyes for serum albumin removal (60, 215, 513, 714). In addition, affinity columns can also be employed such as the Multiple Affinity Removal Column and the ProteoPrep Spin column (61, 507, 714). These columns are applied to ensure the simultaneous removal of immunoglobulin G and albumin from the serum proteome. However, their efficacies have been previously queried (507, 714). Additional methods incorporate commercially available depletion kits for protein enrichment, although this may introduce risk as they are known to remove non-target proteins of interest (249). Conversely, high-abundant proteins may provide insight (via PTMs) (28, 119) in terms of the onset and progression of diseases (e.g. T2D). In addition, limitations such as extreme costs and inter-assay variations are reasons to exclude depletion from the workflow (565). Furthermore, literature indicates that the loss of valuable proteins have previously occurred due to the effects of albumin (249). This could be due to the 'sponge-effect' of albumin, whereby it becomes negatively charged and 'sticky' at physiologic pH (565) and this may lead to the significant and unintended loss of proteins of interest (598). Enrichment methods can be employed (without prior depletion) to avoid such negative effects and to lower the sample processing steps. Furthermore, enrichment may consist of chromatographic techniques which form an integral part of proteomics. Hence such proteins may be of significance for the current study and should be preserved and enriched along with the low abundant proteins (refer in-depth overview of such methods in later chapters).

1.6.2.2 Chromatography as a mode of separation

Liquid chromatography remains a vital tool for providing accurate results in proteomics research (319, 593). A major advantage of resolving proteins by LC is that ion suppression effects can be minimized (593). Online systems which employ high performance LC (HPLC), can aid with this by concentrating samples and improving separation (137). In comparison to 2D-PAGE, HPLC offers high reproducibility, high resolving power and compatibility with certain modes of MS (319, 593). Multi-dimensional chromatographic steps are conjointly employed to fractionate samples for low-abundance protein retrieval (198). Examples include hydrophilic interaction liquid chromatography (HILIC), strong anion exchange (SAX) and strong cation exchange (SCX) chromatography (400, 735). An important method of enrichment includes immobilized metal affinity chromatography (IMAC) that can be applied to a wide range of retrieval strategies. Here, the coupling of proteins/molecules to specific reactive groups/ions ensures optimal recovery of phospho- and glycoproteins (refer Chapters 2 & 3) (339, 400). It is important to note that although more sample handling steps might improve the identification of proteins of interest, it may also result in higher chances of sample loss (70). An example of this is where sample loss occurs due to surface adsorption (415), hence an important consideration is the number of processing steps involved prior to MS analysis.

Stress research has employed proteomics-based technologies to discover candidate biomarkers and to also identify mechanistic links. For example, a study employing human plasma samples attempted to discover biomarkers which could relate stressful physical activity to inflammation (47). Here, the authors employed kits for abundant protein removal and protein enrichment, while eluates were further processed using MS. Their results revealed proteome alterations before and after intense physical activity (47). Human salivary samples were also previously analyzed in the context of acute and chronic stress (434, 726). For example McKetney *et al.* (2021) employed saliva samples from war veterans to analyze the stress response and associated physical and cognitive links (434). Although they did not employ depletion/enrichment strategies in their untargeted bottom-up experiment, they found significant alterations in numerous proteins in response to simulated war missions (434).

Animal models of stress that involved proteomic analysis were performed using serum, saliva and organ tissue samples (278, 491, 529, 706). For example, a rodent study focusing on chronic restraint stress and exhaustive swimming utilized both serum and

splenic tissue to aid in the identification of candidate biomarkers linking immune suppression and chronic stress (278). Here, the authors depleted the serum of high abundant proteins and performed SCX chromatography to further fractionate samples post-digestion and found 121 proteins which were differentially expressed between the control and stress groups (278). An enzyme-linked immunosorbent assay was also applied to further assess and validate four candidate biomarkers. Overall the study provided insights into differential protein expression involved in multiple processes (278). Moreover, two additional rodent studies employed SCX fractionation prior to LC-MS analysis (706, 733), while others used centrifugation to enrich for synaptosomes in rat hippocampi (706).

Table 1.4 summarizes examples of proteomic techniques that were employed for studying psychosocial stress, with some aiming for biomarker discovery. However, to the best of our knowledge none have interrogated phosphorylated and glycosylated changes in preclinical and clinical chronic psychosocial stress models. Furthermore, intact protein enrichment strategies involving PTMs have not yet been included in sample preparation workflows for this type of research work.

Table 1.4. A brief description of proteomics analyses in stress pathology research and the methods involved. ANS, autonomic nervous system; PTSD, post-traumatic stress disorder; MDD, major depressive disorder; CREB, cAMP-response element binding protein; SDS-PAGE, sodium dodecyl sulfate polyacrylamide gel electrophoresis; IgG, immunoglobulin G; 2-DE, 2-dimensional electrophoresis; SCX, strong cation exchange; UPP, ubiquitin-proteasomal pathway; ERK, extracellular signal regulated kinase; MAPK, mitogen activated protein kinase; PI3K, phosphatidylinositol 3 kinase; Akt, Ak strain transforming; mTOR, mammalian target of rapamycin.

Biological sample	Study overview	Stressor	Methods of enrichment/fractionation	Study outcomes	Reference
Human plasma	Identification of possible biomarkers to understand and link stress to inflammation	Extreme physical stress (246 km run)	Depletion kits for albumin and IgG removal, enrichment kits for low abundant proteins	Distinct alteration of proteomic profile before vs after marathon, related to inflammation	(47)
Human salivary samples	Evaluation of the role of the ANS in acute stress in university students	Acute psychological stress in the form of an oral exam	2-DE and spot excision	Known biomarkers of stress exhibited significant change	(726)
Human salivary samples	Unravelling of the biomolecular components which links physical and cognitive performance in soldiers	Simulated acute & chronic war stress	No protein enrichment	> 300 proteins significantly altered, immune and metabolic perturbation	(434)
Rat serum & splenic tissue	Examination of serum proteins which link chronic stress and the immune system, whilst identifying candidate biomarkers	Chronic restraint stress & exhaustive swimming	Cell preparation using panning and microbeads, SCX fractionation	New insight into molecular mechanisms gained, 121 proteins changed between groups, metabolism plays a major role	(278)
Rat liver tissue	Gaining a better understanding of the relationship between liver dysfunction/injury and depression	Chronic restraint stress	No protein enrichment	2 176 proteins identified, 98 differentially expressed, new insight into potential pathophysiological mechanisms	(379)
Rat saliva	Understanding the mechanisms which link chronic psychological stress and oral disease	Chronic restraint stress	Centrifugal filtration, 2-DE & spot excision	Bacteria & seven oral proteins significantly altered between groups,	(491)
Rat hippocampi	Investigation of extreme psychological trauma, stress susceptibility and mental illness (PTSD)	Foot shock stress	No protein enrichment	Overall protein changes indicative of redox changes, top protein changes were also validated proteins, potential relation to stress observed	(171)

Rat hippocampi	Elucidating the pathogenesis of MDD	Chronic unpredictable mild stress	SCX fractionation	Alteration of proteins involved in synaptic transmission, coupled with metabolic & enzymatic changes	(733)
Rat hippocampi	Evaluating hippocampal function in depression, as well as synaptic plasticity	Chronic mild stress	Density gradient centrifugation for synaptosome enrichment, SCX fractionation	21 mitochondrial proteins significantly altered, suggestive of oxidative phosphorylation implication	(706)
Rat hippocampal hemispheres	Examination of the hippocampal proteome profiles in depression	Chronic social isolation	Electrophoretic separation of proteins	Global, cytosolic and metabolic protein changes, UPP implication, potential biomarkers	(200)
Rat hippocampus	Identification of molecular changes induced by constant psychosocial stress	Chronic social defeat stress	2-DE followed by spot excision	Several changes in protein expression	(93)
Rat nucleus accumbens	Anti-depressant effects of the environment and its relation to stress, examining pathways such as CREB	Acute restraint stress	Delipidation, 2-DE followed by spot excision	Change in ERK, MAPK & PI3K/Akt pathways, 14-3-3 protein alteration and relation to phosphorylation, energy metabolism alteration	(193)
Mouse limbic brain regions & serum	Examining the molecular changes in limbic regions for insight into stress and MDD	Chronic social stress	Delipidation, abundant protein depletion via spin cartridges	51 altered proteins, widespread molecular changes, 3 specific protein alterations in serum	(256)
Mouse prefrontal cortex	Revealing the correlation between the pathophysiology of MDD and inflammation	Chronic social defeat stress	SCX fractionation	Inflammasome pathway alteration and proteins involved in inflammation	(360)
Zebrafish telencephalon	The effect of depression and mood disorders on neurogenesis	Chronic unpredictable stress	SDS-PAGE protein separation and visualization by Coomassie staining followed by spot excision	58 protein alterations, implication of mTOR and opioid signaling pathways	(529)
Zebrafish brain samples	Molecular basis of anxiety and depression w.r.t. neuroglia	Chronic unpredictable stress	2-DE, spot excision	18 proteins deregulated which link to anxiety, mitochondrial changes and decreased neurogenesis	(98)

1.6.2.3 Mass spectrometry as a high-throughput technique

MS is a key high-throughput technique used to determine the mass-to-charge ratio (m/z) of ionic species (36, 244). The high specificity and detection range of this technique enables protein identification in the femtomolar concentration ranges (141). Every proteomic experimental procedure comprises of a step involving MS (100) and it contains three main parts, i.e. (1) molecules transitioning to gas phase ions via an *ion source*, (2) separation of such ions based on their m/z values in the presence of a magnetic field released by a *mass analyzer*, and (3) the measurement of the amount of ions separated by virtue of their values by a *detector* (36, 100). Multiple MS processes can take place in one experiment whereby the mass analyzers are used in tandem (36).

Tandem MS (MS/MS) is regularly employed in biomedical research involving proteomics workflows (459). Here, mass analyzers are connected by a collision cell where precursor ions of a specific m/z ratio are selected to collide with gas molecules (3, 459). This results in fragmentation into smaller product ions for identification, which provide information on the make-up of the peptide in the form of MS/MS spectra (3, 319). Bioinformatic processes are then incorporated into the workflow to interpret the spectral data (189).

1.6.2.4 Data analysis

The analysis of MS/MS data is a very important step in the proteomics pipeline (189), as well as a complex multistep process (100). It includes the processing of raw spectral data to extract relevant information, querying a sequence database for peptide selection, scoring of peptides against *in silico* spectra and validation of the identified peptides and proteins (164). Various commercial and open-source database search tools exist (307), which include Sequest (188), MaxQuant (134), MyriMatch (637) and MSFragger (345). Such search engines may yield varying results as they are based on different algorithms (164). The choice of a search tool(s) is therefore a very important aspect of such studies. Although they may differ in data output, most of them still retain the same basic functions (189). For example, the database search tool employs a sequence database from which it selects peptides that can be matched to MS/MS spectra (189). The sequence database is usually in FASTA format containing all the

known proteins of the organism (133) and is often acquired from UniProt (130). Specification of the enzyme employed for digestion is necessary to generate such peptides *in silico*, followed by spectral matching (189). Contaminants are often added to the sequence database which assist with identifying peptides which are not of host origin and explaining the spectra obtained in relation to them (189). Furthermore, decoy sequences are added by reversing the sequence database (8). This enables a threshold of a false discovery rate (FDR) to be achieved that allows for a statistical estimation of the amount of false positive identifications (187).

Fixed and variable modifications are set within the database search tool. An example of a fixed modification is setting the mass change of cysteine due to the alkylation step in sample preparation (355), whereas a variable modification includes the oxidation of methionine, deamidation or phosphorylation (84, 189, 487). This therefore assists with PTM identification (84). Additional important parameters for search input include peptide/precursor mass tolerance, as well as fragment mass tolerance (189). The former is essential for identifying candidate peptides of which the highest-ranked is compared to a MS/MS spectrum (189). The latter helps to assign a peptide spectrum match (PSM) which has a score relating the probable correctness of the observed peptide identification (283). Further validation of the data is crucial for confident statistical analysis of the peptide sequences and the probabilities of their inferred proteins (189), and the method chosen here may vary between researchers as different algorithms exist for this (164). Examples of these include PeptideProphet for peptide validation (326) and ProteinProphet for protein validation (461). Moreover, the investigator defines a threshold for acceptance of the generated information that will ultimately be reported to the scientific community (283). There is no clear consensus regarding the optimal choice in search strategy that should be employed (189). However, each user should construct a bioinformatics workflow in relation to their research question(s) and in line with the available resources.

1.7 AIMS AND OBJECTIVES

We aim to establish and validate two distinct methods of enrichment for phosphoproteins and glycoproteins. These will be tested using a purified protein and serum from our in-house model of chronic restraint stress. The eluted fractions will

then be analyzed using MS to further assess the efficacy of our unique enrichment techniques in comparison to standard enrichment techniques. The specific aims of this study are:

1. To construct a unique method of intact phosphoprotein enrichment. Here, the Zirconium (Zr)-IMAC beads from Resyn Biosciences will be employed, while the original protocol for phosphopeptide enrichment will be altered to prevent protein loss and to retrieve intact phosphoproteins. The efficacy of this technique will be assessed using SDS-PAGE analysis. Suitable positive and negative controls will be included, i.e. a) the enrichment of the phospho-residues present in hen egg ovalbumin (OVA) with Zr-IMAC beads as a positive control, and b) beads not binding phosphoproteins will be employed as a negative control.
2. To create and assess the suitability of lectin-functionalized magnetic beads for the retrieval of glycoproteins. For this aim, carboxyl beads from Resyn Biosciences will be employed onto which a lectin (concanavalin A [ConA]) will be covalently coupled. As ConA possesses an affinity for a specific glycan moiety present on OVA, it will be used as a positive control to determine the suitability of the technique. The carboxyl bead without the lectin attached will be employed as the negative control.
3. To enable tryptic digestion of the enriched glycoproteins prior to LC-MS by employing chemical deglycosylation. Here, trifluoromethanesulfonic (TFMS) acid will be added to OVA to assess the success of deglycosylation and identifying whether protein degradation occurred. In addition, rodent serum will be deglycosylated and the overall assessment of this technique be done using SDS-PAGE with fluorescent staining to visualize protein stability and glycan loss.
4. To investigate the efficacy of these unique enrichment methods by comparison to standard bottom-up enrichment techniques. Here, a Q Exactive mass spectrometer will be employed to generate data that will be analyzed using MS Fragger and the Philosopher toolkit. This should assist with assessments of the enrichment technique(s) for isolated phosphopeptides and glycopeptides, respectively, and also to compare our proposed mode of enrichment. Quality control analysis of the workflow will be evaluated by examining the number of spectra obtained from the RAW files and

incorporating a suitable positive control. Furthermore, the ability to enrich for the specified and modified peptides will be done by investigating the number of peptide spectral matches (PSMs) identified in each technical repeat and the number of glycosylated/phosphorylated peptides observed in each repeat. A comparison between the enriched and unenriched (control) populations will be made to determine the overall efficacy of the technique in serum.

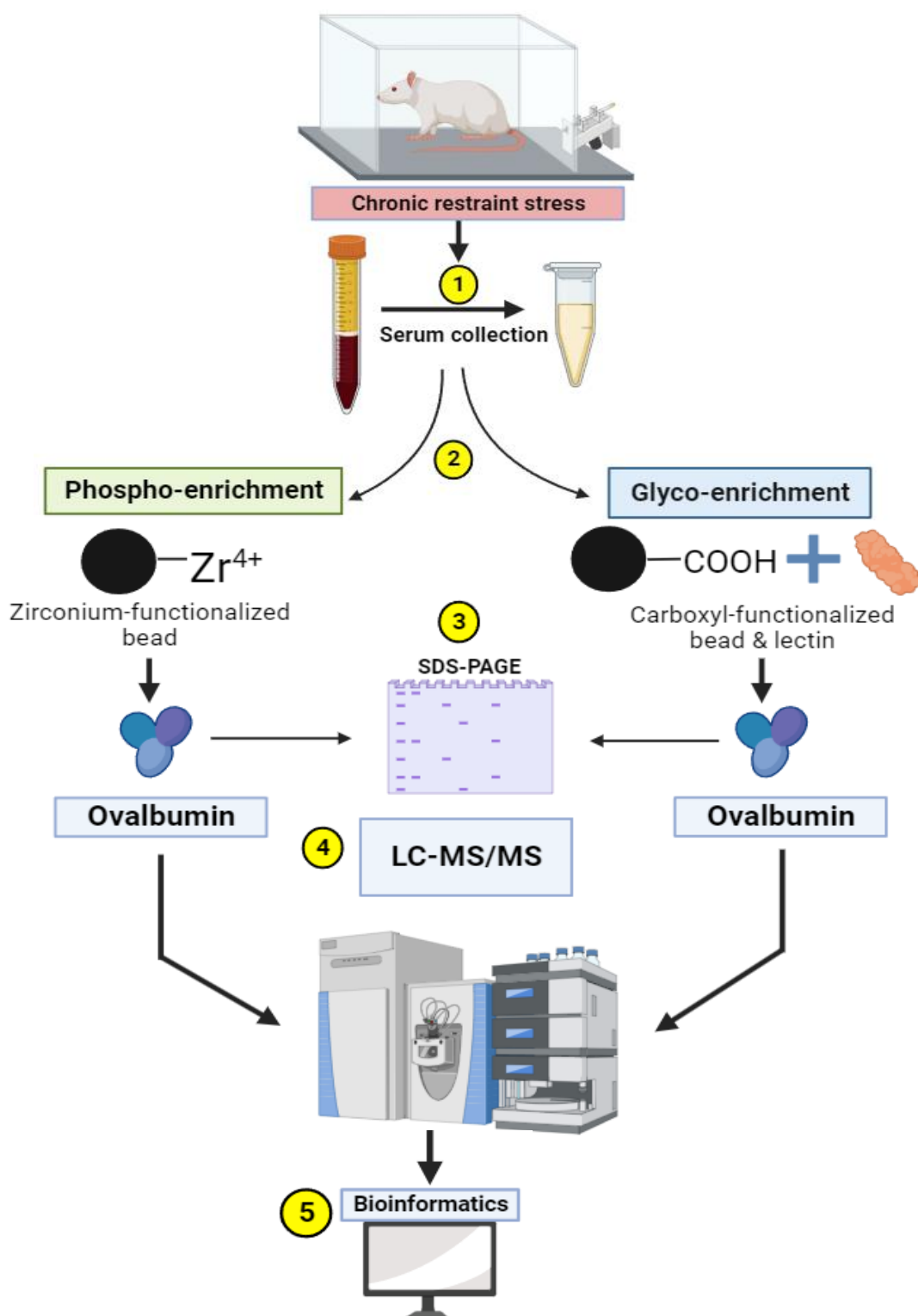


Figure 1.5. A summarized visual representation of our workflow. Step 1: Acquisition of serum from stressed rats; Step 2: Phosphoprotein and glycoprotein enrichment; Step 3: Evaluating unique methods by SDS-PAGE and staining from OVA enrichment; Step 4: Data acquisition using LC-MS/MS; Step 5: Data processing. Zr, zirconium; COOH, carboxyl group; SDS-PAGE, sodium dodecyl sulfate polyacrylamide gel electrophoresis; LC-MS/MS, Liquid chromatography tandem mass spectrometry. Image created using Biorender.com.

**CHAPTER 2 - PHOSPHOPROTEIN ENRICHMENT USING ZR-IMAC
MAGNETIC MICROPARTICLES**

2.1 INTRODUCTION

Protein phosphorylation is one of the most extensively studied PTM and hence underscores its integral physiological role (29). This occurs principally on Ser, Thr and Tyr residues in eukaryotes, in a ratio of 1800:200:1, respectively (386). Of note, up to 30% of the human proteome can be phosphorylated at any given time point and it is a dynamic process as rapid changes (in phosphorylation) are essential for normal cellular functioning (29, 400). However, atypical modifications are linked to diseases such as CVD, T2D and neurodegeneration (102, 122, 268). In the context of psychosocial stress, phosphorylation influences the localization of the GR (329), while MAPK, ERK and JNK pathways are known to also be involved in this instance (43, 190) (refer Chapter 1). Moreover, chronic restraint of male Wistar rats revealed decreased neural ERK phosphorylation that could potentiate abnormalities in cell proliferation and survival (689). These findings alert to the potential detrimental role of abnormal phosphorylation in the context of chronic psychosocial stress. It also draws attention to the potential utility of this particular PTM as a putative clinical tool for monitoring various health outcomes. However, its analysis is complicated as such modifications occur in relatively small amounts (370) and hence this requires unique sample preparation techniques such as phospho-enrichment.

2.1.1 The enrichment of phosphoproteins

Although up to 30% of the proteome can be phosphorylated (400), the wide dynamic range of biological samples decrease the detection of such important PTMs (612). Furthermore, the complexity and high dynamic range of the serum proteome lowers the stoichiometry of phosphorylation and masks its identification (502), therefore enrichment methods are needed to improve their analysis (412). Prefractionation can also be employed prior to enrichment, such as SAX or SCX chromatography, as well as HILIC (201). Strong anion exchange chromatography is often used to retain phosphoproteins as the negative charge present on the phosphate molecule possesses an affinity for the positively charged matrix (400). However, additional steps in sample preparation can result in protein losses and a subsequent decrease in terms of its detection (70, 201). Overall, phosphoprotein enrichment is based on electronegativity and hydrophilicity with contributions by the phosphate molecule (201, 400).

2.1.2 Phosphopeptide versus phosphoprotein enrichment

Enrichment at the peptide level offers numerous advantages. These can occur due to their lesser structural complexity compared to proteins, compatibility with chromatographic methods, easy identification and usefulness for singular organelles (201). A disadvantage of such peptide applications is a decrease in confidence for protein identification and biomarker discovery (325) (refer Chapter 1). Protein level enrichment can potentially bypass this limitation (96), with IMAC and metal oxide affinity chromatography (MOAC) regularly employed because of their high sensitivity and selectivity (42, 44). However, this is not without drawbacks as their complexity in relation to peptides can lead to difficulties in terms of sample preparation. Protein enrichment is relatively underdeveloped in comparison to the dominantly used bottom-up approaches (96, 285). However, this has been performed for phosphoprotein experiments (103, 285, 542) where some were done using the serum proteome (301, 302, 377). For example, researchers successfully employed Fe³⁺-IMAC material to enrich serum phosphoproteins. It is important to note that the researchers chose to deplete their crude serum using the Multiple Affinity Removal System column before enrichment. The caveats of incorporating such commercially available systems and the inclusion of additional processing steps are further discussed in Chapter 1. Nevertheless, these findings show that metal affinity chromatography exhibits great potential for protein enrichment.

2.1.3 Metal oxide affinity chromatography

The affinity of phosphate groups for metal oxides form the basis of MOAC enrichment, where the mechanism of Lewis acid-base interactions and the phosphate group adopting a bidentate binding mode takes place (373). This interaction occurs through the amphoteric nature of metal oxides which allows the capture of peptides at low pH, and the elution thereof at a relatively high pH (176, 373). Titanium dioxide was the first to be applied, followed by others such as Zr dioxide, iron (II,III) oxide and aluminium oxide (109, 356, 382, 505). This material is more tolerant to buffers and detergents such as those containing ethylenediamine tetraacetic acid (EDTA) which chelates metal ions involved in IMAC (304). However, various manufacturers' products often yield different results despite employing the same metal oxides (31, 92). It is also possible for differences in affinity between these groups, as singly and multiply

phosphorylated peptides are enriched in differing orders of magnitude (201). Mesoporous materials are selected as the matrix of choice for both IMAC and MOAC due to their higher surface area and increased reactive sites (386, 404, 641). Despite the similarity between the two enrichment techniques, some studies also found differences in terms of their specificity (32, 227).

2.1.3.1 Immobilized metal affinity chromatography

IMAC enrichment techniques are based on the interaction between positively charged metal cations and the negatively charged phosphate group (201, 386). This strong interaction prevents the leakage of metal ions and was initially used for phosphoprotein enrichment, although numerous studies published data on peptide enrichment due to its overall ease of operation (359, 382, 512, 666). Peptide-level enrichment assists in the easy binding and elution of phosphates through both low pH and high pH levels, respectively (201). These pH levels are not suitable for protein enrichment as it will result in overall protein precipitation (201). Another disadvantage includes the bias observed between metal ions for either singly or multiply phosphorylated peptides. Gallium has been noted to bind multi-phosphorylated peptides, whereas ferric iron is known to collect those remaining (666). Moreover, the method used to chelate these cations to the matrix (either iminodiacetic acid or nitrilotriacetic acid) exhibits further differences in terms of binding (257, 462, 512, 713). These reasons contribute to its rare usage at the protein level. However their long traditional use, ease of operation and large amount of available data (at peptide level) compared to other methods supports the standard choice of this material (201, 385, 386).

In addition to overcoming the complications associated with the dynamic range of serum (mentioned in Chapter 1), enriching for undigested phosphoproteins enables a higher chance of confident identification (80, 96). Resyn Bioscience's MagReSyn® high performance Zr-IMAC magnetic microparticles were chosen for this application. Since Zr^{4+} is a high valence metal cation, its coordination specificity with phosphates are unique and enables it to bind to numerous phosphorylated residues (257). In this case, the metal ion is bound to activated phosphonate groups connected to a flexible linker that increases stability and limits steric hindrance (402, 631). It was also shown to have little to no bias towards singly and multiply phosphorylated residues (31).

Increased stability over time is another reason why this was chosen over traditional titanium(IV)-IMAC material (31). To the best of our knowledge, no intact protein enrichment experiments have been done using Zr-IMAC material, and specifically using ReSyn Biosciences' high performance zirconium beads. As these were only been employed for phosphopeptide enrichment (31, 351, 729), optimization of the current protocol was necessary as the buffers employed for peptide experiments are unsuitable for intact protein retrieval.

2.1.3.2 The presence of nucleic acids in serum

The loss of phosphoproteome information can occur due to the presence of nucleic acids (387). This is because these macromolecules contain abundant phosphate groups that can bind to the IMAC/MOAC material and hence negating phosphopeptide enrichment (452). Serum DNA and RNA can be derived from bacteria and viruses, cell and tissue apoptosis/necrosis, blood cell breakdown, extracellular vesicles and other cell-free sources (218). For this reason, relatively low levels of nucleic acids are usually found in serum. This can range between 1.8 – 474 ng/mL DNA and 2 – 12 ng/mL RNA (277, 352, 354, 383), while relatively higher serum DNA levels were observed in disease states such as cancer (354). However, the latter was not applicable to our rat CRS model. It is important to note that the concentration of serum proteins is 60 mg/mL – 80 mg/mL (87), meaning a 6-fold greater abundance compared to circulating nucleic acids. Despite this, we performed an extraction of DNA and RNA fractions to determine their levels in our serum samples.

2.2 AIMS AND OBJECTIVES

The aim of this chapter is to establish an intact phosphoprotein enrichment method. Here, unique Zr-IMAC particles will be employed as the material for enrichment, where the original protocol (designed for peptide enrichment) will be altered to enrich for intact proteins. A phosphorylated protein, namely OVA (335), will be incorporated as the positive control. The negative control will be magnetic beads that only consists of the phosphoryl backbone present on its surface. Moreover, Zr-IMAC beads which were previously employed for OVA enrichment will be reused to test whether the adapted elution method was successful. The analysis of this method will be done using SDS-PAGE.

2.3 MATERIALS AND METHODS

Although the product and supplier details are stated in this section, information regarding buffers consisting of multiple constituents are listed in the relevant appendices.

2.3.1 Chemicals and Materials

Hen egg OVA (A5503, Sigma-Aldrich, St. Louis, MO, USA) was chosen to assess the enrichment experiments. Here, Zr-IMAC beads (MR-ZHP002, ReSyn Biosciences Ltd., Gauteng, SA) were tested to enrich intact proteins and were the positive control. Resyn's Phosphoryl beads (MR-PHOS-SAMPLE, ReSyn Biosciences Ltd., Gauteng, SA) were employed as the negative control. TRIzol[®] Reagent (15596026, Thermo Fisher Scientific, Waltham, MA, USA) was employed for RNA and DNA extraction.

2.3.2 TRIzol extraction

The extraction of DNA and RNA was performed according to the manufacturer's instructions (Appendix B). Protocol alterations were similar to those of Trakunran *et al.* (2019) as they employed rat serum for their miRNA experiments (662). The protein content of the chosen male rat serum was measured using the A280 function on a NanoDrop[™] One (ND-ONEC, Thermo Fisher Scientific, Waltham, MA, USA). Briefly, 250 μ L of male rat serum was added to 750 μ L of TRIzol[®] reagent and mixed by gentle inversion, followed by 15 minutes of incubation. Two hundred microliters of chloroform (C2432, Sigma Aldrich, St. Louis, MO, USA) was added to the mixture followed by gentle inversion and 5 minutes of incubation. The mixture was then centrifuged (Eppendorf[®] Centrifuge 5810 R, Hamburg, Germany) at 12 000 $\times g$ for 15 minutes at 4°C. After this, an upper aqueous phase, interphase, and lower red phenol-chloroform phase became visible. The upper aqueous phase was transferred into a new tube to which 500 μ L of isopropanol (19516, Sigma Aldrich, St. Louis, MO, USA) was added. All other RNA extraction steps proceeded as indicated in the manufacturer's instructions, except for air-drying time which occurred for 20 minutes. For protein extraction, the interphase was removed and put into a new tube after removal of the aqueous phase. Three hundred microliters of 100% ethanol (E7023, Sigma Aldrich, St. Louis, MO, USA) was added and the tube was gently inverted for sufficient mixing. The mixture was then centrifuged at 2000 $\times g$ for 5 minutes at 4°C. This ensured that

the DNA formed a pellet, and the supernatant (protein fraction) was transferred to a new tube for processing. All further centrifugation, wash and resuspension steps took place according to the original protocol; however, 100% ethanol was employed for washing the protein fraction. The DNA pellet was resuspended in 1 mL of 0.1 M sodium citrate (S4641, Sigma Aldrich, St. Louis, MO, USA) in 10% ethanol, pH 8.5. All steps after this were completed according to the original protocol (Appendix B). The end-point measurements were taken with the Nanodrop One, with an A280 measurement employed for protein concentration determination, and the respective settings for the DNA and RNA measurements. This experiment was repeated on three separate occasions.

2.3.3 Phosphoprotein enrichment

Alterations were made to the original protocol to suit enrichment on an intact protein level. These include buffer substitutions, increased incubation periods and altered washing and elution procedures. The original and final altered protocol is provided in Appendix B. The original protocol employed an acidic solution for binding, and a basic solution for elution (536) which could not be incorporated for intact protein enrichment as this would result in protein precipitation and loss (201). The buffer substitutions and reasons for it are detailed in Table 2.1.

Table 2.1. A comparison between the originally specified buffers and their replacements, including the reason for their substitutions. NA, not applicable.

Purpose	Protocol buffers	Replacement	Explanation
Loading buffer	0.1 M glycolic acid, 80% acetonitrile, 5% trifluoroacetic acid (also employed as the solubilization buffer)	0.1 M glycolic acid in 10 mM ammonium acetate solution, pH 7	This was used for the sole purpose of equilibrating the beads before sample loading. The ammonium acetate was incorporated as it is volatile and used for LC-MS experiments (344). Acetonitrile and trifluoroacetic acid were excluded due to their potential contribution to protein precipitation.
Wash buffer 1	80% acetonitrile, 1% trifluoroacetic acid	10 mM ammonium acetate, pH 7	Utilized for washes and sample solubilization instead of the proposed organic solvent and acid, for reasons mentioned previously.
Wash buffer 2	10% acetonitrile, 0.2% trifluoroacetic acid	NA	NA
Elution buffer	1% ammonium hydroxide	10 mM EDTA, pH 7	A strong base could not be used for elution as it could result in protein precipitation, therefore EDTA was chosen due to its strong chelating ability (228) which could elute the bound protein by removing the Zr ion.

Fifty micrograms of OVA were solubilized in 10 mM ammonium acetate (pH 7, AM9070G, Thermo Fisher Scientific, Waltham, MA, USA) for both enrichment and phospho-fluorescence detection. Twenty microliters of Zr-IMAC, MagResyn Phosphoryl and previously used Zr-IMAC (now referred to as “stripped”) beads were removed from their respective vials and separated from the solution prior to equilibration using a magnetic separator (MagReSyn®, ReSyn Biosciences Ltd., Gauteng, SA). The volumes removed were based on the recommendations of the original protocol. The stripped beads were washed three times with wash buffer 1 to ensure removal of any residual protein from a previous experiment. Thereafter, all the material was washed once with 0.1 M glycolic acid (124737, Sigma-Aldrich, St. Louis, MO, USA) in 10 mM ammonium acetate (pH 7), followed by two washes with wash buffer 1. This was done to remove any excess glycolic acid present in the tube. Thereafter the incubation with sample occurred for 3 hours at 4°C on a rotational mixer (Labnet International, Inc., Edison, NJ, USA). Once complete, the supernatant (unretained fraction) was removed and the material was washed once with loading buffer (glycolic wash fraction), followed by the removal of unbound proteins with wash buffer 1 (wash fraction). Lastly, proteins were eluted with 10 mM EDTA (pH 7, CalBiochem 34103, Sigma Aldrich, St. Louis, MO, USA) for three separate washes of 10 minutes each, and the elutes were pooled to form a single fraction. This fraction, as well as the unretained and two separate wash fractions, were lyophilized and stored for later analysis. All lyophilization took place in a bench top freeze dryer (VirTis BenchTop Pro Freeze Dryer, SP Scientific, Warminster, PA, USA). Storage of the dried fractions prior to SDS-PAGE was at -80°C.

2.3.4 Protein determination, SDS-PAGE analysis and staining

Both a Bradford assay and BCA assay kit (23225, Thermo Fisher Scientific, Waltham, MA, USA) were completed to determine the protein content present in the various fractions. The Bradford assay was done according to the protocol produced by Dr. Danzil Joseph (Department of Physiological Sciences, Stellenbosch University), whereas the manufacturer’s instructions were followed for the BCA assay (refer Appendix D for both protocols). Absorbance was measured at 595 nm using a spectrophotometer (E-SP1000-V-P, Eins-Sci, Gauteng, SA) and 562 nm using a FLUOstar Omega UV/vis Microplate Reader (Ortenberg, Germany) for the Bradford and BCA assays, respectively. SDS-PAGE analysis was employed to inspect the

efficiency of phosphoprotein retrieval. The appropriate steps were followed according to the protocol received from Dr. Danzil Joseph (Department of Physiological Sciences, Stellenbosch University) (refer Appendix D).

2.3.4.1 Laemmli sample preparation

The dried samples were resuspended in ultrapure water and combined in a 1:1 ratio with 2X Laemmli buffer (details in Appendix D). Such prepared samples were heated at 95°C for five minutes, put on ice and stored at -20°C for up to a week before gel loading.

2.3.4.2 Protein loading and staining

A 10% hand-cast gel (refer Appendix D for gel constituents) was utilized for OVA visualization, while a 4% – 20% precast gradient gel (456-1094, Bio-Rad Inc., Hercules, CA, USA) was used for the phospho-fluorescent image analysis of OVA. The first lane always consisted of the protein ladder (26616, Thermo Fisher Scientific, Waltham, MA, USA) and the proteins were separated using the Bio-Rad PowerPac300 (Bio-Rad Inc., Hercules, CA, USA) set at 120 V for approximately one hour. Once separated, the gel which required fluorescent visualization was stained with a specific commercial Pro-Q Diamond fluorescent stain (Invitrogen™, P33301, Thermo Fisher Scientific, Waltham, MA, USA) by following the required protocol (Appendix D). Briefly, the gel was fixed in a 10% glacial acetic acid and 50% methanol solution for one hour, followed by three washes in ultrapure water. Pro-Q staining occurred for 90 minutes, with 50 mM sodium acetate and 20% acetonitrile (pH 4) used for destaining for 90 minutes. Ultrapure water was once more employed for 10 minutes of washing before fluorescent imaging. All images were documented using the ChemiDoc™ MP Imaging System using Image Lab™ software (Universal Hood III, Bio-Rad Laboratories Inc., Hercules, CA, USA). Fluorescent imaging was recorded by utilizing the Pro-Q Diamond setting (filter 3, green epi-illumination) and thereafter gels were immersed in a Coomassie stain (ab119211, Abcam, Cambridge, UK) for at least 15 minutes until the bands were fully visible. This image was taken using the Coomassie protein gel setting with white transillumination. Here, the gel was placed on a white light conversion screen (1708289, Bio-Rad Inc., Hercules, CA, USA) (refer Figure 2.1 for phosphoprotein retrieval and analysis). The stain free setting was chosen to image the

hand cast gel. Every wash and incubation step took place in polypropylene holders placed on rotational mixers (FMH200, Labotec, Gauteng, SA).

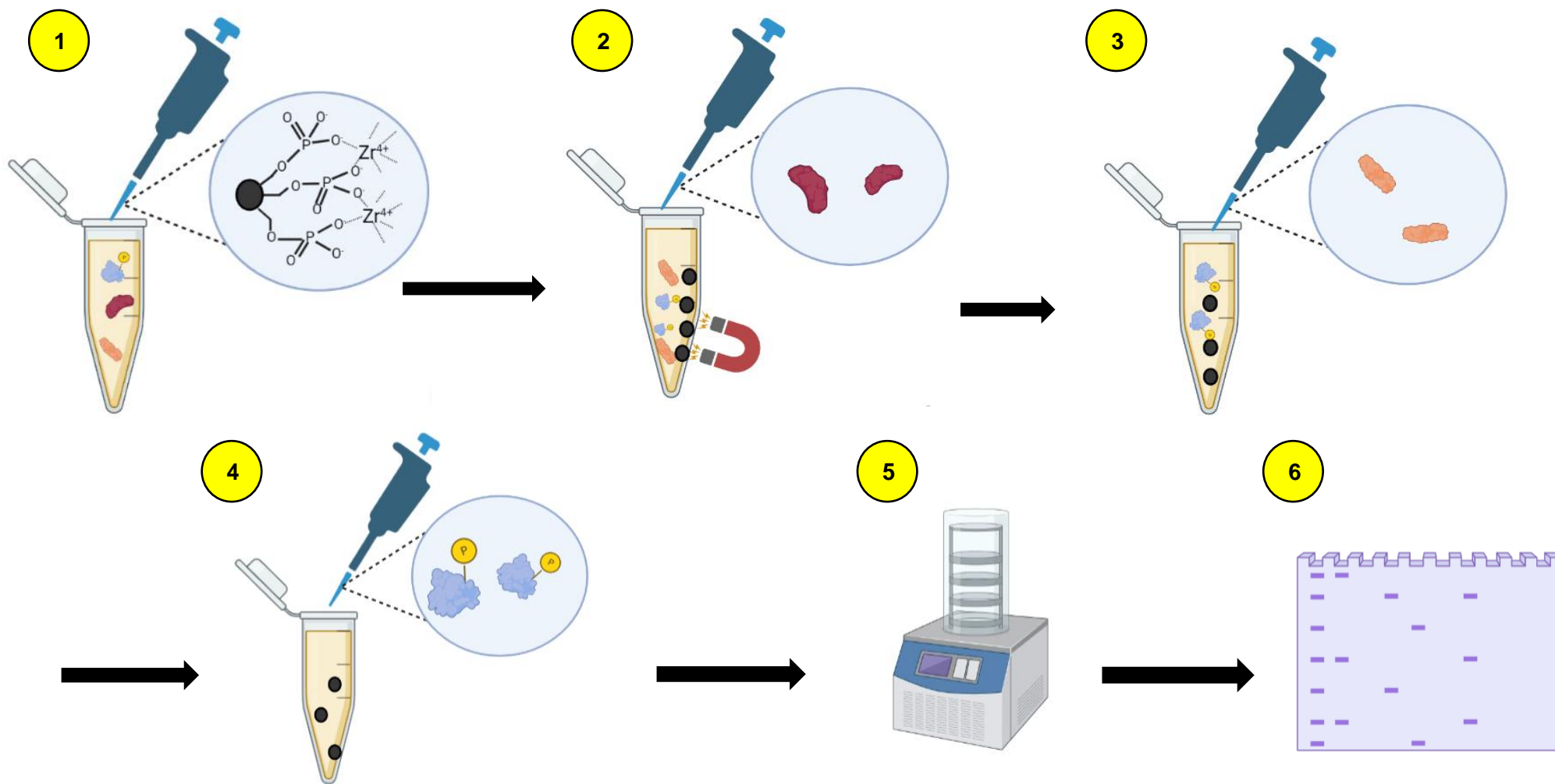


Figure 2.1. A visual summary of the workflow for evaluating the efficacy of phosphoprotein enrichment. Step 1: Incubation of sample with microparticles; Step 2: Unretained fraction removal; Step 3: Material washing and unbound fraction removal; Step 4: Elution; Step 5: Lyophilization; Step 6: SDS-PAGE and staining analysis. SDS-PAGE, sodium dodecyl sulfate polyacrylamide gel electrophoresis. Image created in Biorender.com.

2.4 RESULTS

2.4.1 OVA results

Figure 2.2 shows the total protein and OVA phospho-fluorescent image. The total protein results of the Zr-IMAC beads OVA experiments are displayed in Figure 2.3A, whereas the negative control and stripped beads are shown in Figure 2.3B. The Coomassie-stained gel revealed an OVA band at ~45 kDa (Fig 2.2A), while the phospho-fluorescent staining showed a strong signal at ~45 kDa (Fig 2.2B). The original uncropped gel images are provided in Appendix B.

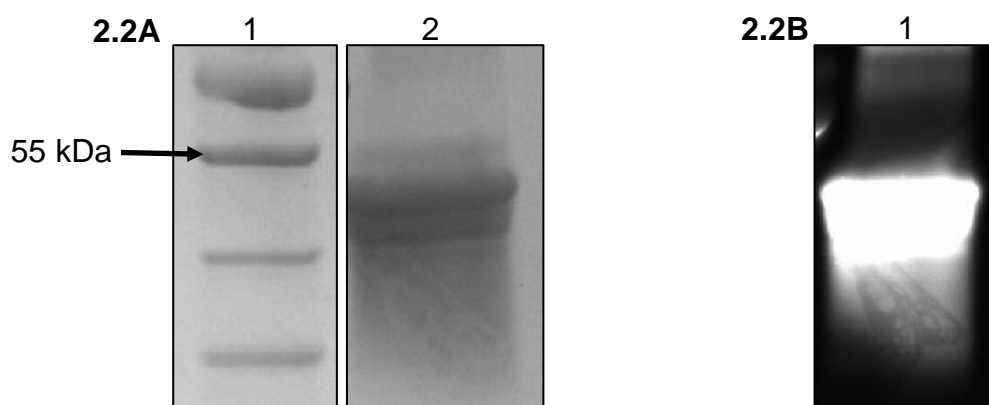


Figure 2.2. 4% - 20% gradient gel displays the (A) total protein stain of OVA and (B) the fluorescent intensity of OVA. **A** - Lane 1: Protein ladder; Lane 2: OVA. **B** - Lane 1: OVA fluorescence.

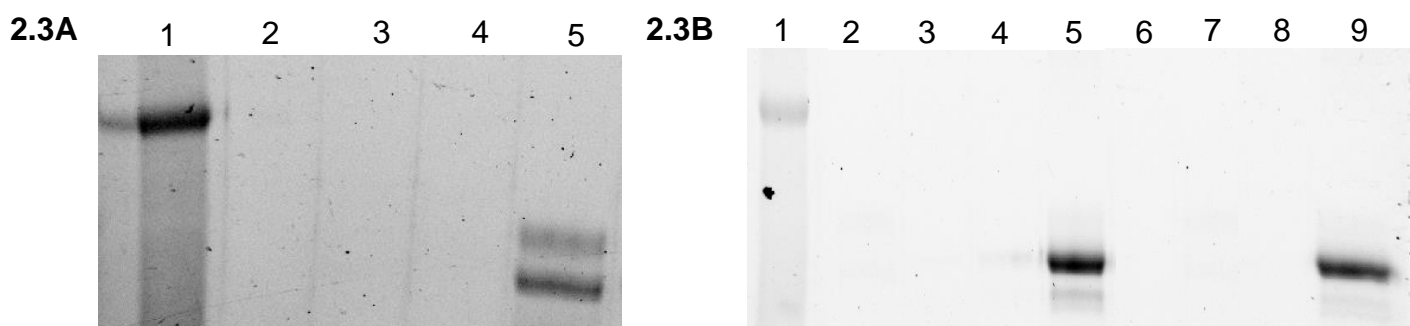


Figure 2.3. Stain free 10% mini-protean gels which display the efficiency of the intact protein enrichment technique. 2.2A represents the new Zr-IMAC beads which were employed as a positive control, whereas 2.2B represents the negative control (lanes 2-5) and stripped beads (lanes 6-9). **A** - Lane 1: Protein ladder; Lane 2: Unretained fraction; Lane 3: Glycolic wash fraction; Lane 4: Unbound fraction; Lane 5: Eluted fraction. **B** - Lane 1: Protein ladder; Lane 2: Unretained fraction; Lane 3: Glycolic wash fraction; Lane 4: Unbound fraction; Lane 5: Eluted fraction Lane 6: Unretained fraction; Lane 7: Glycolic wash fraction; Lane 8: Unbound fraction; Lane 9: Eluted fraction.

2.4.2 Nucleic acids in rat serum

Table 2.2 represents the protein, DNA and RNA measurements obtained from the three separate TRIzol extraction experiments. Relatively high protein concentrations were observed for unprocessed serum and for TRIzol-extracted proteins compared to extracted nucleic acids.

Table 2.2. Protein (including unprocessed from serum), DNA and RNA concentrations obtained from the Nanodrop One are listed, including purity ratios. NA, not applicable.

Repeat	Sample type	Concentration	A260/A280	A260/A230
1	Protein (unprocessed serum)	40 mg/mL	0.64	NA
	Protein	9 mg/mL	0.74	NA
	DNA	16 ng/ μ L	1.1	0.19
	RNA	21 ng/ μ L	1.5	2.3
2	Protein (unprocessed serum)	42 mg/mL	0.64	NA
	Protein	2.21 mg/mL	0.65	NA
	DNA	1.2 ng/ μ L	0.92	0.2
	RNA	1.4 ng/ μ L	1.418	0.027
3	Protein (unprocessed serum)	41 mg/mL	0.64	NA
	Protein	2.26 mg/mL	0.69	NA
	RNA	1.7 ng/ μ L	0.835	0.034
	DNA	0.59 ng/ μ L	0.54	0.037

2.5 DISCUSSION

Protein phosphorylation is a pivotal regulator of numerous intracellular functions through various signaling cascades (525). Research suggests that its dysregulation is involved in the pathogenesis of diseases such as cancer, neurodegeneration and CVD, as well as potentially linking psychosocial stress and pathology (122, 391, 509, 553, 645) (refer Chapter 1). However, its analysis poses significant challenges due to the masking effects of high abundance proteins (386). Techniques such as affinity chromatography must therefore be employed to enrich such specific populations to then gain mechanistic insights into the role of dysregulated phosphorylation and diseases onset and progression. In unison with the aim outlined in Chapter 1, the aim of this chapter was to establish and validate a unique intact phosphoprotein retrieval method.

2.5.1 The efficiency of the unique phosphoprotein enrichment technique

The proposed unique phosphoprotein enrichment technique was tested using OVA which is known to be phosphorylated (335). Moreover, protein determination of the various fractions yielded inconsistent results (refer Appendix B) which could be due to the chemical nature of each method, the detectable limits (116, 589) and the protein-to-protein variation involved for detection (i.e. BSA versus OVA measurements) (651). The phosphorylation of OVA was first investigated by SDS-PAGE fluorescent staining. This was done as dephosphorylation may occur in the absence of protein phosphatases (254). We therefore analyzed this on a 4% - 20% gradient gel and it was evident that OVA was phosphorylated (Figure 2.2B). Moreover, the protein was stored at 4°C and not subjected to extreme conditions which could have resulted in phosphate loss.

The intact protein enrichment technique was assessed using SDS-PAGE analysis. Figure 2.3A represents the positive control employed (Zr-IMAC beads with OVA) and shows the potential of the IMAC material to enrich 50 µg of intact phosphoprotein, as there are no other bands present in lanes 2-4. However, when assessing the results of the negative control (Figure 2.3B), the phosphoryl beads bound all the OVA with which it was incubated. This type of bead should not bind any protein as it does not possess the Zr⁴⁺ ion that attracts the negatively charged phosphate moiety of proteins. An explanation for this occurrence could be the mesoporous structure of the bead, as many enrichment strategies employ porous particles for greater surface area to provide increased binding (713). Coupled with the complexity of native proteins compared to peptides (201), OVA may have lodged within the pores of the bead. The longer incubation and constant agitation of the elution step could then have resulted in the retrieval of OVA. This demonstrates that the mechanism of interaction between the microparticle and the intact phosphoprotein is non-specific. In addition, the adapted elution procedure utilizing EDTA may not be useful as the stripped beads could retrieve OVA and could indicate that the new elution mechanism is unable to chelate the Zr⁴⁺ ions.

2.5.2 The presence of nucleic acids in rat serum

The presence of nucleic acids in biological samples could interfere with phospho-retrieval techniques for proteomics (201). With regards to serum, literature indicates that the levels of nucleic acids are relatively low (218, 352, 383). A TRIzol extraction was utilized to assess the levels of nucleic acids in our rat serum to ensure that this would not interfere with enrichment. Table 2.2 displays the results obtained from this experiment. The purity ratios for all three experiments were not optimal. An A260/280 ratio for DNA and RNA of ~1.8 and ~2.0, respectively, would usually be considered as pure (652). The obtained ratios for all three repeats demonstrate the presence of contaminants such as protein and phenolic compounds (406, 653) of which the latter forms part of the TRIzol reagent (541). Experiments 1 - 3 produced less protein than was first determined in the unprocessed serum. Variance between replicates may have influenced the macromolecular measurements as all three replicates were obtained from different male rats. In addition, pipetting errors may have occurred and also result in the variable measurements. Despite the relatively low levels of nucleic acids found in the rat serum (on three different occasions), protein levels were still 6-fold higher. Thus, for the phosphoenrichment of serum we conclude that the presence of nucleic acids would cause minimal to no interference.

2.6 CONCLUSION

The results from our OVA enrichment with Zr-IMAC beads demonstrate that intact phosphoprotein retrieval is non-specific and thus not feasible to pursue. There is an even higher probability of non-specific enrichment occurring in samples such as serum that display a relatively high dynamic range. The implementation of a technique which is meant for phosphopeptide enrichment is therefore not recommended for protein retrieval. Lastly, enriching serum phosphoproteins/peptides should not be hindered by the presence of serum nucleic acids as their levels are relatively low.

2.7 LIMITATIONS AND FUTURE RECOMMENDATIONS

The main limitation is that Zr-IMAC material intended for phosphopeptide retrieval was employed for protein enrichment and hence future experiments should employ other methods such as that described by Jaros *et al.* (2012, 2015) for phosphoprotein enrichment (301, 302). Iron-oxide (285, 542) and cobalt ferrite (103) nanoparticles

were also employed for phosphoprotein enrichment and thus smaller particles should be used in the place of microparticles. The Zr-IMAC particles should therefore only be utilized for phosphopeptide retrieval as done previously (351, 571, 729).

**CHAPTER 3 - THE ENRICHMENT OF GLYCOPROTEINS USING LECTIN
AFFINITY CHROMATOGRAPHY**

3.1 INTRODUCTION

Glycosylated proteins attract interest from the scientific community due to their integral role in various biological processes (533). This complex form of PTM refers to the enzyme-catalyzed reaction whereby a glycan moiety is attached to the peptide backbone, resulting in a biological response (533, 698). The overall roles of glycosylation include alterations in cell-to-cell communication, protein folding and immune reactions (477, 698). It is known that glycosylation is one of the most common and heterogenous forms of PTMs in the proteome (540, 574). Such modifications also play a role in pathology as evidence shows that their aberrant attachment leads to congenital disorders, CVD and cancer (436, 477, 495, 533, 679).

Despite their relative importance, protein enrichment from samples with a high dynamic range remains a dilemma due to the masking effects of highly abundant proteins. This results in difficulties in terms of its analysis and therefore enrichment first needs to occur (540). Although the repertoire of glycopeptide/protein retrieval techniques has expanded (385), a universal method in this instance still does not exist (540). Moreover, commercially available enrichment kits are expensive and have limited usage (217, 654). Thus, the choice of enrichment must be specifically designed to match the aim and constraints of the intended study. For the current investigation, the intact protein level enrichment method was chosen as it is applied in glycoproteomics (194, 243, 661) and may assist with improved protein identification later-on in the workflow (325). This method was designed to suit the capture of glycoproteins from rat serum by first evaluating its efficiency with a test protein. This was followed by the adaptation of deglycosylation as it forms an integral part of glycoproteomics (46, 648).

3.1.1 Enrichment strategies for glycoproteins

Glycosylated protein enrichment regularly employs functionalized particles which involve HILIC, hydrazide chemistry, boronate affinity chromatography, IMAC/MOAC and lectin affinity chromatography (LAC) (68, 305, 380, 540, 661, 707). Each method has its own advantages but is also not without disadvantages. For example, HILIC is well-characterized and has been utilized in glycoproteomic sample preparation (287, 453, 485) as the attached glycan moiety imparts a degree of hydrophilicity which

enables separation from an organic loading buffer (251). This technique was previously involved in serum and plasma glycoprotein retrievals but only at the level of peptide compliance (453). Furthermore, it is not the most favorable technique due to the hydrophilicity of non-glycans and concealment of glycans (518) that can result in non-specific interactions. Hydrazide chemistry is an additional and widely employed technique for enrichment and requires periodate oxidation of sialyl groups that results in an aldehyde with which hydrazide groups can react (482, 736). However, a drawback includes side reactions that may occur during this process, as well as a lack of specificity of this method (280, 385). It has also mainly been used for glycopeptide enrichment (482).

Boronic acid-based enrichments utilize the affinity of boronic acids for cis-diol-containing moieties (305). However, this approach is not useful for intact protein retrieval as an alkaline pH is necessary for binding, coupled with dissociation at an acidic pH (68, 707). The weak boronate ester bond also results in weak glycoprotein adsorption, relatively poor selectivity and adsorption of non-glycoproteins (68, 305, 707). Immobilized metal affinity chromatography and MOAC may also be employed for glycoprotein enrichment (362). This employs similar binding modes as discussed in Chapter 2 where deprotonated carboxyl groups on Asp and Glu enable enrichment (540). Metal oxide affinity chromatography material such as titanium dioxide particles can also enrich for glycosylated residues which contain sialic acid (362, 485). Conversely, immobilized metal affinity enrichment focuses on *N*-linked glycopeptides as they can be enriched with iron (III, III)-IMAC and titanium (IV)-IMAC (339, 362). However, this has mainly been employed for glycopeptide enrichment (339, 362, 485, 486) and presents with similar limitations for protein enrichment as mentioned in Chapter 2, such as low pH buffer usage (362, 485). These reasons do not exclude the use of magnetic particles as support structures for enrichment methods such as LAC.

3.1.2 The use of lectins for affinity chromatography

Plant lectins have been widely used for decades and are considered one of the most significant discoveries of the century (286, 458). These proteins are not only applied for the separation of biological molecules, but also in clinical environments for drug delivery (318, 331, 716). Such widespread usage stems from their ability to recognize specific carbohydrate components on cell surfaces, proteins and lipids, as well as their

sensitivity to changes in glycosylation patterns (194, 586, 715). All plant lectins exhibit the ability to bind reversibly to a specific mono- or oligosaccharide through the possession of a catalytic domain(s) (732). ConA, wheat germ agglutinin, jacalin and ricinus communis agglutinin I are among the most popular ones (210). Drawbacks of LAC include the weak interactions with glycoproteins and also that no lectin contains an affinity for all potential glycan structures (194).

To combat the limitation of specificity, researchers make use of multi-lectin affinity approaches for the enrichment of glycoproteins (243). For example, Totten *et al.* (2018) employed three lectins on a HPLC system to investigate glycoprotein levels in prostate cancer patients, while Durham *et al.* (2006) studied the human blood proteome using lectin columns in a serial manner (178, 661). Furthermore, wheat germ agglutinin only exhibits an affinity for GlcNAcylated residues. However if it is paired with others such as ConA, a broader range of protein enrichment can be achieved (540). ConA is the most extensively used lectin due to its ability to bind high mannose residues arranged in a branched or terminal manner (58, 139, 237, 732). In light of this, we chose to immobilize this lectin on a specific support structure for the purification of glycoproteins.

3.1.3 Support structures for lectin affinity chromatography

The choice of support structure is pivotal for the application of LAC in sample preparation workflows (243). Formats of support structures include monoliths, column setups, silica particles, and magnetic microparticles/beads (45, 217, 458, 527, 640). Silica particles are traditionally used for their high pressure resistance and variability in particle and pore size. However, their application can include drawbacks such as limited pH stability, and the presence of increased silanols which may interact with basic compounds and result in decreased chromatographic performance (629). Monoliths are a continuous porous sorbent which contains varying sized pores (243) and offer advantages such as high permeability and high porosity, which also saves time for analysis (180). However, irreversible binding, clogging and the loss of small molecules decrease its efficacy (523). Commercial lectin affinity materials usually consist of agarose-based materials (243) and exhibit low non-specific binding to proteins and a hydrophilic surface area large enough for proteins to diffuse into.

However, they are known for limited chemical, biological and mechanical stability (243, 272, 446) whereas magnetic microparticles are regularly used (13, 243, 517, 632).

Enrichment strategies for glycoproteins regularly adopt the use of magnetic microparticles as they exhibit a wide variety of beneficial characteristics. These include effective support of biological materials, high convenience, reversible binding and easy resuspension and separation from complex mixtures (286, 570, 732). They are also able to be combined with other proteins which increase binding capacity and specificity, while retaining magnetic durability (732). Chromatographic techniques using magnetic microparticles are well-established in various sample preparation workflows (243, 397, 412, 454). Coupling lectins with magnetic particles has been done previously, however, the use of these particles is not without limitations as magnetic aggregation, variations between different batches of the same beads and lack of reusability has been reported (412, 578). Despite this, they are relatively low-cost compared to other support structures, easy to use, stable under numerous conditions, useful for high-throughput experiments and easy to couple with multiple sample processing steps (397, 578). Magnetic microparticles are therefore often the first choice as a support structure in sample enrichment for cells, nucleic acids and proteins (286). Moreover, when coupled with LAC this can be effective for glycoprotein retrieval from complex samples such as serum (104, 414, 517).

The application of ConA for glycopeptide/protein retrieval has been well-documented (16, 65, 165, 286, 371, 575, 716). Furthermore, this lectin has been employed for glycoprotein analysis of serum and plasma (104, 313, 414, 519), for example Qui *et al.* (2008) utilized a ConA column for the enrichment of human plasma. However, the samples first underwent delipidation followed by immunoaffinity depletion (519). Similarly, Madera *et al.* (2008) depleted their samples with the Multiple Affinity Removal System column prior to enrichment with two different commercially available ConA agarose gels (414). Others did not employ a depletion strategy, but rather used a commercially available ConA resin coupled with 2-DE (104). Moreover, there are reports that ConA appears to possess a relatively low affinity for serum albumin (166) and contradicts the use of serum depletion strategies. However, we chose not to employ a depletion strategy for the reasons discussed in Chapter 1 of

this thesis. Furthermore, none of these methods employed carboxyl magnetic microparticles as the support structure for their enrichment.

3.1.4 ConA immobilized onto carboxyl magnetic microparticles

The coupling of ConA to magnetic beads for glyco-enrichment was previously achieved (13, 286, 517). For this chapter, unique carboxyl-functionalized magnetic microparticles were chosen for the covalent immobilization of ConA. The present carboxyl groups enable mild coupling to attain covalent immobilization since Glu and Asp constitute the majority of amino acids on protein surfaces (554). This is done by using a carbodiimide, i.e. 1-ethyl-3-(3-dimethylamino) propyl carbodiimide (EDC) (226, 696) as it is a convenient and relatively inexpensive water soluble crosslinker used to couple carboxyl groups to primary amines (95, 696). Limitations involving EDC crosslinking include reversion reactions and potential hydrolysis (696) due to EDC's secondary intermediate, *O*-acylisourea, which is unstable in aqueous solutions and may result in hydrolysis (650). For this reason, *N*-hydroxysuccinimide (NHS) is coupled with EDC to ensure covalent immobilization, as NHS forms a more stable secondary intermediate prior to amination (625, 680). In this reaction, EDC couples NHS to carboxyls, forming an NHS ester which allows for primary amine conjugation under physiological conditions (625, 650, 680). This enables the coupling of ligands such as ConA.

ConA exhibits an affinity for α -D-mannose and α -D-glucose which are branched in a terminal manner (65, 530). To prove the applicability of the affinity material, a known glycosylated protein such as OVA can be employed as it contains a single *N*-linked glycosylation site at the Asn292 residue (266, 635). The glycan present on the Asn292 residue consists of [Mannose]₅[*N*-acetylglucosamine]₂ / [Mannose]₆[*N*-acetylglucosamine]₂, constituting ~2 kDa of the 45 kDa (266). Previous studies employed ConA affinity material to enrich OVA (394, 531, 632, 692). For example, Liu *et al.* (2015) employed silica-bonded ConA (394) whereas Sugawara utilized magnetic particles as the support structure (632). Additionally, Reichelt *et al.* (2012) immobilized ConA onto monolithic material (531). This points towards the applicability of employing OVA to test ConA affinity material, irrespective of the support structure to which ConA is immobilized. For a sugar residue to be bound by the lectin, ConA must undergo a conformational change through its interaction with manganese and calcium cations

(530). Furthermore, a competing sugar is needed to elute the protein for downstream applications (286, 649). Deglycosylation is another important aspect of glycoproteomics which ensures HPLC-MS/MS compatibility (540).

3.1.5 The importance of deglycosylation in proteomics workflows

Bottom-up proteomics exploit proteins which have been proteolytically cleaved into constituent peptides for MS analysis (30). Proteases such as trypsin and chymotrypsin can be applied here and a requirement is an interaction with their respective “cutting sites” (refer Chapter 4) (401). Glycans increase the structural complexity of proteins and can often block such cutting sites to thereby lower confident protein identification especially under limited sample conditions (46). Thus, deglycosylation is employed to circumvent this obstacle (46). This can occur enzymatically and chemically, although neither is without drawbacks (46, 179, 490).

Enzymatic deglycosylation employs glycosidases such as peptide N-glycosidase F which cleaves between the Asn residue and the innermost N-acetylglucosamine (623). Although it exhibits few caveats, it is universally employed as it assists with O-glycoproteomic data interpretation (623). This is possible as the removal of larger N-linked glycans assist with complete digestion to enable MS analysis and to retain O-glycopeptides (623). An unfortunate drawback is that the non-enzymatic re-addition of N-glycans was observed and can therefore introduce artifacts (324). It also often requires the addition of denaturing agents for the process to fully proceed (183). In light of this, the use of hydrazine for release of both N- and O-linked glycans is possible but not favorable, due to long preparation time and hydrazine toxicity (455). The β -elimination (base hydrolysis) with Michael addition is another method for glycan release while still confidently identifying the glycosylation site (694). A drawback here includes the introduction of artifacts, as well as difficulty in distinguishing between glycosylation and phosphorylation (540, 646).

Chemical deglycosylation with TFMS is another approach to non-specific glycan removal. Its effectivity is based on acid volume employed, reaction time, free radical scavenger use and temperature (183). This mode preserves the core protein and can remove the sugar moieties of complex glycoproteins, although certain glycans still remain such as those on the innermost Asn (183). A limitation is the non-specific

removal of glycans as it complicates the identification of O-linked sugars (183). Despite this drawback, this procedure is regularly employed as it chemical deglycosylation enables simple and affordable glycan cutting (183, 611). Moreover, PTMs such as phosphorylation remain intact and can be distinguished from glycosylation through TFMS supplementation (183).

By taking all this into account, we chose to make use of carboxyl surface-functionalized magnetic beads as an immobilization support for ConA. Chemical deglycosylation via TFMS was included after enrichment. This procedure was designed and performed according to previous literature and the supplied carboxyl bead protocol (refer Appendix C) (243, 286, 517, 535).

3.2 AIMS AND OBJECTIVES

The aims of this chapter is to a) construct and evaluate the enrichment efficiency of the unique ConA-functionalized carboxyl magnetic microparticles, and b) to ensure adequate deglycosylation of glycoproteins. For aim (a), we will couple ConA to Resyn Biosciences' carboxyl beads using EDC and NHS. We will then assess the coupling efficiency of ConA by employing the Nanodrop One to determine how much protein was covalently immobilized onto the magnetic particle. Furthermore, we will employ OVA as the control protein to evaluate whether the affinity material can bind specific glycan moieties. The carboxyl bead without ConA will be included as a negative control to assess the non-specific enrichment of the material. For aim (b), TFMS will be employed for non-specific deglycosylation of OVA. Different concentrations of acid at various time points will be tested to prevent protein degradation while maximizing deglycosylation. This will also be repeated with serum. Overall, protein determination and SDS-PAGE with total protein visualization and glyco-fluorescent staining will be utilized for analyses.

3.3 MATERIALS AND METHODS

Although product numbers and supplier details of the materials used for experiments are provided, we excluded certain information as it was already stated in Chapter 2. Furthermore, constituents of buffers and optimized protocols can be found in the relevant appendices.

3.3.1 Biological sample origin

Ethical approval was obtained from the Stellenbosch University animal ethics committee (ACU-2021-19400) (Appendix A). The rats were treated according to the Guidelines for the Care and Use of Laboratory Animals of the National Academy of Science (NIH publication no. 85-23, revised 1996), as well as the South African National Standard for the care and use of animals for scientific purposes (SANS 10386). The animals were handled by researchers authorized by the South African Veterinary Council.

Both male and female Wistar rats ($n = 16$ per sex) were chosen for the CRS model and were obtained at an age of around seven and a half weeks old. After one and a half weeks of handler habituation, plasma samples were collected for baseline measurements. This was done by employing isoflurane for anesthesia and drawing blood from the jugular vein. Plasma was then separated from whole blood using VacuCare blood tubes (AXI11EZZ, Axiology labs (Pty) Ltd., Gauteng, SA) and centrifuged (Eppendorf® Centrifuge 5810 R, Hamburg, Germany) at $1,500 \times g$ for 10 minutes at 4°C . The rats were then equally divided into the stress and control groups ($n = 8$ per group/sex) for the duration of the CRS protocol. Four weeks of restraint for one hour per day occurred between 10h00 and 11h30 for seven days of the week. After the four weeks, blood plasma was once again taken for end-point measurements and enzyme-linked immunosorbent assays were completed to assess plasma corticosterone and ACTH (results available in Appendix A).

Here, trunk blood was collected following rapid decapitation of the rats. Serum was obtained from whole blood using Vacuette blood tubes (456018, Greiner Bio-One, Kremsmünster, Austria) and centrifuged at $2,000 \times g$ for 10 minutes at 4°C . The serum fraction was separated into 4 mL microfuge tubes and phosphatase (PhosStop, 04906837001, Roche Holding AG, Basel, Switzerland) and protease inhibitors (Complete Mini EDTA free protease inhibitor cocktail tablets, 04693159001, Roche Holding AG, Basel, Switzerland) were added. Their initial concentration was determined according to the manufacturer's instructions and diluted 9.25X into the serum fraction. The fractions were further aliquoted into $\sim 600 \mu\text{L}$ portions into 2 mL DNA lobind microfuge tubes and stored at -80°C .

3.3.2 Building and testing novel affinity material for glycoprotein enrichment

MagReSyn® Carboxyl-functionalized magnetic microparticles were purchased from ReSyn BioScience's (MR-CBX002, Gauteng, SA) and stored at 4°C prior to use. 0.1 M 2-(N-morpholino) ethanesulfonic acid (M3671, Sigma-Aldrich, St. Louis, MO, USA), 20 mM EDC (22980, Thermo Fisher Scientific, Waltham, MA, USA) and 50 mM NHS (24500, Thermo Fisher Scientific, Waltham, MA, USA) were utilized to couple ConA (C2010, Sigma-Aldrich, St. Louis, MO, USA) to the beads. Five hundred micrograms of magnetic particles were inserted into a 2 mL tube and separated from the shipping solution. All separations were performed using Resyn Bioscience's magnetic separator (suitable for up to four tubes). The microparticles exhibit a binding capacity of ≥ 20 mg/mL BSA, therefore ConA has a 50% less binding capacity as it is almost double the size of BSA at physiologic pH (398). According to this, it is possible to immobilize ~ 250 μ g of lectin onto the bead. We therefore loaded ConA in excess, with ~ 500 μ g solubilized in phosphate buffered saline (PBS, pH 7.4, P4417, Sigma-Aldrich, St. Louis, MO, USA). Once the carboxyl residues were activated after incubation with EDC and NHS, the particles were equilibrated in PBS and then allowed to couple to the lectin overnight at 4°C. Each incubation step took place with gentle agitation at either 60 rpm (Rocker 25, Labnet International, Inc., Edison, NJ, USA) or a fixed rotational speed.

The unretained ConA fraction was removed the following day and stored for protein determination using the A280 assay on a NanoDrop™ One (ND-ONEC, Thermo Fisher Scientific, Waltham, MA, USA). Following this, any remaining unbound protein was washed away with PBS whereafter the lectin-bound microparticles were incubated in 200 mM ethanolamine (E9508, Sigma-Aldrich, St. Louis, MO, USA) for three hours at 4°C to quench remaining active residues. The affinity material was then washed with 1M NaCl (S9888, Sigma-Aldrich, St. Louis, MO, USA) to remove non-covalently bound particles. Numerous studies employed ConA affinity chromatography and therefore a variety of protocols exist (217, 575, 614, 654). Since it is also one of the most commonly used lectins (210), its function is well-defined and the protocol was constructed based on existing literature and product information (24, 202, 393, 535, 597). Table 3.1 briefly explains the choice of buffers and their uses.

Table 3.1 The buffers, their respective constituents, and explanations for use. ConA, concanavalin A.

Buffer	Buffer constituents	Explanation
Loading buffer	PBS (0.01 M phosphate buffer, 0.0027 M potassium chloride and 0.137 M NaCl, pH 7.4), 1 mM MnCl ₂ , 1 mM CaCl ₂	PBS is a non-toxic solution which is used in a variety of biological applications at physiologic pH (424). Other loading buffers usually consist of Tris with the addition of salt at pH ~7-8 (24, 202, 217); however, PBS already contains salt which can assist with protein solubility and enhance enrichment (614). Moreover, ConA requires metal cations such as Mn ²⁺ and Ca ²⁺ for sugar binding (530).
Wash buffer	PBS	This was employed to remove any unbound/non-specifically bound/residual proteins.
Elution buffer	100 mM methyl- α -D- mannopyranoside in PBS	Various concentrations of this competing sugar are employed for glycoprotein elution. A range between 50 mM to 200 mM is regularly used (210, 614). We chose 100 mM to limit interference with protein determination and sample clean-up in later workflows. Higher concentrations of competing sugar can negatively affect enrichment (196, 649).

After washing with NaCl, more washing with PBS was done before the incubation of glycoproteins with the affinity material. Here, the loading buffer consisted of PBS with metal cations (1 mM manganese (II) chloride, 244589 and 1 mM calcium chloride, C1016, Sigma-Aldrich, St. Louis, MO, USA), and the sample and material were allowed to mix overnight at 4°C.

Fifty micrograms of OVA (A5503, Lot number SLCH2421, Sigma-Aldrich, St. Louis, MO, USA) was incubated with 25 μ L and 50 μ L of affinity material, respectively. This amount of protein was chosen due to the overloading of the affinity material in the original thesis, and we therefore reduced the original amount by 400X. The incubation period ended the following day by removing the supernatant (stored as the unretained fraction), washing with PBS to remove non-specifically bound protein (stored as the wash fraction) and eluting three times for 10 minutes each. The eluent consisted of 100 mM methyl α -D-mannopyranoside (67770, Sigma-Aldrich, St. Louis, MO, USA) which competes for lectin binding sites. Serum samples obtained from rats were enriched in the same way as detailed in the original thesis, but were only incorporated to assess deglycosylation. Total protein measurements of the unenriched serum sample, the enriched fraction, the PBS wash fraction, and the eluted fraction were taken with an A280 assay using the NanoDrop™ One as previously described (refer

to Chapter 2). All protein concentration measurements were calculated according to the total volume of the fraction. The subsequent eluates were pooled, lyophilized with a bench top freeze dryer (refer Chapter 2), and resuspended in PBS for protein determination and SDS-PAGE and staining analysis. The unretained and wash fractions were included for this analysis. Storage of the material occurred at 4°C in 0.05% sodium azide (S2002, Sigma-Aldrich, St. Louis, MO, USA) in PBS (refer Appendix C for full protocol details).

3.3.3 Ensuring sufficient deglycosylation for downstream analysis

Chemical deglycosylation was adapted from the available protocol of Sigma-Aldrich's kit (refer Appendix C, PP0510, Sigma-Aldrich, St. Louis, MO, USA). For testing, we extracted a small portion of the eluted fraction from the OVA enrichment test. It is important to note that the OVA used here was from a different lot (lot number 118K7002, Sigma-Aldrich, St. Louis, MO, USA). We also utilized the same volume of the eluted fraction from our 50 µL serum sample enrichment for deglycosylation testing. To identify the optimal incubation period and volume of TFMS, we performed stepwise deglycosylation experiments. We employed 1 µL, 5 µL and 10 µL volumes of TFMS over a period of 1, 2 and 3 hours, respectively. The inclusion of a control sample (no acid added) allowed for monitoring over the same reaction timeframe and for the comparison of deglycosylation effectivity. A supplementary experiment which consisted of 1 µL and 2 µL of acid was also done by employing the same time limits for serum deglycosylation. TFMS (347817), anisole (296295) and pyridine (360570) were all purchased from Sigma-Aldrich (St. Louis, MO, USA). Anisole was employed as a free radical scavenger while pyridine acted as a strong base for acid neutralization.

Anisole and TFMS were combined prior to sample addition, with 1 µL of anisole present in each acid fraction. The OVA/serum sample was first added to a 1.5 mL glass vial, followed by the addition of the precooled acid-scavenger solution. The reaction was allowed to continue for 1, 2 and 3 hours, respectively, with regular mixing at 4°C. Once the respective reaction times were complete, a dry ice methanol bath was prepared as the addition of 60% pyridine for neutralization results in a highly exothermic reaction. An equal amount of the pyridine solution was first added to

neutralize the samples undergoing deglycosylation, followed by rapid cooling with a dry ice bath. Thereafter, an additional equal volume of pyridine solution was added that ensured the complete endpoint of deglycosylation. 50 μ l of ultrapure water was added before the respective samples were transferred into tubes and centrifuged (E-C15-24.P2R, Eins-Sci, Gauteng, SA) at 10, 000 $\times g$ for 5 minutes. The supernatant was separated from the resultant pyridinium TFMS salt and placed into a new 2 mL tube which underwent vacuum centrifugation (Eppendorf Concentrator 5301, Eppendorf, Hamburg, Germany) at 45°C overnight. Sodium dodecyl sulfate polyacrylamide gel electrophoresis and gel staining were employed for analysis of deglycosylation. Figure 3.1 demonstrates the workflow until this point.

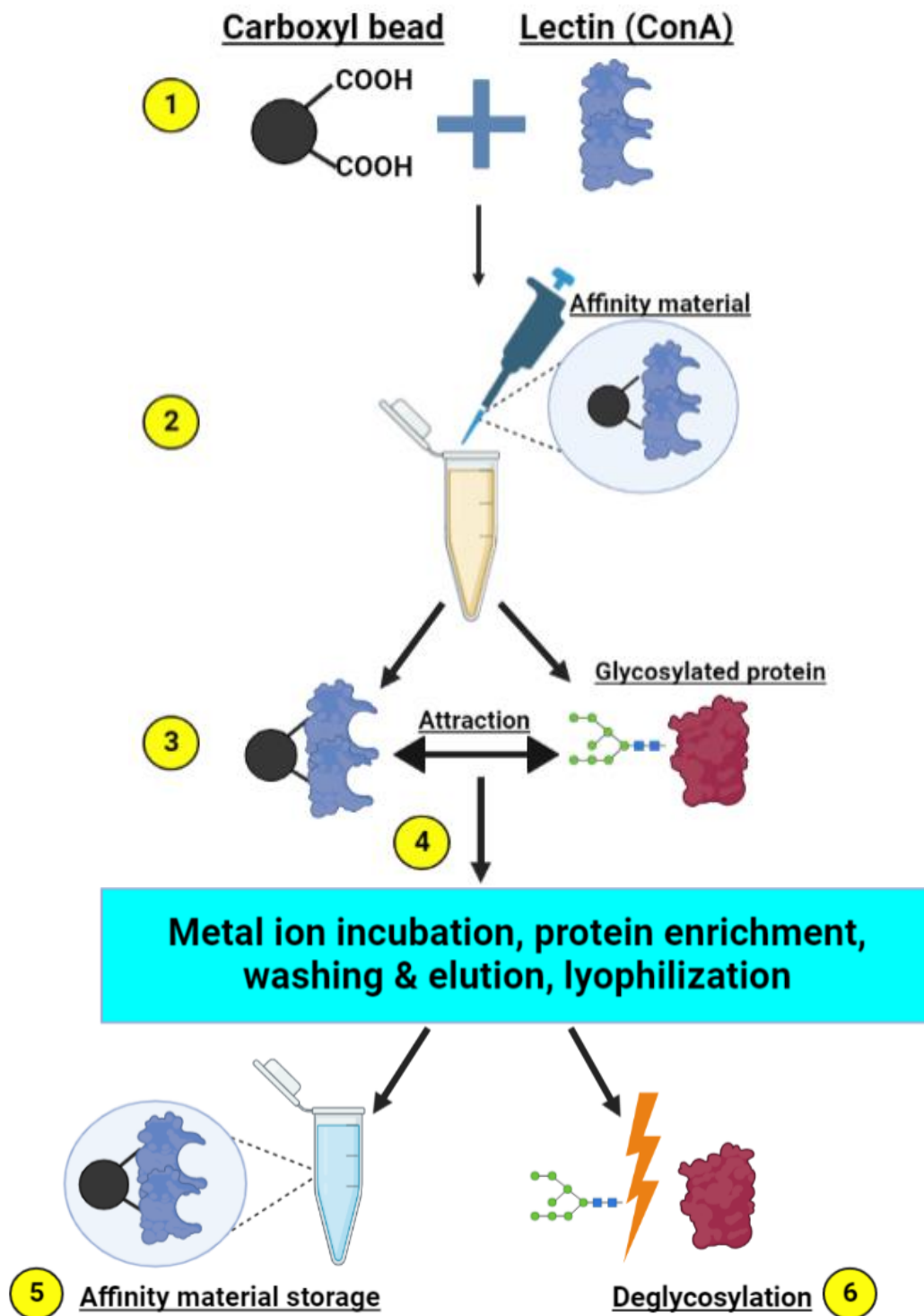


Figure 3.1. A basic representation of the workflow in building, testing, and utilizing the novel affinity material. Step 1: Lectin-bead binding step; Step 2: Incubation with sample; Step 3: The affinity of ConA for specific glycans; Step 4: Protein retrieval and processing; Step 5: Affinity material storage; Step 6: Deglycosylation. ConA, concanavalin A. Image created using Biorender.com.

3.3.4 Protein determination and SDS-PAGE analysis

The SDS-PAGE and total protein visualization analyses occurred as described in Chapter 2. The separation of proteins was performed according to the protocol produced by Dr. Danzil Joseph (Department of Physiological Sciences, Stellenbosch University) (refer Appendix D). The protein ladder was the same as employed in Chapter 2. For all OVA (in the case it being the sole protein used) and deglycosylation results, a 10% hand-cast gel was utilized with 2X Laemmli buffer added to each sample in a 1:1 ratio. Fifty micrograms of OVA were solubilized in PBS and then prepared to be analyzed with fluorescent staining. The gel analysis for this was done using a 4% – 20% TGX mini protein gradient gel (456-1094, Bio-Rad Inc., Hercules, CA, USA).

3.3.4.1 Total protein and glyco-fluorescent staining

Glycoprotein fluorescent staining took place for the serum enrichment and serum deglycosylation experiments, followed by Coomassie staining for total protein visualization. The other gels were only stained with Coomassie (refer Chapter 2). The Pro-Q Emerald 300 gel and Blot Stain Kit (Invitrogen™, P21857, Thermo Fisher Scientific, Waltham, MA, USA) was employed for fluorescent staining. The glycoproteins are visualized through a reaction using periodate-oxidized carbohydrate groups which leads to a fluorescent signal (260). The signal is caused by the stain reacting with oxidized groups (aldehydes) (628) and it is highly sensitive by detecting as little as 0.5 ng of protein per band. Its efficacy has been proven and used previously (129, 260). Briefly, gels were fixed in a 50% methanol and 5% acetic acid solution for 45 minutes for a total of two washes. Gels were then washed twice with washing solution (3% glacial acetic acid) for 20 minutes prior to carbohydrate oxidation with periodic acid in 3% glacial acetic acid. The gels were washed for 1 hour whereafter fluorescent staining occurred (for 2 hours). After such staining the gels were washed twice for 20 minutes and imaging took place by employing the ChemiDoc™ MP Imaging System using Image Lab™ software (Universal Hood III, Bio-Rad Inc., Hercules, CA, USA). The image was taken with the Pro-Q Emerald 300 setting (filter 1, ultraviolet trans-illumination) (refer Appendix D for extended protocol with product and buffer information). Here, every washing and incubation step took place in polypropylene holders placed on rotational mixers (FMH200, Labotec, Gauteng, SA).

3.4 RESULTS

3.4.1 Protein determination results

The ConA unretained fraction was saved to determine the amount of lectin bound to the beads. We calculated ~ 250 µg of lectin to be bound to 500 µg of carboxyl beads and protein determination results confirmed that the average amount of lectin bound in our samples was ~170 µg – 240 µg. In addition, both Bradford and BCA assays were separately completed to determine the OVA amount in the respective fractions from the positive and negative control experiments. Here, inconsistent results (refer Appendix C) were obtained for both assays in relation to the starting amount of protein, like those obtained in Chapter 2. Protein determination of only the 25 µL experiment was done as we anticipated the same result when increasing the volume of affinity material for the following experiment. Moreover, the protein determination values for the 50 µL serum glycoprotein enrichment technique were retained in Appendix C (from the original thesis) as the elutes here generated were employed for deglycosylation analysis.

3.4.2 The glycosylation of OVA

Figure 3.2 shows the total protein and glyco-fluorescent image of OVA, with the total protein result (50 µg OVA) displayed in Figure 3.2A. The Coomassie-stained gel showed an OVA band at ~45 kDa, whereas glyco-fluorescent staining showed a faint signal at ~45 kDa (Fig 3.2B). The original (uncropped) gel images are available in Appendix C.

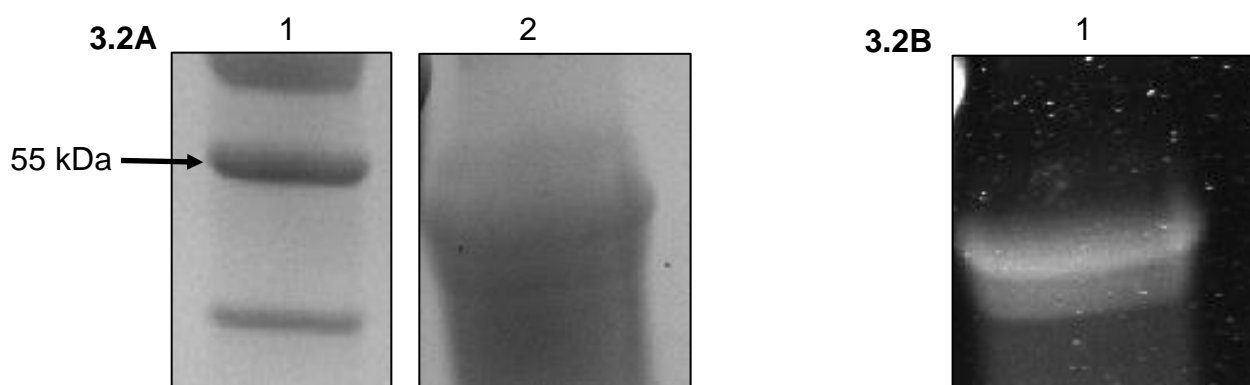


Figure 3.2. 4% - 20% gradient gel displays the (A) total protein stain of OVA and (B) the fluorescent intensity of OVA. **A** - Lane 1: Protein ladder; Lane 2: OVA. **B** - Lane 1: OVA fluorescence.

3.4.3 Testing the affinity material with OVA

Assessment of the enrichment for glycoprotein was tested using OVA as a positive control, as well as the carboxyl bead as a negative control. Here, 25 μ L of affinity material was incubated with 50 μ g of OVA. Figure 3.3 displays the stain-free results of this test where OVA bound to both sets of microparticles.

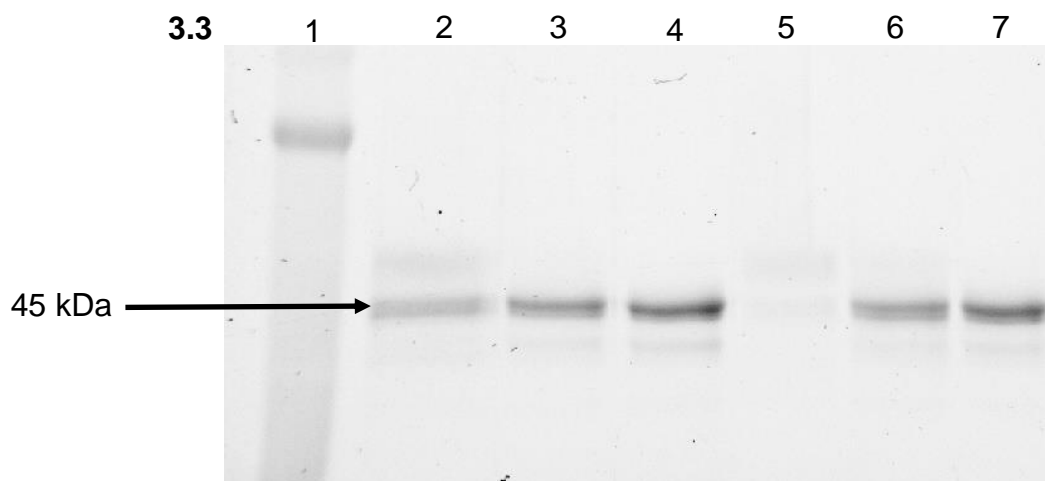


Figure 3.3 A stain free 10% mini-protean gel which displays the enrichment efficiency of the unique method. Here a positive (lanes 2-4) and negative (lanes 5-7) control was employed. Lane 1: Protein ladder; Lane 2: Unretained fraction; Lane 3: Wash fraction; Lane 4: Eluted fraction; Lane 5: Unretained fraction; Lane 6: Wash fraction; Lane 7: Eluted fraction.

3.4.4 Fifty microliters of affinity material employed with 50 µg of OVA

Figure 3.4 displays the SDS-PAGE results for increasing the amount of material utilized to enrich 50 µg of OVA. Figure 3.4A shows the ConA-carboxyl material, whereas Figure 3.4B displays the results from using the carboxyl beads as a negative control. These results were displayed on the same 10% mini-protean gel; however for lanes 1 – 3 (of Fig. 3.4B) the contrast was altered to visualize the protein present in the respective lanes. OVA bound to the material on both occasions. The original gel is available in Appendix C.

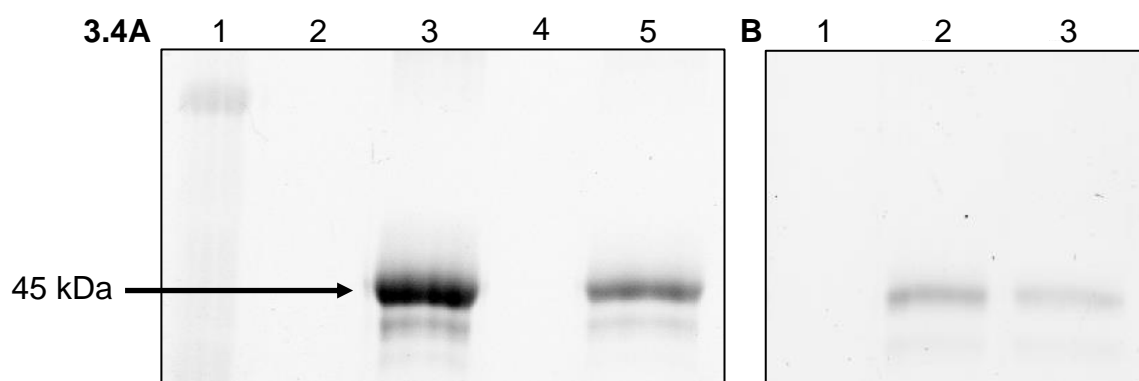


Figure 3.4 The total protein image of an increase in affinity material for enrichment for both positive (A) and negative (B) controls. **A** - Lane 1: Protein ladder; Lane 2: Skipped; Lane 3: Unretained fraction; Lane 4: Wash fraction; Lane 5: Eluted fraction. **B** - Lane 1: Unretained fraction; Lane 2: Wash fraction; Lane 3: Eluted fraction.

3.4.5 The efficacy of deglycosylation

OVA was employed to test the efficacy of various TFMS volumes for different reaction time periods. The respective volumes were 1 μL , 5 μL , 10 μL , partnered with time intervals of 1, 2 and 3 hours, respectively. Ovalbumin was employed as a control (lane 2), with it being combined with all the reagents (except for TFMS) and left to mix for the previously specified times. Lanes 9 – 14 indicate higher volumes of TFMS with protein degradation.

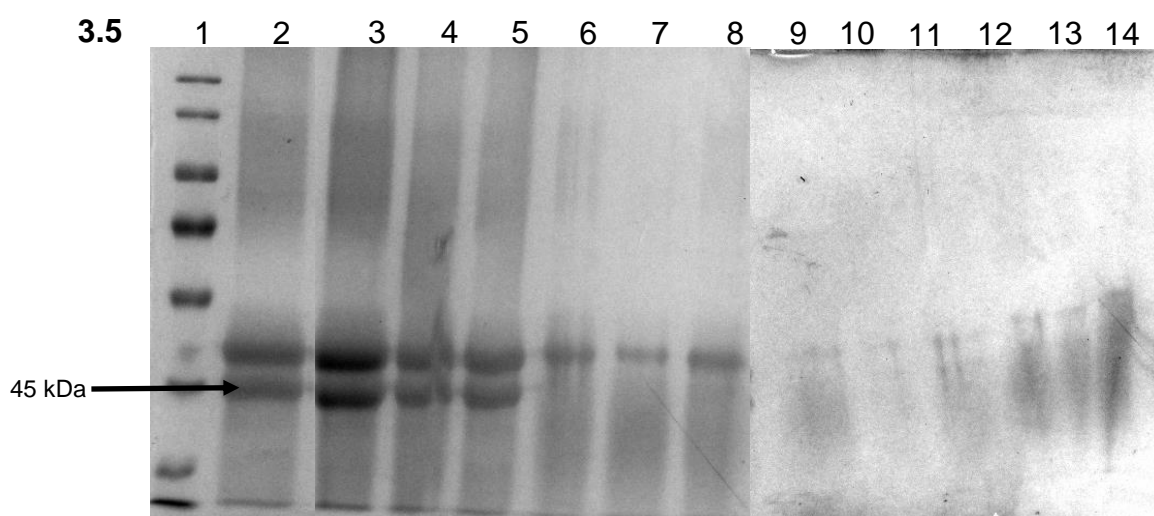


Figure 3.5. Optimization of chemical deglycosylation was assessed using increasing amounts of TFMS. Two 10% hand-cast gels were employed with Coomassie staining. Lane 1: Protein ladder; Lane 2: OVA control; Lane 3: 0 μL at 1 hour; Lane 4: 0 μL at 2 hours; Lane 5: 0 μL at 3 hours; Lane 6 : 1 μL at 1 hour; Lane 7: 1 μL at 2 hours; Lane 8: 1 μL at 3 hours; Lane 9: 5 μL at 1 hour; Lane 10: 5 μL at 2 hours; Lane 11: 5 μL at 3 hours; Lane 12: 10 μL for 1 hour; Lane 13: 10 μL for 2 hours; Lane 14: 10 μL for 3 hours. kDa, kilodaltons.

3.4.6 Serum deglycosylation

The eluted fraction from serum (50 μ L experiment) underwent deglycosylation based on the results of OVA deglycosylation (Figure 3.5). Following this, the eluted fraction from enriched serum underwent deglycosylation with 2 μ L of acid over the different time periods (Figure 3.6). Unfortunately, the 2 hour incubation period sample was lost during gel loading (Figure 3.8, lane 4).

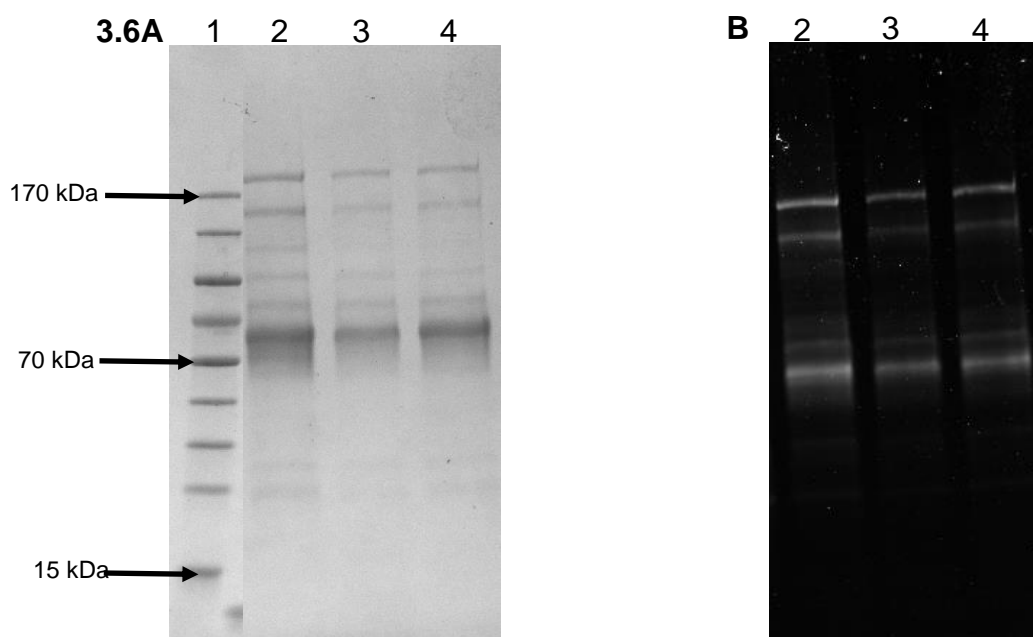


Figure 3.6. One microliter of acid was employed to deglycosylate serum for three different time intervals. 7A displays the total protein, whereas 7B displays the fluorescently stained gel. Lane 1: Protein ladder; Lane 2: 1 μ L for 1 hour; Lane 3: 1 μ L for 2 hours; Lane 4: 1 μ L for 3 hours. kDa, kilodaltons.

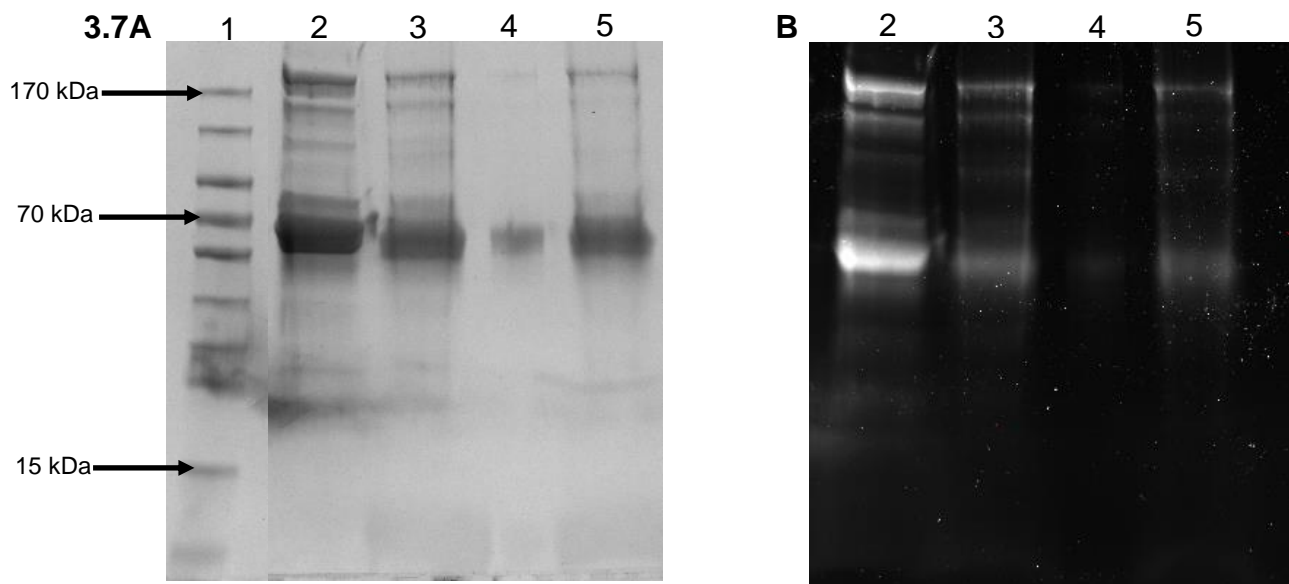


Figure 3.7. Two microliters of TFMS was employed for deglycosylation of the eluted serum fraction. The reaction was monitored for three different time periods, with Coomassie staining (A) and fluorescent staining (B) occurring. Lane 1: Protein ladder; Lane 2: Reference standard; Lane 3: 1 hour incubation; Lane 4: 2 hour incubation; Lane 5: 3 hour incubation. kDa, kilodaltons.

3.5 DISCUSSION

Glycosylation is the most complex protein PTM type and arguably the most abundant (574). Its involvement in diseases such as CVD, cancer and T2D has resulted in the burgeoning of the field of glycoproteomics where researchers aim to discover new methods to increase coverage of the glycoproteome for analysis (540, 704). However, it remains relatively understudied as analytical challenges continue to hamper its effective investigation (478, 648). Affinity chromatography is the mode of choice for protein purification as it enables the retrieval of low titer targets from complex mixtures (142). We opted to use LAC for the glycoprotein enrichment where unique affinity material was made using ConA and carboxyl magnetic microparticles. Testing occurred using multiple purified proteins and serum, with reusability and deglycosylation of enriched proteins also investigated. To the best of our knowledge, this specific material has not been created before.

3.5.1 Investigation of affinity material competence

The initial assessment of whether ConA was immobilized to the surface of the magnetic particles was done with an A280 experiment and it showed that enough lectin was bound to the beads as previously determined (refer Appendix C). This was indicative of the successful EDC/NHS coupling step, and we thereafter determined whether this new material could enrich glycoproteins. However, protein determination of the various fractions yielded inconsistent results (refer Appendix C) which could be due to the chemical nature of each method, the detectable limits (116) and the protein-to-protein variation involved (651). SDS-PAGE thus became the main method to assess the unique enrichment technique. Although OVA was employed to assess the enrichment of ConA affinity material (394, 531, 632, 692), we still assessed whether OVA was glycosylated. This was done using a 4% - 20% gradient gel which was visualized using a Coomassie stain and a glyco-fluorescent stain. Figure 3.2B reveals a fluorescent signal that shows OVA glycosylation.

The efficiency of 25 μ L of affinity material was thereafter assessed by incubating it with 50 μ g of OVA. The stain free image (Figure 3.3) showed that OVA was present in all three fractions of the positive control experiment. The negative control also bound OVA as there was protein present in the wash and eluted fractions

of this experiment. The results of our positive control experiment are in accordance with the findings of others who employed ConA enrichment of OVA (394, 531). For example, Liu *et al.* (2015) observed unbound OVA prior to the addition of methyl- α -D-mannopyranoside, and profiling of the glycan composition led them to believe that most of this fraction was non-glycosylated OVA (394). In addition, Reichelt *et al.* (2012) found excess OVA in the wash fractions of their experiment with specifically bound OVA present in the eluates (531). This shows that the OVA present in lanes 2 and 3 of Figure 3.3 could potentially be non-glycosylated. Magnetic microparticle size could also be a reason for our results as such differences were shown to affect ConA-OVA binding (632). Despite these potential explanations, the negative control showed that OVA was bound to the carboxyl bead (Figure 3.3, lanes 6-7). This highlights non-specific binding mechanisms and that further experiments are required to help clarify this.

Fifty microliters of affinity material and carboxyl beads were incubated with 50 μ g of OVA in a follow-up experiment (Figure 3.4). Here, we did not observe any proteins in the wash fraction, but only in the unretained and eluted fractions (figure 3.4B). This is in line with the findings observed by Liu *et al.* (2015) (394) and further demonstrates that non-glycosylated OVA may be the reason for non-specific binding. Moreover, isomers of OVA in relation to glycan composition and number were previously documented by others (294, 394, 506). Despite such plausible explanations, an increase in carboxyl microparticles resulted in OVA binding (Figure 3.4B). A significant contributing factor may be the structure of the beads as they are hyperporous (535). This would result in non-specific enrichment of OVA, with wash and elution steps causing the dislodging of protein adhered to the matrix. We therefore cannot conclude that the material enriches glycoproteins.

3.5.2 Ensuring deglycosylation for downstream analysis

3.5.2.1 OVA deglycosylation

The complete removal of glycan moieties via chemical deglycosylation with TFMS was first assessed using OVA. Various acid concentrations were employed – over a period of three hours - to remove its glycan moiety. Figure 3.5 depicts the acid concentrations with time for which the reaction was allowed to proceed. A double band appears in the

OVA molecular weight region and may be indicative of structural isomers consisting of a singly and doubly glycosylated residue (294). This was reported previously as changes in glycan structure can occur (294, 506). It is therefore possible that the isomer with two glycan structures is present at 47 kDa, whereas the expected singly glycosylated isomer of OVA is present at 45 kDa (294). Once these tests were complete, the 1 μ L volume of TFMS showed the disappearance of the 45 kDa OVA isomer. This can represent the applicability of glycosylation using such acid volumes.

3.5.2.2 Serum deglycosylation

Conditions for serum deglycosylation were upheld in relation to OVA glycan trimming, with only 1 μ L utilized for 1, 2 and 3 hours of reaction time. Little to no fluorescent signal should be obtained to enable the conclusion of successful deglycosylation. However, Figure 3.6B highlights a relatively strong signal intensity that indicates incomplete deglycosylation. Increased acid was then administered in a separate experiment utilizing enriched serum (Figure 3.7). Here, a much lower fluorescent signal is recognized especially after three hours of reaction time. The faint signal displayed is related to high molecular weight proteins (~170 kDa) as well as high abundance proteins (~60 kDa – 70 kDa). This may occur due to a greater number of glycans present on such proteins and increased albumin, both which could result in greater structural complexity of the sample and lessened glycan cutting (15). We thus concluded that 2 μ L of acid for a 3 hour reaction was sufficient to deglycosylate the retrieved protein. Following this, numerous sample preparation steps must be undertaken for compatibility with MS analysis.

3.6 CONCLUSION

ConA bound sufficiently to the carboxyl beads by employing carbodiimide-mediated coupling. Further assessment of the affinity material generated contradictory results as OVA presence in specific fractions was in accordance with previous literature that demonstrated glycoprotein enrichment (394, 531). However, OVA that adhered to the carboxyl beads showed that non-specific interactions occur. Thus, glycopeptide enrichment coupled with LC-MS may be more suitable to assess the enrichment capacity of the affinity material. In addition, moderate acid usage coupled to increased reaction periods enabled deglycosylation.

3.7 LIMITATIONS AND FUTURE RECOMMENDATIONS

Limitations include the choice of test protein as the literature indicates that OVA may have glycan isoforms that do not exhibit an affinity for ConA (394). We are thus unable to acknowledge the efficacy of the enrichment material. In addition, the porous structure of the carboxyl beads may increase non-specific enrichment. Future studies should aim to screen additional proteins (e.g. ribonuclease B) with a strong affinity for ConA (58, 394). Moreover, a different and/or validated matrix with fewer pores and a smaller size compared to the carboxyl particles should instead be employed, for example nanoparticles or agarose beads (217, 531).

**CHAPTER 4 - THE EVALUATION OF THE ENRICHMENT METHODS BY LC-
MS**

4.1 INTRODUCTION

Chapters 2 and 3 demonstrated that intact protein enrichment is not feasible as both sets of affinity material enrich in a non-specific manner. Hence a better approach would be to assess the use of this material by a conventional bottom-up experiment where the serum proteins are digested prior to enrichment. This chapter focuses on utilizing LC-MS/MS to compare this versus the intact protein enrichment method.

4.1.1 Chromatography as an integral tool

The high resolving power of HPLC is a considerable incentive for its inclusion in proteomic analyses (593). The broad selection of phases increases its ability to separate complex mixtures into simpler parts (593). For normal phase HPLC the stationary phase is polar while the mobile phase is non-polar. The opposite holds for reversed-phase HPLC that exhibits compatibility with most samples (589, 630). Columns consisting of C18 material are often exploited for the stationary phase, with the carbon chains bonded to silica or other supports (589). The most significant limitation of this approach is its low retention capacity of highly hydrophilic compounds (630). Solvents which differ in polarity are thus employed to optimize partitioning from the stationary phase for enhanced separation (630). For increased analytical sensitivity, nanoflow HPLC is employed to ensure higher chromatographic resolution (141). The flow rates involved here are in the nanoliter per minute range which contribute towards greater separation (141). Moreover, configurations such as column switching between a trap and analytical column enable higher separation, sensitivity and accuracy and minimal sample handling and organic solvent use (137). The former collects and concentrates the sample before it moves over to the analytical column (141, 609). Following this, a gradient elution procedure can be implemented by gradually altering the polarity of the mobile phase (445). Similar to other forms of LC, nanoflow LC is compatible with ionization methods such as electrospray ionization (319, 342) and enables the coupling of such processes for comprehensive proteomic investigation (319).

4.1.2 Electrospray ionization-MS/MS

Electrospray ionization is a soft ionization technique whereby peptides can be ionized for MS analysis (50). Briefly, liquid analytes that contain charged elements can

transition into gas phase ions through the generation of a fine spray (100). This occurs by feeding the solution through a needle held at high voltage (2 – 5 kV), with gas collisions and proton transfers aiding in ionization (2, 50, 100). This assists with the retention of structural information which is advantageous for acquiring PTM data (50, 314, 639). Following ionization, a mass analyzer separates such charged particles based on their m/z ratio (602). The analyzers can either be in the form of a Quadrupole, Time-of-Flight, Orbitrap and Linear Ion Trap (323, 602, 606). Each has its own specifications and limitations. For example, mass spectrometers containing an Orbitrap boast the advantage of high mass resolution, good detection and ease of operation (323, 739). Furthermore, hybrid instruments employ multiple mass analyzers to enhance MS/MS data acquisition processes (192).

Data-dependent acquisition (DDA) is commonly used for bottom-up experiments where the most abundant precursor ions observed in the MS1 scan are selected for fragmentation to produce the MS/MS spectra (55). This is advantageous as little (or none) processing is needed before the spectra can be used. However, a limited number of ions may be fragmented due to small variations between scan times and ion intensities (148). Moreover, lower reproducibility may be observed between technical repeats (55). Despite this, there are well-established free software tools to analyze the acquired data (250, 437). Such analysis is an important and complex component of the proteomics workflow (189). As mentioned in Chapter 1, important aspects of this step include the database search, the configuration thereof, and the validation of such data (189). Important parameters include the modifications set and the specificity of the enzyme used for proteolysis as this assists with peptide identification from the MS/MS data (133).

4.1.3 The role of trypsin

The stringent cleavage specificity of trypsin is the determining factor in its regular employment in bottom-up approaches (274). The kinetics and structure of this serine protease are well characterized as it cleaves at the carboxyl terminus of Lys and Arg (677). This results in fragments that usually range between 0.6 and 1 kDa (363). Additionally, the presence of basic residues at the carboxyl terminus that exist in balance with the free amine amino terminus is favorable for positive ionization (677). Despite its specificity, it can skip a cleavable residue which results in a missed

cleavage (479), for example when trypsin does not cleave Lys or Arg residues when followed by a Pro (677). Likewise, the presence of acidic amino acids (Asp and Glu) near the cleavage site can cause missed cleavages (603). Bioinformatics analysis takes this into account and allows for a set number of miscleavages (479).

Regardless of its wide use, a lack of general consensus exists regarding the parameters which govern its activity, i.e. incubation temperature, pH, type of trypsin used and enzyme to substrate ratio choice (401). A consequence of this is the reproducibility of results due to altered digestion conditions (85, 514). Recent advances in proteolytic techniques produced on-bead digestion which utilizes HILIC microparticles (631) that allow for sample purification by removing unwanted contaminants from the analyte (454, 472). Once the digestion procedure is complete, trypsin's proteolytic activity needs to be stopped (by either cooling or acidification) to avoid unwanted cleavages (677). Reversed-phase solid phase extraction (SPE) material can thereafter be employed to allow for further sample clean-up prior to LC-MS (71). The multi-dimensional process in terms of sample preparation therefore necessitates the implementation of an internal standard to ensure quality control (70).

4.1.4 Ensuring quality control in the proteomics workflow

The contemporary MS experiment consists of multiple intricate processes that assist in acquiring data for important research (70, 638). However, multiple steps in the proteomics pipeline impart a degree of variability that affects the outcomes of numerous workflows (70). The accuracy and reliability of results generated is thus at risk and hence there is a robust need for harmonization of such processes (70, 220). By implementing specific control checks to assess sample preparation and the instrumentation we will be able to judge the suitability of the entire process (75). Although strides have been made to produce a generic standard to determine the uniformity of proteomics experiments (4, 220, 367, 638), there is at present not a general consensus regarding which quality control methodology to incorporate (423). Likewise, the multiple steps in our proteomics workflow require quality control implementation as variation can result from multiple sources (500). Since the focal point of enrichment is glycosylated and phosphorylated proteins, a suitable control protein must be glycosylated and/or phosphorylated (341). Hen egg OVA is therefore a good candidate as its modifications have been well characterized (294, 335).

4.2 AIMS AND OBJECTIVES

The aims and objectives of this section relate to those mentioned in Chapter 1. Briefly, we aim to assess both enrichment methods by employing a conventional bottom-up approach in comparison to our initially described top-down method. Here, rat serum samples will first undergo tryptic digestion, followed by glycopeptide and phosphopeptide enrichment, respectively. Glycopeptides will undergo chemical deglycosylation followed by digestion again. Unenriched rat serum will be employed as controls for both techniques with OVA used as a positive control. Data acquisition will occur by LC-MS/MS and downstream bioinformatics processing for data interpretation. Furthermore, 50 µg of OVA will undergo glycopeptide and phosphopeptide enrichment, respectively, as an additional quality control measure. The number of spectra obtained from RAW files, phosphopeptide and glycopeptide PSMs and comparison between the enriched and control (unenriched) sample populations should assist in terms of determining the repeatability and efficacy of such forms of enrichment.

4.3 METHODS AND MATERIALS

Serum samples for proteomic analyses of the respective enrichment techniques were isolated from rats (refer Chapter 3). The product numbers, supplier details for reagents, and reagents not previously referred to are also mentioned in this chapter. The details for buffers containing multiple components are provided in the relevant appendices.

4.3.1 Sample size

To assess serum phosphopeptide enrichment, 8 rat serum samples were chosen for enrichment, whereas five rat serum samples were utilized as the control (unenriched) sample population. Two additional positive controls were added, i.e. OVA. The same approach was adopted for glycopeptide enrichment analysis, where a total of 8 samples were designated for enrichment, and 7 samples (five rat serum, two OVA) were included as controls. For both sets of analyses an OVA sample was employed for enrichment and served as a quality control check for each respective technique. A total of 32 samples was therefore employed with 16 (9 enriched, 7 unenriched) samples designated for the evaluation of each respective enrichment technique. All

rat serum samples were chosen randomly by noting the remaining unprocessed serum samples and allowing a random number generator to determine their group allocations. Approximately 50 µg of protein was extracted from each individual sample (including OVA) before the commencement of sample preparation.

4.3.2 On-bead digestion procedure

For digestion, the HILIC on-bead digest protocol from ReSyn Biosciences was followed (MagReSyn®, ReSyn Biosciences, Gauteng, SA) - refer Appendix E for full description of method. The protocol itself is designed for 50 µg of protein and this amount was extracted from the serum samples by first quantifying the initial protein concentration with an A280 assay using a Nanodrop One (ND-ONEC, Thermo Fisher Scientific, Waltham, MA, USA). OVA was weighed and diluted to 50 µg. All samples were suspended in 20 µL of 50 mM Tris-HCl, 2% SDS, pH 8. The only adaptations that were made to the digestion protocol included: replacement of dithiothreitol by tris (2-carboxyethyl) phosphine-HCl (C4706, Sigma-Aldrich, St. Louis, MO, USA) as the reducing agent at a final concentration of 5 mM for 1 hour at 37°C; employing S-methyl methane thiosulfonate (208795, Sigma-Aldrich, St. Louis, MO, USA) for alkylation at a final concentration of 10 mM for 30 minutes: 25 mM Tris pH 8 as the trypsin digestion buffer. Moreover, sequencing grade trypsin (VF11A, Promega, Madison, WI, USA) was utilized in a 1:50 ratio and all samples were left to digest for 18 hours at 37°C. Peptides were recovered with 1% trifluoroacetic acid (T6508, Sigma-Aldrich, St. Louis, MO, USA) and all samples were lyophilized in a bench top freeze dryer (refer Chapter 2). Samples were then centrifuged at 10 000 x g for 5 minutes at 4°C (E-C15-24.P2R, Eins-Sci, Gauteng, SA) followed by enrichment. The controls were stored at -80°C before any further preparation was needed.

4.3.3 Phosphopeptide enrichment

Phosphopeptide enrichment of the 9 designated samples was done according to ReSyn Biosciences' Zr-IMAC HP protocol (Appendix B). Briefly, dried samples were resuspended in loading buffer (0.1 M glycolic acid in 80% acetonitrile, 5% TFA) and centrifuged at 10 000 x g for 5 minutes at 4°C to remove any insoluble material. The supernatant was then incubated with 20 µL of equilibrated microparticles and left to mix for 20 minutes at room temperature with gentle agitation. Washing took place with the respective wash buffers, followed by elution with 1% ammonium hydroxide

(221228, Sigma-Aldrich, St. Louis, MO, USA). The elutes of each respective sample were collected into 1.5 mL microfuge tubes containing 50 μ L of 10% formic acid (695076, Sigma-Aldrich, St. Louis, MO, USA). These were once again lyophilized and stored at -80°C with the digested control fractions for LC-MS/MS analysis.

4.3.4 Glycopeptide sample processing

The samples designated for glycopeptide enrichment were resuspended in 50 μ L of PBS, pH 7.4, and enriched according to the unique ConA affinity material protocol discussed in Chapter 3. The pooled elutes of each respective sample was then lyophilized as discussed previously. Once this was complete, the control (unenriched) and enriched samples were resuspended in PBS and transferred to glass vials for deglycosylation (see Chapter 3). Briefly, all samples were incubated with 2 μ L of TFMS and 1 μ L anisole for 3 hours at 4°C under constant agitation, whereafter neutralization occurred with 60% pyridine. The neutralized samples were transferred to their respective 2 mL microfuge tubes and centrifuged at $10\ 000 \times g$ for 5 minutes at 4°C , followed by vacuum drying at 45°C (Eppendorf Concentrator 5301, Eppendorf, Hamburg, Germany). The dried samples were resuspended in 50 mM Tris-HCl, 2% SDS, pH 8, digested as previously mentioned and vacuum dried again. Once dry, all samples were stored at -80°C for LC-MS/MS at the Centre for Proteomic and Genomic Research (CPGR).

4.3.5 Data acquisition by LC-MS/MS

All 32 samples sent for LC-MS/MS were analyzed. The CPGR also created separate pools of the glycopeptide and phosphopeptide samples which acted as a quality control, as well incorporated their own quality control assessment of their instrumentation. Peptide samples were acidified and de-salted by ZipTip (ZTC18S096, Merck Millipore, Darmstadt, Germany) according to the manufacturer's instructions. Samples were then dried down before being resuspended in LC loading buffer 0.1% formic acid (56302, Sigma-Aldrich, St. Louis, MO, USA), 2% acetonitrile (BJLC015CS, Burdick & Jackson, Muskegon, MI, USA). LC-MS analysis was conducted with a Q-Exactive quadrupole-Orbitrap mass spectrometer (Thermo Fisher Scientific, Waltham, MA, USA) coupled with a Dionex Ultimate 3000 nano-UPLC system. Data was acquired using Xcalibur v4.1.31.9, Chromeleon v6.8 (SR13), Orbitrap MS v2.9 (build 2926) and Thermo Foundations 3.1 (SP4). Peptides were dissolved in 0.1% formic

acid, 2% acetonitrile and loaded on a C18 trap column (PepMap100, 9027905000, 300 μm \times 5 mm \times 5 μm). Approximately 400 ng of peptide was injected per sample. Samples were trapped onto the column and washed for three minutes before the valve was switched and peptides eluted onto the analytical column as will be described. Chromatographic separation was performed on a ReproSil-Pur 120 C-18-AQ column (Dr Maisch, r119.aq.n150.075, 75 μm \times 15 cm \times 1.9 μm) as described below. The solvent system employed was solvent A: LC water (BJLC365, Burdick and Jackson, Muskegon, MI, USA), 0.1% formic acid and solvent B: acetonitrile 0.1% formic acid. The multi-step gradient (summarized in Appendix E) for peptide separation was generated at 300 nL/min (for the majority of the peptide elution gradient) as follows: time change 1.5 min, gradient change: 2 – 5% Solvent B, time change 50 min, gradient change 5 – 18% Solvent B, time change 1 min, gradient change 18 – 30% Solvent B, time change 4 min, gradient change 30 – 80% Solvent B. The gradient was then held at 80% Solvent B for 5 minutes before returning it to 2% Solvent B for 5 minutes. All data acquisition was obtained using Proxeon stainless steel emitters (TFES523, Thermo Fisher Scientific, Waltham, MA, USA). The mass spectrometer was operated in positive ion mode with a capillary temperature of 320°C. The applied electrospray voltage was 1.95 kV. Details of data acquisition are shown in Appendix E.

4.3.6 Data interpretation

In total, 34 samples (which includes the pooled samples) were processed using the bioinformatics workflow. The Fragpipe Graphical User Interface version 20.0 was utilized for the comprehensive analysis of the acquired data. Here, MSFragger version 3.8 (345, 644) was employed for the database search and the input included RAW MS data, a sequence database and search configuration. The sequence database included the *Rattus Norvegicus* reference proteome (UP000002494) which was obtained from the UniProt database (47 942 entries, October 2023) (130). Decoys and contaminant sequences were added by employing the formatting function of Philosopher version 5.0 (143). It is important to note that upon closer inspection of the formatted sequence database, OVA was added as a contaminant, and this was used to interpret the OVA sample data acquired from LC-MS/MS. For configuration, the closed default search option was utilized, and a precursor ion mass tolerance and fragment ion mass tolerance of ± 20 ppm was selected. Mass calibration was turned off and we allowed for an isotope error of 1. The search was limited to strict trypsin

peptides of length 7 – 40 amino acids, the cut sites being Arg and Lys but not if they were followed by Pro. The peptide mass range was left as is (500 Da – 5000 Da) and we allowed for a total of two missed cleavages.

Thiomethylation of cysteine was set as a fixed modification, whereas the oxidation of methionine and *N*-terminal acetylation were set as variable modifications. In addition, phosphorylation of Ser, Thr and Tyr was specified as a variable modification for all the phospho-samples, whereas deamidation of Asn was specified for glyco-samples. All other specifications were left as set by the default closed configuration. The validation of the output data for peptide, protein and PTM identification was done using the Philosopher toolkit. Here, PeptideProphet (326) was employed for peptide assignment validation, PTMProphet (594) for PTM site localization (minimum probability set to 50%), and ProteinProphet (461) for protein inference (FDR set to 5%). Additional filtering settings were employed within the previously mentioned software over which we had no control, and the FDR for PSM and peptide identification converged to $\leq 1\%$. The visualization and further analysis of the data took place using the generated MSstats files, as well as PDV (381). Graphpad prism version 8.4.3 (GraphPad Software Inc., La Jolla, CA, USA) was employed to assess the covariance between sample populations by utilizing the RAW spectra generated for serum samples. Additional criteria which we set during data processing included the identification of PSMs, peptides and PTMs based on high confidence ($\geq 95\%$). From this data, we removed contaminants and assessed whether enrichment was successful by comparing the number of modified peptides present in the enriched samples in comparison to the respective controls. Deamidated peptides were further assessed based on whether the consensus sequence for *N*-linked glycosylation existed, thus demonstrating the potential of glycosylation at that site. The percentage of PSMs that displayed a phosphorylation or glycosylation modification was also determined, along with the identification of such modifications in our positive controls.

4.3.7 Supplementary SDS-PAGE experiments

A tricine-SDS-PAGE experiment was employed to assess phosphopeptide enrichment, as initial results from the total ion current chromatograms displayed little intensity in the phospho-enrichment population. Here, the protocol designed by Haider *et al.* (2012) was chosen for peptide visualization using the tricine gel running system

(255). The fractions for this analysis were generated using on-bead digestion and phosphopeptide enrichment as specified earlier. We employed 50 μg and 100 μg , respectively, of the serum protein digest to assess phosphopeptide enrichment. The respective fractions were lyophilized and resuspended in PBS, pH 7.4. The fractions were then added in a 1:1 ratio with a new sample buffer (Appendix D). A 16% gel was made according to the author's instructions (Appendix D) and samples were loaded as described for previous SDS-PAGE experiments (refer Chapter 2). Peptides were separated using the Bio-Rad PowerPac300 (Bio-Rad Inc., Hercules, CA, USA) set at 140 V until the dye front reached the end of the gel. Fixation took place for 25 minutes using a 5% glutaraldehyde solution which was diluted from a 50% stock (02612-AB, West Chester, PA, USA) followed by Coomassie staining and visualization as described previously (refer Chapter 2). A general description of the proteomics workflow is depicted in Figure 4.1.

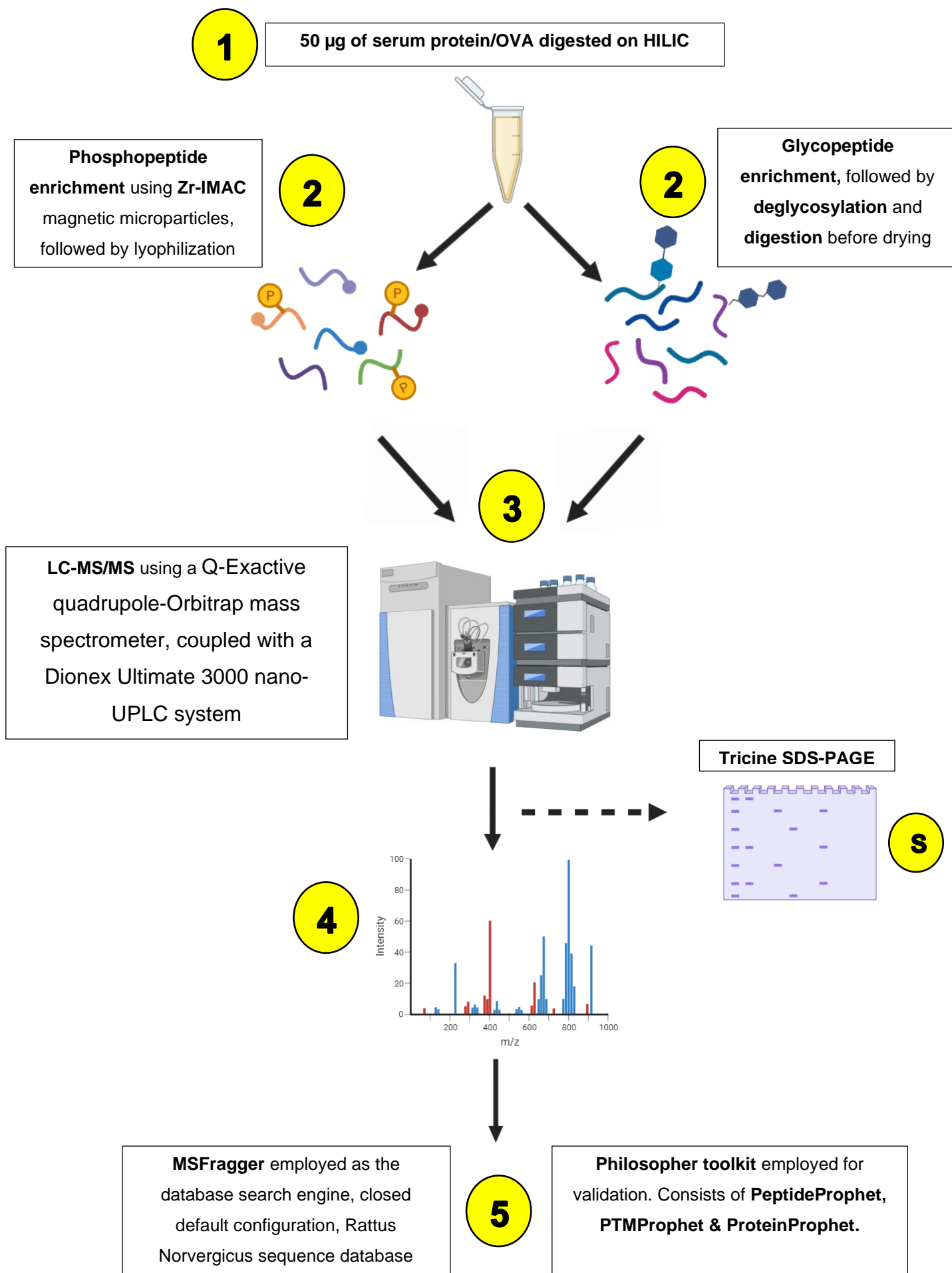


Figure 4.1. An overview of the proteomics workflow from sample preparation to data processing. HILIC, hydrophilic interaction liquid chromatography; Zr-IMAC, zirconium-immobilized metal affinity chromatography; LC-MS, liquid chromatography mass spectrometry; UPLC, ultra (high) pressure liquid chromatography; S, supplementary experiment; SDS-PAGE, sodium dodecyl sulfate polyacrylamide gel electrophoresis. Image created using Biorender.com.

4.4 RESULTS

All the LC-MS/MS results provided are based on the criteria we employed to confidently identify PSMs and peptides. A detailed table summarizing the number of PSMs, peptides and proteins for each sample is included in Appendix F. The raw data (RAW spectra, mzml files generated by Fragpipe, MSstatsfiles) is accessible on massive using the following link: <ftp://massive.ucsd.edu/v02/MSV000093117>, ID: MSV000093117.

4.4.1 The variation of the acquired data

The variance between samples within each sample population (using the RAW MS/MS spectra) was assessed with Graphpad Prism. This is shown in Table 4.1. Here, higher variance was found between samples for phosphopeptide enrichment versus controls, while the opposite was observed between the glycopeptide groups. Moreover, the glycopeptide samples displayed higher variance when compared to the phosphopeptide samples.

Table 4.1 The variance observed between each sample within their respective sample populations.

Sample population	Percentage variance
Phosphopeptide controls	2.3
Phosphopeptide enrichment	8.3
Glycopeptide controls	28.5
Glycopeptide enrichment	24.2

4.4.2 PSMs identified from RAW spectra

The fraction of PSMs produced from raw spectra was calculated and presented as a percentage of successful identifications in Table 4.2. The averages of the sample populations demonstrate that very few PSMs were identified and reported, especially for the glycopeptide sample population. The OVA samples were not considered in this instance, except when they were included with the pooled samples.

Table 4.2 The percentage fraction of PSMs identified and reported from raw spectral data. PSM, peptide spectral match.

Sample(s)	PSMs from raw spectra (%)
Phosphopeptide controls	24.7
Phosphopeptide enriched samples	1.6
Pool of phosphopeptide samples	3.9
Glycopeptide controls	<1
Glycopeptide control population	<1

Pool of glycopeptide samples	<1
------------------------------	----

4.4.3 The number of phospho- and glyco-PSMs identified

The number of phospho- and glyco-PSMs were analyzed within their respective sample groups only. The number of phospho-PSM identifications in the control group was 19, whereas none were observed in the enriched sample population (refer Appendix F). Conversely, numerous deamidated peptides were identified in the glycopeptide enrichment samples. For the controls 44 deamidated PSMs were identified and reported, while 26 was found in the enriched samples. Here, a single deamidated peptide present in replicate 8 of the enriched sample group possessed the consensus sequence for *N*-linked glycosylation (TSKAQEPDNKSVK). Overall <0.01% of PSMs were identified as modified. Table 4.3 gives an account of each observed phosphopeptide.

Table 4.3 Phosphopeptide sequences identified in their respective samples. A lower case ‘p’ represents the residue with the highest probability of phosphorylation, some of which possessed equally high probabilities. The (*) indicates that the specific phosphopeptide was observed multiple times.

Sample	Phosphopeptide
PC 1	pSHpSLpSQHTAISSK
	IDIPPpYEpSpYEKLYEK
	AFpSQpSpSDLTK
PC 4	AELAKpYMCENQATISSK
	NGFpYLAFQDYGGCMSLIAVRVFYR
	LEEDpYPQFSSPK
	IAPASQIDSAWIVpYNKPK
	GQLpTPRANELKATIDQNLEDLR
	TLEASGAVGLGpSQMMPGPK
	HAFSPVApSVEpSApSGEVLHSPK*
	HKPKApTEDQLKTVMGDFAQFVVK

4.4.4 The identification of phosphopeptides and glycopeptides in the positive controls

OVA was incorporated as a positive control for both phosphopeptide and glycopeptide enrichment technique analysis. Neither the phosphorylated residue nor the deamidated residue were observed in the OVA samples. Moreover, the peptide samples which were pooled for glyco- and phospho-enrichment acted as positive controls and were also used as a quality control. For the phosphopool, no phosphorylated residue was observed. Moreover, the glycopool displayed 42 identified deamidated sites, although none had the potential to be glycosylated as the

N-linked consensus sequence was absent. Table 4.4 displays the number of PSMs and peptides identified for each positive control. The number of PSMs between OVA controls in both phospho- and glyco-groups differ by more than 10-fold and 2-fold, respectively.

Table 4.4 The number of PSMs and distinct peptides present in the positive control samples. POVA, OVA employed as a control for phospho-enrichment; GOVA, OVA employed as a control for glyco-enrichment.

Sample	PSMs	Distinct peptides
POVA control 1	307	14
POVA control 2	18	9
Phosphopool	629	296
GOVA control 1	58	10
GOVA control 2	117	11
Glycopool	267	124

4.4.5 Enrichment of OVA

The enrichment of 50 µg of OVA was also employed as a quality control for each respective technique. For glycopeptide enrichment 12 PSMs and 5 distinct peptides were observed, none of which were deamidated. Further inspection showed that the start and end points of these peptides did not include Asn298. OVA that underwent phosphopeptide enrichment produced 369 PSMs and 16 distinct peptides. Here, three phosphorylated peptides were observed, of which one showed a high probability of phosphorylation in the vicinity of the noted phospho-Ser348 of OVA. The sequence here was: ISQAVHAAHAEINEAGREVVGpSAEAGVDAASVSEEFR.

4.4.6 Tricine-SDS-PAGE results

A tricine SDS-PAGE experiment was utilized to further assess phosphopeptide enrichment as low intensity was observed in the total ion current chromatograms at the beginning of data acquisition. Figure 4.2 displays the total protein images of 50 µg (lanes 2-5) and 100 µg (lanes 6-9) phosphopeptide enrichment fractions. Peptide is visible in lanes 1 and 6 which represent the respective unretained fractions. No peptide was visible in any other lanes. Due to the relatively low peptide weight these were near to the dye front which is unfortunately also visible, as gel running was stopped to prevent any sample loss.

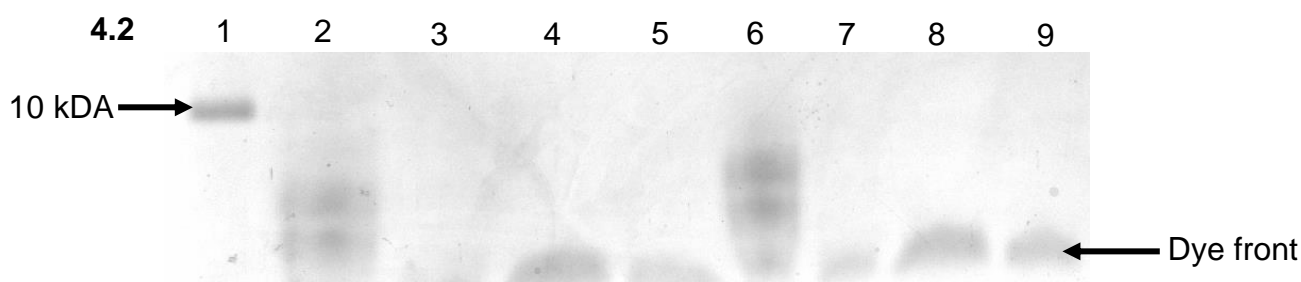


Figure 4.2 A 16% tricine gel was employed to assess phosphopeptide enrichment. Lane 1: Protein ladder; Lane 2: Unretained fraction; Lane 3: Glycolic wash fraction; Lane 4: Combined wash fractions; Lane 5: Pooled eluted fractions; Lane 6: Unretained fraction; Lane 7: Glycolic wash fraction; Lane 8: Combined wash fractions; Lane 9: Pooled eluted fractions.

4.5 DISCUSSION

High precision instrumentation was employed for more robust evaluation of our newly proposed enrichment techniques. This consisted of reversed-phase HPLC coupled to ESI-MS/MS. Of note, sample preparation was tackled in a multi-dimensional manner to ensure compatibility with such equipment (412, 602). The potential variability induced by such additional experimental steps, as well as the nature of the sample through which enrichment took place, resulted in the inclusion of quality control assessment. Overall, the datasets reveal that both enrichment techniques were unable to enrich modified peptides under the current experimental conditions.

4.5.1 The variance between samples

Table 4.1 depicts the variance between the serum sample enrichment and control groups for both phosphopeptide and glycopeptide retrieval techniques. Increased variance was observed in the enriched phosphopeptide sample group versus the control group. This occurred due to more processing steps being required for LC-MS preparation and hence introducing greater variation (70). Moreover, samples that were designated to assess the glycopeptide enrichment technique exhibited much higher variation between results versus the phosphopeptide group. This was expected as there were multiple processing steps such as digestion and deglycosylation, followed by more digestion. Interestingly, the control group demonstrated higher variability between samples compared to the enriched group, and this is likely due to it experiencing more freeze-thaw cycles. This may have resulted in the degradation of our peptide samples (441). Moreover, a striking difference between the number of successfully identified PSMs was observed between positive control samples (Table 4.4) and

indicates that potential differences may have existed in terms of handling the different samples.

4.5.2 Fewer identifications in the enriched samples compared to controls

It is evident that the number of PSMs and peptide identifications in the respective enriched sample populations is lower compared to controls, and both groups displayed very low modified PSM identifications (Appendix F). The overall yield is also very low when compared to existing literature where similar methods were used (619, 734). Moreover, the specific retrieval of glycopeptides and phosphopeptides were unsuccessful as the enriched samples exhibited little to no identifications when compared to the respective control groups. Potential reasons for this result include the loss of the modification site due to sample preparation errors, the instrumentation used and the nature of the biological samples here employed.

4.5.2.1 The loss of the peptide/modification

When the addition of a phosphate moiety occurs, a higher degree of hydrophilicity is acquired (435). Thus if a short, multi-phosphorylated peptide existed in the sample its degree of hydrophilicity would not be compatible with reversed-phase SPE. In addition, its high hydrophilicity could result in lower retention on the trap column and may have been lost (107). The presence of a phosphate molecule in close proximity to the trypsin cutting site may also be a contributor to such an outcome (19). Such issues together with other PTMs can sterically hinder the cleavage site and produce increased missed cleavages (19).

Positive ionization was the mode of choice as it is well characterized and generally preferred (390, 703). Traditionally, an ion relates to a charged species that has either lost or gained electrons. Here, the ions refer to the molecules which accepted a proton and thus become protonated. However, phosphate moieties become neutral due to their negative charge (417, 612) and this results in ionization suppression and a relatively poor identification of phosphorylation (334, 417). Furthermore, operation of the mass spectrometer in DDA mode could have resulted in low abundance precursor ions not being selected for fragmentation (308), hence causing the loss of important information. However, this may not be the case as low intensity was observed in the total ion current chromatograms of the enriched samples.

Moreover, the CPGR employed in-house quality control tests of their instrumentation to ensure optimal function and therefore the instrumentation cannot account for our observations.

For both phosphopeptide and glycopeptide groups, autolysis and loss of stability during digestion could have impacted the identification of modifications (70). A reason for this could be high incubation temperatures with slightly alkaline pH (401). Moreover, excessive enzyme-to-substrate ratios could have caused non-specific cleavage and produced small peptides that are not favorable for MS analysis (274, 401). Although the pH of our digestion solvent was slightly alkaline, we employed a temperature of 37°C which could have lowered the pH (401). No universally employed standard for protein digestion exists, and proteolysis was not performed under extreme conditions. Moreover, we did not allow for non-specific cleavages or semi-tryptic fragments and specified that only peptides longer than 7 amino acids were to be analyzed. This could have resulted in the loss of important information by excluding semi-tryptic peptides for database search and hence decreased identifications (70, 413). In contrast, a 1:50 enzyme to substrate ratio might have been too low and also resulted in decreased cleavage efficiency, therefore a higher concentration of 1:20 or 1:30 might have sufficed (463, 612). If tryptic digestion was inefficient, a combination of proteases which include trypsin and Lys-C might have provided deeper proteomic coverage and better phospho-/glycopeptide identifications (231, 478).

The validation step involving PeptideProphet and PTMProphet did not allow us to alter the FDR threshold for final reporting as only ProteinProphet enabled this. This might be because the validation step was designed to suit protein-centric experiments. This could also be a reason for low PSM identification from RAW spectra as any identifications with an FDR > 1% would not have been reported. This could be rectified by employing other easy-to-use open-source software validation tools which could allow us to alter the FDR for peptide identifications, such as ID Picker (413).

Intact *N*-linked glycans could not be analyzed as we lacked software available for this, and therefore deglycosylation had to be employed (46). The caveats of identifying such glycans based on deamidation is that such induced chemical modification may occur spontaneously (258). The amino acid sequences must

therefore be interrogated to assess the potential of glycosylation. Although multiple PSMs for deamidation were observed, only one exhibited the potential to be glycosylated. The drawback here is that a single PSM existed for this identification and for this protein, and hence the confidence of the assignment of an *N*-linked glycan to this residue on the specific protein is low. Moreover, deglycosylation could have been ineffective for releasing the glycans. Although such reasons may be possible explanations for low PSM and peptide identifications, more plausible reasons are likely the nature of the biological samples and the enrichment techniques employed.

4.5.3 The challenges associated with serum enrichment

The blood proteome is one of the most popular biofluids for candidate biomarker discovery due to its accessibility and biological information it possesses (492, 727). Serum consists of proteins such as albumin and immunoglobulins, lipids, and various small molecules (e.g. salts and sugars) (5). It also exhibits the largest dynamic range of all biological samples, which decreases the detection of lower abundance proteins of interest (22, 727). This is compounded by the relatively low abundance of modified proteins which results in sub-stoichiometric levels of detection (612, 736). Depletion of high abundance proteins and enrichment of proteins of interest (to increase their concentration) can be employed to overcome such complexity (492). However, we propose that interfering non-modified proteins decreased the enrichment capacity of the affinity material for both techniques here employed. Low starting material (50 µg of protein) could also be a reason for the results, as higher amounts of starting protein material has been recommended (612). Others have employed lower amounts of starting material and encountered higher identifications (198, 399), however these took place with samples that had lower dynamic ranges. In addition, commercially available glycoprotein enrichment kits recommend higher amounts of starting material (217, 253, 654). This may also be dependent on the binding ability of the material, for example, how much lectin is immobilized to the support surface. Furthermore, the presence of serum lipoproteins (5) which possess phospholipid components (147) can inhibit phosphoprotein retrieval as the Zr^{4+} ion possesses an attraction towards the negatively charged phosphate moiety. Chloroform-methanol lipid extractions have shown to be beneficial for glycoprotein analysis (584), however, depletion and lipid removal were not tested in this thesis as increased sample processing steps increase the chances of sample loss (70, 300, 598). Despite this, previous studies employing

depletion strategies in conjunction with enrichment revealed sound outcomes (302, 377, 414, 519).

An additional reason for the unsuccessful enrichment of glycopeptides is that ConA exhibits a selective affinity for specific *N*-linked glycan moieties (619) and hence this could further decrease the detection of serum glycopeptides. The structure of the affinity materials may also have contributed to the nature of our results. Both the Zr-IMAC and carboxyl beads are porous (535, 713) and may therefore act as a 'sponge' for non-specifically enriching peptides. Moreover, the positive controls for each respective technique did not show retrieval of the phospho-/glycopeptide. This doesn't necessarily mean that the modification was absent, but rather that the peptide was in relatively low abundance and was therefore not chosen for fragmentation by the instrument (148). However, enrichment of the peptide which carries the Ser348 phospho-residue was observed in the phospho-OVA enriched sample and potentially demonstrates that lower sample complexity may benefit this enrichment technique.

Due to low intensity present in the total ion current chromatograms, 16% tricine gels were employed to visualize the respective phosphopeptide enrichment fractions (Figure 4.2). Peptide was only present in the unretained fractions of both the 50 μg and 100 μg experiments and demonstrates that very little to no enrichment of the serum samples took place. It's possible that only 1% of the total peptide fraction incubated with the beads was enriched. However, it did not appear in the corresponding fractions. The analysis of glycopeptide enrichment was not necessary as lower sample was present in these fractions, therefore a similar result would have been obtained in this case. Even with the high resolution and sensitivity of LC-MS/MS, modified peptide PSMs were low in abundance compared to others.

4.6 CONCLUSION

The use of both sets of affinity material for glycopeptide and phosphopeptide enrichment alone is not suitable for complex samples such as serum. This is mainly due to the high dynamic range of the serum proteome, as well as interfering non-modified proteins and potentially lipids. Moreover, the structure of the affinity material may increase non-specific retrieval of these highly abundant species. Thus such techniques should be employed for the enrichment of phospho- and glycopeptides

within biological matrices which do not possess such a high dynamic range as for serum. Moreover, additional fractionation steps such as depletion should be incorporated into workflows which employ such retrieval techniques. This should first be evaluated for serum peptides retrieval and then followed by a top-down approach for enrichment.

4.7 LIMITATIONS AND FUTURE RECOMMENDATIONS

Limitations include the enrichment techniques that were employed for retrieval of modified peptides in unfractionated serum. Here, serum membrane bound particles could be targeted by employing novel techniques as described by Wu *et al.* (2023). These authors employed a single-step-enrichment of microvesicles, exosomes and apoptotic bodies from the plasma proteome using SAX chromatography (701). This should decrease the dynamic range of blood samples and increase the identification of modified proteins. Furthermore, extracellular vesicles can also be separated from serum by means of ultracentrifugation (105). These can then be lysed and enriched for phosphoprotein/glycoproteins which would assist with candidate biomarker discovery. Additional methods for enrichment can be employed, such as a combination of IMAC materials (31) or multiple lectin affinity chromatography (194). A larger starting amount of serum material should also be employed as the relatively low abundance of modified proteins only constitutes ~1% of the total protein fraction. Automated workflows can also be employed in future experiments to limit sample handling errors (70). Unfortunately, limited reagent availability and financial constraints prevented us from considerably improving the current methodology.

5 A UNIFIED CONCLUSION

SDS-PAGE coupled with total protein visualization displayed non-specific enrichment, and LC-MS/MS evaluation demonstrated that the current affinity material was insufficient for serum glycopeptide and phosphopeptide enrichment. This is due to the porosity of the beads for both techniques as intact protein enrichment results in non-specific capture within the micropores. Contaminants such as lipids may also hinder enrichment in serum samples. Moreover, the high dynamic range of serum and enrichment without depletion decreases the efficiency of peptide enrichment when employing microparticles such as these. Increased starting material and fractionation steps could improve this, such as the coupling of multiple enrichment techniques. We therefore propose that more sample processing might be necessary to extract modified peptides. Moreover, extracellular vesicles present in the blood proteome may be better suited for isolation, followed by lysis and enrichment through the discussed retrieval techniques. Overall, more optimization of these techniques is needed to extract modified proteins from samples such as serum.

6 REFERENCES

1. **Abcam**. Product datasheet InstantBlue® Coomassie Protein Stain ab119211 [Online]. *Abcam* Abcam: 1–3, [date unknown]. <https://www.abcam.com/products/reagents/instantblue-coomassie-protein-stain-isb11-ab119211.html> [9 Sep. 2022].
2. **Abraham RS, Barnidge DR, Lanza IR**. Assessment of proteins of the immune system. In: *Clinical Immunology: Principles and Practice: Fourth Edition*. Elsevier Ltd., p. 1145–1159.
3. **Adaway JE, Keevil BG, Owen LJ**. Liquid chromatography tandem mass spectrometry in the clinical laboratory. *Ann Clin Biochem* 52: 18–38, 2015. doi: 10.1177/0004563214557678.
4. **Addona TA, Abbatiello SE, Schilling B, Skates SJ, Mani DR, et al**. Multi-site assessment of the precision and reproducibility of multiple reaction monitoring-based measurements of proteins in plasma. *Nat Biotechnol* 27: 633–641, 2009. doi: 10.1038/nbt.1546.
5. **Adkins JN, Varnum SM, Auberry KJ, Moore RJ, Angell NH, Smith RD, Springer DL, Pounds JG**. Toward a human blood serum proteome: analysis by multidimensional separation coupled with mass spectrometry. *Mol Cell Proteomics* 1: 947–955, 2002. doi: 10.1074/mcp.M200066-MCP200.
6. **Aebersold R, Agar JN, Amster IJ, Baker MS, Bertozzi CR, Boja ES, Costello CE, Cravatt BF, Fenselau C, Garcia BA, Ge Y, Gunawardena J, Hendrickson RC, Hergenrother PJ, Huber CG, Ivanov AR, Jensen ON, Jewett MC, Kelleher NL, Kiessling LL, Zhang B**. How many human proteoforms are there? *Nat Chem Biol* 14: 206–214, 2018. doi: <https://doi.org/10.1038/nchembio.2576>.
7. **Afrisham R, Paknejad M, Soliemanifar O, Sadegh-Nejadi S, Meshkani R, Ashtary-Larky D**. The influence of psychological stress on the initiation and progression of diabetes and cancer. *Int J Endocrinol Metab* 17: e67400, 2019. doi: 10.5812/ijem.67400.
8. **Aggarwal S, Yadav AK**. False Discovery Rate Estimation in Proteomics. In: *Statistical Analysis in Proteomics*. New York: Humana Press, 2016, p. 119–128.
9. **Agorastos A, Pervanidou P, Chrousos GP, Baker DG**. Developmental trajectories of early life stress and trauma: A narrative review on neurobiological

- aspects beyond stress system dysregulation. *Front Psychiatry* 10: 1–25, 2019. doi: 10.3389/fpsyt.2019.00118.
10. **Aguiló S, García E, Arza A, Garzón-Rey JM, Aguiló J.** Evaluation of chronic stress indicators in geriatric and oncologic caregivers: a cross-sectional study. *Stress* 21: 36–42, 2018. doi: 10.1080/10253890.2017.1391211.
 11. **Aicart-Ramos C, Valero RA, Rodriguez-Crespo I.** Protein palmitoylation and subcellular trafficking. *Biochim Biophys Acta - Biomembr* 1808: 2981–2994, 2011. doi: 10.1016/j.bbamem.2011.07.009.
 12. **Akanji MA, Rotimi DE, Elebiyo TC, Awakan OJ, Adeyemi OS.** Redox homeostasis and prospects for therapeutic targeting in neurodegenerative disorders. *Oxid Med Cell Longev* 2021: 1–14, 2021. doi: 10.1155/2021/9971885.
 13. **Akkaya B, Candan F, Yvuz H, Adil D.** Concanavalin A immobilized magnetic poly(glycidyl methacrylate) beads for antibody purification. *J Appl Polym Sci* 125: 1867–1874, 2012. doi: 10.1002/app.
 14. **Al-Aly Z.** Mental health in people with covid-19. *BMJ* 376: 1, 2022. doi: 10.1136/bmj.o415.
 15. **Alberts B, Johnson A, Lewis J.** The shape and structure of proteins [Online]. *Mol. Biol. Cell* Garland Science: 2002. <https://www.ncbi.nlm.nih.gov/books/NBK26830/> [9 Jun. 2022].
 16. **Alla A, Stine K.** Development of monolithic column materials for the separation and analysis of glycans. *Chromatography* 2: 20–65, 2015. doi: 10.3390/chromatography2010020.
 17. **Allfrey VG, Faulkner R, Mirsky AE.** Acetylation and methylation of histones and their possible role in the regulation of RNA synthesis. *Proc Natl Acad Sci United States* 51: 786–794, 1964. doi: 10.1073/pnas.51.5.786.
 18. **American Psychological Association.** Stress in America 2021: Stress and decision-making during the pandemic [Online]. <https://www.apa.org/news/press/releases/stress/2013/stress-report.pdf>.
 19. **American Psychological Association.** Stress in America™ 2021: Pandemic impedes basic decision-making ability [Online]. *apa.org*: 2021. <https://www.apa.org/news/press/releases/2021/10/stress-pandemic-decision-making> [27 May 2022].
 20. **Amiri-Dashatan N, Koushki M, Abbaszadeh HA, Rostami-Nejad M, Rezaei-**

- Tavirani M.** Proteomics applications in health: Biomarker and drug discovery and food industry. *Iran J Pharm Res IJPR* 17: 1523–1536, 2018.
21. **Amirkhan JH.** Stress overload in the spread of coronavirus. *Anxiety, Stress Coping* 34: 121–129, 2021. doi: 10.1080/10615806.2020.1824271.
22. **Anderson NL, Anderson NG.** The human plasma proteome: history, character, and diagnostic prospects. *Mol Cell Proteomics* 1: 845–867, 2002. doi: 10.1074/mcp.R200007-MCP200.
23. **Anderson NL, Polanski M, Pieper R, Gatlin T, Tirumalai RS, Conrads TP, Veenstra TD, Adkins JN, Pounds JG, Fagan R, Lobley A.** The human plasma proteome. *Mol Cell Proteomics* 3: 311–326, 2004. doi: 10.1074/mcp.M300127-MCP200.
24. **Andersson P.** Comparison of lectins and their suitability in lectin affinity chromatography for isolation of glycoproteins [Online]. *Uppsala Univ.*: 1–78, 2020. <http://www.teknat.uu.se/student> [4 Jul. 2022].
25. **Andrews RC, Walker BR.** Glucocorticoids and insulin resistance: old hormones, new targets. *Clin Sci* 96: 513–523, 1999.
26. **Anisman H, Merali Z.** Understanding stress: Characteristics and caveats. *Alcohol Res Heal* 23: 241–249, 1999.
27. **Arakane F, King SR, Du Y, Kallen CB, Walsh LP, Watari H, Stocco DM, Strauss JF.** Phosphorylation of steroidogenic acute regulatory protein (StAR) modulates its steroidogenic activity. *J Biol Chem* 272: 32656–32662, 1997. doi: 10.1074/jbc.272.51.32656.
28. **Arasteh A, Farahi S, Habibi-Rezaei M, Moosavi-Movahedi AA.** Glycated albumin: An overview of the in vitro models of an in vivo potential disease marker. *J Diabetes Metab Disord* 13: 1–9, 2014. doi: 10.1186/2251-6581-13-49.
29. **Ardito F, Giuliani M, Perrone D, Troiano G, Muzio L Lo.** The crucial role of protein phosphorylation in cell signaling and its use as targeted therapy (review). *Int J Mol Med* 40: 271–280, 2017. doi: 10.3892/ijmm.2017.3036.
30. **Armirotti A.** Bottom-up proteomics. *Curr Anal Chem* 5: 116–130, 2009. doi: 10.2174/157341109787846117.
31. **Arribas Diez I, Govender I, Naicker P, Stoychev S, Jordaan J, Jensen ON.** Zirconium(IV)-IMAC revisited: Improved performance and phosphoproteome coverage by magnetic microparticles for phosphopeptide affinity enrichment. *J Proteome Res* 20: 453–462, 2021. doi: 10.1021/acs.jproteome.0c00508.

32. **Aryal UK, Ross ARS.** Enrichment and analysis of phosphopeptides under different experimental conditions using titanium dioxide affinity chromatography and mass spectrometry. *Rapid Commun Mass Spectrom* 24: 1457–1466, 2010. doi: 10.1002/rcm.
33. **Asaba K, Iwasaki Y, Yoshida M, Asai M, Oiso Y, Murohara T, Hashimoto K.** Attenuation by reactive oxygen species of glucocorticoid suppression on proopiomelanocortin gene expression in pituitary corticotroph cells. *Endocrinology* 145: 39–42, 2004. doi: 10.1210/en.2003-0375.
34. **Aschbacher K, Mason AE.** Eustress, distress, and oxidative stress: Promising pathways for mind-body medicine. In: *Oxidative Stress*, edited by Sies H. Elsevier Inc., p. 583–617.
35. **Aschbacher K, O'Donovan A, Wolkowitz OM, Dhabhar FS, Su Y, Epel E.** Good stress, bad stress and oxidative stress: Insights from anticipatory cortisol reactivity. *Psychoneuroendocrinology* 38: 1698–1708, 2013. doi: 10.1016/j.psyneuen.2013.02.004.
36. **Aslam B, Basit M, Nisar MA, Khurshid M, Rasool MH.** Proteomics: Technologies and their applications. *J Chromatogr Sci* 55: 182–196, 2017. doi: 10.1093/chromsci/bmw167.
37. **Assil IQ, Abou-Samra AB.** N-glycosylation of CRF receptor type 1 is important for its ligand-specific interaction. *Am J Physiol - Endocrinol Metab* 281: E1015–E1021, 2001. doi: 10.1152/ajpendo.2001.281.5.e1015.
38. **Atkinson AJ, Colburn WA, DeGruttola VG, DeMets DL, Downing GJ, Hoth DF, Oates JA, Peck CC, Schooley RT, Spilker BA, Woodcock J, Zeger SL.** Biomarkers and surrogate endpoints: Preferred definitions and conceptual framework. *Clin Pharmacol Ther* 69: 89–95, 2001. doi: 10.1067/mcp.2001.113989.
39. **Atrooz F, Alkadhi KA, Salim S.** Understanding stress: Insights from rodent models. *Curr Res Neurobiol* 2: 100013, 2021. doi: 10.1016/j.crneur.2021.100013.
40. **Audet MC, Mangano EN, Anisman H.** Behavior and pro-inflammatory cytokine variations among submissive and dominant mice engaged in aggressive encounters: Moderation by corticosterone reactivity. *Front Behav Neurosci* 4: 1–12, 2010. doi: 10.3389/fnbeh.2010.00156.
41. **Audet MC, McQuaid RJ, Merali Z, Anisman H.** Cytokine variations and mood

- disorders: Influence of social stressors and social support. *Front Neurosci* 8: 1–12, 2014. doi: 10.3389/fnins.2014.00416.
42. **Avvakumov G V., Warmels-Rodenhiser S, Hammond GL.** Glycosylation of human corticosteroid-binding globulin at asparagine 238 is necessary for steroid binding. *J Biol Chem* 268: 862–866, 1993. doi: 10.1016/s0021-9258(18)54013-8.
43. **Ayroldi E, Cannarile L, Migliorati G, Nocentini G, Delfino D V., Riccardi C.** Mechanisms of the anti-inflammatory effects of glucocorticoids: Genomic and nongenomic interference with MAPK signaling pathways. *FASEB J* 26: 4805–4820, 2012. doi: 10.1096/fj.12-216382.
44. **Badrick E, Kirschbaum C, Kumari M.** The relationship between smoking status and cortisol secretion. *J Clin Endocrinol Metab* 92: 819–824, 2007. doi: 10.1210/jc.2006-2155.
45. **Bag AK, Saha S, Sundar S, Saha B, Chakrabarti A, Mandal C.** Comparative proteomics and glycoproteomics of plasma proteins in Indian visceral leishmaniasis. *Proteome Sci* 12: 1–14, 2014. doi: 10.1186/s12953-014-0048-z.
46. **Bailey UM, Schulz BL.** Deglycosylation systematically improves N-glycoprotein identification in liquid chromatography-tandem mass spectrometry proteomics for analysis of cell wall stress responses in *Saccharomyces cerevisiae* lacking Alg3p. *J Chromatogr B Anal Technol Biomed Life Sci* 923–924: 16–21, 2013. doi: 10.1016/j.jchromb.2013.01.026.
47. **Balfoussia E, Skenderi K, Tsironi M, Anagnostopoulos AK, Parthimos N, Vougas K, Papassotiriou I, Tsangaris GT, Chrousos GP.** A proteomic study of plasma protein changes under extreme physical stress. *J Proteomics* 98: 1–14, 2014. doi: 10.1016/j.jprot.2013.12.004.
48. **Ball J, Micheel C.** Evaluation of biomarkers and surrogate endpoints in chronic disease. Washington DC: The National Academic Press, 2010.
49. **Banerjee PS, Lagerlöf O, Hart GW.** Roles of O-GlcNAc in chronic diseases of aging. *Mol Aspects Med* 51: 1–15, 2016. doi: 10.1016/j.mam.2016.05.005.
50. **Banerjee S, Mazumdar S.** Electrospray ionization mass spectrometry: A technique to access the information beyond the molecular weight of the analyte. *Int J Anal Chem* 2012: 1–40, 2012. doi: 10.1155/2012/282574.
51. **Barbayannis G, Bandari M, Zheng X, Baquerizo H, Pecor KW, Ming X.** Academic stress and mental well-being in college students: correlations,

- affected groups, and COVID-19. *Front Psychol* 13: 1–10, 2022. doi: 10.3389/fpsyg.2022.886344.
52. **Barbosa EB, Vidotto A, Polachini GM, Henrique T, de Marqui ABT, Helena Tajara E.** Proteomics: methodologies and applications to the study of human diseases. *Rev da Assoc Médica Bras (English Ed)* 58: 366–375, 2012. doi: 10.1016/s2255-4823(12)70209-6.
53. **Barua S, Kim JY, Yenari MA, Lee JE.** The role of NOX inhibitors in neurodegenerative diseases. *IBRO Reports* 7: 59–69, 2019. doi: 10.1016/j.ibror.2019.07.1721.
54. **Bassil K, De Nijs L, Rutten BPF, Van Den Hove DLA, Kenis G.** In vitro modeling of glucocorticoid mechanisms in stress-related mental disorders: Current challenges and future perspectives. *Front Cell Dev Biol* 10: 1–9, 2022. doi: 10.3389/fcell.2022.1046357.
55. **Bateman NW, Goulding SP, Shulman NJ, Gadok AK, Szumlinski KK, MacCoss MJ, Wu CC.** Maximizing peptide identification events in proteomic workflows using data-dependent acquisition (DDA). *Mol Cell Proteomics* 13: 329–338, 2014. doi: 10.1074/mcp.M112.026500.
56. **Beauclair G, Bridier-Nahmias A, Zagury JF, Säb A, Zamborlini A.** JASSA: A comprehensive tool for prediction of SUMOylation sites and SIMs. *Bioinformatics* 31: 3483–3491, 2015. doi: 10.1093/bioinformatics/btv403.
57. **Becker M, Pinhasov A, Ornoy A.** Animal models of depression: What can they teach us about the human disease? *Diagnostics* 11: 1–31, 2021. doi: 10.3390/diagnostics11010123.
58. **Bedair M, El Rassi Z.** Affinity chromatography with monolithic capillary columns: II. Polymethacrylate monoliths with immobilized lectins for the separation of glycoconjugates by nano-liquid affinity chromatography. *J Chromatogr A* 1079: 236–245, 2005. doi: 10.1016/j.chroma.2005.02.084.
59. **Behl T, Rana T, Alotaibi GH, Shamsuzzaman M, Naqvi M, Sehgal A, Singh S, Sharma N, Almoshari Y, Abdellatif AAH, Iqbal MS, Bhatia S, Al-Harrasi A, Bungau S.** Polyphenols inhibiting MAPK signalling pathway mediated oxidative stress and inflammation in depression. *Biomed Pharmacother* 146: 112545, 2022. doi: 10.1016/j.biopha.2021.112545.
60. **Bellei E, Bergamini S, Monari E, Fantoni LI, Cuoghi A, Ozben T, Tomasi A.** High-abundance proteins depletion for serum proteomic analysis: Concomitant

- removal of non-targeted proteins. *Amino Acids* 40: 145–156, 2011. doi: 10.1007/s00726-010-0628-x.
61. **Bellei E, Rustichelli C, Bergamini S, Monari E, Baraldi C, Lo Castro F, Tomasi A, Ferrari A.** Proteomic serum profile in menstrual-related and post menopause migraine. *J Pharm Biomed Anal* 184: 113165, 2020. doi: 10.1016/j.jpba.2020.113165.
 62. **Bergsbaken T, Fink SL, Cookson BT.** Pyroptosis: Host cell death and inflammation. *Nat Rev Microbiol* 7: 99–109, 2009. doi: 10.1038/nrmicro2070.
 63. **Bernstein A, Zvolensky MJ, Stewart SH, Nancy Comeau M, Leen-Feldner EW.** Anxiety sensitivity taxonicity across gender among youth. *Behav Res Ther* 44: 679–698, 2006. doi: 10.1016/j.brat.2005.03.011.
 64. **Bhatia N, Maiti PP, Choudhary A, Tuli A, Masih D, Khan MMU, Jaggi AS.** Animal models of stress. *Int J Pharm Sci Res* 2: 1147, 2011. doi: 10.1016/B978-0-12-809324-5.02030-7.
 65. **Bhattacharyya L, Ceccarini C, Lorenzoni P, Brewer CF.** Concanavalin A interactions with asparagine-linked glycopeptides. Bivalency of high mannose and bisected hybrid type glycopeptides. *J Biol Chem* 262: 1288–1293, 1987. doi: 10.1016/s0021-9258(19)75784-6.
 66. **Bhattacharyya S, Brown DE, Brewer JA, Vogt SK, Muglia LJ.** Macrophage glucocorticoid receptors regulate Toll-like receptor 4-mediated inflammatory responses by selective inhibition of p38 MAP kinase. *Blood* 109: 4313–4319, 2007. doi: 10.1182/blood-2006-10-048215.
 67. **Bhosale SD, Moulder R, Venäläinen MS, Koskinen JS, Pitkänen N, Juonala MT, Kähönen MAP, Lehtimäki TJ, Viikari JSA, Elo LL, Goodlett DR, Lahesmaa R, Raitakari OT.** Serum proteomic profiling to identify biomarkers of premature carotid atherosclerosis. *Sci Rep* 8: 1–9, 2018. doi: 10.1038/s41598-018-27265-9.
 68. **Bie Z, Chen Y, Li H, Wu R, Liu Z.** Off-line hyphenation of boronate affinity monolith-based extraction with matrix-assisted laser desorption/ionization time-of-flight mass spectrometry for efficient analysis of glycoproteins/glycopeptides. *Anal Chim Acta* 834: 1–8, 2014. doi: 10.1016/j.aca.2014.04.035.
 69. **Biermann MHC, Griffante G, Podolska MJ, Boeltz S, Stürmer J, Muñoz LE, Bilyy R, Herrmann M.** Sweet but dangerous - The role of immunoglobulin G glycosylation in autoimmunity and inflammation. *Lupus* 25: 934–942, 2016. doi:

- 10.1177/0961203316640368.
70. **Bittremieux W, Tabb DL, Impens F, Staes A, Timmerman E, Martens L, Laukens K.** Quality control in mass spectrometry-based proteomics. *Mass Spectrom Rev* 37: 697–711, 2018. doi: 10.1002/mas.21544.
 71. **Bladergroen MR, Van Der Burgt YEM.** Solid-phase extraction strategies to surmount body fluid sample complexity in high-throughput mass spectrometry-based proteomics. *J Anal Methods Chem* 2015: 8, 2015. doi: 10.1155/2015/250131.
 72. **Blanc M, David F, Abrami L, Migliozzi D, Armand F, Bürgi J, van der Goot FG.** SwissPalm: Protein palmitoylation database. *F1000Research* 4: 1–23, 2015. doi: 10.12688/f1000research.6464.1.
 73. **Blom N, Sicheritz-Pontén T, Gupta R, Gammeltoft S, Brunak S.** Prediction of post-translational glycosylation and phosphorylation of proteins from the amino acid sequence. *Proteomics* 4: 1633–1649, 2004. doi: 10.1002/pmic.200300771.
 74. **Boeck C, Pfister S, Bürkle A, Vanhooren V, Libert C, Salinas-Manrique J, Dietrich DE, Kolassa IT, Karabatsiakakis A.** Alterations of the serum N-glycan profile in female patients with Major Depressive Disorder. *J Affect Disord* 234: 139–147, 2018. doi: 10.1016/j.jad.2018.02.082.
 75. **Bourmaud A, Gallien S, Domon B.** A quality control of proteomic experiments based on multiple isotopologous internal standards. *EuPA Open Proteomics* 8: 16–21, 2015. doi: 10.1016/j.euprot.2015.07.010.
 76. **Bowers SL, Bilbo SD, Dhabhar FS, Nelson RJ.** Stressor-specific alterations in corticosterone and immune responses in mice. *Brain Behav Immun* 22: 105–113, 2008. doi: 10.1016/j.bbi.2007.07.012.
 77. **Brenhouse HC, Danese A, Grassi-Oliveira R.** Neuroimmune impacts of early-life stress on development and psychopathology. In: *Neuroendocrine Regulation of Behavior. Current Topics in Behavioral Neurosciences, Vol 43*, edited by Coolen L, Grattan D. Springer, Cham, p. 289–320.
 78. **Broedbaek K, Hilsted L.** Chromogranin A as biomarker in diabetes. *Biomark Med* 10: 1181–1189, 2016. doi: 10.2217/bmm-2016-0091.
 79. **Brookes PS, Padilla Salinas E, Darley-USmar K, Eiserich JP, Freeman BA, Darley-USmar VM, Anderson PG.** Concentration-dependent effects of nitric oxide on mitochondrial permeability transition and cytochrome c release. *J Biol*

- Chem* 275: 20474–20479, 2000. doi: 10.1074/jbc.M001077200.
80. **Brown K, Melby J, Roberts D, Ge Y.** Top-down proteomics: Challenges, innovations, and applications in basic and clinical research. *Expert Rev Proteomics* 17: 719–733, 2020. doi: 10.1080/14789450.2020.1855982.
 81. **Brown RWB, Sharma AI, Engman DM.** Dynamic protein S-palmitoylation mediates parasite life cycle progression and diverse mechanisms of virulence. *Crit Rev Biochem Mol Biol* 52: 145–162, 2017. doi: 10.1080/10409238.2017.1287161.
 82. **Bruneel A, Habarou F, Stojkovic T, Plouviez G, Bougas L, Guillemet F, Brient N, Henry D, Dupré T, Vuillaumier-Barrot S, Seta N.** Two-dimensional electrophoresis highlights haptoglobin beta chain as an additional biomarker of congenital disorders of glycosylation. *Clin Chim Acta* 470: 70–74, 2017. doi: 10.1016/j.cca.2017.04.022.
 83. **Bueno-Notivol J, Gracia-García P, Olaya B, Lasheras I, López-Antón R, Santabárbara J.** Prevalence of depression during the COVID-19 outbreak: A meta-analysis of community-based studies. *Int J Clin Heal Psychol* 21, 2021. doi: 10.1016/j.ijchp.2020.07.007.
 84. **Bugyi F, Szabó D, Szabó G, Révész Á, Pape VFS, Soltész-Katona E, Tóth E, Kovács O, Langó T, Vékey K, Drahos L.** Influence of post-translational modifications on protein identification in database searches. *ACS Omega* 6: 7469–7477, 2021. doi: 10.1021/acsomega.0c05997.
 85. **Burkhart JM, Schumbrutzki C, Wortelkamp S, Sickmann A, Zahedi RP.** Systematic and quantitative comparison of digest efficiency and specificity reveals the impact of trypsin quality on MS-based proteomics. *J Proteomics* 75: 1454–1462, 2012. doi: 10.1016/j.jprot.2011.11.016.
 86. **Burnett G, Kennedy EP.** The enzymatic phosphorylation of proteins. *J Biol Chem* 211: 969–980, 1954.
 87. **Busher J.** Serum albumin and globulin [Online]. In: *Clinical Methods: The History, Physical, and Laboratory Examinations* <https://www.ncbi.nlm.nih.gov/books/NBK204/>.
 88. **Busillo JM, Cidlowski JA.** The five Rs of glucocorticoid action during inflammation: Ready, reinforce, repress, resolve, and restore. *Trends Endocrinol Metab* 24: 109–119, 2013. doi: 10.1016/j.tem.2012.11.005.
 89. **Byrne J, Eksteen G, Crickmore C.** Cardiovascular disease statistics reference

- document [Online]. *Heart. Stroke Found. South Africa*: 6, 2016. <https://www.heartfoundation.co.za/wp-content/uploads/2017/10/CVD-Stats-Reference-Document-2016-FOR-MEDIA-1.pdf> [29 Sep. 2020].
90. **Calcia MA, Bonsall DR, Bloomfield PS, Selvaraj S, Barichello T, Howes OD.** Stress and neuroinflammation: A systematic review of the effects of stress on microglia and the implications for mental illness. *Psychopharmacology (Berl)* 233: 1637–1650, 2016. doi: 10.1007/s00213-016-4218-9.
 91. **Califf RM.** Biomarker definitions and their applications. *Exp Biol Med* 243: 213–221, 2018. doi: 10.1177/1535370217750088.
 92. **Cantin GT, Shock TR, Sung KP, Madhani HD, Yates JR.** Optimizing TiO₂-based phosphopeptide enrichment for automated multidimensional liquid chromatography coupled to tandem mass spectrometry. *Anal Chem* 79: 4666–4673, 2007. doi: 10.1021/ac0618730.
 93. **Carboni L, Piubelli C, Pozzato C, Astner H, Arban R, Righetti PG, Hamdan M, Domenici E.** Proteomic analysis of rat hippocampus after repeated psychosocial stress. *Neuroscience* 137: 1237–1246, 2006. doi: 10.1016/j.neuroscience.2005.10.045.
 94. **Carpenter GSJ, Carpenter TP, Kimbrel NA, Flynn EJ, Pennington ML, Cammarata C, Zimering RT, Kamholz BW, Gulliver SB.** Social support, stress, and suicidal ideation in professional firefighters. *Am J Health Behav* 39: 191–196, 2015. doi: 10.5993/AJHB.39.2.5.
 95. **Carter JD, LaBean TH.** Coupling strategies for the synthesis of peptide-oligonucleotide conjugates for patterned synthetic biomineralization. *J Nucleic Acids* 2011: 1–8, 2011. doi: 10.4061/2011/926595.
 96. **Catherman A, Skinner O, Kelleher N.** Top Down proteomics: Facts and perspectives. *Biochem Biophys Res Commun* 445: 683–693, 2014. doi: <https://doi.org/10.1016/j.bbrc.2014.02.041>.
 97. **Chacko BK, Scott DW, Chandler RT, Patel RP.** Endothelial surface N-glycans mediate monocyte adhesion and are targets for anti-inflammatory effects of peroxisome proliferator-activated receptor γ ligands. *J Biol Chem* 286: 38738–38747, 2011. doi: 10.1074/jbc.M111.247981.
 98. **Chakravarty S, Reddy BR, Sudhakar SR, Saxena S, Das T, Meghah V, Brahmendra Swamy C V., Kumar A, Idris MM.** Chronic unpredictable stress (CUS)-induced anxiety and related mood disorders in a zebrafish model: Altered

- brain proteome profile implicates mitochondrial dysfunction. *PLoS One* 8, 2013. doi: 10.1371/journal.pone.0063302.
99. **Chandel NS, Budinger GRS.** The cellular basis for diverse responses to oxygen. *Free Radic Biol Med* 42: 165–174, 2007. doi: 10.1016/j.freeradbiomed.2006.10.048.
 100. **Chandramouli K, Qian PY.** Proteomics: Challenges, techniques and possibilities to overcome biological sample complexity. *Hum Genomics Proteomics* 1: 1–22, 2009. doi: 10.4061/2009/239204.
 101. **Charmandari E, Tsigos C, Chrousos G.** Endocrinology of the stress response. *Annu Rev Physiol* 67: 259–284, 2005. doi: 10.1146/annurev.physiol.67.040403.120816.
 102. **Chatterjee B, Thakur SS.** Investigation of post-translational modifications in type 2 diabetes. *Clin Proteomics* 15: 1–11, 2018. doi: 10.1186/s12014-018-9208-y.
 103. **Chen B, Hwang L, Ochowicz W, Lin Z, Guardado-Alvarez TM, Cai W, Xiu L, Dani K, Colah C, Jin S, Ge Y.** Coupling functionalized cobalt ferrite nanoparticle enrichment with online LC/MS/MS for top-down phosphoproteomics. *Chem Sci* 8: 4306–4311, 2017. doi: 10.1039/c6sc05435h.
 104. **Chen HM, Lee LC, Hu KY, Tsai WJ, Huang C, Jen Tsay H, Liu HK.** The application of post-translational modification oriented serum proteomics to assess experimental diabetes with complications. *PLoS One* 13: 1–22, 2018. doi: 10.1371/journal.pone.0206509.
 105. **Chen IH, Xue L, Hsu CC, Paez JSP, Panb L, Andaluz H, Wendt MK, Iliuk AB, Zhu JK, Tao WA.** Phosphoproteins in extracellular vesicles as candidate markers for breast cancer. *Proc Natl Acad Sci U S A* 114: 3175–3180, 2017. doi: 10.1073/pnas.1618088114.
 106. **Chen W, Dang T, Blind RD, Wang Z, Cavasotto CN, Hittelman AB, Rogatsky I, Logan SK, Garabedian MJ.** Glucocorticoid receptor phosphorylation differentially affects target gene expression. *Mol Endocrinol* 22: 1754–1766, 2008. doi: 10.1210/me.2007-0219.
 107. **Chen X, Wu D, Zhao Y, Wong BHC, Guo L.** Increasing phosphoproteome coverage and identification of phosphorylation motifs through combination of different HPLC fractionation methods. *J Chromatogr B Anal Technol Biomed Life Sci* 879: 25–34, 2011. doi: 10.1016/j.jchromb.2010.11.004.

108. **Cheng D, Côté J, Shaaban S, Bedford MT.** The arginine methyltransferase CARM1 regulates the coupling of transcription and mRNA processing. *Mol Cell* 25: 71–83, 2007. doi: 10.1016/j.molcel.2006.11.019.
109. **Choi S, Kim J, Cho K, Park G, Yoon JH, Park S, Yoo JS, Ryu SH, Kim YH, Kim J.** Sequential Fe₃O₄/TiO₂ enrichment for phosphopeptide analysis by liquid chromatography/tandem mass spectrometry. *Rapid Commun Mass Spectrom* 24: 1467–1474, 2010. doi: 10.1002/rcm.4541.
110. **Chothia A.** Lockdown: 87 000 cases of gender-based violence reported [Online]. *The South African:* 2020. <https://www.thesouthafrican.com/news/gender-based-violence-reported-during-lockdown-cele/> [8 Mar. 2021].
111. **Choudhari SK, Chaudhary M, Gadbail AR, Sharma A, Tekade S.** Oxidative and antioxidative mechanisms in oral cancer and precancer: A review. *Oral Oncol* 50: 10–18, 2014. doi: 10.1016/j.oraloncology.2013.09.011.
112. **Choudhary C, Kumar C, Gnäd F, Nielsen ML, Rehman M, Walther TC, Olsen J V., Mann M.** Lysine acetylation targets protein complexes and co-regulates major cellular functions. *Science (80-)* 325: 834–840, 2009. doi: 10.1126/science.1175371.
113. **Choudhary C, Mann M.** Decoding signalling networks by mass spectrometry-based proteomics. *Nat Rev Mol Cell Biol* 11: 427–439, 2010. doi: 10.1038/nrm2900.
114. **Chrousos G.** The role of stress and the hypothalamic - pituitary - adrenal axis in the pathogenesis of the metabolic syndrome : neuro-endocrine and target tissue-related causes. *Int J Obes* 24: 50–55, 2000. doi: 10.1038/sj.ijo.0801278.
115. **Chung IM.** Stress-induced atherosclerosis: Clinical evidence and possible underlying mechanism. *Korean Circ J* 35: 101, 2005. doi: 10.4070/kcj.2005.35.2.101.
116. **Chutipongtanate S, Watcharatanyatip K, Homvises T, Jaturongkakul K, Thongboonkerd V.** Systematic comparisons of various spectrophotometric and colorimetric methods to measure concentrations of protein, peptide and amino acid: Detectable limits, linear dynamic ranges, interferences, practicality and unit costs. *Talanta* 98: 123–129, 2012. doi: 10.1016/j.talanta.2012.06.058.
117. **City Press.** SA is the second most stressed country in the world. Here's how you can cope | Citypress [Online]. *news24:* 2019.

- <https://www.news24.com/citypress/Careers/sa-is-the-second-most-stressed-country-in-the-world-heres-how-you-can-cope-20190423> [16 Jun. 2020].
118. **City Press**. SA is the second most stressed country in the world. Here's how you can cope | Citypress [Online]. *news24*: 2019. <https://www.news24.com/citypress/careers/sa-is-the-second-most-stressed-country-in-the-world-heres-how-you-can-cope-20190423> [14 Nov. 2022].
 119. **Clerc F, Reiding KR, Jansen BC, Kammeijer GSM, Bondt A, Wuhrer M**. Human plasma protein N-glycosylation. *Glycoconj J* 33: 309–343, 2016. doi: 10.1007/s10719-015-9626-2.
 120. **Cogswell PC, Kashatus DF, Keifer JA, Guttridge DC, Reuther JY, Bristow C, Roy S, Nicholson DW, Baldwin AS**. NF- κ B and I κ B α are found in the mitochondria. Evidence for regulation of mitochondrial gene expression by NF- κ B. *J Biol Chem* 278: 2963–2968, 2003. doi: 10.1074/jbc.M209995200.
 121. **Cohen P**. The regulation of protein function by multisite phosphorylation - A 25 year update. *Trends Biochem Sci* 25: 596–601, 2000. doi: 10.1016/S0968-0004(00)01712-6.
 122. **Cohen P**. The role of protein phosphorylation in human health and disease: Delivered on June 30th 2001 at the FEBS meeting in Lisbon. *Eur J Biochem* 268: 5001–5010, 2001. doi: 10.1046/j.0014-2956.2001.02473.x.
 123. **Cohen P**. Protein kinases - The major drug targets of the twenty-first century? *Nat Rev Drug Discov* 1: 309–315, 2002. doi: 10.1038/nrd773.
 124. **Cohen S, Doyle WJ, Skoner DP**. Psychological stress, cytokine production, and severity of upper respiratory illness. *Psychosom Med* 61: 175–180, 1999. doi: 10.1097/00006842-199903000-00009.
 125. **Cohen S, Janicki-Deverts D, Doyle WJ, Miller GE, Frank E, Rabin BS, Turner RB**. Chronic stress, glucocorticoid receptor resistance, inflammation, and disease risk. *Proc Natl Acad Sci U S A* 109: 5995–5999, 2012. doi: 10.1073/pnas.1118355109.
 126. **Cohen S, Janicki-Deverts D, Miller GE**. Psychological stress and disease. *J Am Med Assoc* 298: 1685–1687, 2007. doi: 10.1001/jama.298.14.1685.
 127. **Comes AL, Papiol S, Mueller T, Geyer PE, Mann M, Schulze TG**. Proteomics for blood biomarker exploration of severe mental illness: pitfalls of the past and potential for the future. *Transl Psychiatry* 8: 1–15, 2018. doi: 10.1038/s41398-018-0219-2.

128. **Condrat CE, Thompson DC, Barbu MG, Bugnar OL, Boboc A, Cretoiu D, Suci N, Cretoiu SM, Voinea SC.** miRNAs as biomarkers in disease: Latest findings regarding their role in diagnosis and prognosis. *Cells* 9: 1–32, 2020. doi: 10.3390/cells9020276.
129. **Cong W, Zhou A, Liu Z, Shen J, Zhou X, Ye W, Zhu Z, Zhu X, Lin J, Jin L.** Highly sensitive method for specific, brief, and economical detection of glycoproteins in sodium dodecyl sulfate-polyacrylamide gel electrophoresis by the synthesis of a new hydrazide derivative. *Anal Chem* 87: 1462–1465, 2015. doi: 10.1021/ac503543z.
130. **Consortium TU.** UniProt: the Universal Protein Knowledgebase in 2023. *Nucleic Acids Res* 51: D523–D531, 2023. doi: <https://doi.org/10.1093/nar/gkac1052>.
131. **Contesse T, Broussot L, Fofu H, Vanhoutte P, Fernandez SP, Barik J.** Dopamine and glutamate receptors control social stress-induced striatal ERK1/2 activation. *Neuropharmacology* 190: 108534, 2021. doi: 10.1016/j.neuropharm.2021.108534.
132. **Conway-Campbell BL, McKenna MA, Wiles CC, Atkinson HC, De Kloet ER, Lightman SL.** Proteasome-dependent down-regulation of activated nuclear hippocampal glucocorticoid receptors determines dynamic responses to corticosterone. *Endocrinology* 148: 5470–5477, 2007. doi: 10.1210/en.2007-0585.
133. **Cottrell JS.** Protein identification using MS/MS data. *J Proteomics* 74: 1842–1851, 2011. doi: 10.1016/j.jprot.2011.05.014.
134. **Cox J, Mann M.** MaxQuant enables high peptide identification rates, individualized p.p.b.-range mass accuracies and proteome-wide protein quantification. *Nat Biotechnol* 26: 1367–1372, 2008. doi: 10.1038/nbt.1511.
135. **Crosswell AD, Lockwood KG.** Best practices for stress measurement: How to measure psychological stress in health research. *Heal Psychol Open* 7, 2020. doi: 10.1177/2055102920933072.
136. **Cruz-Topete D, Cidlowski JA.** One hormone, two actions: Anti- And pro-inflammatory effects of glucocorticoids. *Neuroimmunomodulation* 22: 20–32, 2014. doi: 10.1159/000362724.
137. **Cruz JC, de Souza ID, Grecco CF, Figueiredo EC, Queiroz MEC.** Recent advances in column switching high-performance liquid chromatography for

- bioanalysis. *Sustain Chem Pharm* 21, 2021. doi: 10.1016/j.scp.2021.100431.
138. **Cui B, Wu M, She X, Liu H.** Impulse noise exposure in rats causes cognitive deficits and changes in hippocampal neurotransmitter signaling and tau phosphorylation. *Brain Res* 1427: 35–43, 2012. doi: 10.1016/j.brainres.2011.08.035.
139. **Cummings RD.** Use of lectins in analysis of glycoconjugates. *Methods Enzymol* 230: 66–86, 1994. doi: 10.1016/0076-6879(94)30008-9.
140. **Cupp-Sutton K, Wu S.** High-throughput quantitative top-down proteomics. *Mol Omi* 16: 91–99, 2020. doi: 10.1039/c9mo00154a.
141. **Cutillas P.** Principles of nanoflow liquid chromatography and applications to proteomics. *Curr Nanosci* 1: 65–71, 2006. doi: 10.2174/1573413052953093.
142. **Cutler P.** Affinity chromatography. In: *Protein Purification Protocols*, edited by Walker JM. Totowa: Humana Press, 2004, p. 139–149.
143. **da Veiga Leprevost F, Haynes SE, Avtonomov DM, Chang HY, Shanmugam AK, Mellacheruvu D, Kong AT, Nesvizhskii AI.** Philosopher: A versatile toolkit for shotgun proteomics data analysis. *Nat Methods* 17: 869–870, 2020. doi: 10.1038/s41592-020-0912-y.
144. **Dabelić S, Flögel M, Maravić G, Lauc G.** Stress causes tissue-specific changes in the sialyltransferase activity. *Zeitschrift fur Naturforsch - Sect C J Biosci* 59: 276–280, 2004. doi: 10.1515/znc-2004-3-427.
145. **Dalvie S, Chatzinakos C, Al Zoubi O, Georgiadis F, Lancashire L, Daskalakis NP.** From genetics to systems biology of stress-related mental disorders. *Neurobiol Stress* 15, 2021. doi: 10.1016/j.ynstr.2021.100393.
146. **Dasgupta A, Klein K.** Psychological stress-induced oxidative stress. In: *Antioxidants in Food, Vitamins and Supplements*, edited by Dasgupta A, Klein K. Elsevier, 2014, p. 97–111.
147. **Dashti M, Kulik W, Hoek F, Veerman EC, Peppelenbosch MP, Rezaee F.** A phospholipidomic analysis of all defined human plasma lipoproteins. *Sci Rep* 1: 1–11, 2011. doi: 10.1038/srep00139.
148. **Davies V, Wandy J, Weidt S, Van Der Hooff JJJ, Miller A, Daly R, Rogers S.** Rapid development of improved data-dependent acquisition strategies. *Anal Chem* 93: 5676–5683, 2021. doi: 10.1021/acs.analchem.0c03895.
149. **De Bosscher K, Haegeman G.** Minireview: Latest perspectives on antiinflammatory actions of glucocorticoids. *Mol Endocrinol* 23: 281–291, 2009.

- doi: 10.1210/me.2008-0283.
150. **De Bosscher K, Vanden Berghe W, Haegeman G.** The interplay between the glucocorticoid receptor and nuclear factor- κ B or activator protein-1: Molecular mechanisms for gene repression. *Endocr Rev* 24: 488–522, 2003. doi: 10.1210/er.2002-0006.
 151. **de Haan N, Wuhrer M, Ruhaak LR.** Mass spectrometry in clinical glycomics: The path from biomarker identification to clinical implementation. *Clin Mass Spectrom* 18: 1–12, 2020. doi: 10.1016/j.clinms.2020.08.001.
 152. **de Kloet ER, Meijer OC.** MR/GR signaling in the brain during the stress response. In: *Aldosterone-Mineralocorticoid Receptor - Cell Biology to Translational Medicine*, edited by Harvey B, Jaisser F. Intech Open, p. 1–18.
 153. **de la Morena-Barrio ME, Martínez-Martínez I, de Cos C, Wypasek E, Roldán V, Undas A, van Scherpenzeel M, Lefeber DJ, Toderici M, Sevivas T, España F, Jaeken J, Corral J, Vicente V.** Hypoglycosylation is a common finding in antithrombin deficiency in the absence of a SERPINC1 gene defect. *J Thromb Haemost* 14: 1549–1560, 2016. doi: 10.1111/jth.13372.
 154. **de la Morena-Barrio ME, Suchon P, Jacobsen EM, Iversen N, Miñano A, de la Morena-Barrio B, Bravo-Pérez C, Padilla J, Cifuentes R, Asenjo S, Deleuze JF, Trégouët DA, Lozano ML, Vicente V, Sandset PM, Morange PE, Corral J.** Two SERPINC1 variants affecting N-glycosylation of Asn224 cause severe thrombophilia not detected by functional assays. *Blood* 140: 140–151, 2022. doi: 10.1182/blood.2021014708.
 155. **Deacon BJ, Abramowitz JS, Woods CM, Tolin DF.** The Anxiety Sensitivity Index - Revised: Psychometric properties and factor structure in two nonclinical samples. *Behav Res Ther* 41: 1427–1449, 2003. doi: 10.1016/S0005-7967(03)00065-2.
 156. **del Monte F, Agnetti G.** Protein post-translational modifications and misfolding: New concepts in heart failure. *Proteomics - Clin Appl* 8: 534–542, 2014. doi: 10.1002/prca.201400037.
 157. **Dempski RE, Imperiali B.** Oligosaccharyl transferase: Gatekeeper to the secretory pathway. *Curr Opin Chem Biol* 6: 844–850, 2002. doi: 10.1016/S1367-5931(02)00390-3.
 158. **Dhama K, Latheef SK, Dadar M, Samad HA, Munjal A, Khandia R, Karthik K, Tiwari R, Yattoo MI, Bhatt P, Chakraborty S, Singh KP, Iqbal HMN,**

- Chaicumpa W, Joshi SK.** Biomarkers in stress related diseases/disorders: Diagnostic, prognostic, and therapeutic values. *Front Mol Biosci* 6, 2019. doi: 10.3389/fmolb.2019.00091.
159. **Dienel GA.** Brain glucose metabolism: Integration of energetics with function. *Physiol Rev* 99: 949–1045, 2019. doi: 10.1152/physrev.00062.2017.
160. **Diez IA, Govender I, Naicker P, Stoychev S, Jordaan J, Jensen ON.** Zirconium(IV)-IMAC for phosphopeptide enrichment in phosphoproteomics. *bioRxiv* : 1–34, 2020. doi: 10.1101/2020.04.13.038810.
161. **Distelhorst CW.** Recent insights into the mechanism of glucocorticosteroid-induced apoptosis. *Cell Death Differ* 9: 6–19, 2002. doi: 10.1038/sj.cdd.4400969.
162. **Dobric M.** 46 stunning stress statistics & facts for 2020 [Online]. *loudcloudhealth*: 2019. <https://loudcloudhealth.com/stress-statistics/> [16 Jun. 2020].
163. **Dobric M.** 39 new stress statistics we have taken part in [Online]. *loudcloudhealth*: 2022. <https://loudcloudhealth.com/resources/stress-statistics/> [28 May 2022].
164. **Domon B, Aebersold R.** Challenges and opportunities in proteomics data analysis. *Mol Cell Proteomics* 5: 1921–1926, 2006. doi: 10.1074/mcp.R600012-MCP200.
165. **Dong Z, Ye L, Zhang Y, Chen Z, Li B, Zhang T, Zhao P.** Identification of N-linked glycoproteins in silkworm serum using Con A lectin affinity chromatography and mass spectrometry. *J Insect Sci* 21: 1–11, 2021. doi: 10.1093/jisesa/ieab057.
166. **Drake RR, Cazares LH, Jones EE, Fuller TW, Semmes OJ, Laronga C.** Challenges to developing proteomic-based breast cancer diagnostics. *Omi A J Integr Biol* 15: 251–259, 2011. doi: 10.1089/omi.2010.0120.
167. **Droescher M, Chaugule VK, Pichler A.** SUMO rules: Regulatory concepts and their implication in neurologic functions. *NeuroMolecular Med* 15: 639–660, 2013. doi: 10.1007/s12017-013-8258-6.
168. **Du J, McEwen B, Manji HK.** Glucocorticoid receptors modulate mitochondrial function: A novel mechanism for neuroprotection. *Commun Integr Biol* 2: 350–352, 2009. doi: 10.4161/cib.2.4.8554.
169. **Du J, Wang Y, Hunter R, Wei Y, Blumenthal R, Falke C, Khairova R, Zhou**

- R, Yuan P, Machado-Vieira R, McEwen BS, Manji HK.** Dynamic regulation of mitochondrial function by glucocorticoids. *Proc Natl Acad Sci U S A* 106: 3543–3548, 2009. doi: 10.1073/pnas.0812671106.
170. **Duan G, Walther D.** The roles of post-translational modifications in the context of protein interaction networks. *PLoS Comput Biol* 11: 1–23, 2015. doi: 10.1371/journal.pcbi.1004049.
171. **Duan J, Li W, Li W, Liu Q, Tian M, Chen C, Zhang L, Zhang M.** Quantitative proteomics analysis of susceptibility and resilience to stress in a rat model of PTSD. *Behav Brain Res* 415: 113509, 2021. doi: 10.1016/j.bbr.2021.113509.
172. **Duffin KL, Welply JK, Huang E, Henion JD, Huang E, Henion JD.** Characterization of N-linked oligosaccharides by electrospray and tandem mass spectrometry. *Anal Chem* 64: 1440–1448, 1992. doi: 10.1021/ac00037a024.
173. **Duffy MJ, Shering S, Sherry F, McDermott E, O’Higgins N.** CA 15-3: A prognostic marker in breast cancer. *Int J Biol Markers* 15: 330–333, 2000. doi: 10.1177/172460080001500410.
174. **Dunbar C, Kushnir MM, Yang YK.** Glycosylation profiling of the neoplastic biomarker alpha fetoprotein through intact mass protein analysis. *J Proteome Res* 22: 226–234, 2023. doi: 10.1021/acs.jproteome.2c00656.
175. **Duncan JG, Fong JL, Medeiros DM, Finck BN, Kelly DP.** Insulin-resistant heart exhibits a mitochondrial biogenic response driven by the peroxisome proliferator-activated receptor- α /PGC-1 α gene regulatory pathway. *Circulation* 115: 909–917, 2007. doi: 10.1161/CIRCULATIONAHA.106.662296.
176. **Dunn JD, Reid GE, Bruening ML.** Techniques for phosphopeptide enrichment prior to analysis by mass spectrometry. *Mass Spectrom Rev* 29: 29–54, 2010. doi: 10.1002/mas.20219.
177. **Durden T.** Prozac world: These are the most stressed out countries [Online]. *zerohedge*: 2013. <https://www.zerohedge.com/news/2013-07-17/prozac-world-these-are-most-stressed-out-countries> [16 Jun. 2020].
178. **Durham M, Regnier FE.** Targeted glycoproteomics: Serial lectin affinity chromatography in the selection of O-glycosylation sites on proteins from the human blood proteome. *J Chromatogr A* 1132: 165–173, 2006. doi: 10.1016/j.chroma.2006.07.070.
179. **Dwek RA, Edge C, Harvey D, Wormald MR.** Analysis of glycoprotein-associated oligosaccharides. *Analysis* 62: 65–100, 1993. doi:

- 10.1146/annurev.bi.62.070193.000433.
180. **Dziomba S, Araya-Farias M, Smadja C, Taverna M, Carbonnier B, Tran NT.** Solid supports for extraction and preconcentration of proteins and peptides in microfluidic devices: A review. *Anal Chim Acta* 955: 1–26, 2017. doi: 10.1016/j.aca.2016.12.017.
 181. **Dziurkowska E, Wesolowski M.** Cortisol as a biomarker of mental disorder severity. *J Clin Med* 10, 2021. doi: 10.3390/jcm10215204.
 182. **Ebner K, Singewald N.** Individual differences in stress susceptibility and stress inhibitory mechanisms. *Curr Opin Behav Sci* 14: 54–64, 2017. doi: 10.1016/j.cobeha.2016.11.016.
 183. **Edge ASB.** Deglycosylation of glycoproteins with trifluoromethanesulphonic acid: Elucidation of molecular structure and function. *Biochem J* 376: 339–350, 2003. doi: 10.1042/BJ20030673.
 184. **Edwards AS, Scott JD.** A-kinase anchoring proteins: Protein kinase A and beyond. *Curr Opin Cell Biol* 12: 217–221, 2000. doi: 10.1016/S0955-0674(99)00085-X.
 185. **Eifler K, Vertegaal ACO.** Mapping the SUMOylated landscape. *FEBS J* 282: 3669–3680, 2015. doi: 10.1111/febs.13378.
 186. **Eik-Nes TT, Tokatlian A, Raman J, Spirou D, Kvaløy K.** Depression, anxiety, and psychosocial stressors across BMI classes: A Norwegian population study - The HUNT Study. *Front Endocrinol (Lausanne)* 13: 1–11, 2022. doi: 10.3389/fendo.2022.886148.
 187. **Elias JE, Gygi SP.** Target-decoy search strategy for increased confidence in large-scale protein identifications by mass spectrometry. *Nat Methods* 4: 207–214, 2007. doi: 10.1038/nmeth1019.
 188. **Eng J, McCormack A, Yates J.** An approach to correlate tandem mass spectral data of peptides with amino acid sequences in a protein database. *J Am Soc Mass Spectrom* 5: 976–989, 1994. doi: [https://doi.org/10.1016/1044-0305\(94\)80016-2](https://doi.org/10.1016/1044-0305(94)80016-2).
 189. **Eng JK, Searle BC, Clauser KR, Tabb DL.** A face in the crowd: Recognizing peptides through database search. *Mol Cell Proteomics* 10: R111.009522, 2011. doi: 10.1074/mcp.R111.009522.
 190. **Engelbrecht AM, Smith C, Neethling I, Thomas M, Ellis B, Mattheyse M, Myburgh KH.** Daily brief restraint stress alters signaling pathways and induces

- atrophy and apoptosis in rat skeletal muscle. *Stress* 13: 132–141, 2010. doi: 10.3109/10253890903089834.
191. **Epel ES, Crosswell AD, Mayer SE, Prather AA, Slavich GM, Puterman E, Mendes WB.** More than a feeling: A unified view of stress measurement for population science. *Front Neuroendocrinol* 49: 146–169, 2018. doi: 10.1016/j.yfrne.2018.03.001.
192. **Espadas G, Borràs E, Chiva C, Sabidó E.** Evaluation of different peptide fragmentation types and mass analyzers in data-dependent methods using an Orbitrap Fusion Lumos Tribrid mass spectrometer. *Proteomics* 17: 1–9, 2017. doi: 10.1002/pmic.201600416.
193. **Fan X, Li D, Lichti CF, Green TA.** Dynamic proteomics of nucleus accumbens in response to acute psychological stress in environmentally enriched and isolated rats. *PLoS One* 8, 2013. doi: 10.1371/journal.pone.0073689.
194. **Fanayan S, Hincapie M, Hancock WS.** Using lectins to harvest the plasma/serum glycoproteome. *Electrophoresis* 33: 1746–1754, 2012. doi: 10.1002/elps.201100567.
195. **Fang X, Zhang WW.** Affinity separation and enrichment methods in proteomic analysis. *J Proteomics* 71: 284–303, 2008. doi: 10.1016/j.jprot.2008.06.011.
196. **Feng S, Yang N, Pennathur S, Goodison S, Lubman D.** Enrichment of glycoproteins using nanoscale chelating concanavalin A monolithic capillary chromatography. *Anal Chem* 15: 3776–3783, 2009. doi: 10.1021/ac900085k.Enrichment.
197. **Ferrie J., Kivimäki M, Shipley M., Davey Smith G, Virtanen MJ.** Job insecurity and incident coronary heart disease: The Whitehall II prospective cohort study. *Atherosclerosis* 227: 178–181, 2013. doi: 10.1016/j.atherosclerosis.2012.12.027.Job.
198. **Ficarro SB, Zhang Y, Carrasco-Alfonso MJ, Garg B, Adelmant G, Webber JT, Luckey CJ, Marto JA.** Online nanoflow multidimensional fractionation for high efficiency phosphopeptide analysis. *Mol Cell Proteomics* 10: 1–19, 2011. doi: 10.1074/mcp.O111.011064.
199. **Figueira TR, Barros MH, Camargo AA, Castilho RF, Ferreira JCB, Kowaltowski AJ, Sluse FE, Souza-Pinto NC, Vercesi AE.** Mitochondria as a source of reactive oxygen and nitrogen species: From molecular mechanisms to human health. *Antioxidants Redox Signal* 18: 2029–2074, 2013. doi:

- 10.1089/ars.2012.4729.
200. **Filipović D, Perić I, Costina V, Stanisavljević A, Gass P, Findeisen P.** Social isolation stress-resilient rats reveal energy shift from glycolysis to oxidative phosphorylation in hippocampal nonsynaptic mitochondria. *Life Sci* 254: 117790, 2020. doi: 10.1016/j.lfs.2020.117790.
 201. **Fílla J, Honys D.** Enrichment techniques employed in phosphoproteomics. *Amino Acids* 43: 1025–1047, 2012. doi: 10.1007/s00726-011-1111-z.
 202. **Fitchette A, Benchabane M, Paccalet T, Faye L, Gomord V.** Simple tools for complex N-glycan analysis. In: *The Protein Protocols Handbook*, edited by Walker JM. Hatfield: Humana Press, 1997, p. 1187–1197.
 203. **Fleshner M.** Stress-evoked sterile inflammation, danger associated molecular patterns (DAMPs), microbial associated molecular patterns (MAMPs) and the inflammasome. *Brain Behav Immun* 27: 1–7, 2013. doi: 10.1016/j.bbi.2012.08.012.
 204. **Flotho A, Melchior F.** Sumoylation: A regulatory protein modification in health and disease. *Annu Rev Biochem* 82: 357–385, 2013. doi: 10.1146/annurev-biochem-061909-093311.
 205. **Foot N, Henshall T, Kumar S.** Ubiquitination and the regulation of membrane proteins. *Physiol Rev* 97: 253–281, 2017. doi: 10.1152/physrev.00012.2016.
 206. **Förstermann U.** Oxidative stress in vascular disease: Causes, defense mechanisms and potential therapies. *Nat Clin Pract Cardiovasc Med* 5: 338–349, 2008. doi: 10.1038/ncpcardio1211.
 207. **Francisco R, Marques-da-Silva D, Brasil S, Pascoal C, dos Reis Ferreira V, Morava E, Jaeken J.** The challenge of CDG diagnosis. *Mol Genet Metab* 126: 1–5, 2019. doi: 10.1016/j.ymgme.2018.11.003.
 208. **Frank MG, Miguel ZD, Watkins LR, Maier SF.** Prior exposure to glucocorticoids sensitizes the neuroinflammatory and peripheral inflammatory responses to *E. coli* lipopolysaccharide. *Brain Behav Immun* 24: 19–30, 2010. doi: 10.1016/j.bbi.2009.07.008.
 209. **Fransson EI, Nordin M, Magnusson Hanson LL, Westerlund H.** Job strain and atrial fibrillation – Results from the Swedish Longitudinal Occupational Survey of Health and meta-analysis of three studies. *Eur J Prev Cardiol* 25: 1142–1149, 2018. doi: 10.1177/2047487318777387.
 210. **Freeze HH.** Lectin affinity chromatography. In: *Current Protocols in Protein*

- Science*. John Wiley & Sons, Inc., 1995, p. 9.1.1-9.1.9.
211. **Freeze HH, Chong JX, Bamshad MJ, Ng BG**. Solving glycosylation disorders: Fundamental approaches reveal complicated pathways. *Am J Hum Genet* 94: 161–175, 2014. doi: 10.1016/j.ajhg.2013.10.024.
 212. **Freire C, Ferradás M del M, Regueiro B, Rodríguez S, Valle A, Núñez JC**. Coping strategies and self-efficacy in university students: A person-centered approach. *Front Psychol* 11: 1–11, 2020. doi: 10.3389/fpsyg.2020.00841.
 213. **Frey FJ, Odermatt A, Frey BM**. Glucocorticoid-mediated mineralocorticoid receptor activation and hypertension. *Curr Opin Nephrol Hypertens* 13: 451–458, 2004. doi: 10.1097/01.mnh.0000133976.32559.b0.
 214. **Fricchione GL**. The challenge of stress-related non-communicable diseases. *Med Sci Monit Basic Res* 24: 93–95, 2018. doi: 10.12659/MSMBR.911473.
 215. **Fu Q, Garnham CP, Elliott ST, Bovenkamp DE, Van Eyk JE**. A robust, streamlined, and reproducible method for proteomic analysis of serum by delipidation, albumin and IgG depletion, and two-dimensional gel electrophoresis. *Proteomics* 5: 2656–2664, 2005. doi: 10.1002/pmic.200402048.
 216. **Fujimoto S, Nomura M, Niki M, Motoba H, Ieishi K, Mori T, Ikefuji H, Ito S**. Evaluation of stress reactions during upper gastrointestinal endoscopy in elderly patients: assessment of mental stress using chromogranin A. *J Med Investig* 54: 140–145, 2007. doi: <https://doi.org/10.2152/jmi.54.140>.
 217. **G Biosciences**. Concanavalin A (Con A) Agarose [Online]. *G Biosci. A Geno Technology Inc.:* 7–8, 2014. http://www.gbiosciences.com/ResearchProducts/cona_agarose.aspx [9 Jun. 2021].
 218. **Gahan PB**. Circulating nucleic acids in plasma and serum: Diagnosis and prognosis in cancer. *EPMA J* 1: 503–512, 2010. doi: 10.1007/s13167-010-0021-6.
 219. **Galea S, Lurie N**. The mental health consequences of COVID-19 and physical distancing: The need for prevention and early intervention. *JAMA Intern Med* 8: 817–818, 2020. doi: 10.1002/da.20838.
 220. **Gallien S, Bourmaud A, Domon B**. A simple protocol to routinely assess the uniformity of proteomics analyses. *J Proteome Res* 13: 2688–2695, 2014. doi: 10.1021/pr4011712.

221. **Gallagher-Beckley AJ, Cidlowski JA.** Emerging roles of glucocorticoid receptor phosphorylation in modulating glucocorticoid hormone action in health and disease. *IUBMB Life* 61: 979–986, 2009. doi: 10.1002/iub.245.
222. **Gallup Inc.** Gallup Global Emotions 2021 [Online]. <https://www.gallup.com/analytics/349280/gallup-global-emotions-report.aspx>.
223. **Gambini J, Stromsnes K.** Oxidative stress and inflammation: From mechanisms to therapeutic approaches. *Biomedicines* 10: 753, 2022. doi: 10.3390/biomedicines10040753.
224. **Gao Y, Rodríguez L V.** The effect of chronic psychological stress on lower urinary tract function: An animal model perspective. *Front Physiol* 13: 1–14, 2022. doi: 10.3389/fphys.2022.818993.
225. **García A, Martí O, Vallès A, Dal-Zotto S, Armario A.** Recovery of the hypothalamic-pituitary-adrenal response to stress. *Neuroendocrinology* 72: 114–125, 2000. doi: 10.1159/000054578.
226. **Garny S, Beeton-Kempen N, Gerber I, Verschoor J, Jordaan J.** The co-immobilization of P450-type nitric oxide reductase and glucose dehydrogenase for the continuous reduction of nitric oxide via cofactor recycling. *Enzyme Microb Technol* 85: 71–81, 2016. doi: 10.1016/j.enzmictec.2015.10.006.
227. **Gates MB, Tomer KB, Deterding LJ.** Comparison of metal and metal oxide media for phosphopeptide enrichment prior to mass spectrometric analyses. *J Am Soc Mass Spectrom* 21: 1649–1659, 2010. doi: 10.1016/j.jasms.2010.06.005.
228. **George T, Brady M.** Ethylenediaminetetraacetic Acid (EDTA) [Online]. StatPearls Publishing. <https://www.ncbi.nlm.nih.gov/books/NBK565883/> [19 Aug. 2023].
229. **Ghallab A.** In vitro test systems and their limitations. *EXCLI J* 12: 1024–1026, 2013.
230. **Gibbs A, Mkhwanazi S.** Poverty, violence and stress: Why South Africa’s young people are anxious – Bhekisisa [Online]. *Bhekisisa*: 2021. <https://bhekisisa.org/article/2021-09-01-poverty-violence-and-stress-why-south-africas-young-people-are-anxious/> [14 Nov. 2022].
231. **Gilmore JM, Kettenbach AN, Gerber SA.** Increasing phosphoproteomic coverage through sequential digestion by complementary proteases. *Anal Bioanal Chem* 402: 711–720, 2011. doi: 10.1007/s00216-011-5466-5.

232. **Giorgianni F, Beranova-Giorgianni S.** Phosphoproteome discovery in human biological fluids. *Proteomes* 4: 1–21, 2016. doi: 10.3390/proteomes4040037.
233. **Gjerstad JK, Lightman SL, Spiga F.** Role of glucocorticoid negative feedback in the regulation of HPA axis pulsatility. *Stress* 21: 403–416, 2018. doi: 10.1080/10253890.2018.1470238.
234. **Godoy LD, Rossignoli MT, Delfino-Pereira P, Garcia-Cairasco N, Umeoka EH de L.** A comprehensive overview on stress neurobiology: Basic concepts and clinical implications. *Front Behav Neurosci* 12: 1–23, 2018. doi: 10.3389/fnbeh.2018.00127.
235. **Gold PW, Gabry KE, Yasuda MR, Chrousos GP.** Divergent endocrine abnormalities in melancholic and atypical depression: Clinical and pathophysiologic implications. *Endocrinol Metab Clin North Am* 31: 37–62, 2002. doi: 10.1016/S0889-8529(01)00022-6.
236. **Goldstein G, Scheid M, Hammerling U, Schlesinger DH, Niall HD, Boyse EA.** Isolation of a polypeptide that has lymphocyte differentiating properties and is probably represented universally in living cells. *Proc Natl Acad Sci U S A* 72: 11–15, 1975. doi: 10.1073/pnas.72.1.11.
237. **Goldstein IJ, Reichert CM, Misaki A.** Interaction of concanavalin a with model substrates. *Ann N Y Acad Sci* 234: 283–296, 1974. doi: 10.1111/j.1749-6632.1974.tb53040.x.
238. **Gonzalez MW, Kann MG.** Chapter 4: Protein interactions and disease. *PLoS Comput Biol* 8: e1002819, 2012. doi: 10.1371/journal.pcbi.1002819.
239. **Gonzalo-Calvo D, Pérez-Boza J, Curado J, Devaux Y.** Challenges of microRNA-based biomarkers in clinical application for cardiovascular diseases. *Clin Transl Med* 12: 10–12, 2022. doi: 10.1002/ctm2.585.
240. **Goth CK, Tuhkanen HE, Khan H, Lackman JJ, Wang S, Narimatsu Y, Hansen LH, Overall CM, Clausen H, Schjoldager KT, Petäjä-Repo UE.** Site-specific O-glycosylation by polypeptide N-acetylgalactosaminyltransferase 2 (GalNAc-transferase T2) co-regulates β 1-adrenergic receptor N-terminal cleavage. *J Biol Chem* 292: 4714–4726, 2017. doi: 10.1074/jbc.M116.730614.
241. **Gouin JP, Glaser R, Malarkey WB, Beversdorf D, Kiecolt-Glaser J.** Chronic stress, daily stressors, and circulating inflammatory markers. *Heal Psychol* 31: 264–268, 2012. doi: 10.1037/a0025536.
242. **Goulabchand R, Vincent T, Batteux F, Eliaou J François, Guilpain P.** Impact

- of autoantibody glycosylation in autoimmune diseases. *Autoimmun Rev* 13: 742–750, 2014. doi: 10.1016/j.autrev.2014.02.005.
243. **Goumenou A, Delaunay N, Pichon V.** Recent advances in lectin-based affinity sorbents for protein glycosylation studies. *Front Mol Biosci* 8: 1–27, 2021. doi: 10.3389/fmolb.2021.746822.
244. **Graves P, Haystead T.** Molecular biologist's guide to proteomics. *Microbiol Mol Biol Rev* 66: 39–63, 2002. doi: 10.1128/MMBR.66.1.39.
245. **Greff MJE, Levine JM, Abuzgaia AM, Elzagallaai AA, Rieder MJ, van Uum SHM.** Hair cortisol analysis: An update on methodological considerations and clinical applications. *Clin Biochem* 63: 1–9, 2019. doi: 10.1016/j.clinbiochem.2018.09.010.
246. **Grotenberg G, Ploegh H.** Dressed-up proteins. *Nature* 446: 994–995, 2007. doi: 10.1038/446993a.
247. **Guillard M, Morava E, Van Delft FL, Hague R, Körner C, Adamowicz M, Wevers RA, Lefeber DJ.** Plasma N-glycan profiling by mass spectrometry for congenital disorders of glycosylation type II. *Clin Chem* 57: 593–602, 2011. doi: 10.1373/clinchem.2010.153635.
248. **Guilliams TG, Edwards L.** Chronic stress and the HPA axis: Clinical assessment and therapeutic considerations. *Stand* 9: 1–12, 2010.
249. **Gundry RL, Fu Q, Jelinek CA, Van Eyk JE, Cotter RJ.** Investigation of an albumin-enriched fraction of human serum and its albuminome. *Proteomics - Clin Appl* 1: 73–88, 2007. doi: 10.1002/prca.200600276.Investigation.
250. **Guo J, Huan T.** Comparison of full-scan, data-dependent, and data-independent acquisition modes in liquid chromatography-mass spectrometry based untargeted metabolomics. *Anal Chem* 92: 8072–8080, 2020. doi: 10.1021/acs.analchem.9b05135.
251. **Guo Y.** Recent progress in the fundamental understanding of hydrophilic interaction chromatography (HILIC). *Analyst* 140: 6452–6466, 2015. doi: 10.1039/c5an00670h.
252. **Gut P, Czarnywojtek A, Fischbach J, Baczyk M, Ziemnicka K, Wrotkowska E, Gryczyńska M, Ruchała M.** Chromogranin A - Unspecific neuroendocrine marker. Clinical utility and potential diagnostic pitfalls. *Arch Med Sci* 12: 1–9, 2016. doi: 10.5114/aoms.2016.57577.
253. **Gutiérrez A, Cerón JJ, Razzazi-Fazeli E, Schlosser S, Tecles F.** Influence of

- different sample preparation strategies on the proteomic identification of stress biomarkers in porcine saliva. *BMC Vet Res* 13: 1–11, 2017. doi: 10.1186/s12917-017-1296-9.
254. **Ha J, Kang E, Seo J, Cho S.** Phosphorylation dynamics of JNK signaling: Effects of dual-specificity phosphatases (dusps) on the jnk pathway. *Int J Mol Sci* 20: 1–19, 2019. doi: 10.3390/ijms20246157.
255. **Haider SR, Reid HJ, Sharp BL.** Tricine-SDS-PAGE. In: *Methods in Molecular Biology*, edited by Kurien B, Scofield R, p. 81–91.
256. **Hamilton PJ, Chen EY, Tolstikov V, Peña CJ, Picone JA, Shah P, Panagopoulos K, Strat AN, Walker DM, Lorsch ZS, Robinson HL, Mervosh NL, Kiraly DD, Sarangarajan R, Narain NR, Kiebish MA, Nestler EJ.** Chronic stress and antidepressant treatment alter purine metabolism and beta oxidation within mouse brain and serum. *Sci Rep* 10: 1–14, 2020. doi: 10.1038/s41598-020-75114-5.
257. **Han G, Ye M, Zou H.** Development of phosphopeptide enrichment techniques for phosphoproteome analysis. *Analyst* 133: 1128–1138, 2008. doi: 10.1039/b806775a.
258. **Hao P, Ren Y, Alpert AJ, Siu KS.** Detection, evaluation and minimization of nonenzymatic deamidation in proteomic sample preparation. *Mol Cell Proteomics* 10: O111.009381, 2011. doi: 10.1074/mcp.O111.009381.
259. **Hariri AR, Holmes A.** Finding translation in stress research. *Nat Neurosci* 18: 1347–1352, 2015. doi: 10.1038/nn.4111.
260. **Hart C, Schulenberg B, Steinberg TH, Leung W-Y, Patton WF.** Detection of glycoproteins in polyacrylamide gels using Pro-Q emerald 300 dye, a fluorescent periodate schiff-base stain. *Electrophoresis* 24: 588–598, 2003. doi: 10.1007/978-1-4939-8745-0_14.
261. **Hart G., Kelly W., Blomberg, M.A. Roquemore EP, Dong L, Kreppel L, Chou T, Snow D, Greis K.** Glycosylation of nuclear and cytoplasmic proteins is as abundant and as dynamic as phosphorylation. In: *Glyco- and Cellbiology*, edited by Wieland F, Reutter W. Springer, 1994, p. 91–103.
262. **Hart GW.** Glycosylation. *Curr Opin Cell Biol* 4: 1017–1023, 1992. doi: 10.1016/0955-0674(92)90134-X.
263. **Hart GW.** Nutrient regulation of signaling and transcription. *J Biol Chem* 294: 2211–2231, 2019. doi: 10.1074/jbc.AW119.003226.

264. **Hart GW, Slawson C, Ramirez-Correa G, Lagerlof O.** Cross talk Between O-GlcNAcylation and phosphorylation: Roles in signaling, transcription, and chronic disease. *Annu Rev Biochem* 7: 825–858, 2011. doi: 10.1146/annurev-biochem-060608-102511.
265. **Harvard Medical School.** Understanding the stress response - Harvard Health [Online]. *Harvard Heal. Publ.*: 2011. <https://www.health.harvard.edu/staying-healthy/understanding-the-stress-response> [29 Oct. 2020].
266. **Harvey DJ, Wing DR, Küster B, Wilson IBH.** Composition of N-linked carbohydrates from ovalbumin and co-purified glycoproteins. *J Am Soc Mass Spectrom* 11: 564–571, 2000. doi: 10.1016/S1044-0305(00)00122-7.
267. **Hayashi T.** Conversion of psychological stress into cellular stress response: Roles of the sigma-1 receptor in the process. *Psychiatry Clin Neurosci* 69: 179–191, 2015. doi: 10.1111/pcn.12262.
268. **Heinisch JJ, Brandt R.** Signaling pathways and posttranslational modifications of tau in Alzheimer's disease: The humanization of yeast cells. *Microb Cell* 3: 135–146, 2016. doi: 10.15698/mic2016.04.489.
269. **Helander A, Wielders J, Anton R, Arndt T, Bianchi V, Deenmamode J, Jeppsson JO, Whitfield JB, Weykamp C, Schellenberg F.** Standardisation and use of the alcohol biomarker carbohydrate-deficient transferrin (CDT). *Clin Chim Acta* 459: 19–24, 2016. doi: 10.1016/j.cca.2016.05.016.
270. **Helgesson Ö, Cabrera C, Lapidus L, Bengtsson C, Lissner L.** Self-reported stress levels predict subsequent breast cancer in a cohort of Swedish women. *Eur J Cancer Prev* 12: 377–381, 2003. doi: 10.1097/00008469-200310000-00006.
271. **Helman TJ, Headrick JP, Stapelberg NJC, Braidy N.** The sex-dependent response to psychosocial stress and ischaemic heart disease. *Front Cardiovasc Med* 10, 2023. doi: 10.3389/fcvm.2023.1072042.
272. **Helmholz H, Cartellieri S, He L, Thiesen P, Niemeyer B.** Process development in affinity separation of glycoconjugates with lectins as ligands. *J Chromatogr A* 1006: 127–135, 2003. doi: 10.1016/S0021-9673(03)00783-0.
273. **Henry H, Froehlich F, Perret R, Tissot JD, Eilers-Messerli B, Lavanchy D, Dionisi-Vici C, Gonvers JJ, Bachmann C.** Microheterogeneity of serum glycoproteins in patients with chronic alcohol abuse compared with carbohydrate-deficient glycoprotein syndrome type I. *Clin Chem* 45: 1408–1413,

1999. doi: 10.1093/clinchem/45.9.1408.
274. **Hildonen S, Halvorsen TG, Reubsaet L.** Why less is more when generating tryptic peptides in bottom-up proteomics. *Proteomics* 14: 2031–2041, 2014. doi: 10.1002/pmic.201300479.
275. **Hill LA, Bodnar TS, Weinberg J, Hammond GL.** Corticosteroid-binding globulin is a biomarker of inflammation onset and severity in female rats. *J Endocrinol* 230: 215–225, 2016. doi: 10.1530/JOE-16-0047.
276. **Honda M, Kuwano Y, Katsuura-Kamano S, Kamezaki Y, Fujita K, Akaike Y, Kano S, Nishida K, Masuda K, Rokutan K.** Chronic academic stress increases a group of microRNAs in peripheral blood. *PLoS One* 8, 2013. doi: 10.1371/journal.pone.0075960.
277. **Hoque A, Goodman P, Ambrosone C, Figg W, Price D, Kopp W, Wu X, Conroy J, Lehman T, Santella R.** Extraction of DNA from serum for high-throughput genotyping: findings from pilot studies within the Prostate Cancer Prevention Trial. *Urology* 71: 967–970, 2008. doi: 10.1016/j.urology.2007.11.042.
278. **Hou DD, Zhu RZ, Sun Z, Ma XD, Wang DC, Timothy H, Chen WN, Yan F, Lei P, Han XW, Chen DX, Cai LP, Guan HQ.** Serum proteomics analysis in rats of immunosuppression induced by chronic stress. *Scand J Immunol* 84: 165–173, 2016. doi: 10.1111/sji.12461.
279. **Hsieh SY, Chen RK, Pan YH, Lee HL.** Systematical evaluation of the effects of sample collection procedures on low-molecular-weight serum/plasma proteome profiling. *Proteomics* 6: 3189–3198, 2006. doi: 10.1002/pmic.200500535.
280. **Huang J, Qin H, Sun Z, Huang G, Mao J, Cheng K, Zhang Z, Wan H, Yao Y, Dong J, Zhu J, Wang F, Ye M, Zou H.** A peptide N-terminal protection strategy for comprehensive glycoproteome analysis using hydrazide chemistry based method. *Sci Rep* 5: 1–15, 2015. doi: 10.1038/srep10164.
281. **Huang KY, Lee TY, Kao HJ, Ma CT, Lee CC, Lin TH, Chang WC, Huang H Da.** DbPTM in 2019: Exploring disease association and cross-Talk of post-Translational modifications. *Nucleic Acids Res* 47: D298–D308, 2019. doi: 10.1093/nar/gky1074.
282. **Huang P, Li C, Fu T, Zhao D, Yi Z, Lu Q, Guo L, Xu X.** Flupirtine attenuates chronic restraint stress-induced cognitive deficits and hippocampal apoptosis in male mice. *Behav Brain Res* 288: 1–10, 2015. doi: 10.1016/j.bbr.2015.04.004.

283. **Hubler SL, Kumar P, Mehta S, Easterly C, Johnson JE, Jagtap PD, Griffin TJ.** Challenges in peptide-spectrum matching: A robust and reproducible statistical framework for removing low-accuracy, high-scoring hits. *J Proteome Res* 19: 161–173, 2020. doi: 10.1021/acs.jproteome.9b00478.
284. **Hussain T, Tan B, Yin Y, Blachier F, Tossou MCB, Rahu N.** Oxidative stress and inflammation: What polyphenols can do for us? *Oxid Med Cell Longev* 2016, 2016. doi: 10.1155/2016/7432797.
285. **Hwang L, Ayaz-Guner S, Gregorich Z, Cai W, Valeja S, Jin S, Ge Y.** Specific enrichment of phosphoproteins using functionalized multivalent nanoparticles. *J Am Chem Soc* 137: 2432–2435, 2015. doi: 10.1021/ja511833y.
286. **Idil N, Perçin I, Karakoç V, Yavuz H, Aksöz N, Denizli A.** Concanavalin A immobilized magnetic poly(glycidyl methacrylate) beads for prostate specific antigen binding. *Colloids Surfaces B Biointerfaces* 134: 461–468, 2015. doi: 10.1016/j.colsurfb.2015.06.050.
287. **Ikegami T.** Hydrophilic interaction chromatography for the analysis of biopharmaceutical drugs and therapeutic peptides: A review based on the separation characteristics of the hydrophilic interaction chromatography phases. *J Sep Sci* 42: 130–213, 2019. doi: 10.1002/jssc.201801074.
288. **Iliuk A.** Identification of phosphorylated proteins on a global scale. *Curr Protoc Chem Biol* 10: e48, 2018. doi: 10.1002/cpch.48.
289. **Imhof JT, Coelho ZMI, Schmitt ML, Morato GS, Carobrez AP.** Influence of gender and age on performance of rats in the elevated plus maze apparatus. *Behav Brain Res* 56: 177–180, 1993. doi: 10.1016/0166-4328(93)90036-P.
290. **Immordino-Yang MH, Yang XF, Damasio H.** Cultural modes of expressing emotions influence how emotions are experienced. *Emotion* 16: 1033–1039, 2016. doi: 10.1037/emo0000201.
291. **International Human Genome Sequencing Consortium.** Finishing the euchromatic sequence of the human genome. *Nature* 431: 931–945, 2004. doi: 10.1038/nature03001.
292. **Islam MR, Islam MR, Ahmed I, Moktadir A AI, Nahar Z, Islam MS, Shahid SFB, Islam SN, Islam MS, Hasnat A.** Elevated serum levels of malondialdehyde and cortisol are associated with major depressive disorder: A case-control study. *SAGE Open Med* 6, 2018. doi: 10.1177/2050312118773953.

293. **Ismaili N, Garabedian MJ.** Modulation of glucocorticoid receptor function via phosphorylation. *Ann N Y Acad Sci* 1024: 86–101, 2004. doi: 10.1196/annals.1321.007.
294. **Ito K, Matsudomi N.** Structural characteristics of hen egg ovalbumin expressed in yeast *Pichia pastoris*. *Biosci Biotechnol Biochem* 69: 755–761, 2005. doi: 10.1271/bbb.69.755.
295. **Iwata M, Ota KT, Duman RS.** The inflammasome: Pathways linking psychological stress, depression, and systemic illnesses. *Brain Behav Immun* 31: 105–114, 2013. doi: 10.1016/j.bbi.2012.12.008.
296. **Jack CR, Bennett DA, Blennow K, Carrillo MC, Dunn B, Haeberlein SB, Holtzman DM, Jagust W, Jessen F, Karlawish J, Liu E, Molinuevo JL, Montine T, Phelps C, Rankin KP, Rowe CC, Scheltens P, Siemers E, Snyder HM, Sperling R, Elliott C, Masliah E, Ryan L, Silverberg N.** NIA-AA Research Framework: Toward a biological definition of Alzheimer’s disease. *Alzheimer’s Dement* 14: 535–562, 2018. doi: 10.1016/j.jalz.2018.02.018.
297. **Jaeken J, Morava E.** Congenital disorders of glycosylation, dolichol and glycosylphosphatidylinositol metabolism. In: *Inborn metabolic diseases diagnosis and treatment*, edited by J-M M, Baumgartner M, Walter J. Berlin: Springer, 2016, p. 607–622.
298. **Jaeken J, Péanne R.** What is new in CDG? *J Inherit Metab Dis* 40: 569–586, 2017. doi: 10.1007/s10545-017-0050-6.
299. **Jaggi AS, Bhatia N, Kumar N, Singh N, Anand P, Dhawan R.** A review on animal models for screening potential anti-stress agents. *Neurol Sci* 32: 993–1005, 2011. doi: 10.1007/s10072-011-0770-6.
300. **Jankovska E, Svitek M, Holada K, Petrak J.** Affinity depletion versus relative protein enrichment: a side-by-side comparison of two major strategies for increasing human cerebrospinal fluid proteome coverage. *Clin Proteomics* 16: 1–10, 2019. doi: 10.1186/s12014-019-9229-1.
301. **Jaros JA, Rahmoune H, Wesseling H, Leweke FM, Ozcan S, Guest PC, Bahn S.** Effects of olanzapine on serum protein phosphorylation patterns in patients with schizophrenia. *Proteomics - Clin Appl* 9: 907–916, 2015. doi: 10.1002/prca.201400148.
302. **Jaros JAJ, Guest PC, Ramoune H, Rothermundt M, Leweke FM, Martins-de-Souza D, Bahn S.** Clinical use of phosphorylated proteins in blood serum

- analysed by immobilised metal ion affinity chromatography and mass spectrometry. *J Proteomics* 76: 36–42, 2012. doi: 10.1016/j.jprot.2012.02.015.
303. **Jensen ON**. Modification-specific proteomics: Characterization of post-translational modifications by mass spectrometry. *Curr Opin Chem Biol* 8: 33–41, 2004. doi: 10.1016/j.cbpa.2003.12.009.
304. **Jensen S, Larsen M**. Evaluation of the impact of some experimental procedures on different phosphopeptide enrichment techniques. *Rapid Commun Mass Spectrom* 21: 3635–3645, 2007. doi: 10.1002/rcm.
305. **Jiang L, Messing ME, Ye L**. Temperature and pH dual-responsive core-brush nanocomposite for enrichment of glycoproteins. *ACS Appl Mater Interfaces* 9: 8985–8995, 2017. doi: 10.1021/acsami.6b15326.
306. **Jin J, Pawson T**. Modular evolution of phosphorylation-based signalling systems. *Philos Trans R Soc B Biol Sci* 367: 2540–2555, 2012. doi: 10.1098/rstb.2012.0106.
307. **Joh Y, Lee K, Kim H, Park H**. Progressive search in tandem mass spectrometry. *BMC Bioinformatics* 24: 1–16, 2023. doi: 10.1186/s12859-023-05222-2.
308. **Johnson D, Boyes B, Fields T, Kopkin R, Orlando R**. Optimization of data-dependent acquisition parameters for coupling high-speed separations with LC-MS/MS for protein identifications. *J Biomol Tech* 24: 62–72, 2013. doi: 10.7171/jbt.13-2402-003.
309. **Johnson GL, Lapadat R**. Mitogen-activated protein kinase pathways mediated by ERK, JNK, and p38 protein kinases. *Science (80-)* 298: 1911–1912, 2002. doi: 10.1126/science.1072682.
310. **Joshi HJ, Jørgensen A, Schjoldager KT, Halim A, Dworkin LA, Steentoft C, Wandall HH, Clausen H, Vakhrushev SY**. GlycoDomainViewer: A bioinformatics tool for contextual exploration of glycoproteomes. *Glycobiology* 28: 131–136, 2018. doi: 10.1093/glycob/cwx104.
311. **Jovicic MJ, Lukic I, Radojicic M, Adzic M, Maric NP**. Modulation of c-Jun N-terminal kinase signaling and specific glucocorticoid receptor phosphorylation in the treatment of major depression. *Med Hypotheses* 85: 291–294, 2015. doi: 10.1016/j.mehy.2015.05.015.
312. **Jung C, Greco S, Nguyen HHT, Ho JT, Lewis JG, Torpy DJ, Inder WJ**. Plasma, salivary and urinary cortisol levels following physiological and stress

- doses of hydrocortisone in normal volunteers. *BMC Endocr Disord* 14: 1–10, 2014. doi: 10.1186/1472-6823-14-91.
313. **Jung K, Cho W, Regnier FE.** Glycoproteomics of plasma based on narrow selectivity lectin affinity chromatography. *J Proteome Res* 8: 643–650, 2009. doi: 10.1021/pr8007495.
314. **Kaltashov IA, Abzalimov RR.** Do ionic charges in ESI-MS provide useful information on macromolecular structure? *J Am Soc Mass Spectrom* 19: 1239–1246, 2008. doi: 10.1016/j.jasms.2008.05.018.
315. **Kambe Y, Miyata A.** Potential involvement of the mitochondrial unfolded protein response in depressive-like symptoms in mice. *Neurosci Lett* 588: 166–171, 2015. doi: 10.1016/j.neulet.2015.01.006.
316. **Kanwar J, Kanwar R, Burrow H, Baratchi S.** Recent advances on the roles of NO in cancer and chronic inflammatory disorders. *Curr Med Chem* 16: 2373–2394, 2009. doi: 10.2174/092986709788682155.
317. **Karanikas E, Vlasidou DI.** Psychologically traumatic stress inducing redox – inflammation interplay; which comes first? *Pharmacol Biochem Behav* 209: 1–3, 2021. doi: 10.1016/j.pbb.2021.173254.
318. **Karimi M, Malekzad H, Mirshekari H, Sahandi P, Basri SMM, Baniasadi F, Aghdam MS, Hamblin MR, Hospital MG, Education US.** Plant protein-based hydrophobic fine and ultrafine carrier particles in drug delivery systems. *Crit Rev Biotechnol* 38: 47–67, 2018. doi: 10.1080/07388551.2017.1312267.
319. **Karpievitch Y V., Polpitiya AD, Anderson GA, Smith RD, Dabney AR.** Liquid chromatography mass spectrometry-based proteomics: Biological and technological aspects. *Ann Appl Stat* 4: 1797–1823, 2010. doi: 10.1214/10-AOAS341.
320. **Karve TM, Cheema AK.** Small changes huge impact: The role of protein posttranslational modifications in cellular homeostasis and disease. *J Amino Acids* 2011: 1–13, 2011. doi: 10.4061/2011/207691.
321. **Karyotaki E, Cuijpers P, Albor Y, Alonso J, Auerbach RP, Bantjes J, Bruffaerts R, Ebert DD, Hasking P, Kiekens G, Lee S, McLafferty M, Mak A, Mortier P, Sampson NA, Stein DJ, Vilagut G, Kessler RC.** Sources of stress and their associations with mental disorders among college students: Results of the World Health Organization world mental health surveys international college student initiative. *Front Psychol* 11: 1–11, 2020. doi: 10.3389/fpsyg.2020.01759.

322. **Katsuura S, Kuwano Y, Yamagishi N, Kurokawa K, Kajita K, Akaike Y, Nishida K, Masuda K, Tanahashi T, Rokutan K.** MicroRNAs miR-144/144* and miR-16 in peripheral blood are potential biomarkers for naturalistic stress in healthy Japanese medical students. *Neurosci Lett* 516: 79–84, 2012. doi: 10.1016/j.neulet.2012.03.062.
323. **Kaufmann A, Teale P.** Capabilities and limitations of high-resolution mass spectrometry (HRMS): time-of-flight and Orbitrap. In: *Chemical analysis of non-antimicrobial veterinary drug residues in food*. John Wiley & Sons, Inc., 2016, p. 93–139.
324. **Keating CL, Kuhn E, Bals J, Cocco AR, Yousif AS, Matysiak C, Sangesland M, Ronsard L, Smoot M, Moreno TB, Okonkwo V, Setliff I, Georgiev I, Balazs AB, Carr SA, Lingwood D.** Spontaneous glycan reattachment following N-glycanase treatment of influenza and HIV vaccine antigens. *J Proteome Res* 19: 733–743, 2020. doi: 10.1021/acs.jproteome.9b00620.
325. **Kelleher N, Thomas P, Ntai I, Compton P, LeDuc R.** Deep and quantitative top-down proteomics in clinical and translational research. *Expert Rev Proteomics* 11: 649–651, 2014. doi: 10.1586/14789450.2014.976559.
326. **Keller A, Nesvizhskii AI, Kolker E, Aebersold R.** Empirical statistical model to estimate the accuracy of peptide identifications made by MS/MS and database search. *Anal Chem* 74: 5383–5392, 2002. doi: 10.1021/ac025747h.
327. **Kennedy BM, Kumanyika S, Ard JD, Reams P, Johnson CA, Karanja N, Charleston JB, Appel LJ, Maurice V, Harsha DW.** Overall and minority-focused recruitment strategies in the PREMIER multicenter trial of lifestyle interventions for blood pressure control. *Contemp Clin Trials* 31: 49–54, 2010. doi: <https://doi.org/10.1016/j.cct.2009.10.002>.
328. **Kermott CA, Johnson RE, Sood R, Jenkins SM, Sood A.** Is higher resilience predictive of lower stress and better mental health among corporate executives? *PLoS One* 14: 1–14, 2019. doi: 10.1371/journal.pone.0218092.
329. **Khan SH, McLaughlin WA, Kumar R.** Site-specific phosphorylation regulates the structure and function of an intrinsically disordered domain of the glucocorticoid receptor. *Sci Rep* 7: 1–8, 2017. doi: 10.1038/s41598-017-15549-5.
330. **Khoury GA, Baliban RC, Floudas CA.** Proteome-wide post-translational modification statistics: Frequency analysis and curation of the swiss-prot

- database. *Sci Rep* 1: 1–5, 2011. doi: 10.1038/srep00090.
331. **Kianfar E.** Protein nanoparticles in drug delivery: animal protein, plant proteins and protein cages, albumin nanoparticles. *J Nanobiotechnology* 19: 1–32, 2021. doi: 10.1186/s12951-021-00896-3.
332. **Kim Y, Carver CS, Shaffer KM, Gansler T, Cannady RS.** Cancer caregiving predicts physical impairments: Roles of earlier caregiving stress and being a spousal caregiver. *Cancer* 121: 302–310, 2015. doi: 10.1002/cncr.29040.
333. **King CC, Sastri M, Chang P, Pennypacker J, Taylor SS.** The rate of NF- κ B nuclear translocation is regulated by PKA and A kinase interacting protein 1. *PLoS One* 6: 1–15, 2011. doi: 10.1371/journal.pone.0018713.
334. **King R, Bonfiglio R, Fernandez-Metzler C, Miller-Stein C, Olah T.** Mechanistic investigation of ionization suppression in electrospray ionization. *J Am Soc Mass Spectrom* 11: 942–950, 2000. doi: 10.1016/S1044-0305(00)00163-X.
335. **Kinoshita-Kikuta E, Kinoshita E, Koike T.** Separation and identification of four distinct serine-phosphorylation states of ovalbumin by Phos-tag affinity electrophoresis. *Electrophoresis* 33: 849–855, 2012. doi: 10.1002/elps.201100518.
336. **Kirwan A, Utratna M, O'Dwyer ME, Joshi L, Kilcoyne M.** Glycosylation-based serum biomarkers for cancer diagnostics and prognostics. *Biomed Res Int* 2015, 2015. doi: 10.1155/2015/490531.
337. **Kitchener P, Di Blasi F, Borrelli E, Piazza PV.** Differences between brain structures in nuclear translocation and DNA binding of the glucocorticoid receptor during stress and the circadian cycle. *Eur J Neurosci* 19: 1837–1846, 2004. doi: 10.1111/j.1460-9568.2004.03267.x.
338. **Kivimäki M, Nyberg ST, Batty GD, Kawachi I, Jokela M, et al.** Long working hours as a risk factor for atrial fibrillation: A multi-cohort study. *Eur Heart J* 38: 2621–2628, 2017. doi: 10.1093/eurheartj/ehx324.
339. **Klement E, Raffai T, Medzihradszky KF.** Immobilized metal affinity chromatography optimized for the analysis of extracellular phosphorylation. *Proteomics* 16: 1858–1862, 2016. doi: 10.1002/pmic.201500520.
340. **Knorre DG, Kudryashova N V, Godovikova TS.** Chemical and functional aspects of posttranslational modification of proteins. *Acta Naturae* 1: 29–51, 2009. doi: 10.32607/actanaturae.10755.

341. **Köcher T, Pichler P, Swart R, Mechtler K.** Quality control in LC-MS/MS. *Proteomics* 11: 1026–1030, 2011. doi: 10.1002/pmic.201000578.
342. **Kocher T, Swart R, Mechtler K.** Ultra-high-pressure RPLC hyphenated to an LTQ-Orbitrap Velos reveals a linear relation between peak capacity and number of identified peptides. *Anal Chem* 83: 2699–2704, 2011. doi: 10.1021/ac103243t |.
343. **Kokras N, Dalla C.** Sex differences in animal models of psychiatric disorders. *Br J Pharmacol* 171: 4595–4619, 2014. doi: 10.1111/bph.12710.
344. **Konermann L.** Addressing a common misconception: Ammonium acetate as neutral pH “Buffer” for native electrospray mass spectrometry. *J Am Soc Mass Spectrom* 28: 1827–1835, 2017. doi: 10.1007/s13361-017-1739-3.
345. **Kong AT, Leprevost F V., Avtonomov DM, Mellacheruvu D, Nesvizhskii AI.** MSFragger: Ultrafast and comprehensive peptide identification in mass spectrometry-based proteomics. *Nat Methods* 14: 513–520, 2017. doi: 10.1038/nmeth.4256.
346. **Konjevod M, Tudor L, Svob Strac D, Nedic Erjavec G, Barbas C, Zarkovic N, Nikolac Perkovic M, Uzun S, Kozumplik O, Lauc G, Pivac N.** Metabolomic and glycomic findings in posttraumatic stress disorder. *Prog Neuro-Psychopharmacology Biol Psychiatry* 88: 181–193, 2019. doi: 10.1016/j.pnpbp.2018.07.014.
347. **Kouzarides T.** Acetylation: a regulatory modification to rival phosphorylation? *EMBO J* 19: 1176–1179, 2000. doi: 10.1093/emboj/19.6.1176.
348. **Krištić J, Vučković F, Menni C, Klarić L, Keser T, Beccheli I, Pučić-Baković M, Novokmet M, Mangino M, Thaqi K, Rudan P, Novokmet N, Šarac J, Missoni S, Kolčić I, Polašek O, Rudan I, Campbell H, Hayward C, Aulchenko Y, Valdes A, Wilson JF, Gornik O, Primorac D, Zoldoš V, Spector T, Lauc G.** Glycans are a novel biomarker of chronological and biological ages. *Journals Gerontol - Ser A Biol Sci Med Sci* 69: 779–789, 2014. doi: 10.1093/gerona/glt190.
349. **Kucharz EJ, Stajszczyk M, Kotulska-Kucharz A, Batko B, Brzosko M, Jeka S, Leszczyński P, Majdan M, Olesińska M, Samborski W, Wiland P.** Tofacitinib in the treatment of patients with rheumatoid arthritis: Position statement of experts of the Polish Society for Rheumatology. *Reumatologia* 56: 203–211, 2018. doi: 10.5114/reum.2018.77971.

350. **Kumar A, Zhang KYJ.** Advances in the development of SUMO specific protease (SENPs) inhibitors. *Comput Struct Biotechnol J* 13: 204–211, 2015. doi: 10.1016/j.csbj.2015.03.001.
351. **Kumar S, Haile MT, Hoopmann MR, Tran LT, Michaels SA, Morrone SR, Ojo KK, Reynolds LM, Kusebauch U, Vaughan AM, Moritz RL.** Plasmodium falciparum calcium-dependent protein kinase 4 is critical for male gametogenesis and transmission to the mosquito vector. *Mol Biol Microbiol* 12: e02575-21, 2021. doi: 10.1128/mBio.02575-21.
352. **Kumar SR, Kimchi ET, Manjunath Y, Gajagowni S, Stuckel AJ.** RNA cargos in extracellular vesicles derived from blood serum in pancreas associated conditions. *Sci Rep* 10: 1–10, 2020. doi: 10.1038/s41598-020-59523-0.
353. **Kuo T, McQueen A, Chen T, Wang J.** Regulation of glucose homeostasis by glucocorticoids. In: *Glucocorticoid Signaling Advances in experimental medicine and biology*, edited by Wang J, Harris C, p. 99–126.
354. **Kustanovich A, Schwartz R, Peretz T, Grinshpun A.** Life and death of circulating cell-free DNA. *Cancer Biol Ther* 20: 1057–1067, 2019. doi: 10.1080/15384047.2019.1598759.
355. **Kuznetsova KG, Solovyeva EM, Kuzikov A V., Gorshkov M V., Moshkovskii SA.** Modification of cysteine residues for mass spectrometry-based proteomic analysis: Facts and artifacts. *Biochem Suppl Ser B Biomed Chem* 14: 204–215, 2020. doi: 10.1134/S1990750820030087.
356. **Kweon HK, Håkansson K.** Selective zirconium dioxide-based enrichment of phosphorylated peptides for mass spectrometric analysis. *Anal Chem* 78: 1743–1749, 2006. doi: 10.1021/ac0522355.
357. **Kyrou I, Chrousos GP, Tsigos C.** Stress, visceral obesity, and metabolic complications. *Ann N Y Acad Sci* 1083: 77–110, 2006. doi: 10.1196/annals.1367.008.
358. **Kyrou I, Tsigos C.** Stress mechanisms and metabolic complications. *Horm Metab Res* 39: 430–438, 2007. doi: 10.1055/s-2007-981462.
359. **Lai ACY, Tsai CF, Hsu CC, Sun YN, Chen YJ.** Complementary Fe³⁺- and Ti⁴⁺-immobilized metal ion affinity chromatography for purification of acidic and basic phosphopeptides. *Rapid Commun Mass Spectrom* 26: 2186–2194, 2012. doi: 10.1002/rcm.6327.
360. **Lan T, Bai M, Chen X, Wang Y, Li Y, Tian Y, He Y, Wu Z, Yu H, Chen Z, Chen**

- C, Yu Y, Cheng K, Xie P.** iTRAQ-based proteomics implies inflammasome pathway activation in the prefrontal cortex of CSDS mice may influence resilience and susceptibility. *Life Sci* 262: 118501, 2020. doi: 10.1016/j.lfs.2020.118501.
361. **Larsen ISB, Narimatsu Y, Joshi HJ, Siukstaite L, Harrison OJ, Brasch J, Goodman KM, Hansen L, Shapiro L, Honig B, Vakhrushev SY, Clausen H, Halim A.** Discovery of an O-mannosylation pathway selectively serving cadherins and protocadherins. *Proc Natl Acad Sci U S A* 114: 11163–11168, 2017. doi: 10.1073/pnas.1708319114.
362. **Larsen MR, Jensen SS, Jakobsen LA, Heegaard NHH.** Exploring the sialome using titanium dioxide chromatography and mass spectrometry. *Mol Cell Proteomics* 6: 1778–1787, 2007. doi: 10.1074/mcp.M700086-MCP200.
363. **Laskay ŪA, Lobas AA, Szentić K, Gorshkov M V., Tsybin YO.** Proteome digestion specificity analysis for rational design of extended bottom-up and middle-down proteomics experiments. *J Proteome Res* 12: 5558–5569, 2013. doi: 10.1021/pr400522h.
364. **Lauc G, Flögel M.** Glycobiology of stress. In: *Encyclopedia of Stress second edition*. Oxford: Academic Press, 2007, p. 222–227.
365. **Lauc G, Huffman JE, Pučić M, Zgaga L, Adamczyk B, Mužinić A, et al.** Loci associated with N-glycosylation of human immunoglobulin G show pleiotropy with autoimmune diseases and haematological cancers. *PLoS Genet* 9, 2013. doi: 10.1371/journal.pgen.1003225.
366. **Law V.** Coronavirus is disproportionately killing African Americans [Online]. *Al Jazeera*: 2020. <https://www.aljazeera.com/news/2020/4/10/coronavirus-is-disproportionately-killing-african-americans> [8 Jul. 2023].
367. **Lebert D, Louwagie M, Goetze S, Picard G, Ossola R, Duquesne C, Basler K, Ferro M, Rinner O, Aebersold R, Garin J, Mouz N, Brunner E, Brun V.** DIGESTIF: A universal quality standard for the control of bottom-up proteomics experiments. *J Proteome Res* 14: 787–803, 2015. doi: 10.1021/pr500834z.
368. **Lederbogen F, Kühner C, Kirschbaum C, Meisinger C, Lammich J, Holle R, Krumm B, Von Lengerke T, Wichmann HE, Deuschle M, Ladwig KH.** Salivary cortisol in a middle-aged community sample: Results from 990 men and women of the KORA-F3 Augsburg study. *Eur J Endocrinol* 163: 443–451, 2010. doi: 10.1530/EJE-10-0491.

369. **Lee KM, Kang D, Yoon K, Kim SY, Kim H, Yoon HS, Trout DB, Hurrell JJ.** A pilot study on the association between job stress and repeated measures of immunological biomarkers in female nurses. *Int Arch Occup Environ Health* 83: 779–789, 2010. doi: 10.1007/s00420-010-0544-0.
370. **Lee SY, Kang D, Hong J.** Enrichment strategies for identification and characterization of phosphoproteome. *Mass Spectrom Lett* 6: 31–37, 2015. doi: 10.5478/MSL.2015.6.2.31.
371. **Lee YC, Block G, Chen H, Folch-Puy E, Foronjy R, Jalili R, Jendresen CB, Kimura M, Kraft E, Lindemose S, Lu J, McLain T, Nutt L, Ramon-Garcia S, Smith J, Spivak A, Wang ML, Zanic M, Lin SH.** One-step isolation of plasma membrane proteins using magnetic beads with immobilized concanavalin A. *Protein Expr Purif* 62: 223–229, 2008. doi: 10.1016/j.pep.2008.08.003.
372. **Lefeber DJ, Morava E, Jaeken J.** How to find and diagnose a CDG due to defective N-glycosylation. *J Inherit Metab Dis* 34: 849–852, 2011. doi: 10.1007/s10545-011-9370-0.
373. **Leitner A.** Phosphopeptide enrichment using metal oxide affinity chromatography. *TrAC - Trends Anal Chem* 29: 177–185, 2010. doi: 10.1016/j.trac.2009.08.007.
374. **Lennartsson AK, Theorell T, Kushnir MM, Jonsdottir IH.** Changes in DHEA-s levels during the first year of treatment in patients with clinical burnout are related to health development. *Biol Psychol* 120: 28–34, 2016. doi: 10.1016/j.biopsycho.2016.08.003.
375. **Lennartsson AK, Theorell T, Kushnir MM, Jonsdottir IH, Meijer OC.** Low levels of dehydroepiandrosterone sulfate in younger burnout patients. *PLoS One* 10: 4–10, 2015. doi: 10.1371/journal.pone.0140054.
376. **Levene PA, Alsberg CL.** The cleavage products of vitellin. *J Biol Chem* 2: 127–133, 1906. doi: 10.1016/s0021-9258(17)46054-6.
377. **Levin Y, Jaros JAJ, Schwarz E, Bahn S.** Multidimensional protein fractionation of blood proteins coupled to data-independent nanoLC-MS/MS analysis. *J Proteomics* 73: 689–695, 2010. doi: 10.1016/j.jprot.2009.10.013.
378. **Lewis JG, Bagley CJ, Elder PA, Bachmann AW, Torpy DJ.** Plasma free cortisol fraction reflects levels of functioning corticosteroid-binding globulin. *Clin Chim Acta* 359: 189–194, 2005. doi: 10.1016/j.cccn.2005.03.044.
379. **Li C, Guo Z, Zhao R, Sun W, Xie M.** Proteomic analysis of liver proteins in a

- rat model of chronic restraint stress-induced depression. *Biomed Res Int* 2017, 2017. doi: 10.1155/2017/7508316.
380. **Li J, Wang F, Wan H, Liu J, Liu Z, Cheng K, Zou H.** Magnetic nanoparticles coated with maltose-functionalized polyethyleneimine for highly efficient enrichment of N-glycopeptides. *J Chromatogr A* 1425: 213–220, 2015. doi: 10.1016/j.chroma.2015.11.044.
381. **Li K, Vaudel M, Zhang B, Ren Y, Wen B.** PDV: An integrative proteomics data viewer. *Bioinformatics* 35: 1249–1251, 2019. doi: 10.1093/bioinformatics/bty770.
382. **Li M, Liu J, Xu Y, Qian G.** Phosphate adsorption on metal oxides and metal hydroxides: A comparative review. *Environ Rev* 24: 319–332, 2016. doi: 10.1139/er-2015-0080.
383. **Li M, Zeringer E, Barta T, Schageman J, Cheng A, Vlassov A.** Analysis of the RNA content of the exosomes derived from blood serum and urine and its potential as biomarker. *Philos Trans R Soc B* 369: 20130502., 2014. doi: <http://dx.doi.org/10.1098/rstb.2013.0502>.
384. **Li MD, Ruan H Bin, Singh JP, Zhao L, Zhao T, Azarhoush S, Wu J, Evans RM, Yang X.** O-GlcNAc transferase is involved in glucocorticoid receptor-mediated transrepression. *J Biol Chem* 287: 12904–12912, 2012. doi: 10.1074/jbc.M111.303792.
385. **Li X.** Affinity materials for phosphorylated and glycosylated proteins/peptides enrichment. *J Phys Conf Ser* 1759, 2021. doi: 10.1088/1742-6596/1759/1/012026.
386. **Li XS, Yuan BF, Feng YQ.** Recent advances in phosphopeptide enrichment: Strategies and techniques. *TrAC - Trends Anal Chem* 78: 70–83, 2016. doi: 10.1016/j.trac.2015.11.001.
387. **Li Y, Luo Y, Wu S, Gao Y, Liu Y, Zheng D.** Nucleic acids in protein samples interfere with phosphopeptide identification by immobilized-metal-ion affinity chromatography and mass spectrometry. *Mol Biotechnol* 43: 59–66, 2009. doi: 10.1007/s12033-009-9176-6.
388. **Li YH, Zhang CH, Qiu J, Wang SE, Hu SY, Huang X, Xie Y, Wang Y, Cheng TL.** Antidepressant-like effects of Chaihu-Shugan-San via SAPK/JNK signal transduction in rat models of depression. *Pharmacogn Mag* 10: 271–277, 2014. doi: 10.4103/0973-1296.137367.

389. **Liang H, Ward WF.** PGC-1 α : A key regulator of energy metabolism. *Am J Physiol - Adv Physiol Educ* 30: 145–151, 2006. doi: 10.1152/advan.00052.2006.
390. **Liigand P, Kaupmees K, Haav K, Liigand J, Leito I, Girod M, Antoine R, Kruve A.** Think negative: Finding the best electrospray ionization/MS mode for your analyte. *Anal Chem* 89: 5665–5668, 2017. doi: 10.1021/acs.analchem.7b00096.
391. **Liu T, Lv YF, Zhao JL, You QD, Jiang ZY.** Regulation of Nrf2 by phosphorylation: Consequences for biological function and therapeutic implications. *Free Radic Biol Med* 168: 129–141, 2021. doi: 10.1016/j.freeradbiomed.2021.03.034.
392. **Liu X, Dang W, Liu H, Song Y, Li Y, Xu W.** Associations between chronic work stress and plasma chromogranin A/catestatin among healthy workers. *J Occup Health* 64: 1–9, 2022. doi: 10.1002/1348-9585.12321.
393. **Liu Y, Cao Q, Li L.** Isolation and characterization of glycosylated neuropeptides. 1st ed. Elsevier Inc.
394. **Liu Y, Fu D, Xiao Y, Guo Z, Yu L, Liang X.** Synthesis and evaluation of a silica-bonded concanavalin A material for lectin affinity enrichment of N-linked glycoproteins and glycopeptides. *Anal Methods* 7: 25–28, 2015. doi: 10.1039/c4ay02286f.
395. **Liu YZ, Wang YX, Jiang CL.** Inflammation: The common pathway of stress-related diseases. *Front Hum Neurosci* 11: 1–11, 2017. doi: 10.3389/fnhum.2017.00316.
396. **Longo VD, Mattson MP.** Fasting: Molecular mechanisms and clinical applications. *Cell Metab* 19: 181–192, 2014. doi: 10.1016/j.cmet.2013.12.008.
397. **Loo D, Jones A, Hill MM.** Lectin magnetic bead array for biomarker discovery. *J Proteome Res* 9: 5496–5500, 2010. doi: 10.1021/pr100472z.
398. **López-Jaramillo FJ, González-Ramírez LA, Albert A, Santoyo-González F, Vargas-Berenguel A, Otálora F.** Structure of concanavalin A at pH 8: Bound solvent and crystal contacts. *Acta Crystallogr Sect D Biol Crystallogr* 60: 1048–1056, 2004. doi: 10.1107/S0907444904007000.
399. **Loroch S, Zahedi RP, Sickmann A.** Highly sensitive phosphoproteomics by tailoring solid-phase extraction to electrostatic repulsion-hydrophilic interaction chromatography. *Anal Chem* 87: 1596–1604, 2015. doi: 10.1021/ac502708m.
400. **Low TY, Mohtar MA, Lee PY, Omar N, Zhou H, Ye M.** Widening the bottleneck

- of phosphoproteomics: Evolving strategies for phosphopeptide enrichment. *Mass Spectrom Rev* 40: 309–333, 2020. doi: 10.1002/mas.21636.
401. **Loziuk PL, Wang J, Li Q, Sederoff RR, Chiang VL, Muddiman DC.** Understanding the role of proteolytic digestion on discovery and targeted proteomic measurements using liquid chromatography tandem mass spectrometry and design of experiments. *J Proteome Res* 12: 5820–5829, 2013. doi: 10.1021/pr4008442.
402. **Lu J, Li Y, Deng C.** Facile synthesis of zirconium phosphonate-functionalized magnetic mesoporous silica microspheres designed for highly selective enrichment of phosphopeptides. *Nanoscale* 3: 1225–1233, 2011. doi: 10.1039/c0nr00896f.
403. **Lu Q, Li S, Shao F.** Sweet talk: Protein glycosylation in bacterial interaction with the host. *Trends Microbiol* 23: 630–641, 2015. doi: 10.1016/j.tim.2015.07.003.
404. **Lu Z, Duan J, He L, Hu Y, Yin Y.** Mesoporous TiO₂ nanocrystal clusters for selective enrichment of phosphopeptides. *Anal Chem* 82: 7249–7258, 2010. doi: 10.1021/ac1011206.
405. **Lucassen P, Pruessner J, Sousa N, Almeida O, Van Dam A, Rajkowska G, Swaab D, Czéh B.** Neuropathology of stress. *Acta Neuropathol* 1: 109–135, 2014. doi: 10.1007/s00401-013-1223-5.
406. **Lucena-Aguilar G, Sánchez-López AM, Barberán-Aceituno C, Carrillo-Ávila JA, López-Guerrero JA, Aguilar-Quesada R.** DNA source selection for downstream applications based on DNA quality indicators analysis. *Biopreserv Biobank* 14: 264–270, 2016. doi: 10.1089/bio.2015.0064.
407. **Lui A, Vanleuven J, Perekopskiy D, Liu D, Xu D, Alzayat O, Elgokhy T, Do T, Gann M, Martin R, Liu DZ.** FDA-approved kinase inhibitors in preclinical and clinical trials for neurological disorders. *Pharmaceuticals* 15: 1–30, 2022. doi: 10.3390/ph15121546.
408. **Luine VN, Beck K, Bowman R, Kneavel M.** Sex differences in chronic stress effects on cognitive function and brain neurochemistry. *Neuroplast Dev Steroid Horm Action* 1: 287–300, 2001. doi: 10.1201/9781420041194.ch23.
409. **Lundström SL, Yang H, Lyutvinskiy Y, Rutishauser D, Herukka SK, Soininen H, Zubarev RA.** Blood plasma IgG Fc glycans are significantly altered in Alzheimer's disease and progressive mild cognitive impairment. *J Alzheimer's Dis* 38: 567–579, 2014. doi: 10.3233/JAD-131088.

410. **Luo J, Zhang B, Cao M, Roberts BW.** The stressful personality: A meta-analytical review of the relation between personality and stress. *Personal Soc Psychol Rev* 27: 128–194, 2023. doi: 10.1177/10888683221104002.
411. **Lupien SJ, Juster RP, Raymond C, Marin MF.** The effects of chronic stress on the human brain: From neurotoxicity, to vulnerability, to opportunity. *Front Neuroendocrinol* 49: 91–105, 2018. doi: 10.1016/j.yfrne.2018.02.001.
412. **Luque-Garcia JL, Neubert TA.** Sample preparation for serum/plasma profiling and biomarker identification by mass spectrometry. *J Chromatogr A* 1153: 259–276, 2007. doi: 10.1016/j.chroma.2006.11.054.
413. **Ma ZQ, Dasari S, Chambers MC, Litton MD, Sobocki SM, Zimmerman LJ, Halvey PJ, Schilling B, Drake PM, Gibson BW, Tabb DL.** IDPicker 2.0: Improved protein assembly with high discrimination peptide identification filtering. *J Proteome Res* 8: 3872–3881, 2009. doi: 10.1021/pr900360j.
414. **Madera M, Mann B, Mechref Y, Novotny M V.** Efficacy of glycoprotein enrichment by microscale lectin affinity chromatography. *J Sep Sci* 31: 2722–2732, 2008. doi: 10.1002/jssc.200800094.
415. **Magdeldin S, Moresco JJ, Yamamoto T, Yates JR.** Off-line multidimensional liquid chromatography and auto sampling result in sample loss in LC/LC-MS/MS. *J Proteome Res* 13: 3826–3836, 2014. doi: 10.1021/pr500530e.
416. **Majer AD, Fasanello VJ, Tindle K, Frenz BJ, Ziur AD, Fischer CP, Fletcher KL, Seecof OM, Gronsky S, Vassallo BG, Reed WL, Paitz RT, Stier A, Haussmann MF.** Is there an oxidative cost of acute stress? Characterization, implication of glucocorticoids and modulation by prior stress experience. *Proc R Soc B Biol Sci* 286, 2019. doi: 10.1098/rspb.2019.1698.
417. **Mann M, Ong SE, Grønborg M, Steen H, Jensen ON, Pandey A.** Analysis of protein phosphorylation using mass spectrometry: Deciphering the phosphoproteome. *Trends Biotechnol* 20: 261–268, 2002. doi: 10.1016/S0167-7799(02)01944-3.
418. **Mann SP, Treit P V., Geyer PE, Omenn GS, Mann M.** Ethical principles, constraints, and opportunities in clinical proteomics. *Mol Cell Proteomics* 20: 100046, 2021. doi: 10.1016/J.MCPRO.2021.100046.
419. **Manna PR, Dyson MT, Stocco DM.** Regulation of the steroidogenic acute regulatory protein gene expression: Present and future perspectives. *Mol Hum Reprod* 15: 321–333, 2009. doi: 10.1093/molehr/gap025.

420. **Manoli I, Alesci S, Blackman MR, Su YA, Rennert OM, Chrousos GP.** Mitochondria as key components of the stress response. *Trends Endocrinol Metab* 18: 190–198, 2007. doi: 10.1016/j.tem.2007.04.004.
421. **Manousek J, Kala P, Lokaj P, Ondrus T, Helanova K, Miklikova M, Brazdil V, Tomandlova M, Parenica J, Pavkova Goldbergova M, Hlasensky J.** Oxidative stress in Takotsubo syndrome—Is it essential for an acute attack? Indirect evidences support multisite impact including the calcium overload—Energy failure hypothesis. *Front Cardiovasc Med* 8, 2021. doi: 10.3389/fcvm.2021.732708.
422. **Mapanga RF, Essop MF.** Damaging effects of hyperglycemia on cardiovascular function: Spotlight on glucose metabolic pathways. *Am J Physiol - Hear Circ Physiol* 310: H153–H173, 2016. doi: 10.1152/ajpheart.00206.2015.
423. **Martens L.** A report on the ESF workshop on quality control in proteomics. *Mol Biosyst* 6: 935–938, 2010. doi: 10.1039/c003912h.
424. **Martin NC, Pirie AA, Ford L V., Callaghan CL, McTurk K, Lucy D, Scrimger DG.** The use of phosphate buffered saline for the recovery of cells and spermatozoa from swabs. *Sci Justice - J Forensic Sci Soc* 46: 179–184, 2006. doi: 10.1016/S1355-0306(06)71591-X.
425. **Martínez MC, Andriantsitohaina R.** Reactive nitrogen species: Molecular mechanisms and potential significance in health and disease. *Antioxidants Redox Signal* 11: 669–702, 2009. doi: 10.1089/ars.2007.1993.
426. **Masuda T, Mori A, Ito S, Ohtsuki S.** Quantitative and targeted proteomics-based identification and validation of drug efficacy biomarkers. *Drug Metab Pharmacokinet* 36: 1–9, 2021. doi: 10.1016/j.dmpk.2020.09.006.
427. **Matthews G, Lin J, Wohleber R.** Personality, stress and resilience. *Psychol Top* 26: 139–162, 2017. doi: 10.31820/pt.26.1.6.
428. **Mattsson N, Ewers M, Rich K, Kaiser E, Mulugeta E, Rose E.** CSF biomarkers and incipient Alzheimer disease in patients with mild cognitive impairment. *JAMA* 302: 385–393, 2009.
429. **Mauri P, Petretto A, Cuccabita D, Basilico F, Silvestre D, Levreri I, Melioli G.** Fractionation techniques improve the proteomic analysis of human serum. *Curr Pharm Anal* 4: 69–77, 2008. doi: 10.2174/157341208784246297.
430. **Mbalo N, Zhang M, Ntuli S.** Risk factors for PTSD and depression in female survivors of rape. *Psychol Trauma Theory, Res Pract Policy* 9: 301–308, 2017.

- doi: <https://doi.org/10.1037/tra0000228>.
431. **McCurlley JL, Mills PJ, Roesch SC, Carnethon M, Giacinto RE, Isasi CR, Teng Y, Sotres-Alvarez D, Llabre MM, Penedo FJ, Schneiderman N, Gallo LC.** Chronic stress, inflammation, and glucose regulation in U.S. Hispanics from the HCHS/SOL Sociocultural Ancillary Study. *Psychophysiology* 52: 1071–1079, 2015. doi: 10.1111/psyp.12430.
 432. **McEwen BS.** Protection and damage from acute and chronic stress: Allostasis and allostatic overload and relevance to the pathophysiology of psychiatric disorders. *Ann N Y Acad Sci* 1032: 1–7, 2004. doi: 10.1196/annals.1314.001.
 433. **McEwen BS.** Protective and damaging effects of stress mediators: Central role of the brain. *Dialogues Clin Neurosci* 8: 367–381, 2006. doi: 10.31887%2FDCNS.2006.8.4%2FbmcEwen.
 434. **McKetney J, Jenkins CC, Minogue C, Mach PM, Hussey EK, Glaros TG, Coon J, Dhummakupt ES.** Proteomic and metabolomic profiling of acute and chronic stress events associated with military exercises. *Mol Omi* 18: 279–295, 2021. doi: 10.1039/d1mo00271f.
 435. **McNulty DE, Annan RS.** Hydrophilic interaction chromatography reduces the complexity of the phosphoproteome and improves global phosphopeptide isolation and detection. *Mol Cell Proteomics* 7: 971–980, 2008. doi: 10.1074/mcp.M700543-MCP200.
 436. **Mereiter S, Balmaña M, Campos D, Gomes J, Reis CA.** Glycosylation in the era of cancer-targeted therapy: Where are we heading? *Cancer Cell* 36: 6–16, 2019. doi: 10.1016/j.ccell.2019.06.006.
 437. **Meyer JG.** Fast proteome identification and quantification from data-dependent acquisition–tandem mass spectrometry (DDA MS/MS) using free software tools. *Methods Protoc* 2: 1–17, 2019. doi: 10.3390/mps2010008.
 438. **Micel LN, Tentler JJ, Smith PG, Eckhardt SG.** Role of ubiquitin ligases and the proteasome in oncogenesis: Novel targets for anticancer therapies. *J Clin Oncol* 31: 1231–1238, 2013. doi: 10.1200/JCO.2012.44.0958.
 439. **Mifsud KR, Reul JM.** Mineralocorticoid and glucocorticoid receptor-mediated control of genomic responses to stress in the brain. *Stress* 21: 389–402, 2018. doi: 10.1080/10253890.2018.1456526.
 440. **Mihrshahi R, Lewis JG, Ali SO.** Hormonal effects on the secretion and glycoform profile of corticosteroid-binding globulin. *J Steroid Biochem Mol Biol*

- 101: 275–285, 2006. doi: 10.1016/j.jsbmb.2006.06.031.
441. **Mitchell BL, Yasui Y, Li CI, Fitzpatrick AL, Lampe PD.** Impact of freeze-thaw cycles and storage time on plasma samples used in mass spectrometry based biomarker discovery projects. *Cancer Inform* 1: 98–104, 2005. doi: 10.1177/117693510500100110.
442. **Mitic M, Lukic I, Bozovic N, Djordjevic J, Adzic M.** Fluoxetine signature on hippocampal MAPK signalling in sex-dependent manner. *J Mol Neurosci* 55: 335–346, 2015. doi: 10.1007/s12031-014-0328-1.
443. **Mitic M, Simic I, Djordjevic J, Radojicic MB, Adzic M.** Gender-specific effects of fluoxetine on hippocampal glucocorticoid receptor phosphorylation and behavior in chronically stressed rats. *Neuropharmacology* 70: 100–111, 2013. doi: 10.1016/j.neuropharm.2012.12.012.
444. **Moggetti P, Bacchi E, Brangani C, Donà S, Negri C.** Metabolic effects of exercise. *Front Horm Res* 47: 44–57, 2016. doi: 10.1159/000445156.
445. **Moldoveanu SC, David V.** Gradient Elution. In: *Selection of the HPLC Method in Chemical Analysis*, edited by Moldoveanu SC, David V. 2017, p. 451–462.
446. **Monzo A, Bonn GK, Guttman A.** Lectin-immobilization strategies for affinity purification and separation of glycoconjugates. *TrAC - Trends Anal Chem* 26: 423–432, 2007. doi: 10.1016/j.trac.2007.01.018.
447. **Moran KE, Ommerborn MJ, Blackshear CT, Sims M, Clark CR.** Financial stress and risk of coronary heart disease in the Jackson Heart Study. *Am J Prev Med* 56: 224–231, 2019. doi: 10.1016/j.amepre.2018.09.022.
448. **Morena-Barrio MED La, Wypasek E, Owczarek D, Miñano A, Vicente V, Corral J, Undas A.** MPI-CDG with transient hypoglycosylation and antithrombin deficiency. *Haematologica* 104: e79–e82, 2019. doi: 10.3324/haematol.2018.211326.
449. **Morgan DJ, Poolman TM, Williamson AJK, Wang Z, Clark NR, Ma'ayan A, Whetton AD, Brass A, Matthews LC, Ray DW.** Glucocorticoid receptor isoforms direct distinct mitochondrial programs to regulate ATP production. *Sci Rep* 6: 1–10, 2016. doi: 10.1038/srep26419.
450. **Mottaz-Brewer HM, Norbeck AD, Adkins JN, Manes NP, Ansong C, Shi L, Rikihisa Y, Kikuchi T, Wong SW, Estep RD, Heffron F, Pasa-Tolic L, Smith RD.** Optimization of proteomic sample preparation procedures for comprehensive protein characterization of pathogenic systems. *J Biomol Tech*

- 19: 285–295, 2008.
451. **Müller MM**. Post-translational modifications of protein backbones: Unique functions, mechanisms, and challenges. *Biochemistry* 57: 177–185, 2018. doi: 10.1021/acs.biochem.7b00861.
452. **Murphy JC, Jewell DL, White KI, Fox GE, Willson RC**. Nucleic acid separations Utilizing immobilized metal affinity chromatography. *Biotechnol Prog* 19: 982–986, 2003. doi: Murphy, J. C., Jewell, D. L., White, K. I., Fox, G. E., & Willson, R. C. (2003). Nucleic Acid Separations Utilizing Immobilized Metal Affinity Chromatography. *Biotechnology Progress*, 19(3), 982–986. doi:10.1021/bp025563o.
453. **Mysling S, Palmisano G, Højrup P, Thaysen-andersen M**. Utilizing ion-pairing hydrophilic interaction chromatography solid phase extraction for efficient glycopeptide enrichment in glycoproteomics. *Anal Chem* 82: 5598–5609, 2010. doi: 10.1021/ac100530w.
454. **Naicker P, Govender I, Crampton M, Gerber I, Mancama D, Damelin, Demetra Stoychev S, Jordaan J**. Rapid and automatable magnetic microparticle-based methods for clinical proteogenomic studies [Online]. *Resyn Biosciences*: 2019. https://resynbio.com/wp-content/uploads/2020/01/HUPO_Poster_JJ_SAX_2019_Urine_Clean-up.pdf.
455. **Nakakita S ichi, Sumiyoshi W, Miyanishi N, Hirabayashi J**. A practical approach to N-glycan production by hydrazinolysis using hydrazine monohydrate. *Biochem Biophys Res Commun* 362: 639–645, 2007. doi: 10.1016/j.bbrc.2007.08.032.
456. **Nakanishi K, Nishida M, Harada M, Ohama T, Kawada N, Murakami M, Moriyama T, Yamauchi-Takahara K**. Klotho-related molecules upregulated by smoking habit in apparently healthy men: A cross-sectional study. *Sci Rep* 5: 1–9, 2015. doi: 10.1038/srep14230.
457. **Nakanishi K, Nishida M, Taneike M, Yamamoto R, Adachi H, Moriyama T, Yamauchi-Takahara K**. Implication of alpha-Klotho as the predictive factor of stress. *J Investig Med* 67: 1082–1086, 2019. doi: 10.1136/jim-2018-000977.
458. **Nascimento KS, Cunha AI, Nascimento KS, Cavada BS, Azevedo AM, Aires-Barros MR**. An overview of lectins purification strategies. *J Mol Recognit* 25: 527–541, 2012. doi: 10.1002/jmr.2200.
459. **Neagu AN, Jayathirtha M, Baxter E, Donnelly M, Petre BA, Darie CC**.

- Applications of tandem Mass spectrometry (MS/MS) in protein analysis for biomedical research. *Molecules* 27, 2022. doi: 10.3390/molecules27082411.
460. **Nehring S, Goyal A, Patel B.** C Reactive Protein [Online]. StatPearls Publishing. <https://www.ncbi.nlm.nih.gov/books/NBK441843/> [8 Jul. 2023].
461. **Nesvizhskii AI, Keller A, Kolker E, Aebersold R.** A statistical model for identifying proteins by tandem mass spectrometry. *Anal Chem* 75: 4646–4658, 2003. doi: 10.1021/ac0341261.
462. **Neville DCA, Rozanas CR, Price EM, Gruis DB, Verkman AS, Townsend RR.** Evidence for phosphorylation of serine 753 in CFTR using a novel metal-ion affinity resin and matrix-assisted laser desorption mass spectrometry. *Protein Sci* 6: 2436–2445, 1997. doi: 10.1002/pro.5560061117.
463. **New England Biolabs.** Glycoproteomics technical guide. New England Biolabs Inc.: 2021.
464. **Nguse S, Wassenaar D.** Mental health and COVID-19 in South Africa. *South African J Psychol* 51: 304–313, 2021. doi: 10.1177/00812463211001543.
465. **Nguyen JT, Evans DP, Galvan M, Pace KE, Leitenberg D, Bui TN, Baum LG.** CD45 modulates galectin-1-induced T cell death: Regulation by expression of core 2 O-glycans. *J Immunol* 167: 5697–5707, 2001. doi: 10.4049/jimmunol.167.10.5697.
466. **Nicholson LM, Schwirian PM, Groner JA.** Recruitment and retention strategies in clinical studies with low-income and minority populations: Progress from 2004-2014. *Contemp Clin Trials* 45: 34–40, 2015. doi: 10.1016/j.cct.2015.07.008.
467. **Nieto-Quero A, Chaves-Peña P, Santín LJ, Pérez-Martín M, Pedraza C.** Do changes in microglial status underlie neurogenesis impairments and depressive-like behaviours induced by psychological stress? A systematic review in animal models. *Neurobiol Stress* 15: 1–23, 2021. doi: 10.1016/j.ynstr.2021.100356.
468. **Nirupama R, Rajaraman B, Yajurvedi H.** Stress and glucose metabolism: A review. *Imaging J Clin Med Sci* 5: 8–12, 2018. doi: <http://doi.org/10.17352/2455-8702.000037>.
469. **Nissen RM, Yamamoto KR.** The glucocorticoid receptor inhibits NFκB by interfering with serine-2 phosphorylation of the RNA polymerase II carboxy-terminal domain. *Genes Dev* 14: 2314–2329, 2000. doi: 10.1101/gad.827900.

470. **Noushad S, Ahmed S, Ansari B, Mustafa U-H, Saleem Y, Hazrat H.** Physiological biomarkers of chronic stress: A systematic review. [Online]. *Int J Health Sci (Qassim)* 15: 46–59, 2021. <http://www.ncbi.nlm.nih.gov/pubmed/34548863><http://www.pubmedcentral.nih.gov/articlerender.fcgi?artid=PMC8434839>.
471. **Nsiah-Sefaa A, McKenzie M.** Combined defects in oxidative phosphorylation and fatty acid β -oxidation in mitochondrial disease. *Biosci Rep* 36, 2016. doi: 10.1042/BSR20150295.
472. **Nweke EE, Naicker P, Aron S, Stoychev S, Devar J, Tabb DL, Omshoro-Jones J, Smith M, Candy G.** SWATH-MS based proteomic profiling of pancreatic ductal adenocarcinoma tumours reveals the interplay between the extracellular matrix and related intracellular pathways. *PLoS One* 15: 1–18, 2020. doi: 10.1371/journal.pone.0240453.
473. **Nyberg ST, Fransson EI, Heikkilä K, Ahola K, Alfredsson L, et al.** Job strain as a risk factor for type 2 diabetes: A pooled analysis of 124,808 men and women. *Diabetes Care* 37: 2268–2275, 2014. doi: 10.2337/dc13-2936.
474. **O'Connor D, Thayer J, Vedhara K.** Stress and health: A review of psychobiological processes. *Annu Rev Psychol* 72: 1–53, 2020. doi: 10.1146/annurev-psych-062520-122331.
475. **Oakley RH, Cidlowski JA.** The biology of the glucocorticoid receptor: New signaling mechanisms in health and disease. *J Allergy Clin Immunol* 132: 1033–1044, 2013. doi: 10.1016/j.jaci.2013.09.007.
476. **Oberholzer C, Oberholzer A, Clare-Salzler M, Moldawer LL.** Apoptosis in sepsis: A new target for therapeutic exploration. *FASEB J* 15: 879–892, 2001. doi: 10.1096/fsb2fj00058rev.
477. **Ohtsubo K, Marth JD.** Glycosylation in cellular mechanisms of health and disease. *Cell* 126: 855–867, 2006. doi: 10.1016/j.cell.2006.08.019.
478. **Oliveira T, Thaysen-Andersen M, Packer NH, Kolarich D.** The Hitchhiker's guide to glycoproteomics. *Biochem Soc Trans* 49: 1643–1662, 2021. doi: <https://doi.org/10.1042/BST20200879>.
479. **Olsen J V., Ong SE, Mann M.** Trypsin cleaves exclusively C-terminal to arginine and lysine residues. *Mol Cell Proteomics* 3: 608–614, 2004. doi: 10.1074/mcp.T400003-MCP200.
480. **Olver JS, Pinney M, Maruff P, Norman TR.** Impairments of spatial working

- memory and attention following acute psychosocial stress. *Stress Health* 31: 115–123, 2015. doi: 10.1002/smi.2533.
481. **Omer B, Charney DS.** Neuropathology of stress: Prospects and caveats. *Psychiatry* 67: 407–411, 2004. doi: 10.1521/psyc.67.4.407.56561.
482. **Ongay S, Boichenko A, Govorukhina N, Bischoff R.** Glycopeptide enrichment and separation for protein glycosylation analysis. *J Sep Sci* 35: 2341–2372, 2012. doi: 10.1002/jssc.201200434.
483. **Orth-Gomér K, Wamala SP, Horsten M, Schenck-Gustafsson K, Schneiderman N, Mittleman MA.** Marital stress worsens prognosis in women with coronary heart disease: The Stockholm female coronary risk study. *Jama* 284: 3008–3014, 2000. doi: 10.1001/jama.284.23.3008.
484. **Ottesen AH, Carlson CR, Louch WE, Dahl MB, Sandbu RA, Johansen RF, Jarstadmarken H, Bjørås M, Høiseith AD, Brynildsen J, Sjaastad I, Stridsberg M, Omland T, Christensen G, Røsjø H.** Glycosylated Chromogranin A in heart failure: Implications for processing and cardiomyocyte calcium homeostasis. *Circ Hear Fail* 10: 1–11, 2017. doi: 10.1161/CIRCHEARTFAILURE.116.003675.
485. **Palmisano G, Lendal SE, Engholm-keller K, Leth-larsen R, Parker BL, Larsen MR.** Selective enrichment of sialic acid – containing glycopeptides using titanium dioxide chromatography with analysis by HILIC and mass spectrometry. *Nat Protoc* 5: 1974–1982, 2010. doi: 10.1038/nprot.2010.167.
486. **Palmisano G, Lendal SE, Larsen MR.** Titanium dioxide enrichment of sialic acid-containing glycopeptides. In: *Methods in Molecular Biology*, edited by Gevaert K, Vandekerckhove J. Clifton: Springer Science & Business Media LLC 2011, 2011, p. 309–322.
487. **Palmisano G, Melo-Braga MN, Engholm-Keller K, Parker BL, Larsen MR.** Chemical deamidation: A common pitfall in large-scale N-Linked glycoproteomic mass spectrometry-based analyses. *J Proteome Res* 11: 1949–1957, 2012. doi: 10.1021/pr2011268.
488. **Park DI, Štambuk J, Razdorov G, Pučić-Baković M, Martins-De-Souza D, Lauc G, Turck CW.** Blood plasma/IgG N-glycome biosignatures associated with major depressive disorder symptom severity and the antidepressant response. *Sci Rep* 8: 1–11, 2018. doi: 10.1038/s41598-017-17500-0.
489. **Patchev VK, Patchev A V.** Experimental models of stress. *Dialogues Clin*

- Neurosci* 8: 417–432, 2006. doi: 10.31887/dcms.2006.8.4/vpatchev.
490. **Patel T, Bruce J, Merry A, Bigge C, Parekh R, Wormald M, Jaques A.** Use of hydrazine to release intact and unreduced Form both N- and O-linked oligosaccharides from glycoproteins. *Biochemistry* 32: 679–693, 1993. doi: 10.1021/bi00053a037.
491. **Paudel D, Kuramitsu Y, Uehara O, Morikawa T, Yoshida K, Giri S, Islam ST, Kitagawa T, Kondo T, Sasaki K, Matsuoka H, Miura H, Abiko Y.** Proteomic and microbiota analyses of the oral cavity during psychological stress. *PLoS One* 17: e0268155, 2022. doi: 10.1371/journal.pone.0268155.
492. **Paul J, Veenstra TD.** Separation of serum and plasma proteins for in-depth proteomic analysis. *Separations* 9, 2022. doi: 10.3390/separations9040089.
493. **Perogamvros I, Ray DW, Trainer PJ.** Regulation of cortisol bioavailability - Effects on hormone measurement and action. *Nat Rev Endocrinol* 8: 717–727, 2012. doi: 10.1038/nrendo.2012.134.
494. **Petersen KS, Smith C.** Ageing-associated oxidative stress and inflammation are alleviated by products from grapes. *Oxid Med Cell Longev* 2016, 2016. doi: 10.1155/2016/6236309.
495. **Peterson SB, Hart GW.** New insights: A role for O-GlcNAcylation in diabetic complications. *Crit Rev Biochem Mol Biol* 51: 150–161, 2016. doi: 10.3109/10409238.2015.1135102.
496. **Petrosyan A.** Unlocking Golgi: Why does morphology matter? *Biochem* 84: 1490–1501, 2019. doi: 10.1134/S0006297919120083.
497. **Pfeifer LS, Heyers K, Ocklenburg S, Wolf OT.** Stress research during the COVID-19 pandemic and beyond. *Neurosci Biobehav Rev* 131: 581–596, 2021. doi: <https://doi.org/10.1016/j.neubiorev.2021.09.045>.
498. **Pharma Dynamics.** South Africans' stress levels have shot up by 56% since start of pandemic according to survey [Online]. 2020. <https://pharmadynamics.co.za/south-africans-stress-levels-have-shot-up-by-56-since-start-of-pandemic-according-to-survey/> [27 May 2022].
499. **Piechaczek CE, Pehl V, Feldmann L, Haberstroh S, Allgaier AK, Freisleder FJ, Schulte-Körne G, Greimel E.** Psychosocial stressors and protective factors for major depression in youth: Evidence from a case-control study. *Child Adolesc Psychiatry Ment Health* 14: 1–11, 2020. doi: 10.1186/s13034-020-0312-1.

500. **Piehowski PD, Petyuk VA, Orton DJ, Xie F, Moore RJ, Ramirez-Restrepo M, Engel A, Lieberman AP, Albin RL, Camp DG, Smith RD, Myers AJ.** Sources of technical variability in quantitative LC-MS proteomics: Human brain tissue sample analysis. *J Proteome Res* 12: 2128–2137, 2013. doi: 10.1021/pr301146m.
501. **Pierobon M, Wulfschlegel J, Liotta L, Petricoin E.** Application of molecular technologies for phosphoproteomic analysis of clinical samples. *Oncogene* 34: 805–814, 2015. doi: 10.1038/onc.2014.16.
502. **Pietrowska M, Wlosowicz A, Gawin M, Widlak P.** MS-based proteomic analysis of serum and plasma: Problem of high abundant components and lights and shadows of albumin removal. In: *Emerging Sample Treatments in Proteomics, Advances in Experimental Medicine and Biology*. Springer Nature Switzerland AG, 2019, p. 57–76.
503. **Pillay Y.** State of mental health and illness in South Africa. *South African J Psychol* 49: 463–466, 2019. doi: 10.1177/0081246319857527.
504. **Pinho SS, Reis CA.** Glycosylation in cancer: mechanisms and clinical implications. *Nat Rev Cancer* 15: 540–555, 2015. doi: 10.1038/nrc3982.ABSTRACT.
505. **Pinkse MWH, Uitto PM, Hilhorst MJ, Ooms B, Heck AJR.** Selective isolation at the femtomole level of phosphopeptides from proteolytic digests using 2D-NanoLC-ESI-MS/MS and titanium oxide precolumns. *Anal Chem* 76: 3935–3943, 2004. doi: 10.1021/ac0498617.
506. **Plasencia MD, Isailovic D, Merenbloom S. ., Mechref Y, Clemmer DE.** Resolving and assigning N-linked glycan structural isomers from ovalbumin by IMS-MS. *J Am Soc Mass Spectrom* 19: 1706–1715, 2008. doi: <https://doi.org/10.1016/j.jasms.2008.07.020>.
507. **Polaskova V, Kapur A, Khan A, Molloy MP, Baker MS.** High-abundance protein depletion: Comparison of methods for human plasma biomarker discovery. *Electrophoresis* 31: 471–482, 2010. doi: 10.1002/elps.200900286.
508. **Poljsak B, Šuput D, Milisav I.** Achieving the balance between ROS and antioxidants: When to use the synthetic antioxidants. *Oxid Med Cell Longev* 2013, 2013. doi: 10.1155/2013/956792.
509. **Ponce-Lina R, Serafín N, Carranza M, Arámburo C, Prado-Alcalá RA, Luna M, Quirarte GL.** Differential phosphorylation of the glucocorticoid receptor in

- hippocampal subregions induced by contextual fear conditioning training. *Front Behav Neurosci* 14: 1–13, 2020. doi: 10.3389/fnbeh.2020.00012.
510. **Poornima IG, Parikh P, Shannon RP.** Diabetic cardiomyopathy: The search for a unifying hypothesis. *Circ Res* 98: 596–605, 2006. doi: 10.1161/01.RES.0000207406.94146.c2.
511. **Popovic D, Vucic D, Dikic I.** Ubiquitination in disease pathogenesis and treatment. *Nat Med* 20: 1242–1253, 2014. doi: 10.1038/nm.3739.
512. **Posewitz MC, Tempst P.** Immobilized gallium (III) affinity chromatography of phosphopeptides [Online]. *Biosystems* 71: 29520–29529, 1999. <http://www.ncbi.nlm.nih.gov/pubmed/10424175>.
513. **Prieto DA, Johann DJ, Wei BR, Ye X, Chan KC, Nissley D V., Simpson RM, Citrin DE, Mackall CL, Linehan WM, Blonder J.** Mass spectrometry in cancer biomarker research: A case for immunodepletion of abundant blood-derived proteins from clinical tissue specimens. *Biomark Med* 8: 269–286, 2014. doi: 10.2217/bmm.13.101.
514. **Proc JL, Kuzyk MA, Hardie DB, Yang J, Smith DS, Jackson AM, Parker CE, Borchers CH.** A quantitative study of the effects of chaotropic agents, surfactants, and solvents on the digestion efficiency of human plasma proteins by trypsin. *J Proteome Res* 9: 5422–5437, 2010. doi: 10.1021/pr100656u.
515. **Pulvirenti A, Rao D, McIntyre CA, Gonen M, Tang LH, Klimstra DS, Fleisher M, Ramanathan L V., Reidy-Lagunes D, Allen PJ.** Limited role of Chromogranin A as clinical biomarker for pancreatic neuroendocrine tumors. *Hpb* 21: 612–618, 2019. doi: 10.1016/j.hpb.2018.09.016.
516. **Punita P, Saranya K, Chandrasekar M, Kumar SS.** Gender difference in heart rate variability in medical students and association with the level of stress. *Natl J Physiol Pharm Pharmacol* 6: 431–437, 2016. doi: 10.5455/njppp.2016.6.0102325042016.
517. **Qin Y, Zhong Y, Yang G, Ma T, Jia L, Huang C, Li Z.** Profiling of concanavalin a-binding glycoproteins in human hepatic stellate cells activated with transforming growth factor- β 1. *Molecules* 19: 19845–19867, 2014. doi: 10.3390/molecules191219845.
518. **Qing G, Yan J, He X, Li X, Liang X.** Recent advances in hydrophilic interaction liquid interaction chromatography materials for glycopeptide enrichment and glycan separation. *TrAC - Trends Anal Chem* 124: 115570, 2020. doi:

- 10.1016/j.trac.2019.06.020.
519. **Qiu Y, Patwa TH, Xu L, Shedden K, Misek DE, Tuck M, Jin G, Ruffin MT, Turgeon DK, Synal S, Bresalier R, Marcon N, Brenner DE, Lubman DM.** Plasma glycoprotein profiling for colorectal cancer biomarker identification by lectin glycoarray and lectin blot. *J Proteome Res* 7: 1693–1703, 2008. doi: 10.1021/pr700706s.
520. **Racine N, McArthur BA, Cooke JE, Eirich R, Zhu J, Madigan S.** Global prevalence of depressive and anxiety symptoms in children and adolescents during COVID-19: A meta-analysis. *JAMA Pediatr* 175: 1142–1150, 2021. doi: 10.1001/jamapediatrics.2021.2482.
521. **Radivojac P, Vacic V, Haynes C, Cocklin RR, Mohan A, Heyen JW, Goebel MG, Iakoucheva LM.** Identification, analysis, and prediction of protein ubiquitination sites. *Proteins Struct Funct Bioinforma* 78: 365–380, 2010. doi: 10.1002/prot.22555.
522. **Rahal A, Kumar A, Singh V, Yadav B, Tiwari R, Chakraborty S, Dhama K.** Oxidative stress, prooxidants, and antioxidants: The interplay. *Biomed Res Int* 2014, 2014. doi: 10.1155/2014/761264.
523. **Rajamanickam V, Herwig C, Spadiut O.** Monoliths in bioprocess technology. *Chromatography* 2: 195–212, 2015. doi: 10.3390/chromatography2020195.
524. **Ramazi S, Allahverdi A, Zahiri J.** Evaluation of post-translational modifications in histone proteins: A review on histone modification defects in developmental and neurological disorders. *J Biosci* 45: 3–9, 2020. doi: 10.1007/s12038-020-00099-2.
525. **Ramazi S, Zahiri J.** Post-translational modifications in proteins: Resources, tools and prediction methods. *Database* 2021: 1–20, 2021. doi: 10.1093/database/baab012.
526. **Ranabir S, Reetu K.** Stress and hormones. *Indian J Endocrinol Metab* 15: 18–22, 2011. doi: 10.4103/2230-8210.77573.
527. **Rathnasekara R, El Rassi Z.** Polar silica-based stationary phases. Part III- Neutral silica stationary phase with surface bound maltose for affinity chromatography at reduced non-specific interactions. *J Chromatogr A* 1508: 33–41, 2017. doi: 10.1016/j.chroma.2017.05.060.
528. **Reddin C, Murphy R, Hankey GJ, Judge C, Xavier D, Rosengren A, Ferguson J, Alvarez-Iglesias A, Oveisgharan S, Iversen HK, Lanas F, Al-**

- Hussein F, Czlonkowska A, Oguz A, McDermott C, Pogossova N, Málaga G, Langhorne P, Wang X, Wasay M, Yusuf S, O'Donnell M.** Association of psychosocial stress with risk of acute stroke. *JAMA Netw Open* 5: E2244836, 2022. doi: 10.1001/jamanetworkopen.2022.44836.
529. **Reddy BR, Babu NS, Das T, Bhattacharya D, Murthy CLN, Kumar A, Idris MM, Chakravarty S.** Proteome profile of telencephalon associates attenuated neurogenesis with chronic stress induced mood disorder phenotypes in zebrafish model. *Pharmacol Biochem Behav* 204: 173170, 2021. doi: 10.1016/j.pbb.2021.173170.
530. **Reeke GN, Becker JW, Cunningham BA, Wang JL, Yahara I, Edelman GM.** Structure and function of concanavalin A. *Adv Exp Med Biol* 55: 13–33, 1975. doi: https://doi.org/10.1007/978-1-4684-0949-9_2.
531. **Reichelt S, Elsner C, Prager A, Naumov S, Kuballa J, Buchmeiser MR.** Amino-functionalized monolithic spin-type columns for high-throughput lectin affinity chromatography of glycoproteins. *Analyst* 137: 2600–2607, 2012. doi: 10.1039/c2an16087k.
532. **Reiding KR, Ruhaak LR, Uh HW, El Bouhaddani S, van den Akker EB, Plomp R, McDonnell LA, Houwing-Duistermaat JJ, Slagboom PE, Beekman M, Wuhrer, M.** Human plasma N-glycosylation as analyzed by MALDI-FTICR-MS associates with markers of inflammation and metabolic health. *Mol Cell Proteomics* 16: 228–242, 2017.
533. **Reily C, Stewart TJ, Renfrow MB, Novak J.** Glycosylation in health and disease. *Nat Rev Nephrol* 15: 346–366, 2019. doi: 10.1038/s41581-019-0129-4.
534. **Resh MD.** Palmitoylation of proteins in cancer. *Biochem Soc Trans* 45: 409–416, 2017. doi: 10.1042/BST20160233.
535. **ReSyn Biosciences.** MagReSyn® Carboxyl [Online]. *ReSyn Biosci.* © ReSyn Biosciences (Pty) Ltd 2012-2020: 1–2, 2017. https://resynbio.com/wp-content/uploads/2020/IFU_Carboxyl.pdf [8 Mar. 2021].
536. **ReSyn Biosciences.** MagReSyn® Zr-IMAC HP Zirconium-ion (Zr 4+) functional magnetic microparticles [Online]. *ReSyn Biosci.* © ReSyn Biosciences (Pty) Ltd 2012-2020: 2, 2020. https://resynbio.com/wp-content/uploads/2022/09/IFU_ZrIMAC_HP.pdf [8 Mar. 2021].
537. **Rhein C, Hepp T, Kraus O, von Majewski K, Lieb M, Rohleder N, Erim Y.**

- Interleukin-6 secretion upon acute psychosocial stress as a potential predictor of psychotherapy outcome in posttraumatic stress disorder. *J Neural Transm* 128: 1301–1310, 2021. doi: 10.1007/s00702-021-02346-8.
538. **Rhen T, Cidlowski JA.** Antiinflammatory action of glucocorticoids — New mechanisms for old drugs. *N Engl J Med* 353: 1711–1723, 2005. doi: 10.1056/nejmra050541.
539. **Rice JC, Allis CD.** Lysine methylation and acetylation of histones. *Curr Opin Cell Biol* 13: 263–273, 2001. doi: [https://doi.org/10.1016/S0955-0674\(00\)00208-8](https://doi.org/10.1016/S0955-0674(00)00208-8).
540. **Riley NM, Bertozzi CR, Pitteri SJ.** A pragmatic guide to enrichment strategies for mass spectrometry–based glycoproteomics. *Mol Cell Proteomics* 20: 100029, 2021. doi: 10.1074/mcp.R120.002277.
541. **Rio DC, Ares M, Hannon GJ, Nilsen TW.** Purification of RNA using TRIzol (TRI Reagent). *Cold Spring Harb Protoc* 5: 1–4, 2010. doi: 10.1101/pdb.prot5439.
542. **Roberts DS, Chen B, Tiambeng TN, Wu Z, Ge Y, Jin S.** Reproducible large-scale synthesis of surface silanized nanoparticles as an enabling nanoproteomics platform: Enrichment of the human heart phosphoproteome. *Nano Res* 12: 1473–1481, 2019. doi: 10.1007/s12274-019-2418-4.
543. **Rogne P, Rosselin M, Grundström C, Hedberg C, Sauer UH, Wolf-Watz M.** Molecular mechanism of ATP versus GTP selectivity of adenylate kinase. *Proc Natl Acad Sci U S A* 115: 3012–3017, 2018. doi: 10.1073/pnas.1721508115.
544. **Rohleder N.** Stimulation of systemic low-grade inflammation by psychosocial stress. *Psychosom Med* 76: 181–189, 2014. doi: 10.1097/PSY.000000000000049.
545. **Rosengren A, Hawken S, Ôunpuu S, Sliwa PK, Zubaid M, Almahmeed WA, Ngu Blackett K, Sitthi-Amorn C, Sato H, Yusuf PS.** Association of psychosocial risk factors with risk of acute myocardial infarction in 11 119 cases and 13 648 controls from 52 countries (the INTERHEART study): Case-control study. *Lancet* 364: 953–962, 2004. doi: 10.1016/S0140-6736(04)17019-0.
546. **Roskoski R.** A historical overview of protein kinases and their targeted small molecule inhibitors. *Pharmacol Res* 100: 1–23, 2015. doi: 10.1016/j.phrs.2015.07.010.
547. **Roskoski R.** Properties of FDA-approved small molecule protein kinase inhibitors: A 2022 update. *Pharmacol Res* 175: 106037, 2022. doi:

- 10.1016/j.phrs.2021.106037.
548. **Roth GA, Mensah GA, Johnson CO, Addolorato G, Ammirati E, Ai E.** Global burden of cardiovascular diseases and risk factors, 1990–2019: Update from the GBD 2019 study. *J Am Coll Cardiol* 76: 2982–3021, 2020. doi: 10.1016/j.jacc.2020.11.010.
549. **Rothman SM, Griffioen KJ, Wan R, Mattson MP.** Brain-derived neurotrophic factor as a regulator of systemic and brain energy metabolism and cardiovascular health. *Ann N Y Acad Sci* 1264: 49–63, 2012. doi: 10.1111/j.1749-6632.2012.06525.x.
550. **Roy B, Sobhani M.** Biomolecular basis of the role of chronic psychological stress in the development and progression of Atherosclerosis. *Int J Med Med Sci* 3: 339–350, 2013.
551. **Royce M, Osgood C, Mulkey F, Bloomquist E, Pierce WF, Roy A, Kalavar S, Ghosh S, Philip R, Rizvi F, Mixter BD, Tang S, Pazdur R, Beaver JA, Amiri-Kordestani L.** FDA approval summary: Abemaciclib with endocrine therapy for high-risk early breast cancer. *J Clin Oncol* 40: 1155–1162, 2022. doi: 10.1200/JCO.21.02742.
552. **Rugulies R, Bültmann U, Aust B, Burr H.** Psychosocial work environment and incidence of severe depressive symptoms: Prospective findings from a 5-year follow-up of the Danish work environment cohort study. *Am J Epidemiol* 163: 877–887, 2006. doi: 10.1093/aje/kwj119.
553. **Ruprecht B, Lemeer S.** Proteomic analysis of phosphorylation in cancer. *Expert Rev Proteomics* 11: 259–267, 2014. doi: 10.1586/14789450.2014.901156.
554. **Rusmini F, Zhong Z, Feijen J.** Protein immobilization strategies for protein biochips. *Biomacromolecules* 8: 1775–1789, 2007. doi: 10.1021/bm061197b.
555. **Russ T, Hamer M, Stamatakis E, Starr J, Batty G.** Psychological distress as a risk factor for dementia death. *Arch Intern Med* 170: 1859, 2011. doi: 10.1001/archinternmed.2011.521.
556. **Russell E, Koren G, Rieder M, Van Uum S.** Hair cortisol as a biological marker of chronic stress: Current status, future directions and unanswered questions. *Psychoneuroendocrinology* 37: 589–601, 2012. doi: 10.1016/j.psyneuen.2011.09.009.
557. **Russell LK, Mansfield CM, Lehman JJ, Kovacs A, Courtois M, Saffitz JE, Medeiros DM, Valencik ML, McDonald JA, Kelly DP.** Cardiac-specific

- induction of the transcriptional coactivator peroxisome proliferator-activated receptor γ coactivator-1 α promotes mitochondrial biogenesis and reversible cardiomyopathy in a developmental stage-dependent manner. *Circ Res* 94: 525–533, 2004. doi: 10.1161/01.RES.0000117088.36577.EB.
558. **Ryder AG, Chentsova-Dutton YE.** Depression in cultural context: “Chinese somatization,” revisited. *Psychiatr Clin North Am* 35: 15–36, 2012. doi: 10.1016/j.psc.2011.11.006.
559. **Ryšlavá H, Doubnerová V, Kavan D, Vaněk O.** Effect of posttranslational modifications on enzyme function and assembly. *J Proteomics* 92: 80–109, 2013. doi: 10.1016/j.jprot.2013.03.025.
560. **Sailaja Rao P, Kalva S, Yerramilli A, Mamidi S.** Free radicals and tissue damage: Role of antioxidants. *Free Radicals Antioxidants* 1: 2–7, 2011. doi: 10.5530/ax.2011.4.2.
561. **Salim Y, Hawken S, Ôunpuu S, Dans T, Avezum A, Lanus F, McQueen M, Budaj A, Pais P, Varigos J, Lisheng L.** Effect of potentially modifiable risk factors associated with myocardial infarction in 52 countries (the INTERHEART study): case-control study. *Lancet* 364: 937–952, 2004.
562. **Salomon RE, Tan KR, Vaughan A, Adynski H, Keely A, St SC, Hill C, Hill C, Hill C.** Minimally-invasive methods for examining biological changes in response to chronic stress: A scoping review. *Int J Nurs Stud* 103: 1–34, 2020. doi: 10.1016/j.ijnurstu.2019.103419.
563. **Sammul S, Viigimaa M.** Rapid socio-economic changes, psychosocial factors and prevalence of hypertension among men and women aged 55 years at baseline in Estonia: a 13-year follow-up study. *Blood Press* 27: 351–357, 2018. doi: 10.1080/08037051.2018.1476054.
564. **Santosa A, Rosengren A, Ramasundarahettige C, Rangarajan S, Chifamba J, Lear SA, Poirier P, Yeates KE, Yusuf R, Orlandini A, Weida L, Sidong L, Yibing Z, Mohan V, Kaur M, Zatonska K, Ismail N, Lopez-Jaramillo P, Iqbal R, Palileo-Villanueva LM, Yusufali AH, Alhabib KF, Yusuf S.** Psychosocial risk factors and cardiovascular disease and death in a population-based cohort from 21 low-, middle-, and high-income countries. *JAMA Netw Open* 4, 2021. doi: 10.1001/jamanetworkopen.2021.38920.
565. **Sarihan M, Bal Albayrak MG, Kasap M, Akpınar G, Kocyigit E.** An experimental workflow for enrichment of low abundant proteins from human

- serum for the discovery of serum biomarkers. *J Biol Methods* 10: e99010001, 2023. doi: 10.14440/jbm.2023.394.
566. **Sato H, Takahashi T, Sumitani K, Takatsu H, Urano S.** Glucocorticoid generates ROS to induce oxidative injury in the hippocampus, leading to impairment of cognitive function of rats. *J Clin Biochem Nutr* 47: 224–232, 2010. doi: 10.3164/jcbrn.10-58.
567. **Sato Y, Nakata K, Kato Y, Shima M, Ishii N, Koji T, Taketa K, Endo Y, Nagataki S.** Early recognition of hepatocellular carcinoma based on altered profiles of alpha-fetoprotein. *N Engl J Med* 328: 1802–1806, 1993.
568. **Sauer H, Wartenberg M, Hescheler J.** Reactive oxygen species as intracellular messengers during cell growth and differentiation. *Cell Physiol Biochem* 11: 173–186, 2001. doi: 10.1159/000047804.
569. **Savaryn JP, Catherman AD, Thomas PM, Abecassis MM, Kelleher NL.** The emergence of top-down proteomics in clinical research. *Genome Med* 5: 1–8, 2013. doi: 10.1186/gm457.
570. **Sawakami-Kobayashi K, Segawa O, Obata K, Hornes E, Yohda M, Tajima H, Machida M.** Multipurpose robot for automated cycle sequencing. *Biotechniques* 34: 634–637, 2003. doi: 10.2144/03343pf01.
571. **Scherma M, Qvist JS, Asok A, Huang SSC, Masia P, Deidda M, Wei YB, Soni RK, Fratta W, Fadda P, Kandel ER, Kandel DB, Melas PA.** Cannabinoid exposure in rat adolescence reprograms the initial behavioral, molecular, and epigenetic response to cocaine. *Proc Natl Acad Sci U S A* 117: 9991–10002, 2020. doi: 10.1073/pnas.1920866117.
572. **Schiavone S, Jaquet V, Trabace L, Krause KH.** Severe life stress and oxidative stress in the brain: From animal models to human pathology. *Antioxidants Redox Signal* 18: 1475–1490, 2013. doi: 10.1089/ars.2012.4720.
573. **Schiavone S, Sorce S, Dubois-Dauphin M, Jaquet V, Colaianna M, Zotti M, Cuomo V, Trabace L, Krause KH.** Involvement of NOX2 in the development of behavioral and pathologic alterations in isolated rats. *Biol Psychiatry* 66: 384–392, 2009. doi: 10.1016/j.biopsych.2009.04.033.
574. **Schjoldager KT, Narimatsu Y, Joshi HJ, Clausen H.** Global view of human protein glycosylation pathways and functions. *Nat Rev Mol Cell Biol* 21: 729–749, 2020. doi: 10.1038/s41580-020-00294-x.
575. **Schmelter C, Brueck A, Perumal N, Qu S, Pfeiffer N, Grus FH.** Lectin-based

- affinity enrichment and characterization of N-glycoproteins from human tear film by mass spectrometry. *Molecules* 28, 2023. doi: 10.3390/molecules28020648.
576. **Schneiderman N, Ironson G, Siegel SD.** Stress and health: Psychological, behavioral, and biological determinants. *Annu Rev Clin Psychol* 1: 607–628, 2005. doi: 10.1146/annurev.clinpsy.1.102803.144141.
577. **Schoenheimer R, Ratner S, Rittenberg D.** Studies in protein metabolism. *J Biol Chem* 127: 333–344, 1939. doi: 10.1016/s0021-9258(18)73846-5.
578. **Schwaminger SP, Fraga-García P, Eigenfeld M, Becker TM, Berensmeier S.** Magnetic separation in bioprocessing beyond the analytical scale: From biotechnology to the food industry. *Front Bioeng Biotechnol* 7, 2019. doi: 10.3389/fbioe.2019.00233.
579. **Seet BT, Dikic I, Zhou MM, Pawson T.** Reading protein modifications with interaction domains. *Nat Rev Mol Cell Biol* 7: 473–483, 2006. doi: 10.1038/nrm1960.
580. **Seewoo BJ, Hennessy LA, Feindel KW, Etherington SJ, Croarkin PE, Rodger J.** Validation of chronic restraint stress model in young adult rats for the study of depression using longitudinal multimodal MR imaging. *eNeuro* 7: 1–22, 2020. doi: 10.1523/ENEURO.01113-20.2020.
581. **Selye H.** A syndrome produced by diverse noxious agents. *Nature* 138: 32, 1936. doi: 10.1038/138032a0.
582. **Shah PK, Lecis D.** Inflammation in atherosclerotic cardiovascular disease [version 1; peer review: 4 approved]. *F1000Research* 8: 1–10, 2019. doi: 10.12688/f1000research.18901.1.
583. **Shah TR, Misra A.** Proteomics. In: *Challenges in Delivery of Therapeutic Genomics and Proteomics*, edited by Misra A. Gujarat: Elsevier, 2011, p. 387–427.
584. **Shajahan A, Heiss C, Ishihara M, Azadi P.** Glycomic and glycoproteomic analysis of glycoproteins—a tutorial. *Anal Bioanal Chem* 409: 4483–4505, 2017. doi: 10.1007/s00216-017-0406-7.
585. **Shakeel M.** Recent advances in understanding the role of oxidative stress in diabetic neuropathy. *Diabetes Metab Syndr Clin Res Rev* 9: 373–378, 2015. doi: 10.1016/j.dsx.2014.04.029.
586. **Sharon N.** Lectin-carbohydrate complexes of plants and animals: an atomic view. *Trends Biochem Sci* 18: 221–226, 1993. doi: 10.1016/0968-

- 0004(93)90193-Q.
587. **Shavers-Hornaday VL, Lynch CF, Burmeister LF, Torner JC.** Why are African Americans under-represented in medical research studies? Impediments to participation. *Ethn Heal* 2: 31–45, 1997. doi: 10.1080/13557858.1997.9961813.
 588. **Sheikh MO, Halmo SM, Wells L.** Recent advancements in understanding mammalian O-mannosylation. *Glycobiology* 27: 806–819, 2017. doi: 10.1093/glycob/cwx062.
 589. **Shen C.** Quantification and analysis of proteins. In: *Diagnostic Molecular Biology*. Elsevier Inc., 2019, p. 187–214.
 590. **Shen CP, Tsimberg Y, Salvatore C, Meller E.** Activation of Erk and JNK MAPK pathways by acute swim stress in rat brain regions. *BMC Neurosci* 5: 1–13, 2004. doi: 10.1186/1471-2202-5-36.
 591. **Sher LD, Geddie H, Olivier L, Cairns M, Truter N, Beselaar L, Essop MF.** Chronic stress and endothelial dysfunction: Mechanisms, experimental challenges, and the way ahead. *Am J Physiol - Hear Circ Physiol* 319: H488–H506, 2020. doi: 10.1152/ajpheart.00244.2020.
 592. **Shi Y, Song R, Wang L, Qi Y, Zhang H, Zhu J, Zhang X, Tang X, Zhan Q, Zhao Y, Swaab DF, Bao AM, Zhang Z.** Identifying plasma biomarkers with high specificity for major depressive disorder: A multi-level proteomics study. *J Affect Disord* 277: 620–630, 2020. doi: 10.1016/j.jad.2020.08.078.
 593. **Shi Y, Xiang R, Horváth C, Wilkins JA.** The role of liquid chromatography in proteomics. *J Chromatogr A* 1053: 27–36, 2004. doi: 10.1016/j.chroma.2004.07.044.
 594. **Shteynberg DD, Deutsch EW, Campbell DS, Hoopmann MR, Kusebauch U, Lee D, Mendoza L, Midha MK, Sun Z, Whetton AD, Moritz RL.** PTMProphet: Fast and accurate mass modification localization for the trans-proteomic pipeline. *J Proteome Res* 18: 4262–4272, 2019. doi: 10.1021/acs.jproteome.9b00205.
 595. **Shuaib A, Hartwell A, Kiss-toth E, Holcombe M.** Multi-compartmentalisation in the MAPK signalling pathway contributes to the emergence of oscillatory behaviour and to ultrasensitivity. *PLoS One* 11: e0156139, 2016. doi: 10.1371/journal.pone.0156139.
 596. **Siddiqui A, Desai NG, Sharma SB, Aslam M, Sinha UK, Madhu S V.**

- Association of oxidative stress and inflammatory markers with chronic stress in patients with newly diagnosed type 2 diabetes. *Diabetes Metab Res Rev* 35: 1–8, 2019. doi: 10.1002/dmrr.3147.
597. **Sigma Aldrich**. Concanavalin A product specification. *Ind. Compet. Cost Reduct.*: 75–92, 2006.
598. **Silva-Costa LC, Garcia-Rosa S, Smith BJ, Baldasso PA, Steiner J, Martins-de-Souza D**. Blood plasma high abundant protein depletion unintentionally carries over 100 proteins. *Sep Sci Plus* 2: 449–456, 2019. doi: 10.1002/sscp.201900057.
599. **Silverman MN, Sternberg EM**. Glucocorticoid regulation of inflammation and its functional correlates: From HPA axis to glucocorticoid receptor dysfunction. *Ann N Y Acad Sci* 1261: 55–63, 2012. doi: 10.1111/j.1749-6632.2012.06633.x.
600. **Simard M, Underhill C, Hammond GL**. Functional implications of corticosteroid-binding globulin N-glycosylation. *J Mol Endocrinol* 60: 71–84, 2018. doi: 10.1530/JME-17-0234.
601. **Simpson DSA, Oliver PL**. ROS generation in microglia: Understanding oxidative stress and inflammation in neurodegenerative disease. *Antioxidants* 9: 1–27, 2020. doi: 10.3390/antiox9080743.
602. **Sinha A, Mann M**. A beginner's guide to mass spectrometry-based proteomics. Portland Press Limited, 2020.
603. **Šlechtová T, Gilar M, Kalíková K, Tesařová E**. Insight into trypsin miscleavage: Comparison of kinetic constants of problematic peptide sequences. *Anal Chem* 87: 7636–7643, 2015. doi: 10.1021/acs.analchem.5b00866.
604. **Smith C**. Using rodent models to simulate stress of physiologically relevant severity: When, why and how. In: *Glucocorticoids - New Recognition of Our Familiar Friend*. Cape Town: 2012, p. 211–230.
605. **Smith C, Essop M**. Influence of lifestyle choices on metabolic risk has distinct gender and age differences. *Int J Clin Exp Physiol* 1: 13, 2014. doi: 10.4103/2348-8093.129722.
606. **Smith RW**. Mass Spectrometry. *Encycl. Forensic Sci*. Elsevier Ltd.: 603–608, 2013.
607. **Smoller JW**. The genetics of stress-related disorders: PTSD, depression, and anxiety disorders. *Neuropsychopharmacology* 41: 297–319, 2016. doi:

- 10.1038/npp.2015.266.
608. **Smyth A, O'Donnell M, Lamelas P, Teo K, Rangarajan S, Yusuf S.** Physical activity and anger or emotional upset as triggers of acute myocardial infarction: The INTERHEART Study. *Circulation* 134: 1059–1067, 2016. doi: 10.1161/CIRCULATIONAHA.116.023142.
609. **Sneekes E-J, Rieux L, Swart R.** Nano LC: Principles, evolution, and state-of-the-art of the technique [Online]. *LCGC North Am* 29: 926–9344, 2011. <https://www.chromatographyonline.com/view/nano-lc-principles-evolution-and-state-art-technique> [7 Oct. 2022].
610. **Søberg K, Skålhegg BS.** The molecular basis for specificity at the level of the protein kinase a catalytic subunit. *Front Endocrinol (Lausanne)* 9: 1–22, 2018. doi: 10.3389/fendo.2018.00538.
611. **Sojar HT, Bahl OP.** Chemical deglycosylation of glycoproteins. In: *Methods in Enzymology*. Academic Press, 1987, p. 341–350.
612. **Solari FA, Dell'Aica M, Sickmann A, Zahedi RP.** Why phosphoproteomics is still a challenge. *Mol Biosyst* 11: 1487–1493, 2015. doi: 10.1039/c5mb00024f.
613. **Soomro S.** Oxidative stress and inflammation. *Open J Immunol* 9: 1–20, 2019. doi: 10.4236/oji.2019.91001.
614. **Soper A, Aird S.** Elution of tightly bound solutes of ConA Sepharose factors affecting the desorption of cottonmouth venom glycoprotein. *J Chromatogr* 1154: 308–318, 2008.
615. **Sorce S, Krause K-H.** NOX enzymes in the central nervous system: From signaling to Disease. *Antioxidants Redox Signal* 11: 2481–2504, 2009.
616. **Sorrells SF, Caso JR, Munhoz CD, Sapolsky RM.** The stressed CNS: When glucocorticoids aggravate inflammation. *Neuron* 64: 33–39, 2009. doi: 10.1016/j.neuron.2009.09.032.
617. **South African Depression and Anxiety Group.** SADAG's online survey findings on COVID-19 and mental health (21 April 2020) [Online]. *South African J Psychiatr* 2020. http://www.sadag.org/index.php?option=com_content&view=article&id=3092:sadag-s-online-survey-findings-on-covid-19-and-mental-health-21-april-2020&catid=149&Itemid=226 [19 Oct. 2020].
618. **Southwick SM, Sippel L, Krystal J, Charney D, Mayes L, Pietrzak RH.** Why are some individuals more resilient than others: The role of social support. *World*

- Psychiatry* 15: 77–79, 2016. doi: 10.1002/wps.20282.
619. **Sparbier K, Koch S, Kessler I, Wenzel T, Kostrzewa M.** Selective isolation of glycoproteins and glycopeptides for MALDI-TOF MS detection supported by magnetic particles. *J Biomol Tech* 16: 407–411, 2005.
620. **Spiers JG, Chen HJC, Sernia C, Lavidis NA.** Activation of the hypothalamic-pituitary-adrenal stress axis induces cellular oxidative stress. *Front Neurosci* 9: 1–6, 2015. doi: 10.3389/fnins.2014.00456.
621. **Spiga F, Walker JJ, Terry JR, Lightman SL.** HPA axis-rhythms. *Compr Physiol* 4: 1273–1298, 2014. doi: 10.1002/cphy.c140003.
622. **Spiro RG.** Protein glycosylation: Nature, distribution, enzymatic formation, and disease implications of glycopeptide bonds. *Glycobiology* 12: 43R-56R, 2002. doi: 10.1093/glycob/12.4.43R.
623. **Stadlmann J, Hoi DM, Taubenschmid J, Mechtler K, Penninger JM.** Analysis of PNGase F-resistant N-glycopeptides using sugarQb for pProteome Discoverer 2.1 reveals cryptic substrate specificities. *Proteomics* 18: 1–5, 2018. doi: 10.1002/pmic.201700436.
624. **Stanta JL, Saldova R, Struwe WB, Byrne JC, Leweke FM, Rothermund M, Rahmoune H, Levin Y, Guest PC, Bahn S, Rudd PM.** Identification of N-glycosylation changes in the CSF and serum in patients with schizophrenia. *J Proteome Res* 9: 4476–4489, 2010. doi: 10.1021/pr100897p.
625. **Staros J V., Wright RW, Swingle DM.** Enhancement by N-hydroxysulfosuccinimide of water-soluble carbodiimide-mediated coupling reactions. *Anal Biochem* 156: 220–222, 1986. doi: 10.1016/0003-2697(86)90176-4.
626. **Steen H.** Introduction to proteomics. In: *Concepts and Techniques in Genomics and Proteomics*. Woodhead Publishing Limited, 2007, p. 147–158.
627. **Steinberg TH, Agnew BJ, Gee KR, Leung WY, Goodman T, Schulenberg B, Hendrickson J, Beechem JM, Haugland RP, Patton WF.** Global quantitative phosphoprotein analysis using multiplexed proteomics technology. *Proteomics* 3: 1128–1144, 2003. doi: 10.1002/pmic.200300434.
628. **Steinberg TH, Pretty K, Berggren KN, Kemper C, Jones L, Diwu Z, Haugland RP, Patton WF.** Rapid and simple single nanogram detection of glycoproteins in polyacrylamide gels and on electroblots. *Proteomics* 1: 841–855, 2001. doi: 10.1002/1615-9861(200107)1:7<841::AID-PROT841>3.0.CO;2-

- E.
629. **Stella C, Rudaz S, Veuthey JL, Tchaplal A.** Silica and other materials as supports in liquid chromatography. Chromatographic tests and their importance for evaluating these supports. Part I. *Chromatographia* 53, 2001. doi: 10.1007/bf02490318.
 630. **Stoll DR.** Reversed-phase liquid chromatography and water, Part I: How much is too much? [Online]. *LCGC North Am.*: 2019. <https://www.chromatographyonline.com/view/reversed-phase-liquid-chromatography-and-water-part-i-how-much-too-much> [30 Apr. 2021].
 631. **Stoychev S, Naicker P, Govender I, Gerber I, Jordaan J.** Development of fully automated pipeline for phosphoproteome profiling: optimisation of phosphopeptide enrichment [Online]. *Am. Soc. Mass Spectrom. Resyn Biosciences*: 2019. https://resynbio.com/wp-content/uploads/2020/01/HUPO_2019_Poster_SS_Phos_coupled_clean-up.pdf [8 Sep. 2022].
 632. **Sugawara K, Yugami A, Kadoya T, Kuramitz H, Hosaka K.** Electrochemical assay of concanavalin A-ovalbumin binding on magnetic beads. *Analyst* 137: 3781–3786, 2012. doi: 10.1039/c2an35667h.
 633. **Sulkava S, Haukka J, Sulkava R, Laatikainen T, Paunio T.** Association between psychological distress and incident dementia in a population-based cohort in Finland. *JAMA Netw Open* 5: E2247115, 2022. doi: 10.1001/jamanetworkopen.2022.47115.
 634. **Sun GD, Cui WP, Guo QY, Miao LN.** Histone lysine methylation in diabetic nephropathy. *J Diabetes Res* 2014: 1–9, 2014. doi: 10.1155/2014/654148.
 635. **Suzuki T, Kitajima K, Emori Y, Inoue Y, Inoue S.** Site-specific de-N-glycosylation of diglycosylated ovalbumin in hen oviduct by endogenous peptide: N-glycanase as a quality control system for newly synthesized proteins. *Proc Natl Acad Sci U S A* 94: 6244–6249, 1997. doi: 10.1073/pnas.94.12.6244.
 636. **Szendroedi J, Phielix E, Roden M.** The role of mitochondria in insulin resistance and type 2 diabetes mellitus. *Nat Rev Endocrinol* 8: 92–103, 2012. doi: 10.1038/nrendo.2011.138.
 637. **Tabb DL, Fernando CG, Chambers MC.** MyriMatch: highly accurate tandem mass spectral peptide identification by multivariate hypergeometric analysis. *J Proteome Res* 6: 654–661, 2007. doi: <https://doi.org/10.1021/pr0604054>.

638. **Tabb DL, Vega-Montoto L, Rudnick PA, Variyath AM, Ham AJL, Bunk DM, Kilpatrick LE, Billheimer DD, Blackman RK, Cardasis HL, Carr SA, Clauser KR, Jaffe JD, Kowalski KA, Neubert TA, Regnier FE, Schilling B, Tegeler TJ, Wang M, Wang P, Whiteaker JR, Zimmerman LJ, Fisher SJ, Gibson BW, Kinsinger CR, Mesri M, Rodriguez H, Stein SE, Tempst P, Paulovich AG, Liebler DC, Spiegelman C.** Repeatability and reproducibility in proteomic identifications by liquid chromatography-tandem mass spectrometry. *J Proteome Res* 9: 761–776, 2010. doi: 10.1021/pr9006365.
639. **Takio K, Titani K.** Plasma desorption mass spectral (PDMS) analysis of polypeptides containing some post-translational modifications; Scission of covalent bonds. In: *Techniques in Protein Chemistry III*, edited by Angeletti R. Academic Press, p. 497–504.
640. **Tan Z, Yin H, Nie S, Lin Z, Zhu J, Ruffin MT, Anderson MA, Simeone DM, Lubman DM.** Large-scale identification of core-fucosylated glycopeptide sites in pancreatic cancer serum using mass spectrometry. *J Proteome Res* 14: 1968–1978, 2015. doi: 10.1021/acs.jproteome.5b00068.
641. **Tang J, Yin P, Lu X, Qi D, Mao Y, Deng C, Yang P, Zhang X.** Development of mesoporous TiO₂ microspheres with high specific surface area for selective enrichment of phosphopeptides by mass spectrometric analysis. *J Chromatogr A* 1217: 2197–2205, 2010. doi: 10.1016/j.chroma.2010.02.008.
642. **Taniguchi N, Kizuka Y.** Glycans and cancer: Role of N-glycans in cancer biomarker, progression and metastasis, and therapeutics. 1st ed. Elsevier Inc.
643. **Temporini C, Calleri E, Massolini G, Caccialanza G.** Integrated analytical strategies for the study of phosphorylation and glycosylation in proteins. *Mass Spectrom Rev* 27: 207–236, 2008. doi: 10.1002/mas.
644. **Teo GC, Polasky DA, Yu F, Nesvizhskii AI.** Fast deisotoping algorithm and its implementation in the MSFragger search engine. *J Proteome Res* 20: 498–505, 2021. doi: 10.1021/acs.jproteome.0c00544.
645. **Tepper K, Biernat J, Kumar S, Wegmann S, Timm T, Hübschmann S, Redecke L, Mandelkow EM, Müller DJ, Mandelkow E.** Oligomer formation of tau protein hyperphosphorylated in cells. *J Biol Chem* 289: 34389–34407, 2014. doi: 10.1074/jbc.M114.611368.
646. **Thaler F, Valsasina B, Baldi R, Xie J, Stewart A, Isacchi A, Kalisz HM, Rusconi L.** A new approach to phosphoserine and phosphothreonine analysis

- in peptides and proteins: Chemical modification, enrichment via solid-phase reversible binding, and analysis by mass spectrometry. *Anal Bioanal Chem* 376: 366–373, 2003. doi: 10.1007/s00216-003-1919-9.
647. **Thau L, Gandhi J, Sharma S.** Physiology, Cortisol [Online]. StatPearls Publishing. <https://www.ncbi.nlm.nih.gov/books/NBK538239/> [7 Jul. 2023].
648. **Thaysen-Andersen M, Packer NH, Schulz BL.** Maturing glycoproteomics technologies provide unique structural insights into the N-glycoproteome and its regulation in health and disease. *Mol Cell Proteomics* 15: 1773–1790, 2016. doi: 10.1074/mcp.O115.057638.
649. **The Protein Man.** How to elute tightly bound glycoproteins from concanavalin A (Con A) agarose [Online]. *G-Biosciences*: 2015. <https://info.gbiosciences.com/blog/how-to-elute-tightly-bound-glyoproteins-from-concanavalin-a-con-a-agarose> [7 Jun. 2021].
650. **The Protein Man's Blog - A discussion of Protein Research.** High efficiency & stability protein crossLinking with EDC & NHS [Online]. *G-Biosciences*: 2017. <https://info.gbiosciences.com/blog/2-step-protein-coupling-edc-nhs> [9 Apr. 2022].
651. **Thermo Fisher Scientific.** Overview of protein assays methods [Online]. *Thermo Fish. Sci.*: [date unknown]. <https://www.thermofisher.com/za/en/home/life-science/protein-biology/protein-biology-learning-center/protein-biology-resource-library/pierce-protein-methods/overview-protein-assays.html> [5 May 2023].
652. **Thermo Fisher Scientific.** NanoDrop Lite: Interpretation of nucleic acid 260/280 ratios. *Protoc. Prod. Manuals* Thermo Fisher Scientific: 1, 2012.
653. **Thermo Fisher Scientific.** NanoDrop One User Guide. Thermo Fisher Scientific: 2016.
654. **Thermo Scientific.** Instructions glycoprotein isolation kit , ConA [Online]. *Thermo Sci.* Thermo Fisher Scientific: 1–3, 2013. https://www.thermofisher.com/document-connect/document-connect.html?url=https://assets.thermofisher.com/TFS-Assets%2FSLSG%2Fmanuals%2FMAN0011534_Glycoprotein_Isolat_ConA_U G.pdf [9 Jul. 2023].
655. **Therrien F, Drapeau V, Lalonde J, Lupien SJ, Beaulieu S, Tremblay A, Richard D.** Awakening cortisol response in lean, obese, and reduced obese

- individuals: Effect of gender and fat distribution. *Obesity* 15: 377–385, 2007. doi: 10.1038/oby.2007.509.
656. **Thinon E, Serwa RA, Broncel M, Brannigan JA, Brassat U, Wright MH, Heal WP, Wilkinson AJ, Mann DJ, Tate EW.** Global profiling of co- and post-translationally N-myristoylated proteomes in human cells. *Nat Commun* 5, 2014. doi: 10.1038/ncomms5919.
657. **Thomas SR, Witting PK, Drummond GR.** Redox control of endothelial function and dysfunction: Molecular mechanisms and therapeutic opportunities. *Antioxidants Redox Signal* 10: 1713–1765, 2008. doi: 10.1089/ars.2008.2027.
658. **Tian R, Hou G, Li D, Yuan TF.** A possible change process of inflammatory cytokines in the prolonged chronic stress and its ultimate implications for health. *Sci World J* 2014, 2014. doi: 10.1155/2014/780616.
659. **Timmermans S, Souffriau J, Libert C.** A general introduction to glucocorticoid biology. *Front Immunol* 10: 1–17, 2019. doi: 10.3389/fimmu.2019.01545.
660. **Toth I, Neumann ID.** Animal models of social avoidance and social fear. *Cell Tissue Res* 354: 107–118, 2013. doi: 10.1007/s00441-013-1636-4.
661. **Totten SM, Adusumilli R, Kullolli M, Tanimoto C, Brooks JD, Mallick P, Pitteri SJ.** Multi-lectin affinity chromatography and quantitative proteomic analysis reveal differential glycoform levels between prostate cancer and benign prostatic hyperplasia sera. *Sci Rep* 8: 1–13, 2018. doi: 10.1038/s41598-018-24270-w.
662. **Trakunram K, Champoochana N, Chaniad P, Thongsuksai P, Raungrut P.** MicroRNA isolation by trizol-based method and its stability in stored serum and cDNA derivatives. *Asian Pacific J Cancer Prev* 20: 1641–1647, 2019. doi: 10.31557/APJCP.2019.20.6.1641.
663. **Trombetta ES.** The contribution of N-glycans and their processing in the endoplasmic reticulum to glycoprotein biosynthesis. *Glycobiology* 13: 77R-91R, 2003. doi: 10.1093/glycob/cwg075.
664. **Tromp B, Dolley C, Laganparsad M, Goveneder S.** SA's sick state of mental health [Online]. *The Sunday Times*: 2014. <https://www.timeslive.co.za/sunday-times/lifestyle/2014-07-06-sas-sick-state-of-mental-health/> [28 May 2022].
665. **Trost B, Kusalik A.** Computational prediction of eukaryotic phosphorylation sites. *Bioinformatics* 27: 2927–2935, 2011. doi: 10.1093/bioinformatics/btr525.
666. **Tsai CF, Hsu CC, Hung JN, Wang YT, Choong WK, Zeng MY, Lin PY, Hong**

- RW, Sung TY, Chen YJ.** Sequential phosphoproteomic enrichment through complementary metal-directed immobilized metal ion affinity chromatography. *Anal Chem* 86: 685–693, 2014. doi: 10.1021/ac4031175.
667. **Tsigos C, Chrousos GP.** Physiology of the hypothalamic-pituitary-adrenal axis in health and dysregulation in psychiatric and autoimmune disorders. *Endocrinol Metab Clin North Am* 23: 451–466, 1994. doi: 10.1016/s0889-8529(18)30078-1.
668. **Tsigos C, Kyrou I, Chrousos, George P. and Papanicolaou DA.** Prolonged suppression of corticosteroid-binding globulin by recombinant human interleukin-6 in man. *J Clin Endocrinol Metab* 83: 3379–3379, 1998. doi: 10.1210/jcem.83.9.5100-2.
669. **Tsukada H, Seino Y, Ueda S, Uchino H, Sakai M.** Influence of water-immersion stress on synthesis of mucus glycoprotein in the rat gastric mucosa. *Scand J Gastroenterol* 24: 19–22, 1989. doi: 10.3109/00365528909091115.
670. **Turkina M.** Functional proteomics of protein phosphorylation in algal photosynthetic membranes (dissertation). Linköping University: 2008.
671. **Ubersax JA, Ferrell JE.** Mechanisms of specificity in protein phosphorylation. *Nat Rev Mol Cell Biol* 8: 530–541, 2007. doi: 10.1038/nrm2203.
672. **Um SH, D’Alessio D, Thomas G.** Nutrient overload, insulin resistance, and ribosomal protein S6 kinase 1, S6K1. *Cell Metab* 3: 393–402, 2006. doi: 10.1016/j.cmet.2006.05.003.
673. **Vaccarino V, Almuwaqqat Z, Kim JH, Hammadah M, Shah AJ, Ko YA, Elon L, Sullivan S, Shah A, Alkholder A, Lima BB, Pearce B, Ward L, Kutner M, Hu Y, Lewis TT, Garcia E V., Nye J, Sheps DS, Raggi P, Bremner JD, Quyyumi AA.** Association of mental stress-induced myocardial ischemia with cardiovascular events in patients with coronary heart disease. *JAMA - J Am Med Assoc* 326: 1818–1828, 2021. doi: 10.1001/jama.2021.17649.
674. **Vaishya S, Sarwade RD, Seshadri V.** MicroRNA, proteins, and metabolites as novel biomarkers for prediabetes, diabetes, and related complications. *Front Endocrinol (Lausanne)* 9: 1–12, 2018. doi: 10.3389/fendo.2018.00180.
675. **Van Cromphaut SJ.** Hyperglycaemia as part of the stress response: The underlying mechanisms. *Best Pract Res Clin Anaesthesiol* 23: 375–386, 2009. doi: 10.1016/j.bpa.2009.08.005.
676. **van der Kooij MA.** The impact of chronic stress on energy metabolism. *Mol Cell*

- Neurosci* 107: 103525, 2020. doi: 10.1016/j.mcn.2020.103525.
677. **Vandermarliere E, Mueller M, Martens L.** Getting intimate with trypsin, the leading protease in proteomics. *Mass Spectrom Rev* 32: 453–465, 2013. doi: <https://doi.org/10.1002/mas.21376>.
678. **Vanmechelen E, Vanderstichele H, Davidsson P, Van Kerschaver E, Van Der Perre B, Sjögren M, Andreasen N, Blennow K.** Quantification of tau phosphorylated at threonine 181 in human cerebrospinal fluid: A sandwich ELISA with a synthetic phosphopeptide for standardization. *Neurosci Lett* 285: 49–52, 2000. doi: 10.1016/S0304-3940(00)01036-3.
679. **Varki A.** Biological roles of glycans. *Glycobiology* 27: 3–49, 2017. doi: 10.1093/glycob/cww086.
680. **Vashist SK.** Comparison of 1-ethyl-3-(3-dimethylaminopropyl) carbodiimide based strategies to crosslink antibodies on amine-functionalized platforms for immunodiagnostic applications. *Diagnostics* 2: 23–33, 2012. doi: 10.3390/diagnostics2030023.
681. **Vassiliou AG, Athanasiou N, Vassiliadi DA, Jahaj E, Keskinidou C, Kotanidou A, Dimopoulou I.** Glucocorticoid and mineralocorticoid receptor expression in critical illness: A narrative review. *World J Crit Care Med* 10: 102–111, 2021. doi: 10.5492/wjccm.v10.i4.102.
682. **Vaudel M, Sickmann A, Martens L.** Current methods for global proteome identification. *Expert Rev Proteomics* 9: 519–532, 2012. doi: 10.1586/epr.12.51.
683. **Vegiopoulos A, Herzig S.** Glucocorticoids, metabolism and metabolic diseases. *Mol Cell Endocrinol* 275: 43–61, 2007. doi: 10.1016/j.mce.2007.05.015.
684. **Verónica A, Friedman PA.** Minireview: Ubiquitination-regulated G protein-coupled receptor signaling and trafficking. *Mol Endocrinol* 27: 558–572, 2013. doi: 10.1210/me.2012-1404.
685. **Vlahou A.** Implementation of clinical proteomics: A step closer to personalized medicine? *Proteomics - Clin Appl* 13: 1–8, 2019. doi: 10.1002/prca.201800088.
686. **Walsh C.** Posttranslational modification of proteins: expanding nature's inventory [Online]. *Harvard Med. Sch.* Roberts & Company Publishers: 576, 2006.
https://books.google.co.za/books?hl=en&lr=&id=JGBfQXlzdWgC&oi=fnd&pg=PR15&ots=v9WBuZ0rNO&sig=pn4hn5oNOCJ5IMh_ecsWlyevST8&redir_esc=y

#v=onepage&q&f=false [6 Jun. 2022].

687. **Walsh GM, Rogalski JC, Klockenbusch C, Kast J.** Mass spectrometry-based proteomics in biomedical research: Emerging technologies and future strategies. *Expert Rev Mol Med* 12: 1–28, 2010. doi: 10.1017/S1462399410001614.
688. **Wang H, Xu J, Lazarovici P, Quirion R, Zheng W.** cAMP response element-binding protein (CREB): A possible signaling molecule link in the pathophysiology of Schizophrenia. *Front Mol Neurosci* 11: 1–14, 2018. doi: 10.3389/fnmol.2018.00255.
689. **Wang X, Xie Y, Zhang T, Bo S, Bai X, Liu H, Li T, Liu S, Zhou Y, Cong X, Wang Z, Liu D.** Resveratrol reverses chronic restraint stress-induced depression-like behaviour: Involvement of BDNF level, ERK phosphorylation and expression of Bcl-2 and Bax in rats. *Brain Res Bull* 125: 134–143, 2016. doi: 10.1016/j.brainresbull.2016.06.014.
690. **Wang YC, Peterson SE, Loring JF.** Protein post-translational modifications and regulation of pluripotency in human stem cells. *Cell Res* 24: 143–160, 2014. doi: 10.1038/cr.2013.151.
691. **Watanabe Y, Allen JD, Wrapp D, McLellan JS, Crispin M.** Site-specific glycan analysis of the SARS-CoV-2 spike. *Science (80-)* 369: 330–333, 2020. doi: 10.1126/science.abb9983.
692. **Welch CJ, Talaga ML, Kadav PD, Edwards JL, Bandyopadhyay P, Dam TK.** A capture and release method based on noncovalent ligand cross-linking and facile filtration for purification of lectins and glycoproteins. *J Biol Chem* 295: 223–236, 2020. doi: 10.1074/jbc.RA119.010625.
693. **Wellen KE, Hatzivassiliou G, Sachdeva UM, Bui T V., Cross JR, Thompson CB.** ATP-citrate lyase links cellular metabolism to histone acetylation. *Science (80-)* 324: 1076–1080, 2009. doi: 10.1126/science.1164097.
694. **Wells L, Vosseller K, Cole RN, Cronshaw JM, Matunis MJ, Hart GW.** Mapping sites of O-GlcNAc modification using affinity tags for serine and threonine post-translational modifications. *Mol Cell Proteomics* 1: 791–804, 2002. doi: 10.1074/mcp.M200048-MCP200.
695. **Weng SL, Kao HJ, Huang CH, Lee TY.** MDD-palm: Identification of protein palmitoylation sites with substrate motifs based on maximal dependence decomposition. *PLoS One* 12: 1–19, 2017. doi: 10.1371/journal.pone.0179529.

696. **Wickramathilaka MP, Tao BY.** Characterization of covalent crosslinking strategies for synthesizing DNA-based bioconjugates. *J Biol Eng* 13: 8–17, 2019. doi: 10.1186/s13036-019-0191-2.
697. **Wiegand C, Savelsbergh A, Heusser P.** MicroRNAs in psychological stress reactions and their use as stress-associated biomarkers, especially in human saliva. *Biomed Hub* 2: 1–15, 2017. doi: 10.1159/000481126.
698. **Wittmann V.** Glycoproteins: Occurrence and significance. In: *Glycoscience*, edited by Fraser-Reid BO, Tatsuta K, Thiem J. Berlin: Springer-Verlag, 2008, p. 1736–1763.
699. **Woo H, Hong CJ, Jung S, Choe S, Yu SW.** Chronic restraint stress induces hippocampal memory deficits by impairing insulin signaling. *Mol Brain* 11: 1–13, 2018. doi: 10.1186/s13041-018-0381-8.
700. **World Health Organization.** Noncommunicable diseases [Online]. *WHO Int*. 2023. <https://www.who.int/news-room/fact-sheets/detail/noncommunicable-diseases> [30 Jul. 2023].
701. **Wu CC, Tsantilas KA, Park J, Plubell D, Naicker P, MacCoss MJ.** Mag-Net : Rapid enrichment of membrane-bound particles enables high coverage quantitative analysis of the plasma proteome (Preprint). .
702. **Wu Z, Huang X, Feng Y, Handschin C, Feng Y, Gullicksen PS, Bare O, Labow M, Spiegelman B, Stevenson SC.** Transducer of regulated CREB-binding proteins (TORCs) induce PGC-1 α transcription and mitochondrial biogenesis in muscle cells. *Proc Natl Acad Sci U S A* 103: 14379–14384, 2006. doi: 10.1073/pnas.0606714103.
703. **Wysocki VH, Tsaprailis G, Smith LL, Brechi LA.** Mobile and localized protons: A framework for understanding peptide dissociation. *J Mass Spectrom* 35: 1399–1406, 2000. doi: 10.1002/1096-9888(200012)35:12<1399::AID-JMS86>3.0.CO;2-R.
704. **Xiao H, Sun F, Suttapitugsakul S, Wu R.** Global and site-specific analysis of protein glycosylation in complex biological systems with mass spectrometry. *Mass Spectrom Rev* 38: 356–379, 2019. doi: 10.1002/mas.21586.
705. **Xie B, Invernizzi CF, Richard S, Wainberg MA.** Arginine methylation of the human immunodeficiency virus type 1 Tat protein by PRMT6 negatively affects Tat interactions with both cyclin T1 and the Tat transactivation region. *J Virol* 81: 4226–4234, 2007. doi: 10.1128/jvi.01888-06.

706. **Xie H, Huang H, Tang M, Wu Y, Huang R, Liu Z, Zhou M, Liao W, Zhou J.** iTRAQ-based quantitative proteomics suggests synaptic mitochondrial dysfunction in the hippocampus of rats susceptible to chronic mild stress. *Neurochem Res* 43: 2372–2383, 2018. doi: 10.1007/s11064-018-2664-y.
707. **Xie J, Zhong G, Cai C, Chen C, Chen X.** Rapid and efficient separation of glycoprotein using pH double-responsive imprinted magnetic microsphere. *Talanta* 169: 98–103, 2017. doi: 10.1016/j.talanta.2017.03.065.
708. **Xie Y, Xu E, Al-Aly Z.** Risks of mental health outcomes in people with covid-19: Cohort study. *BMJ* 376: 1–13, 2022. doi: 10.1136/bmj-2021-068993.
709. **Xu P, Wang K, Lu C, Dong L, Chen Y, Wang Q, Shi Z, Yang Y, Chen S, Liu X.** Effects of the chronic restraint stress induced depression on reward-related learning in rats. *Behav Brain Res* 321: 185–192, 2017. doi: 10.1016/j.bbr.2016.12.045.
710. **Xu T, Ding W, Ji X, Ao X, Liu Y, Yu W, Wang J.** Oxidative stress in cell death and cardiovascular diseases. *Oxid Med Cell Longev* 2019: 1–12, 2019. doi: 10.1155/2019/9030563.
711. **Xu YY, Ge JF, Liang J, Cao Y, Shan F, Liu Y, Yan CY, Xia QR.** Nesfatin-1 and cortisol: Potential novel diagnostic biomarkers in moderate and severe depressive disorder. *Psychol Res Behav Manag* 11: 495–502, 2018. doi: 10.2147/PRBM.S183126.
712. **Yamakoshi T, Park SB, Jang WC, Kim K, Yamakoshi Y, Hirose H.** Relationship between salivary Chromogranin-A and stress induced by simulated monotonous driving. *Med Biol Eng Comput* 47: 449–456, 2009. doi: 10.1007/s11517-009-0447-y.
713. **Yang C, Zhong X, Li L.** Recent advances in enrichment and separation strategies for mass spectrometry-based phosphoproteomics. *Electrophoresis* 35: 3148–2129, 2014. doi: 10.1002/elps.201400017.
714. **Yang HS, Cho IH, Wang Q, Park YD, Yang JM.** Serum proteomic analyses for probing C3 fragment protein. *Process Biochem* 51: 981–988, 2016. doi: 10.1016/j.procbio.2016.05.009.
715. **Yang Z, Harris LE, Palmer-Toy DE, Hancock WS.** Multilectin affinity chromatography for characterization of multiple glycoprotein biomarker candidates in serum from breast cancer patients. *Clin Chem* 52: 1897–1905, 2006. doi: 10.1373/clinchem.2005.065862.

716. **Yavuz H, Özden K, Kin EP, Denizli A.** Concanavalin A binding on PHEMA beads and their interactions with myeloma cells. *J Macromol Sci Part A Pure Appl Chem* 46: 163–169, 2009. doi: 10.1080/10601320802594774.
717. **Ye Z, Mao Y, Clausen H, Vakhrushev SY.** Glyco-DIA: a method for quantitative O-glycoproteomics with in silico-boosted glycopeptide libraries. *Nat Methods* 16: 902–910, 2019. doi: 10.1038/s41592-019-0504-x.
718. **Yen-Nicolaÿ S, Boursier C, Rio M, Lefeber DJ, Pilon A, Seta N, Bruneel A.** MALDI-TOF MS applied to apoC-III glycoforms of patients with congenital disorders affecting O-glycosylation: Comparison with two-dimensional electrophoresis. *Proteomics - Clin Appl* 9: 787–793, 2015. doi: 10.1002/prca.201400187.
719. **Yi S, Chen K, Zhang L, Shi W, Zhang Y, Niu S, Jia M, Cong B, Li Y.** Endoplasmic reticulum stress is involved in stress-induced hypothalamic neuronal injury in rats via the PERK-ATF4-CHOP and IRE1-ASK1-JNK pathways. *Front Cell Neurosci* 13: 1–13, 2019. doi: 10.3389/fncel.2019.00190.
720. **Yilmaz Y.** Serum proteomics for biomarker discovery in nonalcoholic fatty liver disease. *Clin Chim Acta* 413: 1190–1193, 2012. doi: 10.1016/j.cca.2012.04.019.
721. **Yoshida-Moriguchi T, Campbell KP.** Matriglycan: A novel polysaccharide that links dystroglycan to the basement membrane. *Glycobiology* 25: 702–713, 2014. doi: 10.1093/glycob/cwv021.
722. **Young FB, Butland SL, Sanders SS, Sutton LM, Hayden MR.** Putting proteins in their place: Palmitoylation in Huntington disease and other neuropsychiatric diseases. *Prog Neurobiol* 97: 220–238, 2012. doi: 10.1016/j.pneurobio.2011.11.002.
723. **Young WF.** Endocrine hypertension. In: *Williams Textbook of Endocrinology*. Elsevier Inc., p. 556–588.
724. **Yung HW, Zhao X, Glover L, Burrin C, Pang PC, Jones CJP, Gill C, Duhig K, Olovsson M, Chappell LC, Haslam SM, Dell A, Burton GJ, Charnock-Jones DS.** Perturbation of placental protein glycosylation by endoplasmic reticulum stress promotes maladaptation of maternal hepatic glucose metabolism. *iScience* 26: 105911, 2023. doi: 10.1016/j.isci.2022.105911.
725. **Zafir A, Banu N.** Modulation of in vivo oxidative status by exogenous corticosterone and restraint stress in rats. *Stress* 12: 167–177, 2009. doi: 10.1080/10253890802234168.

726. **Zallocco L, Giusti L, Ronci M, Mussini A, Trerotola M, Mazzoni MR, Lucacchini A, Sebastiani L.** Salivary proteome changes in response to acute psychological stress due to an oral exam simulation in university students: Effect of an olfactory stimulus. *Int J Mol Sci* 22: 1–22, 2021. doi: 10.3390/ijms22094295.
727. **Zhang AH, Sun H, Yan GL, Han Y, Wang XJ.** Serum proteomics in biomedical research: A systematic review. *Appl Biochem Biotechnol* 170: 774–786, 2013. doi: 10.1007/s12010-013-0238-7.
728. **Zhang Q, Raof M, Chen Y, Sumi Y, Sursal T, Junger W, Brohi K, Itagaki K, Hauser CJ.** Circulating mitochondrial DAMPs cause inflammatory responses to injury. *Nature* 464: 104–107, 2010. doi: 10.1038/nature08780.
729. **Zhang X, Wang BZ, Kim M, Nash TR, Liu B, Rao J, Lock R, Tamargo M, Soni RK, Belov J, Li E, Vunjak-Novakovic G, Fine B.** STK25 inhibits PKA signaling by phosphorylating PRKAR1A. *Cell Rep* 40: 1–27, 2022. doi: 10.1016/j.celrep.2022.111203.
730. **Zhang Y, Fonslow B, Shan B, Baek M, Yates J.** Protein analysis by shotgun/bottom-up proteomics. *Chem Rev* 113: 2343–2349, 2013. doi: 10.1021/cr3003533.
731. **Zhang Y, Liu W, Zhou Y, Ma C, Li S, Cong B.** Endoplasmic reticulum stress is involved in restraint stress-induced hippocampal apoptosis and cognitive impairments in rats. *Physiol Behav* 131: 41–48, 2014. doi: 10.1016/j.physbeh.2014.04.014.
732. **Zhao W, Chen Y, Yu H, Zhang H, Yu Z, Ding L, Liu J, Li J, Chen F.** The enrichment and characterization of ginger-derived glycoprotein using magnetic particles. *Food Chem* 244: 164–168, 2018. doi: 10.1016/j.foodchem.2017.10.038.
733. **Zhou J, Liu Z, Yu J, Han X, Fan S, Shao W, Chen J, Qiao R, Xie P.** Quantitative proteomic analysis reveals molecular adaptations in the hippocampal synaptic active zone of chronic mild stress-unsusceptible rats. *Int J Neuropsychopharmacol* 19: 1–19, 2016. doi: 10.1093/ijnp/pyv100.
734. **Zhou W, Ross MM, Tessitore A, Ornstein D, VanMeter A, Liotta LA, Petricoin EF.** An initial characterization of the serum phosphoproteome. *J Proteome Res* 8: 5523–5531, 2009. doi: 10.1021/pr900603n.
735. **Zhu G, Jin L, Sun W, Wang S, Liu N.** Proteomics of post-translational

- modifications in colorectal cancer: Discovery of new biomarkers. *Biochim Biophys Acta - Rev Cancer* 1877: 188735, 2022. doi: 10.1016/j.bbcan.2022.188735.
736. **Zhu R, Zacharias L, Wooding KM, Peng W, Mechref Y.** Glycoprotein enrichment analytical techniques: Advantages and disadvantages. *Methods Enzymol* 585: 397–429, 2017. doi: 10.1016/bs.mie.2016.11.009.
737. **Zhu X, Dong J, Xia Z, Zhang A, Chao J, Yao H.** Repeated restraint stress increases seizure susceptibility by activation of hippocampal endoplasmic reticulum stress. *Neurochem Int* 110: 25–37, 2017. doi: 10.1016/j.neuint.2017.09.002.
738. **Zilmer M, Edmondson AC, Khetarpal SA, Alesi V, Zaki MS, Rostasy K, Madsen CG, Lepri FR, Sinibaldi L, Cusmai R, Novelli A, Issa MY, Fenger CD, Jamra RA, Reutter H, Briuglia S, Agolini E, Hansen L, Petäjä-Repo UE, Hintze J, Raymond KM, Liedtke K, Stanley V, Musaev D, Gleeson JG, Vitali C, O'Brien WT, Gardella E, Rubboli G, Rader DJ, Schjoldager KT, Møller RS.** Novel congenital disorder of O-linked glycosylation caused by GALNT2 loss of function. *Brain* 143: 1114–1126, 2020. doi: 10.1093/brain/awaa063.
739. **Zubarev RA, Makarov A.** Orbitrap mass spectrometry. *Anal Chem* 85: 5288–5296, 2013. doi: 10.1021/ac4001223.

APPENDICES

APPENDIX A – CRS STUDY

The serum samples used to evaluate our glyco- and phosphoenrichment methods were taken from this rat stress study which formed part of a larger study. Another final year MSc student (Minette van Wyk) and I worked together on this for the duration of the stress run until euthanasia. The results below are a product of her own work for her thesis.

A1. Ethical approval letter



REC: Animal Care and Use

[Project Approval Letter](#)

Date: 19 November 2021

PI Name: Prof MF Essop

Protocol #: ACU-2021-19400

Title: The effects of chronic stress on cardiovascular, brain and metabolic function

Dear MF Essop ,

Your project application, was reviewed by the Research Ethics Committee: Animal Care and Use (**REC: ACU**) via committee review procedures and was approved. Please note that this clearance is only valid for a period of twelve months. Ethics approval of projects spanning more than one year must be renewed annually through submission of a progress report, up to a maximum of three years.

Approval Date: **19 November 2021 - 18 November 2022**

Animal Species: **Wistar Rats**

Animal Numbers: **120**

Applicants are reminded that they are expected to comply with accepted standards for the use of animals in research and teaching as reflected in the South African National Standards 10386: 2008. The SANS 10386: 2008 document is available on the Division for Research Developments website www.sun.ac.za/research.

As provided for in the Veterinary and Para-Veterinary Professions Act, 1982. It is the principal investigator's responsibility to ensure that all study participants are registered with or have been authorised by the South African Veterinary Council (SAVC) to perform the procedures on animals, or will be performing the procedures under the direct and continuous supervision of a SAVC-registered veterinary professional or SAVC-registered para-veterinary professional, who are acting within the scope of practice for their profession.

Please remember to use your protocol number 19400 on any documents or correspondence with the REC: ACU concerning your research protocol.

Please note that the REC: ACU has the prerogative and authority to ask further questions, seek additional information, require further modifications or monitor the conduct of your research.

Any event not consistent with routine expected outcomes that results in any unexpected animal welfare issue (death, disease, or prolonged distress) or human health risks (zoonotic disease or exposure, injuries) must be reported to the committee, by creating an Adverse Event submission within the system.

We wish you the best as you conduct your research.

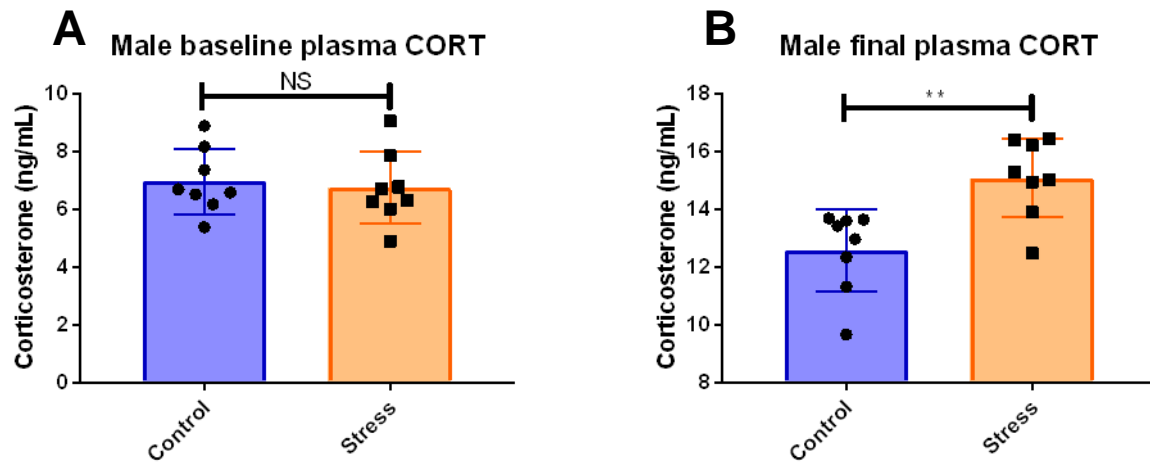
If you have any questions or need further help, please contact the ethics help-desk at applyethics@sun.ac.za or 021 808 9003. This committee is registered with the National Health Research Ethics Council of South Africa - registration number: **AREC-150211-007**.

Sincerely,

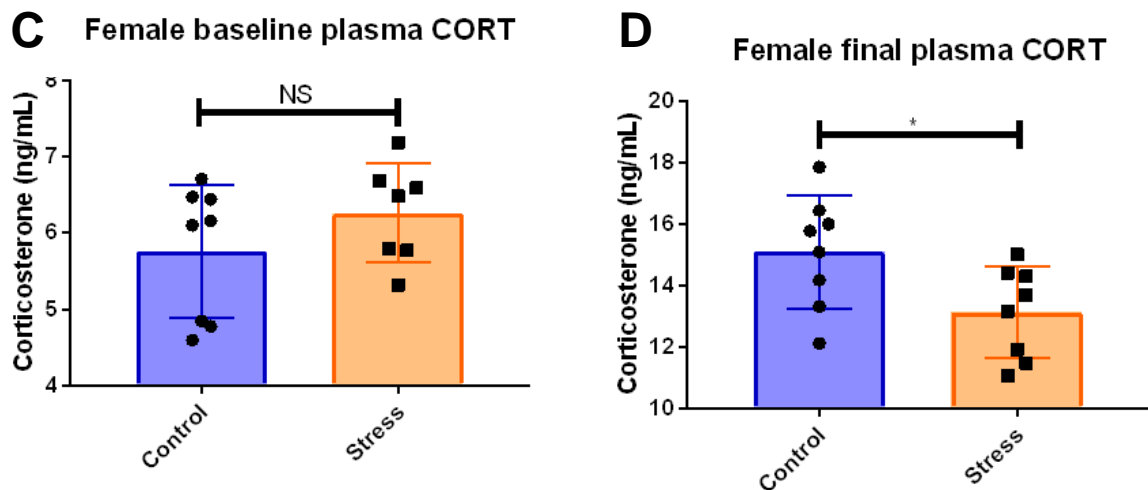
A handwritten signature in black ink, appearing to read 'WA Beukes'.

Mr. WA Beukes
Coordinator: Research Ethics (Animal Use and Biosafety)
E: wabeukes@sun.ac.za

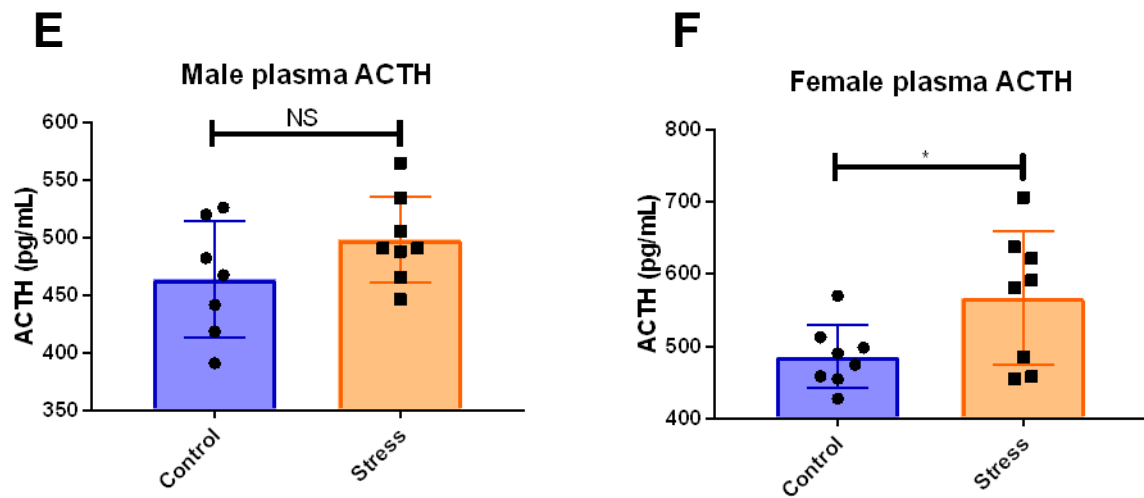
A2. Enzyme-linked immunosorbent assay results



Male plasma corticosterone levels at (a) baseline and (b) final. (a) There was no statistical significance between the experimental (stress) group (6.73 ± 1.24 ng/ml, $n=8$) and the control group (6.96 ± 1.12 ng/ml, $n=8$). (b) A statistical significance ($p<0.01$) was observed between the experimental (stress) group (15.08 ± 1.37 ng/ml, $n=8$) and the control group (12.58 ± 1.43 ng/ml, $n=8$). Analysis done by mixed model ANOVA in R; values represented as mean \pm SD.



Female plasma corticosterone levels at (c) baseline and (d) final. (a) The experimental (stress) group (6.25 ± 0.65 ng/ml, $n=7$) displayed no difference compared to the control group (5.76 ± 0.87 ng/ml, $n=8$). (b) The experimental (stress) group (13.13 ± 1.48 ng/ml, $n=8$) showed a significant difference ($p<0.05$) compared to the control group (15.09 ± 1.84 ng/ml, $n=8$). Analysis done by mixed model ANOVA in R; values represented as mean \pm SD.



(E) Male plasma ACTH levels. No statistical significance was observed between the experimental (stress) group (498.20 ± 37.32 pg/ml, $n=8$) and the control group (463.80 ± 50.41 pg/ml, $n=7$). **(F) Female plasma ACTH levels.** The experimental (stress) group (566.90 ± 91.80 pg/ml, $n=8$) showed a significant difference ($p<0.05$) compared to the control group (485.70 ± 43.36 pg/ml, $n=8$). Analysis done by two-way ANOVA; values represented as mean \pm SD.

APPENDIX B – PHOSPHOPROTEIN ENRICHMENT

This appendix contains all the protocols and protein determination results for phosphoprotein enrichment. The relevant product information can also be found here.

B1. Original Zr-IMAC protocol obtained from ReSyn Biosciences Ltd.

Recommended buffers

Loading Buffer: 0.1 M glycolic acid in 80% acetonitrile and 5% trifluoroacetic acid

Wash Buffer 1: 80% acetonitrile, 1% trifluoroacetic acid

Wash Buffer 2: 10% acetonitrile, 0.2% trifluoroacetic acid

Elution Buffer: 1% ammonium hydroxide

Thoroughly resuspend MagReSyn® Zr-IMAC HP by vortex mixing or inversion to ensure a homogenous suspension.

1.1 Particle equilibration

1. Transfer 100 µL (2 mg of beads, a 1:4 protein to bead ratio) MagReSyn® Zr-IMAC to a 2 mL micro-centrifuge tube.
2. Place the tube on a magnetic separator and allow 10 sec for the microparticles to clear.
3. Remove the shipping solution by aspiration with a pipette and discard.
4. Equilibrate the microparticles in 200 µL Loading Buffer, allow 60 sec for equilibration.
5. Place the tube on the magnetic separator and allow the microparticles to clear. Remove the loading buffer by aspiration with a pipette.
6. Repeat steps 5 and 6 twice for a total of three equilibrations.

1.2 Phosphopeptide enrichment procedure

7. Resuspend 500 µg de-salted protein digest in 200 µL loading buffer and mix by vortexing.
8. Centrifuge at 10,000 xg for 5 minutes at 4°C to remove any insoluble material.
9. Transfer supernatant to the equilibrated MagReSyn® Zr-IMAC microparticle pellet from particle equilibration.
10. Resuspend the microparticles in the peptide sample by vortexing or pipette aspiration.
11. Incubate for 20 min at room temperature with continuous mixing (e.g. slow vortexing) to ensure adequate sample and microparticle interaction.

12. Place the tube on the magnetic separator and allow the microparticles to clear. Remove and discard the coupling supernatant by aspiration with a pipette.
13. Remove unbound sample by washing with 100 μ L of loading buffer for 2 min with gentle agitation.
14. Place the tube on a magnetic separator and allow 10 sec for the microparticles to clear. Remove the supernatant and discard.
15. Remove non-specifically bound peptides by resuspending the microparticles in 100 μ L wash buffer 1 for 2 min with gentle agitation.
16. Place the tube on a magnetic separator and allow 10 sec for the microparticles to clear. Remove the supernatant and discard.
17. Perform an additional 2 min wash using 100 μ L of wash buffer 2.
18. Elute the bound phosphopeptides from the microparticles by adding 150 μ L elution buffer for 10 min. Ensure that the microparticles remain in suspension by constant gentle agitation during the elution step.
19. Place the tube on a magnetic separator and allow 5 to 10 sec to clear.
20. Transfer the supernatant (eluted phosphopeptides) to a 1.5 mL Protein LoBind tubes containing 50 μ L of 10% Formic Acid
21. Repeat elution steps 12 to 14 for improved recovery.
22. Pool eluates for a total of 400 μ L elution.
23. Lyophilize or vacuum dry eluates from frozen (samples frozen at -80°C for 30 minutes).
24. Analyze the sample by MS. Samples can be de-salted prior analysis using C18 SPE or in-line C18 trap cartridge used in a typical pre-concentrations LC-MS setup.

B2. Zr-IMAC protocol for unique phosphoprotein enrichment

Buffers for enrichment

Loading buffer: 0.1 M glycolic acid in 10 mM Ammonium acetate pH 7.4

Wash buffer 1: 10 mM ammonium acetate pH 7.4

Elution buffer: 10 mM EDTA pH 7.4 in deionized water

For every separation step, allow at least 10 seconds in the magnetic separator for microparticles to clear.

Particle equilibration

1. Resuspend Zr-IMAC beads by gently vortex mixing, remove 200 μ L (4 mg beads) and place into a new 2 mL tube.

2. Place on magnetic separator and remove shipping solution.
3. Equilibrate microparticles in 400 μ L of loading buffer for 1 minute.
4. Magnetically separate particles and remove buffer.
5. Wash twice with wash buffer to remove any unbound glycolic acid. The microparticles are now ready to be incubated with sample.

Before sample loading, measure the protein concentration to later determine how much protein was retrieved.

Serum phosphoprotein enrichment and elution procedure

6. Incubate equilibrated microparticles with serum samples with continuous rotational mixing/slow end-over-end mixing (60 rpm) for 3 hours at 4°C.
7. After incubation, place the tube on a magnetic separator, remove the supernatant and store this at -80°C for protein determination and SDS-PAGE analysis.
8. Wash for 2 minutes with 400 μ L wash buffer to remove any sample that may be left on the tube or within the porous microparticles. Repeat this step once more and store supernatants at -80°C for protein determination and SDS-PAGE analysis.
9. Elute the bound proteins by adding 400 μ L of elution buffer for 10 minutes. Gently agitate during this time.
10. Repeat the previous step twice more and pool eluates for a total of 1,2 mL.
11. Freezy dry all the samples intended for SDS-PAGE & staining/LC-MS analysis
12. After drying, proceed to relevant steps (SDS-PAGE and staining analysis – Appendix D / Protein digestion for LC-MS – Appendix E).

B3. TRIzol extraction protocol from Sigma-Aldrich

1. Lyse and homogenize samples in TRIzol™ Reagent according to your starting material.
 - b. Add 0.75 mL of TRIzol™ Reagent per 0.25 mL of sample (5–10 \times 10⁶ cells from animal, plant, or yeast origin or 1 \times 10⁸ cells of bacterial origin) to the pellet.
 - c. Pipet the lysate up and down several times to homogenize.
2. (*Optional*) If samples have a high fat content, centrifuge the lysate for 5 minutes at 12,000 \times g at 4–10°C, then transfer the clear supernatant to a new tube.

3. Incubate for 5 minutes to allow complete dissociation of the nucleoproteins complex.
4. Add 0.2 mL of chloroform per 1 mL of TRIzol™ Reagent used for lysis, securely cap the tube, then thoroughly mix by shaking.
5. Incubate for 2–3 minutes.
6. Centrifuge the sample for 15 minutes at 12,000 × *g* at 4°C. The mixture separates into a lower red phenol-chloroform, an interphase, and a colorless upper aqueous phase.
7. Transfer the aqueous phase containing the RNA to a new tube by angling the tube at 45° and pipetting the solution out.

Isolate RNA

a. (*Optional*) If the starting sample is small (<10⁶ cells or <10 mg of tissue), add 5–10 µg of RNase-free glycogen as a carrier to the aqueous phase.

Note: The glycogen is co-precipitated with the RNA, but does not interfere with subsequent applications.

- b. Add 0.5 mL of isopropanol to the aqueous phase, per 1 mL of TRIzol™ Reagent used for lysis.
- c. Incubate for 10 minutes at 4°C.
- d. Centrifuge for 10 minutes at 12,000 × *g* at 4°C.

Total RNA precipitate forms a white gel-like pellet at the bottom of the tube.

e. Discard the supernatant with a micropipettor.

Precipitate the RNA

a. Resuspend the pellet in 1 mL of 75% ethanol per 1 mL of TRIzol™ Reagent used for lysis.

Note: The RNA can be stored in 75% ethanol for at least 1 year at –20°C, or at least 1 week at 4°C.

- b. Vortex the sample briefly, then centrifuge for 5 minutes at 7500 × *g* at 4°C.
- c. Discard the supernatant with a micropipettor.
- d. Vacuum or air dry the RNA pellet for 5–10 minutes.

IMPORTANT! Do not dry the pellet by vacuum centrifuge. Do not let the RNA pellet dry, to ensure total solubilization of the RNA. Partially dissolved RNA samples have an A₂₃₀/A₂₈₀ ratio <1.6.

Wash the RNA

- a. Resuspend the pellet in 20–50 μL of RNase-free water, 0.1 mM EDTA, or 0.5% SDS solution by pipetting up and down. Do not dissolve the RNA in 0.5% SDS if the RNA is to be used in subsequent enzymatic reactions.
 - b. Incubate in a water bath or heat block set at 55–60°C for 10–15 minutes.
- Proceed to downstream applications, or store the RNA at –70°C.

Solubilize the RNA

- a. Resuspend the pellet in 20–50 μL of RNase-free water, 0.1 mM EDTA, or 0.5% SDS solution by pipetting up and down. Do not dissolve the RNA in 0.5% SDS if the RNA is to be used in subsequent enzymatic reactions.
- b. Incubate in a water bath or heat block set at 55–60°C for 10–15 minutes.
- c. Dilute sample in RNase-free water, then measure absorbance at 260 nm and 280 nm.

Isolate proteins

Isolate the proteins from the organic phase saved from “Isolate RNA” using either “Precipitate the proteins” or “Dialyse the proteins”

- a. Remove any remaining aqueous phase overlying the interphase.
- b. Add 0.3 mL of 100% ethanol per 1 mL of TRIzol™ Reagent used for lysis.
- c. Cap the tube, mix by inverting the tube several times.
- d. Incubate for 2–3 minutes.
- e. Centrifuge for 5 minutes at 2000 $\times g$ at 4°C to pellet the DNA.
- f. Transfer the phenol-ethanol supernatant to a new tube.
- g. Add 1.5 mL of isopropanol to the phenol-ethanol supernatant per 1 mL of TRIzol™ Reagent used for lysis.
- h. Incubate for 10 minutes.
- i. Centrifuge for 10 minutes at 12,000 $\times g$ at 4°C to pellet the proteins.
- j. Discard the supernatant with a micropipettor.

Precipitate the proteins

- a. Prepare a wash solution consisting of 0.3 M guanidine hydrochloride in 95% ethanol.
- b. Resuspend the pellet in 2 mL of wash solution per 1 mL of TRIzol™ Reagent used for lysis.
- c. Incubate for 20 minutes. Note: The proteins can be stored in wash solution for at least 1 month at 4°C or for at least 1 year at –20°C.

- d. Centrifuge for 5 minutes at $7500 \times g$ at 4°C .
- e. Discard the supernatant with a micropipettor.
- f. Repeat step 2b–step 2e twice.
- g. Add 2 mL of 100% ethanol, then mix by vortexing briefly.
- h. Incubate for 20 minutes.
- i. Centrifuge for 5 minutes at $7500 \times g$ at 4°C .
- j. Discard the supernatant with a micropipettor.
- k. Air dry the protein pellet for 5–10 minutes. Do not dry the pellet by vacuum centrifuge.

Wash the proteins

- a. Resuspend the pellet in 200 μL of 1% SDS by pipetting up and down.

Note: To ensure complete resuspension of the pellet, we recommend that you incubate the sample at 50°C in a water bath or heat block.

- b. Centrifuge for 10 minutes at $10,000 \times g$ at 4°C to remove insoluble materials.
- c. Transfer the supernatant to a new tube.

Measure protein concentration by Bradford assay (SDS concentration must be $<0.1\%$), then proceed directly to downstream applications, or store the sample at -20°C .

Isolate DNA

Isolate DNA from the interphase and the lower phenol-chloroform phase.

- a. Remove any remaining aqueous phase overlying the interphase. This is critical for the quality of the isolated DNA.
- b. Add 0.3 mL of 100% ethanol per 1 mL of TRIzol™ Reagent used for lysis.
- c. Cap the tube, mix by inverting the tube several times.
- d. Incubate for 2–3 minutes.
- e. Centrifuge for 5 minutes at $2000 \times g$ at 4°C to pellet the DNA.

f. Transfer the phenol-ethanol supernatant to a new tube. The supernatant is used for protein isolation [refer to *TRIzol™ Reagent User Guide* (Pub. No. MAN0001271)], if needed, and can be stored at -70°C for several months.

Precipitate the DNA

- a. Resuspend the pellet in 1 mL of 0.1 M sodium citrate in 10% ethanol, pH 8.5, per 1 mL of TRIzol™ Reagent used for lysis.
- b. Incubate for 30 minutes, mixing occasionally by gentle inversion. Note: The DNA can be stored in sodium citrate/ethanol for at least 2 hours.

- c. Centrifuge for 5 minutes at $2000 \times g$ at 4°C .
- d. Discard the supernatant with a micropipettor.
- e. Repeat step 2a–step 2d once. Note: Repeat step 2a–step 2d twice for large DNA pellets ($>200 \mu\text{g}$).
- f. Resuspend the pellet in 1.5–2 mL of 75% ethanol per 1 mL of TRIzol™ Reagent used for lysis.
- g. Incubate for 10–20 minutes, mixing occasionally by gentle inversion.
Note: The DNA can be stored in 75% ethanol at several months at 4°C .
- h. Centrifuge for 5 minutes at $2000 \times g$ at 4°C .
- i. Discard the supernatant with a micropipettor.
- j. Vacuum or air dry the DNA pellet for 5–10 minutes. Do not dry the pellet by vacuum centrifuge.

Wash the DNA

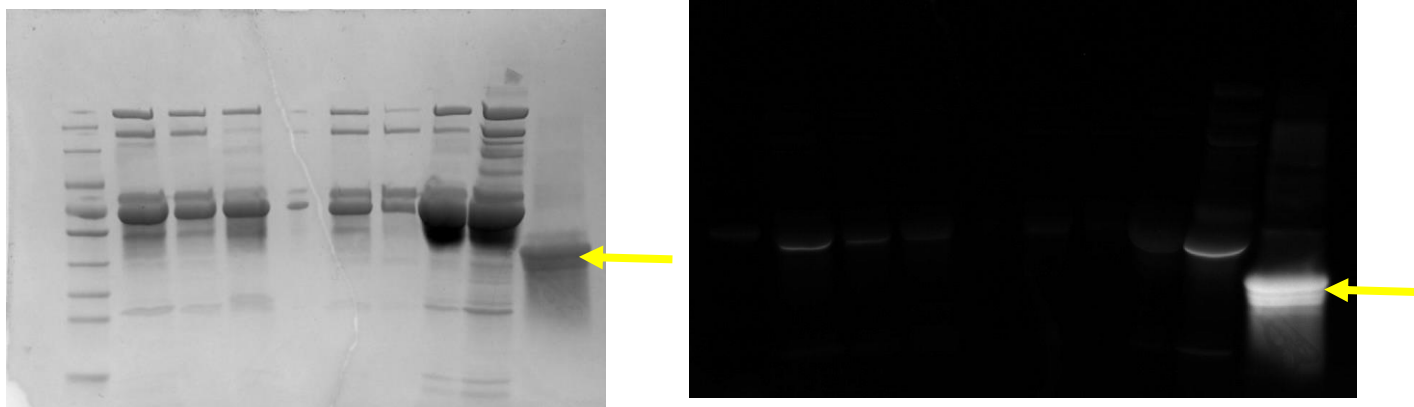
- a. Resuspend the pellet in 0.3–0.6 mL of 8 mM NaOH by pipetting up and down.
Note: We recommend resuspending the DNA in a mild base because isolated DNA does not resuspend well in water or Tris buffer.
- b. Centrifuge for 10 minutes at $12,000 \times g$ at 4°C to remove insoluble materials.
- c. Transfer the supernatant to a new tube, then adjust pH as needed with HEPES.
Proceed to downstream applications, or store the DNA at 4°C overnight. For longer-term storage at -20°C , adjust the pH to 7–8 with HEPES and add 1 mM EDTA.

Solubilize the DNA

- a. Resuspend the pellet in 0.3–0.6 mL of 8 mM NaOH by pipetting up and down.
Note: We recommend resuspending the DNA in a mild base because isolated DNA does not resuspend well in water or Tris buffer.
- b. Centrifuge for 10 minutes at $12,000 \times g$ at 4°C to remove insoluble materials.
- c. Transfer the supernatant to a new tube, then adjust pH as needed with HEPES.
Proceed to downstream applications, or store the DNA at 4°C overnight. For longer-term storage at -20°C , adjust the pH to 7–8 with HEPES and add 1 mM EDTA.
- d. Dilute sample in water or buffer (pH >7.5), then measure absorbance at 260 nm and 280 nm.

B4 Uncropped gel images in results section 2.4

Total protein image (left) and fluorescent image (right), arrow indicates lane for OVA.



B5 Protein determination results for OVA – starting amount = ~50 µg of protein.
 Here, all wash fractions (glycolic wash and unbound wash) were combined to form a single wash fraction.

BCA assay results for Zr beads (in relation to gel images in section 2.3)

Sample	Protein conc. (µg/mL)	Protein content (µg)
Zr-IMAC positive control unretained	488.12	19.52
Unbound fraction	90.51	3.62
Eluted fraction	1537.664362	61.51
Zr-IMAC negative control	0	0
Unbound fraction	0	0
Eluted fraction	954.88	38.2
Stripped beads unretained fraction	985.12	19.7
Unbound fraction	120.98	2.42
Eluted fraction	771.56	38.58

Bradford assay results

Sample	Protein conc. (µg/5µL)	Protein content (µg)
Zr-IMAC positive control unretained	5.73	22.92
Unbound fraction	3.1	18.59
Eluted fraction	0.85	10.26
Zr-IMAC negative control	5.83	23.34
Unbound fraction	0.49	2.92
Eluted fraction	2.91	34.87
Stripped beads unretained fraction	7.11	28.46
Unbound fraction	0.57	3.45
Eluted fraction	2.20	26.46

APPENDIX C – GLYCOPROTEIN ENRICHMENT

All the relevant protocols and protein determination results for glycoprotein enrichment can be found in this appendix. Any outstanding and relevant product information is also stated below.

C1. Original carboxyl bead protocol for ligand coupling, obtained from ReSyn Biosciences Ltd.

1.1 Microparticle equilibration

1. Resuspend MagReSyn® Carboxyl thoroughly by vortex mixing for 3 s to ensure a homogenous suspension.
2. Transfer 50 μ L (1 mg) MagReSyn® Carboxyl to a new tube. We recommend using a low-binding tube such as Eppendorf® Protein LoBind.
3. Place the tube on the magnetic separator and allow the microparticles to clear.
4. Remove the shipping solution by aspiration with a pipette and discard.
5. Wash/equilibrate the microparticles in 200 μ L of compatible buffer selected for ligand conjugation (e.g. activation buffer, 0.1 M MES section 2.3), allow 1 min for equilibration.
6. Place the tube on the magnetic separator and allow the microparticles to clear. Invert the magnet twice with the tube in place to collect any microparticles remaining in the cap.
7. Remove the binding buffer by aspiration with a pipette and repeat steps 5 and 6 twice for a total of three washes.
8. After removal of the buffer from step 6, MagReSyn® Carboxyl is ready to be functionalized for ligand binding.

1.2 Activation of carboxyl residues for coupling using EDC and NHS

9. Prepare sufficient activation solution for your immobilization requirements. Activation solution contains: 20 mM EDC and 50 mM NHS in a suitable buffer, e.g. 0.1 M MES, 0.5 M NaCl, pH 6.0. Example: Dissolve 28.8 mg of NHS and 19.1 mg of EDC in 5 mL of buffer. Ensure the EDC and NHS are completely dissolved before use.
10. Add 0.5 mL activation solution to the 1 mg equilibrated microparticles prepared according to 1.1.

11. Agitate microparticle suspension for 15 minutes at room temperature. We recommend slow end-over-end mixing.
12. Place the tube on the magnetic separator and allow the microparticles to clear. Aspirate the supernatant with a pipette and discard.
13. Wash the microparticles three times with 1 mL of immobilization-compatible buffer, e.g. PBS, pH 7. Allow 10 s for equilibration between each wash procedure.

1.3 Ligand coupling procedure

14. Prepare protein to be coupled in a suitable coupling buffer (free of primary amines, e.g. PBS, pH 7, and add to the microparticle suspension.
15. Agitate using end-over-end mixer or gentle vortexing for 2 – 24 hours at room temperature or at 4°C for temperature sensitive ligands.
16. Place the tube on the magnetic separator and allow the microparticles to clear.
17. Remove the unbound fraction by pipette aspiration and discard or keep for subsequent determination of coupling efficiency.
18. Wash twice with 200 µL coupling buffer only (equilibration for 1 min between washes). Aspirate and discard the wash fractions using a magnetic separator.
19. Add 500 µL of a suitable buffer comprising excess amine-containing blocking agent (e.g. 200 mM ethanolamine or aspartic acid in PBS, pH 7) and incubate for 3 h at room temperature (or 12+ hours at 4°C) to quench any remaining amine-reactive residues on the microparticles.
20. Apply magnetic separator and aspirate and discard excess quenching agent.
21. Optional: Wash three times with 500 µL suitable buffer solution containing 0.5 M – 1 M NaCl to remove possible noncovalently bound proteins and non-reactants. Apply a magnetic separator to recover microparticles and aspirate wash solutions.
22. Wash/equilibrate the microparticles containing your immobilized ligand in a suitable volume of buffer for your further applications or storage. The microparticles are now ready for your downstream experimentation.
23. Immobilized biologicals may be stored with suitable preservatives (e.g. sodium phosphate buffer containing 0.05% sodium azide) at 4°C. DO NOT FREEZE the microparticles.

C2 UNIQUELY DESIGNED AND OPTIMIZED PROTOCOL FOR SERUM GLYCOPROTEIN ENRICHMENT

The protocol can be altered for specific applications, such as changing the amount of microparticles and thereafter protein concentrations for coupling, as well as was and elution volumes based on amount of affinity material.

2.1 Solutions to be made

**Solutions for affinity material are to be freshly made on the day of lab work, with extra care taken regarding the transport and pH of buffers and solutions. Everything to be kept on ice.*

1L PBS – pH 7.4

0.1 M MES – pH 6

1 M NaCl

20 mM EDC & 50 mM NHS in 0.1 M MES - Activation solution

200 mM Ethanolamine in PBS

200 mM Glutamic acid in PBS

0.05% Sodium azide (w/v) in PBS – Storage buffer

ConA in PBS

10 mM MnCl₂

10 mM CaCl₂

100 mM Methyl α -D-mannopyranoside – Elution buffer

2.2 Microparticle equilibration

Allow a minimum of 10 s for magnetic separation

- 1) Resuspend carboxyl microparticles by thoroughly vortex mixing to ensure homogenous solution.
- 2) Transfer 200 μ L (4 mg) carboxyl microparticles to a new 2 mL tube.
- 3) Magnetically separate particles from initial solution and remove by aspiration.
- 4) Resuspend in 400 μ L 0.1 M MES and leave to equilibrate for 1 min.
- 5) Separate microparticles from the solution by magnetic separation.
- 6) Aspirate the washing solution and repeat steps 5 and 6 twice (total of 3 washes).

The beads are now equilibrated.

2.3. Microparticle activation and lectin binding

- 7) Ensure that EDC and NHS are completely dissolved in 0.1 M MES

- 8) Add 300 μL of prepared activation solution to the equilibrated microparticles and slowly mix microparticle suspension for 15 min at room temperature.
9. Separate microparticles from the solution by magnetic separation, aspirate supernatant and discard.
10. Wash microparticles three times with PBS (pH 7.4) allowing 10 seconds for equilibration between wash steps.
11. Immediately add 200 μL (250 mg) of prepared ConA solution to the microparticles, mix overnight at 4°C using a rotational mixer.
12. Separation particles by magnetic separation and remove the supernatant, However instead of discarding, place into separate tube for protein determination to establish coupling efficiency.
13. Wash twice with 400 μL PBS (pH 7.4) with 1 min equilibration between washes. Separate bound affinity material by magnet, aspirate and discard the supernatant.
14. Add 400 μL of 200 mM ethanolamine PBS, as prepared before) and incubate for 3 hours at 4°C to remove remaining amine-reactive residues.
15. Wash 3 times with 1M NaCl to remove non-covalently bound proteins and non-reactants. Magnetically separate bound affinity material and discard supernatant.
16. Wash and equilibrate bound affinity material in PBS (pH 7.4).

2.4 Protein incubation with the lectin-bound microparticles

Prepare a 50 μg OVA (diluted in PBS, 1 mM MnCl_2 , CaCl_2) or serum sample.

17. Add protein solution to affinity material and allow to gently mix at 4°C overnight.
18. Magnetically separate fractions and save supernatant for protein determination.
19. Wash once with 400 μL PBS to remove stuck proteins and save supernatant for analysis.
20. Elute bound proteins by adding 400 μL prepared 100 mM methyl α -D-mannopyranoside solution. Incubate for 10 minutes, thereafter magnetically separating fractions.
21. Perform step 21 twice more, for a total of 3 washes. Pool the eluates, freeze dry and store them at -80°C for SDS-PAGE and staining or deglycosylation.
22. Store the remaining affinity material in 400 μL of prepared storage buffer (0.05% sodium azide in PBS) at 4°C.

C3 SIGMA-ALDRICH'S DEGLYCOSYLATION PROTOCOL

A. Rapid Deglycosylation Procedure

1. Cool the TFMS and the anisole to 2–8 °C. Prepare a volume of a 10% anisole in TFMS solution sufficient for the number of reactions (150 µL per sample). For each sample add 15 µL of the pre-cooled anisole to 140 µL of the pre-cooled TFMS in an empty reaction vial.
2. Invert or gently shake to mix after securely closing the vial. Prepare in a chemical fume hood. Avoid exposure to atmospheric moisture. Cool the 10% anisole in TFMS solution to 2–8 °C. Note: One ampule of TFMS contains sufficient volume to analyze four x 1 mg samples of glycoprotein. Due to the hygroscopic nature of the reagents, it is recommended that any unused portion of either the anisole or TFMS should be disposed of properly.
3. Use one vial of the salt-free, lyophilized glycoprotein Standard (1 mg in a 2 mL screw-top glass vial) as a control. For each sample glycoprotein, lyophilize 1 mg of the sample in an empty reaction vial. Ensure that the sample and the vial are absolutely dry. Cool the sample reaction vial to 2°C – 8°C.
4. Add 150 µL of the pre-cooled 10% anisole in TFMS solution to the sample reaction vial and rapidly seal the vial tightly with the supplied cap. Note: A white vapor due to the TFMS forms in the vial. The vapor will dissipate in several minutes.
5. Gently shake the mixture for 2–5 minutes until completely dissolved.
Note: Do not vortex the mixture as the solution may foam, which could lead to protein degradation.
6. Incubate the sample reaction vial on ice or at 2°C–8°C for a further 3 hours with occasional shaking.
7. Cool the 60% pyridine solution and the sample reaction vial to approximately -15°C in a methanol-dry ice bath. Take appropriate precautions during the cooling of materials in the methanol-dry ice bath as the bath temperature is below -70°C. Occasional inversion or gentle shaking may be required to avoid solidification of the pyridine solution. Should the pyridine solution solidify, remove the vial from methanol-dry ice bath and warm gently until it is completely melted.
8. Add indicator dye along the inside wall of the pre-cooled sample reaction vial and gently shake to mix. The color of the solution should now turn red.

9. Immediately after adding the indicator dye, dropwise, add the pre-cooled 60% Pyridine Solution to the sample reaction vial, taking care to mix and cool the sample reaction vial between drops.
10. Note: The addition of the first drop of the 60% Pyridine Solution is highly exothermic and needs rapid cooling in the methanol-dry ice bath (-20°C to -15°C). With subsequent drops there is less needed to cool to these temperatures. It is recommended to use as low a temperature as possible without freezing the reaction mixture. It is essential that the reaction mixture be maintained in a liquid state at all times.
11. The color of the solution gradually changes from red to yellow as the pH is raised with the addition of the 60% Pyridine Solution.
12. After having added approximately an equal volume of the 60% Pyridine Solution (150 μL), a fine precipitate may develop in the reaction mixture. If a precipitate does form, add 20 μL of water and shake. The precipitate will soon dissolve.
13. Continue the addition of the 60% Pyridine Solution until the color of the solution changes to light purple or blue. The pH is now approximately 6. Routinely, a total of approximately 300 μL of the 60% Pyridine Solution is added to the 150 μL of TFMS, resulting in a final volume of less than 500 μL . Note: The entire process of neutralization should be carried out quickly, keeping the reaction mixture cold at all stages to minimize protein degradation.
14. The deglycosylated protein can now be purified for MS and/or SDS-PAGE analysis using a suitable desalting method.

C4 OPTIMIZED DEGLYCOSYLATION PROTOCOL FOR ENRICHED SERUM GLYCOPROTEINS

Solutions to be made

1 μL anisole in 2 μL of TFMS

60% pyridine

Methanol (34860, Sigma-Aldrich, St. Louis, MO, USA) - dry ice bath

Note: Always work on ice, with precooled vials and under a fume hood. Always wear the necessary personal protective equipment.

1. Prepare all solutions and holders for procedure under an operational fume hood,
2. For every sample that must be deglycosylated, add 2 μL of TFMS with 1 μL of anisole to a pre-cooled glass vial and gently mix.

3. Add up to 100 μL of protein sample to the acid mixture and incubate at 4°C for 3 hours with gentle agitation using an end-over-end mixer.
4. Prepare methanol dry ice bath prior to the end of the incubation period.
5. Using the bath, cool the 60% pyridine solution to $\sim -17^{\circ}\text{C}$. Prevent complete freezing.

NOTE: Next step is highly exothermic and dangerous!!

6. After the 3 hour incubation period, add 6 μL of the pyridine solution to the sample undergoing deglycosylation. Ensure that as soon as the pyridine mixture is added, the vial is placed upright (without its cap) in the dry ice bath with tweezers.
7. Remove the vial and immerse it again to ensure sufficient cooling as the reaction proceeds. Ensure that the mixture is not frozen as this will momentarily stop the reaction. Gently stir the vial during this time.
8. After 1 minute, add an equal amount of pyridine solution to ensure acid neutralization.
9. Add 50 μL of ultrapure water and transfer to a new 2 mL tube.
10. Centrifuge the tubes at $10\,000 \times g$ for 5 minutes.
11. Remove supernatants and place in new 2 mL tubes.
12. Vacuum dry the contents of the tubes for 3 hours.
13. Once dried, continue to SDS-PAGE analysis and staining or to digestion for LC-MS.

C5 PROTEIN DETERMINATION RESULTS OF CONA AND 50 μL SERUM ENRICHMENT FRACTIONS

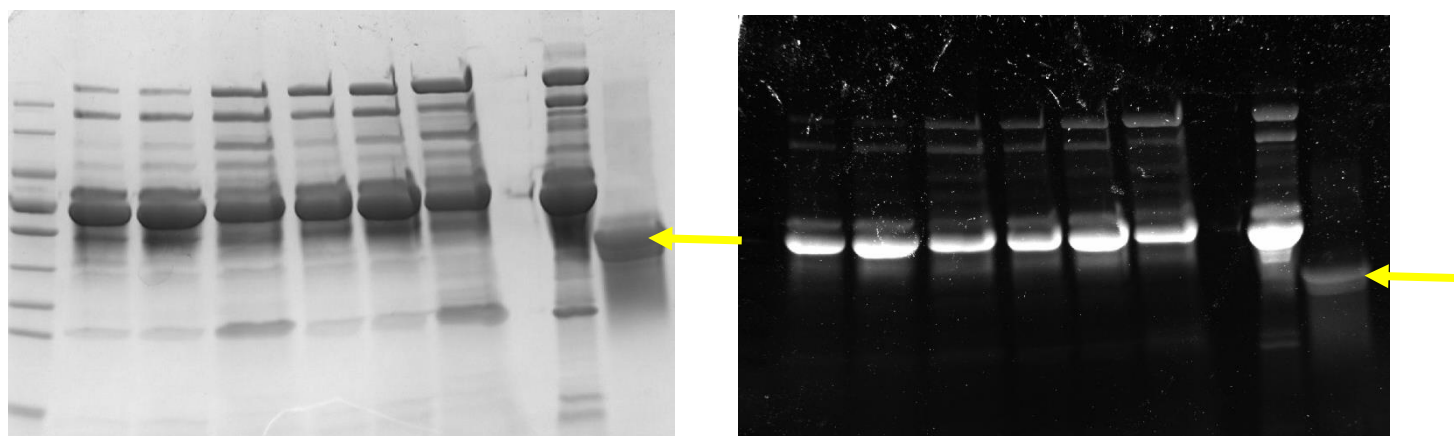
New 20 μL of affinity material	Protein concentration (mg/mL)
ConA unretained	6.301
ConA unretained	6.283
ConA unretained	6.289
Average	6.291
Lectin bound to the particles = $\sim 500 \mu\text{g}$ (originally loaded) – $315 \mu\text{g}$ = $\sim 185 \mu\text{g}$	

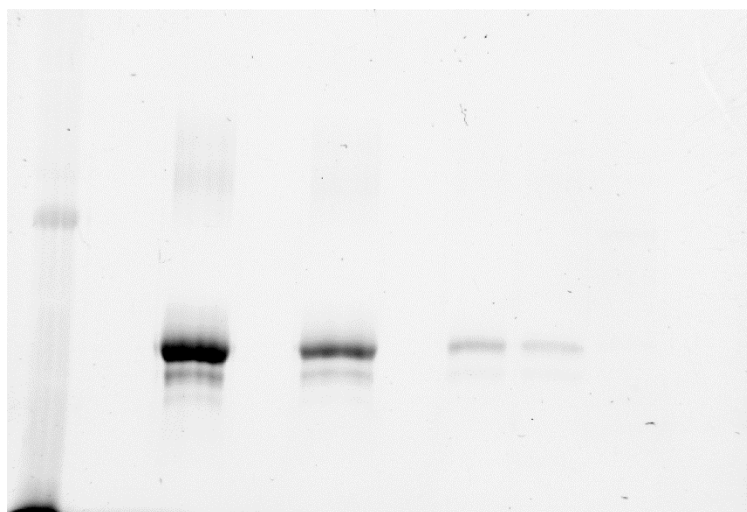
50 μ L of affinity material	Protein concentration (mg/mL)
ConA unretained	6.502
Unretained	6.707
Unretained	6.513
Average	6.574
Lectin bound to the particles = ~1 mg (originally loaded) – 657 μg = ~443 μg	
Unenriched serum	43.665
Unenriched	43.327
Unenriched	43.143
Average	43.378
Unretained	40.378
Unretained	40.256
Unretained	40.405
Average	40.346
Wash	2.583
Wash	2.647
Wash	2.631
Average	2.620
Bound to affinity material = 0.412 mg/mL = 0.95% of original sample	

*Of note, the serum sample elutes from the 50 μ L enrichment experiment were used to assess deglycosylation, therefore these results remain in this appendix.

C6 Uncropped gel images in results section 3.2

Total protein image (left) and fluorescent image (right), arrow indicates lane for OVA



Uncropped gel image in relation to section 3.4.2.3

C7 Protein determination results for OVA – starting amount = ~50 µg of protein.
BCA assay results for glyco affinity material and negative control (in relation to result section 3.4.1)

Sample	Protein conc. (µg/mL)	Protein content (µg)
Lectin affinity material unretained	813.35	32.53
Unbound fraction	989.16	39.57
Eluted fraction	1530.93	61.23
Carboxyl bead (negative control) unretained	95.52	1.91
Unbound fraction	120.98	2.42
Eluted fraction	19.70	19.7

Bradford assay results

Sample	Protein conc. (µg/5µL)	Protein content (µg)
Lectin affinity material unretained	0.02	0.13
Unbound fraction	1.23	9.85
Eluted fraction	2.7	21.6
Carboxyl bead (negative control) unretained	0.06	0.48
Unbound fraction	0.88	7.03
Eluted fraction	3.34	26.74

APPENDIX D - SDS-PAGE, FLUORESCENT STAINING AND PROTEIN DETERMINATION PROTOCOLS

D1 General SDS-PAGE protocol from Danzil Joseph (Department of Physiological Sciences, Stellenbosch University)

This protocol contains all the relevant steps and reagents which were not mentioned in the respective chapters.

Laemmli sample preparation

Stock solutions

1 M Tris (T1503, Sigma-Aldrich, St. Louis, MO, USA)-HCl (1021914, BDH Chemicals Ltd., Poole, England) pH 6.8 – 50 ml

Glycerol

10% (w/v) Sodium dodecyl sulphate (SDS) (75746, Sigma-Aldrich, St. Louis, MO, USA) – 50 ml 1% (w/v)

Bromophenol blue (BPB) – 10 ml

β -mercaptoethanol (BME) (M6250, Sigma-Aldrich, St. Louis, MO, USA)

2X Laemmli sample buffer	Conc. (2X)	Conc. (final)
Tris-HCl, pH 6.8	125 mM	62.5 mM
SDS	4% (w/v)	2% (w/v)
Glycerol	20% (v/v)	10% (v/v)
BPB	0.01% (w/v)	0.005% (w/v)
BME	10% (v/v)	5% (v/v)

All components should be added except BME which degrades in solution. Make up 2X Laemmli stock to a total of 9 ml (excl. BME), aliquot in 0.9 ml portions and add BME to 10% conc. on the day of use.

Method:

1. Set the heating block (Labnet International, Inc., Edison, NJ, USA) to 95°C
2. Make up a working solution of sample buffer by adding β -mercaptoethanol to a final concentration of 10% (v/v) to 2X Laemmli buffer stock solution (see table above) (work in fume cabinet), vortex thoroughly
3. Calculate the appropriate volume of each sample to give equal protein amounts (e.g. 50 μ g or 20 μ g per sample) and calculate the number of sample sets needed
4. Label microcentrifuge tubes for each sample and sample set

5. Add the appropriate volume of protein sample to each tube (as calculated in step 3). Sample volumes can be equalized by addition RIPA buffer (keep samples on ice)
6. Add a volume of working sample buffer that would result in a 1:1 dilution with the protein sample prepared in step 5 to each appropriate tube (work in fume cabinet)
7. Aim to prepare multiple aliquots of each sample, depending on how many times the blots will be repeated (usually 4 to 5 aliquots are enough)
8. Punch small holes in the lid of each tube using the sharp tweezers
9. Heat samples on the heating block (95°C) for 5 min
10. Vortex each tube briefly, spin down contents briefly (~10 seconds) and place on ice immediately
11. Samples can now be applied to gels for SDS-PAGE or stored at -20°C for future use

Sodium dodecyl sulphate-polyacrylamide gel electrophoresis (SDS-PAGE)

Solutions needed

40% Acrylamide solution (01709, Sigma-Aldrich, St. Louis, MO, USA) (biohazard – see MSDS)

1.5 M Tris-HCl, pH 8.8 – 100 ml

0.5 M Tris-HCl, pH 6.8 – 100 ml

10% (w/v) SDS – 50 ml

10% (w/v) Ammonium persulphate (APS) (A3678, Sigma-Aldrich, St. Louis, MO, USA) – 1 ml

Trichloroethanol (TCE) (T54801, Sigma-Aldrich, St. Louis, MO, USA)

TEMED (T9281, Sigma-Aldrich, St. Louis, MO, USA)

10X Tris-Glycine-SDS (TGS) running buffer (Bio-Rad) (1610772, Bio-Rad Laboratories Inc., Hercules, CA, USA)

Materials

Mini gel short plates and spacer plates

Combs (same thickness as spacer plates)

Gel casting stands and rubber gaskets

Green gel assembly frames

Small glass beakers or Erlenmeyer flasks dH₂O in glass beaker

Ethanol

Disposable plastic Pasteur pipettes

Gel tanks and lids

Powerpacks

Method:

1. Clean pairs of spacer plates and short plates, assembly frames, casting stands and rubber gaskets
2. Place gaskets in grooves at the base of the casting stands
3. Assemble glass plates in green casting frames with the short plates facing to the front – push the clips outward to tighten the assembly and secure plates
4. Place the plate assembly onto the rubber gasket in the base of the casting stand, pushing down firmly while securing the clip
5. Add dH₂O between the plates to check for leakage
6. Get three small beakers and three disposable Pasteur pipettes
7. Label one beaker and add dH₂O to it, and label the other two beakers for the resolving and stacking gel, respectively
8. Make up the required resolving gel according to the appropriate recipe (10% relevant in this case):

Gel constituent	10%
dH ₂ O	7.125
40% Acrylamide solution	3.75
1.5 M Tris-HCl, pH 8.8	3.75
10% (w/v) SDS	0.150
TCE	0.075
10% (w/v) APS	0.150
TEMED	0.006

*Gel recipes are for 2 x 1 mm gels; values represent milliliter solution to be added to gel mixture

9. Add all constituents except the APS and TEMED, swirl briefly and let solution stand for a few minutes to degas
10. Add APS and swirl briefly

11. Add TEMED, swirl briefly and quickly pour the gel mixture between the plates using a plastic Pasteur pipette – be sure to avoid bubbles in the gel and leave enough space for the stacking gel (this can be checked beforehand by inserting a comb and marking the position)
12. Add a layer of ethanol on top of the gel to prevent oxidation and bubbles, and to leave a smooth top surface
13. Allow gel to set for 45 min to 1 hour
14. While waiting, start preparing 1X working dilutions of TGS running buffer (from 10X stock) as well as the TBS-T (from 10X TBS), blocking buffer and Transblot Turbo transfer buffer (from 5X stock, according to the Bio-Rad Transblot Turbo transfer kit instructions) (see step 1 under Section G – Transblot Turbo semi-dry transfer below for preparation of TBS-T, blocking buffer and transfer buffer)
15. Once the resolving gel is set, start preparing the stacking gel:
16. 4% stacking gel recipe (for 2 X 1 mm gels):

Gel constituent	Volume (mL)
dH ₂ O	4.84
40% Acrylamide solution	1.0
0.5 M Tris-HCl, pH 6.8	2.0
10% (w/v) SDS	0.08
10% (w/v) APS	0.08
TEMED	0.008

Note: Different Tris-HCl buffers are used for stacking and resolving gels respectively

17. Add all constituents except APS and TEMED, gently swirl and let stand for a few minutes
18. Once resolving gel has set, remove ethanol layer and wash top of gel, use paper towel to draw out all liquid
19. Add APS to the stacking gel solution and gently swirl
20. Add TEMED to the stacking gel solution and gently swirl
21. Quickly pour the stacking gel mixture between the plates to the top of the short plate using a disposable plastic Pasteur pipette
22. Gently insert appropriate combs, pushing down and avoiding bubble formation (make sure combs correspond to gel thickness)
23. Allow to set for ~30 minutes
24. Retrieve standard protein marker from freezer and allow it to equilibrate to room temp

25. Use unstained protein marker in order visualize MW standards using the stain-free setting once gels are activated on the Chemidoc
26. Retrieve samples from freezer (if previously stored) and thaw on ice
27. Boil samples at 95°C for 5 min, allow it to equilibrate to room temp and place on ice
28. Vortex each sample and spin down momentarily (~10 seconds)
29. Carefully remove combs from gels and gently wash wells with dH₂O
30. Remove plates from the casting stands and frames, and place in the U-shaped adaptor with the short plates facing inward
31. Insert assembly into the loading system and close the latches by pushing them inward while pushing down on the plates (the center will now form the buffer dam)
32. Fill the buffer dam with 1X running buffer until the buffer spills into the wells
33. Add 7.5 µl of the protein marker to the first lane on the far left of each gel
34. Add blue samples to the appropriate lane – use a micropipette and loading tips to apply the marker and samples
35. After loading of the gels, place the assembly inside a gel tank, fill the buffer dam to the top and add extra buffer into the tank – fill the tank to approximately 1 cm below the wells
36. Place the green lid with appropriate leads (black-to-black and red-to-red) on top of the tank and connect to the powerpack Switch on the powerpack and perform an initial 10 min run at 100 V (constant) and 400 mA – this run will cause the samples to migrate through the stacking gel
37. Next, run the gels at 120 – 200 V until the sample dye front and smallest standard of the protein marker reaches the bottom of the gel – approximately 1 hour (running times may be adjusted according the specific protein of interest)
38. Before gel electrophoresis is completed (~15 min prior), start preparing for the electrotransfer by getting low fluorescence PVDF membranes and transfer stacks ready for assembly in the Transblot turbo (see step 2 under Section G: Transblot Turbo semi-dry transfer below)
39. Switch off power and disconnect electrodes before removing gel plates from the tank and assembly
40. Do not allow gels to stand at this point as proteins may dissolve from gels – move to gel activation and electrotransfer step immediately

41. Activate/Image stain free gels by gently removing it from the glass plates and placing it on the UV transilluminator tray inside the Chemidoc (use a little dH₂O to pre-wet the tray surface).

42. Choose the following settings:

- Click to open Image Lab software → New single channel → Application select → Protein gels → Stain free gels → Choose gel activation setting (2 min works well) → Select image area → Bio-Rad Mini-Protean gel → Select image exposure → intense/feint/manual exposure → Click yellow “Position gel” button on the left → make sure gel is in the center → click green “Run protocol” button → Save the image.

D2 Pro-Q® Diamond Phosphoprotein Gel Stain protocol

	Reagent	Standard Protocol for Tris-glycine gels
Step 1: Fix	50% methanol (34860, Sigma-Aldrich, St. Louis, MO, USA), 10% acetic acid (10001, BDH Chemicals Ltd., Poole, England)	100 mL, 30 min 2 times
Step 2: Wash	Ultrapure water	100 mL, 10 min 3 times
Step 3: Stain	Pro-Q® Diamond stain	60 mL, 60–90 min
Step 4: Destain	20% acetonitrile (75-05-8, Merck®, Darmstadt, Germany), 50 mM sodium acetate (S-8625, Sigma-Aldrich, St. Louis, MO, USA), pH 4	80–100 mL, 30 min 3 times
Step 5: Wash	Ultrapure water	100 mL, 5 min 2 times
Total solution changes		11
Total time		4.25–4.75 hr

Imaging gel

Pro-Q® Diamond phosphoprotein stain has an excitation maximum at ~555 nm and an emission maximum at ~580 nm (Figure 3). Imaging instruments with light sources and filters that match the excitation and emission maxima result in the highest sensitivity

D3 Pro-Q® Emerald 300 Glycoprotein Gel and Blot Stain Kit protocol

Staining Procedure

The following procedure is optimized for staining 8 cm × 10 cm minigels (0.5–1.0 mm thick) or 8 cm × 10 cm blots. Large 2-D gels (20 cm × 20 cm) require proportionally larger volumes and longer fixation and staining times, as indicated.

1. Perform SDS-PAGE. Separate proteins by standard SDS polyacrylamide gel electrophoresis. Typically, the sample is diluted to about 10–100 µg/mL with sample buffer and 5–10 µL of diluted sample is added per lane for an 8 cm × 10 cm gel. Larger gels require more material.
2. Blot the proteins (optional). Transfer the proteins to a PVDF membrane using standard electroblotting procedures. Note that blotting is not necessary for staining glycoproteins with Pro-Q® Emerald 300 stain; in fact, the stain has somewhat lower sensitivity on blots compared to gels.
3. Fix the gel or blot. Immerse the gel in ~100 mL (~25 mL for blots) of Fix Solution and incubate at room temperature with gentle agitation (e.g., on an orbital shaker at 50 rpm) for 45 minutes. Repeat this fixation step to ensure the SDS is fully washed out of the gel or blot. For large 2-D gels, use two 1 L volumes of Fix Solution and incubate several hours at room temperature including one overnight incubation.
4. Wash. Incubate the gel or blot in ~100 mL (~50 mL for blots or ~1 L for large 2-D gels) of Wash Solution (made in step 1.3) with gentle agitation for 10–20 minutes. Repeat this step once.
5. Oxidize the carbohydrates. Incubate the gel or blot in 25 mL of Oxidizing Solution (made in step 1.4) with gentle agitation for 30 minutes. Large 2-D gels require 500 mL of Oxidizing Solution and should be incubated for 1 hour. (The 250 mL volume of oxidizing solution from step 1.4 can be diluted with 250 mL of 3% acetic acid in order to have an adequate volume for large 2-D gels.)

6. Wash. Incubate the gel or blot in ~100 mL (~50 mL for blots and ~1 L for large 2-D gels) of Wash Solution with gentle agitation for 10–20 minutes. Repeat this step twice more (three times more for large 2-D gels).
7. Prepare fresh Pro-Q® Emerald 300 Staining Solution. Dilute the Pro-Q® Emerald 300 stock solution (made in step 1.1) 50-fold into Pro-Q® Emerald 300 staining buffer. For example, dilute 500 µL of the Pro-Q® Emerald 300 stock solution into 25 mL of staining buffer to make enough staining solution for one 8 cm × 10 cm gel or blot. Large 2-D gels require 250 mL of staining solution.
8. Stain the gel or blot. Incubate the gel or blot in the dark in 25 mL (250 mL for large 2-D gels) of Pro-Q® Emerald 300 Staining Solution (prepared in step 2.7) while gently agitating for 90–120 minutes (2.5 hours for large 2-D gels). The signal can be seen after about 20 minutes and maximum sensitivity is reached at about 120 minutes. Do not stain overnight.
9. Wash. Incubate the gel or blot in ~100 mL (~50 mL for blots or ~1 L for large 2-D gels) of Wash Solution at room temperature for 15-20 minutes. Repeat this wash once for a total of two washes. Do not leave the gel or blot in Wash Solution for more than 2 hours, as the staining will start to decrease. If, upon imaging, the gel background is unacceptably high, then wash the gel a third time

Viewing and Photographing the Gel or Blot

The Pro-Q® Emerald 300 stain has an excitation maximum at ~280 nm and an emission maximum at ~530 nm (Figure 2). Stained gels can be visualized using a 300 nm UV transilluminator. Stained blots are optimally visualized by illuminating the front face using a hand-held UV-B (~300 nm) light source or a top-illuminating imaging system, such as the BioRad Fluor-S™ imager. Alternatively, a UV light box can be placed on its side to illuminate the blot. The use of a photographic camera or CCD camera and the appropriate filters is essential to obtain the greatest sensitivity. The instrument's integrating capability can make bands visible that cannot be detected by eye.

D4 Tricine-SDS-PAGE protocol

Tricine SDS-PAGE components

1. 2.5 M Tris-HCl buffer, pH 8.8 for modified and pH 8.45 for original system (see Notes 1 and 2): Weigh 302.85 g of Tris base and transfer it to a 1-L graduated cylinder or glass beaker. Dissolve the base by adding 600 mL of deionized water and adjust the pH using HCl. Make up to 1 L with water. This gel buffer can be stored at 4–8°C.
2. Polyacrylamide gel solution: 30% (w/v) solution of acrylamide:bis-acrylamide 29:1. Store this polyacrylamide solution at 4–8°C. (It is highly recommended to purchase the ready-made polymer solution from the suppliers instead of preparing it in the laboratory because acrylamide is recognized as a neurotoxin and suspected carcinogen.)
3. Running buffer for modified system: 25 mM Tris, 25 mM tricine, 0.05% (w/v) SDS. Dissolve 3.03 g Tris base, 4.5 g tricine and 0.5 g SDS in 1 L of deionized water (see Note 3). There is no need to adjust the pH. Store at 4–8°C (see Note 4).
4. Running buffer for original system: 100 mM Tris, 100 mM Tricine 0.1% (w/v) SDS. Weigh 12.1 g Tris base, 17.9 g tricine and 1 g SDS and dissolve in 1 L of deionized water (see Notes 3– 5). There is no need to adjust the pH. Store at 4–8°C (see Note 4).
5. Sample or loading buffer: 2x sample buffer containing 100 mM Tris–HCl (pH 6.8) (see Note 6), 1% (w/v) SDS, 4% (v/v) 2-mercaptoethanol, 0.02% (w/v) Coomassie Brilliant Blue (CBB) and 24% (w/v) glycerol. Store at –20°C (see Note 4).
6. Ammonium persulphate (APS) solution: Weigh 0.03 g of APS and dissolve in 1 mL of deionized water (see Note 7).
7. *N*, *N*, *N*′, *N*′-tetramethylethylenediamine (TEMED) (see Note 8).
8. CBB staining solution: Dissolve 0.025–0.030 g of CBB in 100 mL of 10% (v/v) acetic acid solution (see Note 9).
9. Acetic acid (10% v/v) destaining solution: Prepare 100 mL of 10% (v/v) acetic acid solution (see Note 9).
10. Glutaraldehyde (5% v/v) fixing solution: Prepare 5% glutaraldehyde solution by diluting five times the 25% (v/v) glutaraldehyde stock solution (50% stock in our case). Both stock and diluted solutions should be stored at –20°C (see Note 4).

Gel casting – for 1 gel

Gel constituent (resolving gel) – 16%	Volume (mL)
dH ₂ O	0.22
Acrylamide/bis-acrylamide 29:1 30% (w/v) solution (mL)	5.33
2.5 M Tris-HCl, pH 8.8	4.3
APS (30mg/mL)	0.100
TEMED	0.005
Gel constituent (stacking gel) – 4%	Volume (mL)
dH ₂ O	3.42
Acrylamide/bis-acrylamide 29:1 30% (w/v) solution (mL)	0.66
2.5 M Tris-HCl, pH 8.8	0.76
APS (30mg/mL)	0.150
TEMED	0.005

1. Prepare all stacking 4% (w/v) and resolving gel mixtures for 7, 9, and 10% (w/v) gels (16% in our case) for both the original and modified methods as shown in Table 2 (see Notes 12– 14).
2. Cast all the gels in gel cassettes at 7.3-cm height, 8-cm width and 0.75-mm thickness using a mini-gel casting apparatus (Bio-Rad, Hemel Hempstead, UK) (see Notes 15 and 16).
3. Firstly, inject the resolving gel mixture into the gel cassette (see Notes 17 and 18).
4. Do not fill the resolving gel mixture to the top of the gel plates. Leave a space of approximately 1–2 cm from the top. Quickly fill this space with butanol or 70% ethanol (see Notes 19 and 20).
5. The resolving gel usually takes 10–15 min for polymerization. Check for polymerization of the gel in the centrifuge tube and if the gel has been polymerized then pour off the butanol (or 70% ethanol) from the top of the resolving gel. Start injecting the stacking gel mixture onto the polymerized resolving gel in the gel cassette and fill up to the top of the short plates and then quickly insert the gel combs for the loading wells. Check the polymerization of the stacking gel in the centrifuge tube, or by just slightly lifting the combs, and if the stacking gel is polymerized, then remove the gel cassette sandwich from gel casting frame and set this into the electrode assembly. The short plates must be pointing inward in the dual plate electrode assembly

Sample loading and gel running

1. Mix 10 μ L of the sample buffer with 10 μ L of the digest mixture and heat at 70°C for 5–10 minutes. Dilute 20-fold the protein mass ladder (b) with the 1 \times sample buffer and heat at 65°C for 2 minutes (see Note 21).

2. Place the electrode assembly containing the two gel cassettes in the running buffer tank.
3. Fill the tank with the running buffer and gently remove the combs. Wash the loading wells with the running buffer using 1 mL pipette tips to remove any un-polymerized acrylamide.
4. Load protein mass ladder and other samples
5. Apply a constant voltage of 125V –150 V. Do not stop until the dye front touches the bottom (see Note 23).

Gel fixing, staining and destaining

1. Fix the gels for 25 min (using a shaker) with the fixing solution of 5% (v/v) glutaraldehyde.
2. Stain each gel for 20 min (using a shaker) using CBB staining solution. *please note that we used or Abcam Coomassie stain, and no destaining was required after this. Gels were visualized for total protein as stated previously in Chapter 2.

D5 General Bradford protein determination protocol from Dr. Danzil Joseph (Department of Physiological Sciences, Stellenbosch University)

5X Bradford stock solution: Dilute 500 mg Coomassie Brilliant Blue G250 in 250 mL 95% ethanol, Add 500 mL phosphoric acid, mix thoroughly, adjust volume to 1L with dH₂O, filter solution and store at 4°C.

Bradford working solution: Dilute stock in a 1:5 ratio with dH₂O, filter with 2 filter papers.

Materials and solutions: 1 mg/ml bovine serum albumin (BSA) stock solution (stored in freezer, thaw before starting), microcentrifuge tubes (7 for standards, 1 for each sample) dH₂O in a glass beaker, ice, Bradford working reagent, cuvettes, spectrophotometer

Method

1. Thaw the 1 mg/ml BSA stock solution on ice
2. Thaw protein samples on ice if stored – keep on ice at all times
3. Make up a 200 µg/ml BSA working solution by diluting the 1 mg/ml BSA stock 1:4 in dH₂O, vortex thoroughly
4. Mark tubes – 7 for standards (see table below) and 1 each for samples
5. Add BSA and dH₂O to standard tubes as indicated in the table below:

Protein standard (μg protein)	BSA (μL)	dH ₂ O (μL)
Blank (0)	0	100
2	10	90
4	20	80
8	40	60
12	60	40
16	80	20
20	100	0

6. Add 95 μL dH₂O and 5 μL of each protein sample (cell or tissue lysate) to the appropriate tube
7. Vortex all tubes briefly
8. Add 900 μL Bradford working solution to each tube, vortex again
9. Incubate the tubes for at least 5 min at room temp. (*the reaction takes about two minutes to complete and is stable for up to 60 min*)
10. In the meantime, switch on the spectrophotometer, allow it to calibrate, and set the wavelength to 595 nm
11. Read absorbances, twice each, for each tube. Record readings for each standard and sample.
12. If sample values fall outside the range of the highest protein standard, dilute with RIPA buffer and repeat (remember to factor in the dilution if samples are prepared using the original stock lysate)
13. Use Excel to draw a linear plot of standard absorbances, and calculate the protein concentration in each sample by determining the best fit from the equation $y = mx + c$ (y = absorbance; x = protein concentration) in order to make aliquots of equal protein amounts (in μg) to be used for Western blotting

D6 Thermo Fisher Scientific BCA assay kit manual

Preparation of diluted albumin standards

Vial	Volume of Diluent (μL)	Volume and source of BSA (μL)	Final BSA conc ($\mu\text{g}/\text{mL}$)
A	0	300 of stock	2000
B	125	375 of stock	1500
C	325	325 of stock	1000
D	175	175 of vial B dilution	750
E	325	325 of vial C dilution	500
F	325	325 of vial E dilution	250
G	325	325 of vial F dilution	125
H	400	100 of vial G dilution	25
I	400	0	0 = blank

Preparation of the BCA working reagent (WR)

1. Use the following formula to determine the total volume of WR required:

$(\# \text{ standards} + \# \text{ unknowns}) \times (\# \text{ replicates}) \times (\text{volume of WR per sample}) = \text{total volume WR required}$

Example: for the standard test-tube procedure with 3 unknowns and 2 replicates of each sample: $(9 \text{ standards} + 3 \text{ unknowns}) \times (2 \text{ replicates}) \times (2 \text{ mL}) = 48 \text{ mL WR}$ required Note: 2.0 mL of the WR is required for each sample in the test-tube procedure, while only 200 μL of WR reagent is required for each sample in the microplate procedure.

2. Prepare WR by mixing 50 parts of BCA Reagent A with 1 part of BCA Reagent B (50:1, Reagent A:B). For the above example, combine 50 mL of Reagent A with 1 mL of Reagent B. Note: When Reagent B is first added to Reagent A, turbidity is observed that quickly disappears upon mixing to yield a clear, green WR. Prepare sufficient volume of WR based on the number of samples to be assayed. The WR is stable for several days when stored in a closed container at room temperature (RT).

Microplate procedure (sample to WR ratio = 1:8)

1. Pipette 25 μL of each standard or unknown sample replicate into a microplate well (working range = 20–2000 $\mu\text{g/mL}$). Note: If sample size is limited, 10 μL of each unknown sample and standard can be used (sample to WR ratio = 1:20). However, the working range of the assay in this case is limited to 125–2000 $\mu\text{g/mL}$. – this is the amount we used as our sample size was limited.

2. Add 200 μL of the WR to each well and mix plate thoroughly on a plate shaker for 30 seconds.

3. Cover plate and incubate at 37°C for 30 minutes.

4. Cool plate to RT. Measure the absorbance at or near 562 nm on a plate reader.

Note:

- Wavelengths from 540–590 nm have been used successfully with this method.
- Because plate readers use a shorter light path length than cuvette spectrophotometers, the Microplate Procedure requires a greater sample to WR ratio to obtain the same sensitivity as the standard Test Tube Procedure. If higher 562 nm measurements are desired, increase the incubation time to 2 hours.
- Increasing the incubation time or ratio of sample volume to WR increases the net 562 nm measurement for each well and lowers both the minimum detection level of

the reagent and the working range of the assay. As long as all standards and unknowns are treated identically, such modifications may be useful.

5. Subtract the average 562 nm absorbance measurement of the Blank standard replicates from the 562 nm measurements of all other individual standard and unknown sample replicates.

6. Prepare a standard curve by plotting the average Blank–corrected 562 nm measurement for each BSA standard vs. its concentration in $\mu\text{g/mL}$.

Use the standard curve to determine the protein concentration of each unknown sample.

APPENDIX E – HILIC DIGESTION AND LC-MS SETTINGS

E1 HILIC Plasma clean up protocol

PLASMA LYSIS & SOLUBILIZATION:

1. Dilute 5-20 μL plasma 25-fold with 2% SDS in 50 mM Tris-HCl pH 8
NOTE: abundant protein depletion and/or SAX based protein fractionation was performed do not dilute the sample further but proceed from step 2. below
2. Quantify diluted plasma using suitable quantification technique (ensure method is not sensitive to SDS such as the Pierce™ BCA Protein Assay Kit from ThermoFisher Scientific or the 2-D Quant Kit from GE Healthcare)
3. Reduce proteins using a final concentration of 10 mM DTT for 30 min at 60°C
Alkylate proteins using a final concentration of 30 mM IAA for 30 min in the dark
4. Quench IAA by adding a further 10 mM DTT
5. Transfer 20 μg plasma sample to a new eppendorf tube

Note: if the sample volume is less than 50 μL additional Plasma dilution buffer (2% SDS in 50mM Tris-HLC pH 8) should be added.

MICROPARTICLE EQUILIBRATION:

6. Re-suspend MagReSyn® HILIC thoroughly by vortex mixing or inversion to ensure a homogenous suspension. *NOTE: When multiple samples are being prepared, ensure that you maintain a homogeneous suspension by mixing regularly, for example by inversion or pipetting the micro particle mixture up/down before transferring the required volume.*
7. Transfer 10 μL MagReSyn® HILIC (200 μg) microparticles to 2 mL Protein Lo-Bind tube.
8. Place the tube on a magnetic separator and allow 5-10 sec for the microparticles to clear.
9. Remove the shipping solution by aspiration with a pipette and discard.
10. Wash the microparticles by re-suspending in 200 μL of **Equilibration Buffer** (refer above) with agitation (e.g. gentle vortex mixing) for 15-30 sec.
11. Place the tube on the magnetic separator and allow the microparticles to clear.
12. Remove the equilibration solution by aspiration with a pipette and discard.
13. Repeat steps 11 – 13.

NOTE: only remove the 2nd equilibration solution from the microparticles once the sample is ready to be added (see step 15. below). This will ensure that microparticles do not air dry and can be easily resuspended when the sample is added.

SAMPLE BINDING AND WASHING:

11. Mix 20 µg (50 µL) of reduced and alkylated plasma sample from step 6. With 50 µL Binding Buffer (30% ACN, 200 mM NH₄Ac pH 4.5) in 1:1 (v/v) ratio

NOTE: *in order to ensure efficient microparticle mixing and protein binding the total volume (sample plus bind buffer) should be in the range of 100-200 µL.*

Add the plasma – bind buffer mix to the equilibrated microparticles from step 14.

NOTE: *if automating the workflow refer to the volumetric parameters of your instrument to ensure compatibility of your clean-up. We recommend a minimum volume of 5 µL of HILIC beads are used to ensure good bead recovery for both manual and automated sample preparation.*

12. Incubate for 30 min at room temperature with continuous mixing (e.g. slow vortexing) to ensure adequate sample and microparticle interaction.

13. Place the tube on the magnetic separator and allow the microparticles to clear. Remove and discard the unbound fraction by aspiration with a pipette.

14. Wash the microparticles with 200 µL of **Wash Buffer** and mix for 60 sec with gentle agitation.

OPTIONAL: the microparticle mixture can be transferred to a new 2 mL Protein Lo-Bind tube to ensure contaminants left on the tube side walls are not re-introduced in the sample during subsequent digest steps

15. Place the tube on a magnetic separator and allow 5-10 sec for the microparticles to clear. Remove the supernatant and discard.

Repeat steps **19** and **20**.

ON-BEAD PROTEIN DIGESTION:

16. Perform on-bead digestion by adding 200 µL of 25 mM Ammonium Bicarbonate pH 8.0 containing 0.2 µg sequencing grade LysC (1:100 enzyme:protein ratio) and 1 µg sequencing grade Trypsin (1:20 enzyme:protein ratio) and incubate for 2 hrs at 47 °C. Ensure sufficient mixing to keep the particles in solution during digestion.

17. Place the tube on a magnetic separator and allow 5-10 sec for the microparticles to clear

18. Remove peptide solution and place in a 0.5 ml Eppendorf LoBind tube.

OPTIONAL: To improve peptide recovery it is possible to incubate the microparticles with 50 to 100 μ l of 1% TFA for 5 minutes whilst mixing and subsequently to pool the supernatant with digest solution from step 24.

19. Vacuum or freeze-dry the samples and re-suspend in 20-40 μ l LCMS solvent e.g. 2% ACN with 0.2% formic acid

20. Perform a colorimetric Peptide Assay to determine peptide recovery and adjust the loads for LC-MSMS analysis.

OPTIONAL: the efficiency of SDS removal by the HILIC method can be evaluated using a colorimetric assay that can measure SDS concentration in the presence of peptides such as the one described in Arand, Friedberg and Oesch, 1992.

21. Analyse digest by LC-MSMS.

NOTE: *if utilising a nano LCMS set-up without a trap-elute option it is recommended to further desalt the digest using standard C18 desalting workflows*

E2: Table 1: LC gradient for LFQ LC-MS/MS

Time (min)	Flow rate ($\mu\text{l}/\text{min}$)	Solvent A (%)	Solvent B (%)
0.00	0.450	98	2
0.00	0.450	98	2
3.00	0.450	98	2
4.400	0.450	95	5
4.500	0.300	95	5
55.00	0.300	82	18
56.00	0.300	70	30
60.00	0.300	20	80
60.10	0.450	20	80
64.90	0.450	20	80
65.00	0.450	98	2
70.00	0.450	98	2

E3. Table 2: Mass spectrometry data acquisition parameters

Full Scan	
Resolution	70,000 (@ m/z 200)
AGC target value	3e6
Scan range	350-1750 m/z
Maximal injection time (ms)	100
Data-dependent MS/MS	
Inclusion	Off
Resolution	35000 (@ m/z 200)
AGC target value	1e5
Maximal injection time (ms)	100
Loop Count	10
Isolation window width (m/z)	2
NCE (%)	27
Data-dependent Settings	
Underfill ratio (%)	1
Charge exclusion	Unassigned, 1, 5- 8, >8
Peptide match	preferred
Exclusion isotopes	on
Dynamic exclusion (s)	20

APPENDIX F: Data from LC-MS/MS, after applying our choice of filtering ($\geq 95\%$ confident identification of PSMs, peptides and PTM probability) and removal of contaminants. PC, Phospho-control; POVA, OVA for phospho-analysis; PE, Phospho-enriched; GC, Glyco-control; GE, Glyco-enriched, GOVA, OVA for glyco-analysis

Sample	RAW spectra		PSMs	Distinct peptides	Phosphorylated peptide PSMs	Deamidated peptide PSMs	Proteins
PC 1	20159		5181	1514	3		290
PC 2	21383		4799	1491	0		159
PC 3	20294		4833	1483	0		270
PC 4	20404		5209	1494	16		279
PC 5	20380		5344	1504	0		277
POVA control 1	16910		307	14	0		1
POVA control 2	14287		18	9	0		1
Phosphopool	15999		629	296	0		87
PE1	16781		406	221	0		68
PE2	17563		1613	666	0		158
PE3	13428		133	66	0		35
PE4	17072		386	114	0		71
PE5	15390		797	379	0		95
PE6	17162		356	188	0		68
PE7	17205		1383	569	0		134
PE8	16340		398	218	0		75
POVA enriched	14272		369	16	3		1
GC1	15742		787	389		1	82
GC2	15228		449	238		12	72
GC3	6821		189	144		0	35
GC4	14544		563	299		17	74
GC5	16259		886	453		14	104
GOVA control 1	8178		58	10		1	1
GOVA control 2	10989		117	11		2	1
Glycopool	8540		267	124		42	31
GE 1	6500		222	140		8	47
GE 2	4575		70	43		0	22
GE 3	6871		182	127		2	37
GE 4	6153		169	103		5	36
GE 5	5732		152	105		6	37
GE 6	4918		89	53		2	23

GE 7	3795		120	91		1	28
GE 8	3512		50	44		2	14
GOVA enriched	5061		12	5		0	1

The raw data (RAW spectra, mzml files generated by Fragpipe, MSstatsfiles) is accessible on massIVE using the following link: <ftp://massive.ucsd.edu/v02/MSV000093117>, ID: MSV000093117.

APPENDIX G – TURNITIN REPORT

Turnitin Originality Report

[Document Viewer](#)

Processed on: 15-Oct-2023 12:23 SAST

ID: 2196042381

Word Count: 33759

Submitted: 1

Logan Smith Revised MSc Thesis By LOGAN JASON Smith

Similarity by Source	
Similarity Index	
8%	
Internet Sources:	7%
Publications:	5%
Student Papers:	3%